Characterization of the Armcx/Almc10 gene family function in mitochondrial dynamics and neural development

Serena Mirra

UNIVERSIDAD DE BARCELONA
FACULTAD DE BIOLOGÍA
DEPARTAMENTO DE BIOLOGÍA CELULAR

INSTITUTO DE INVESTIGACIÓN BIOMÉDICA
PARQUE CIENTÍFICO DE BARCELONA

Characterization of the Armcx/Armc10 gene family function in mitochondrial dynamics and neural development

Serena Mirra

Barcelona, 2013

UNIVERSIDAD DE BARCELONA
FACULTAD DE BIOLOGÍA
DEPARTAMENTO DE BIOLOGÍA CELULAR

INSTITUTO DE INVESTIGACIÓN BIOMÉDICA
PARQUE CIENTÍFICO DE BARCELONA

Memória presentada por Serena Mirra
para optar al grado de Doctora en Biomedicina en la Universidad de Barcelona

Characterization of the Armcx/Armc10 gene family function in mitochondrial dynamics and neural development

Caracterización funcional de la familia de genes Armcx/Armc10 en la dinámica mitocondrial y en el desarrollo neural

Programa de Doctorado en Biomedicina

Bienio 2009-2011

Julio 2013

Doctorando
Serena Mirra

Director de Tesis
Eduardo Soriano

«*Tutto ciò che esiste nell'universo*
***è frutto del caso e della necessità.*»**
Frammenti, Democrito, V-IV sec. a.e.c.

«*Stat rosa pristina nomine,*
***nomina nuda tenemus*.»**
Il nome della rosa, Umberto Eco, 1980

AGRADECIMIENTOS

Muchas veces me he planteado la posibilidad de comenzar y acabar esta sección únicamente con la palabra "Gracias". Sencillamente por evitar el resumir en unas pocas páginas la mención de aquellas personas que durante estos años de trabajo han estado a mi lado, amigos, familia y compañeros, y que de una u otra forma han contribuido a que esta tesis haya llegado a buen fin.

Mi primer agradecimiento se lo debo a mis padres, a mi querida hermana y a toda mi familia por marcar el camino de mi vida y apoyarme en todas las decisiones que he tomado; al fin y al cabo, siempre han sido buenas, aunque sea sólo por tener el apoyo de los a quien más quiero y por hacerlos sentir orgullosos de mí. A mi familia y a mi ciudad siempre los siento cerca o, más bien, dentro de mí.

Otra familia paralela se ha ido formando aquí, compuesta por mi "grupo de apoyo" y por todas las personas que me ido encontrando durante estos años. A esta familia, también, le agradezco mucho, pues hemos aprendido a conocernos tan rápido y a querernos como si nos conociéramos desde siempre, motivo por el cual me ha animado a enfrentarme a la vida con el coraje de quien sabe que no está solo; esto ha significado mucho para mí.

Gracias a Eduardo por darme la oportunidad de estudiar y trabajar en este laboratorio, por su apoyo constante y por la gran confianza que ha depositado en mí. Mis agradecimientos van también a los compañeros con los que he compartido mi espacio de trabajo a lo largo de estos años, por el apoyo incondicional que me dieron desde el primer momento que llegué. Gracias especialmente a Willy, Román y Martí, los tres mosqueteros al servicio de Alex3 y sus hermanos. Con ellos he compartido gran parte de mi trabajo y les agradezco toda la ayuda que me han prestado, así como los buenos momentos que he pasado en su compañía. ¡Mis mejore deseos para todos ahora que nos hemos separado!

Si pienso en los momentos que pasé entre pipetas, poyatas y centrifugas, no puedo dejar de agradecer también a la gente del primer laboratorio donde estuve, en Nápoles. Allí, también, crecí tanto a nivel profesional como a nivel personal. ¡Fue una excursión en un pequeño y nuevo mundo inolvidable!

Gracias a todas y cada una de las personas que han vivido conmigo la realización de esta tesis. Sin la necesidad de nombrarlas, tanto ellas como yo sabemos que desde los más profundo de mi corazón les agradezco el haberme brindado todo el apoyo, la colaboración, el ánimo y la amistad.

INDEX

RESUMEN

Introducción

1. – Dinámica mitocondrial.

Las mitocondrias son orgánulos celulares encargados de suministrar la mayor parte de la energía necesaria para la actividad celular. Las mitocondrias son muchas veces consideradas como pequeñas centrales eléctricas en las que se produce la síntesis de ATP, mediante un proceso de fosforilación oxidativa, en el que se consume O_2 y se libera CO_2 (Han et al., 2010). Pero en las mitocondrias también se realizan otras muchas funciones como la homeostasis del calcio a nivel intracelular (Rizzuto, 2001) o la regulación de la apoptosis (Kroemer et al., 1998).

Aunque las mitocondrias son orgánulos críticos para todas las células, las neuronas son extremadamente dependientes de la correcta función mitocondrial (Han et al., 2010; Nicholls and Budd, 2000). Las neuronas son células altamente especializadas con largos procesos como los axones y las dendritas. Estos procesos neuronales son muy activos en la transmisión de la señal intercelular mediante la liberación de neurotransmisores desde la sinapsis, proceso que requiera de grandes cantidades de energía (Chen and Chan, 2006). Por ello, la habilidad de las mitocondrias para fusionarse, dividirse y migrar para proporcionar energía a través de los procesos neuronales, es particularmente importante para la función sináptica (MacAskill et al., 2010). Además de una fuente de energía, las mitocondrias también juegan un papel crítico en la plasticidad sináptica a través del mantenimiento de la homeostasis del calcio (Li et al., 2004).

La mitocondria es una organela altamente dinámica. Su forma está controlada por fusión y fisión, su estructura interna cambia en función de su estado fisiológico, y participa en interacciones recíprocas con otras organelas (Chen and Chan, 2004; Chen and Chan, 2009).

Las mitocondrias, como otras organelas, son transportadas por microtúbulos y microfilamentos de actina (Sheng and Cai, 2012). El transporte mitocondrial está altamente regulado, entregando mitocondrias a regiones activas de la célula, particularmente importante en neuronas metabólicamente activas. El transporte mitocondrial depende de la unión y separación de motores del citoesqueleto.

Movimientos de corto alcance en microfilamentos de actina requieren motores de miosina, mientras que movimientos de largo alcance en microtúbulos requieren kinesinas o dineína (Cai and Sheng, 2009).

Miembros de la familia de ATPasas kinesina-1, como KIF5 y KIF1, son responsables del transporte anterógrado rápido de las mitocondrias (Hirokawa and Takemura, 2004). Dos proteínas cargo adaptadoras, Miro y Milton, están involucradas en el enlace de la mitocondria con KIF5 en neuronas (Brickley et al., 2005; Gorska-Andrzejak et al., 2003; Stowers et al., 2002). Miro (*mitocondrial rho*) es una GTPasa de la familia Rho que está anclada a la membrana mitocondrial externa (Fransson et al., 2006). Miro se une a una proteína adaptadora específica mitocondrial llamada Milton (Trak en mamíferos), que está asociada a la cadena pesada KIF5 (MacAskill et al., 2009a). Miro es una proteína ligadora de calcio que puede actuar como un sensor de la concentración local de Ca^{2+}: en su estado libre de Ca^{2+}, Miro se une a Milton, mientras que en su estado ligado a Ca^{2+}, no puede unirse a Milton, resultando en el desacoplamiento de la mitocondria de los microtúbulos (MacAskill and Kittler, 2010; Wang and Schwarz, 2009).

La fusión y fisión de la mitocondria controlan el largo, forma, tamaño y número de las mitocondrias; estos procesos mantienen la forma y propiedades funcionales generales de la población de mitocondrias (Han et al., 2011).

La fusión mitocondrial permite el intercambio de contenidos entre las mitocondrias, permitiendo a las mitocondrias defectivas recobrar componentes de la cadena respiratoria, ADN mitocondrial, y otras moléculas esenciales en el marco del estrés celular (Hoppins and Nunnari, 2009; Sheng and Cai, 2012). La fusión mitocondrial está regulada por diferentes tipos guanosin trifosfato GTPasas. Entre ellas cabe destacar las Mitofusinas (Mfn1 y Mfn2), presentes en la membrana externa de la mitocondria donde forman complejos homo-oligoméricos y hetero-oligoméricos en trans entre mitocondrias cercanas (Chen et al., 2003) y OPA1 (*dynamin- related protein* atrofia óptica 1), localizada en el espacio intermembrana adhiriendo a la membrana mitocondrial interna, esencial para la fusión de las membranas mitocondriales internas (Cipolat et al., 2004).

La fisión de las mitocondrias en mamíferos requiere del reclutamiento de DRP1 (*dynamin-related protein 1*) desde el citosol (Huang et al., 2011). DRP1 se ensambla en depresiones puntiformes en la mitocondria y forma anillos y espirales que rodean y

comprimen el túbulo mitocondrial (Ford et al.; Fukushima et al., 2001; Mears et al., 2011; Yoon and McNiven, 2001). El reclutamiento de DRP1 a los sitios de fisión involucra a la proteína adaptadora FIS1, anclada a la membrana mitocondrial externa y modula el ensamblaje del aparato de fisión (Huang et al., 2011).

La importancia de todos los procesos que regulan la dinámica mitocondrial ha sido descrita tanto en procesos fisiológicos de desarrollo y envejecimiento como en condiciones patológicos de una gran variedad de enfermedades como Alzheimer (AD), Parkinson (PD), la enfermedad de Huntington (HD), Charcot-Marie-Tooth (CMT) o Atrofia óptica dominante (DOA) (Chan, 2006; Cho et al., 2010; Han et al., 2010).

2. – La familia de genes Armcx

Los genes Armcx (Armcx1-6, Gprasp1-2 y bhlhb9) pertenecen a una misma familia localizada en cluster en la región Xq22.1-Xq22.2 del cromosoma X (Armadillo repeat containing X-linked). Esta familia está caracterizada por la posesión de dominios armadillo en su secuencia proteica (Winter and Ponting, 2005). Proteínas con estos dominios se han implicado en procesos de tumorigénesis, desarrollo embrionario o mantenimiento de la integridad tisular (Hatzfeld, 1999). El cluster de genes Armcx se originó por la retrotransposición de un único gen que contiene dominios armadillo (Armc10) exclusivo de y presente en todos los vertebrados, y por subsiguientes duplicaciones en tándem de corto alcance de una región de evolución rápida en el cromosoma X de euterios (Lopez-Domenech et al., 2012).

Los genes Armcx presentan un patrón de expresión casi ubicuo (Kurochkin et al., 2001; Simonin et al., 2004).Sin embargo, es en el cerebro donde se encuentra la mayor expresión de estos genes, lo que ha hecho sugerir que esta familia exclusivas de los mamíferos euterios pueda estar implicadas en la adaptación evolutiva del neocórtex, una región del cerebro anterior exclusiva de los mamíferos (Winter and Ponting, 2005).

Poco se conoce acerca de la función que los genes Armcx desempeñan. Sin embargo su elevada expresión en el sistema nervioso central, su participación en procesos de desarrollo embrionario y su posible implicación en tumorigénesis y enfermedades neurodegenerativas, los convierten en buenos candidatos para realizar un estudio en

profundidad acerca de los mecanismos bioquímicos y biológicos en los que pueden estar implicados.

Alex3 se encontró localizar en diferentes compartimentos celulares, mayoritariamente a núcleo y mitocondria (Lopez-Domenech et al., 2012). La sobreexpresión de Alex3 provoca la agregación y/o tethering mitocondrial tanto en neuronas como células, dando lugar a la formación de un clúster en la zona perinuclear (Lopez-Domenech et al., 2012). La localización en mitocondrias de Alex3 (Mou et al., 2009) y la posesión de dominios armadillo similares a los de la proteína β-catenina, hacen de esta proteína un candidato para estar regulando procesos en la biología mitocondrial donde la vías de señalización de Wnt/β-catenina puede estar implicada.

3. – La vía de señalización de Wnt en desarrollo de la médula espinal

Las proteínas Wnt, representan una gran familia de proteínas secretables, constituida por 19 miembros identificados actualmente en humanos, y que se encuentran altamente conservadas a lo largo de la evolución (Nusse, 2001; Prud'homme et al., 2002). Esta familia de proteínas, está ampliamente descrita por estar implicada en vías de señalización que juegan un papel fundamental en una gran variedad de procesos que incluyen: patrón celular, proliferación, diferenciación, orientación, adhesión, supervivencia y apoptosis (Chong and Maiese, 2004; Li et al., 2006; Nelson and Nusse, 2004; Nusse, 2005; Nusse and Varmus, 1982; Patapoutian and Reichardt, 2000; Smalley and Dale, 1999; van Amerongen and Nusse, 2009; Wodarz and Nusse, 1998).

La vía canónica de señalización por Wnt implica la activación de receptores Frizzled, la estabilización de la β-catenina citoplasmática cuya degradación es inhibida, su translocación al núcleo y su unión a cofactores TCF/LEF para actuar como factor de transcripción. La vía de señalización por Wnt puede actuar sobre células vecinas como señales de corto alcance pero también como morfógenos, induciendo diferentes respuestas sobre células situadas lejos de la fuente de producción en función de la concentración (Lander, 2007). La vía de Wnt juega un papel importante para regular muchos aspectos del desarrollo del sistema nervioso (Ciani and Salinas, 2005; Freese et al., 2010; Ille and Sommer, 2005; Salinas and Zou, 2008). Entre ellos, la vía de

señalización por Wnts actúa de forma clave durante el desarrollo de la médula espinal. Debido a su bien conocida estructura anatómica y a la sencilla tratabilidad experimental, la médula espinal ha sido extensivamente usada como modelo experimental para conocer los mecanismos de acción de los morfógenos.

Muchas proteínas Wnt están expresadas en el tubo neural en desarrollo (Hollyday et al., 1995; Parr et al., 1993). Entre ellos encontramos Wnt1 y Wnt3a, que se expresan ambos en regiones dorsales del tubo neural, actuando en conjunto con otras proteínas de señalización, como Shh, BMPs y FGFs.

La actividad de estas proteínas de señalización regula la expresión de genes de patrón como Pax6, Pax7, Olig2, o Nkx2.2. El perfil de expresión de estos factores de transcripción determina, para cada precursor, la especificación en los distintos tipos de neuronas que se originan a lo largo del eje dorsoventral (Ulloa and Briscoe, 2007; Ulloa and Marti, 2010). Por ejemplo, los ligandos Wnt1 y Wnt3a son necesarios para la formación de las poblaciones más dorsales del tubo neural (Muroyama et al., 2002). Así, embriones de ratón mutantes para Wnt1 y Wnt3a presentan una pérdida o disminución de las tipos celulares característicos del tubo neural dorsal (Muroyama et al., 2002).

Paralelamente a la especificación de los diferentes subtipos neuronales, los progenitores proliferan en la zona ventricular del tubo neural para generar el número adecuado de neuronas de cada subtipo. Número y tamaño celular están controlados por vías de señalización a los componentes de la maquinaria del ciclo celular (Murray, 2004).

El gradiente dorsoventral de Wnts ha sido propuesto como organizador del crecimiento de los progenitores neurales (Megason and McMahon, 2002), siendo capaz, a nivel molecular, de regular la expresión de ciertos moduladores necesarios para la transición G1/S del ciclo celular como CiclinaD1 o N-myc (Megason and McMahon, 2002). Consistente con esto, la expresión de β-catenina constitutivamente activa, en embriones de ratón o de pollo, incrementa la proliferación y disminuye la diferenciación, en contraste con la sobreexpresión de un dominante negativo para Tcf-4 o con la deficiencia de β-catenina (Ille et al., 2007; Megason and McMahon, 2002; Zechner et al., 2003).

El sistema modelo del pollo es un sistema clásico dentro la biología del desarrollo, que permite de realizar experimentos de ganancia y pérdida de función de forma sencilla. El tubo neural representa posiblemente la parte del embrión donde la técnica de

electroporación *in ovo* es más eficiente, permitiendo de generar embriones mosaico (Krull, 2004).

Objectivos

El objetivo de esta Tesis Doctoral es el de caracterizar el papel funcional de las proteínas Alex3 y Armc10 en la dinámica mitocondrial y en el desarrollo neural. La sucesión de resultados obtenidos durante la elaboración de la tesis se ha traducido en la concreción de los siguientes objetivos parciales:

1. Análisis de la función de la proteína Alex3 en la biología y dinámica mitocondrial

2. Análisis de la función de la proteína Armc10, ancestro del cluster Armcx, en la biología y dinámica mitocondrial

3. Análisis de la función de las proteínas Alex3 y Armc10 en desarrollo neural a través de un modelo fisiológico *in vivo*: la medula espinal de pollo.

Resultados

1. La proteína mitocondrial Alex3 regula el tráfico mitocondrial en neuronas y interacciona con el complejo Miro/Trak2 y Mitofusinas.

1.1 Patrón de expresión de los transcriptos Armcx y expresión neuronal de la proteína Alex3

Al analizar la expresión de los genes Armcx durante el desarrollo embrionario, encontramos que, en estadios embrionarios, Armc10 y los genes Armcx3-6 están altamente expresados en los tejidos neurales en desarrollo, en los derivados de la cresta neural y en las extremidades, así como en otros tejidos que eran específicos de cada gen.
Estudios en cortes de cerebro desde E16 hasta Adulto para la proteína Alex3 muestran una elevada expresión de Alex3 en varias regiones del cerebro, siendo especialmente relevante en estructuras laminadas como el córtex cerebral, hipocampo, bulbo olfativo y la capa de células Purkinje y granulares del cerebelo. La expresión de la proteína de

Alex3 disminuye a medida que progresa el desarrollo, manteniéndose significativa en estas estructuras. El estudio detallado de la inmunohistoquímica mostró una localización intracelular diferencial de la proteína Alex3 en diferentes regiones del cerebro, en núcleo o en el citoplasma dependiendo del estadio y del tipo celular.

1.2 Alex3 interactúa con las proteínas Mitofusina1/2 sin alterar fusión mitocondrial

La dinámica mitocondrial es un complejo proceso que implica agregación, tráfico, y eventos de fusión y fisión. Para testar si Alex3 está involucrado en fusión mitocondrial, llevamos a cabo ensayos de co-inmunoprecipitación en células HEK293AD transfectadas con los cDNAs de Alex3-GFP y o Mitofusina1-myc o Mitofusina2-myc, responsables de la fusión mitocondrial. Encontramos que Alex3 interactúa con las dos Mitofusinas.
Para directamente probar si Alex3 regula la fusión mitocondrial, tomamos ventaja de la versión fotoactivable mito-PAGFP (Karbowski et al., 2004). Células HEK293T transfectadas con mito-PAGFP fueron fotoactivadas y videos grabados a lo largo de 15 minutos, y los ratios de fusión mitocondrial a lo largo del tiempo fueron analizados. De acuerdo con estudios previos (Gomes et al., 2011; Karbowski et al., 2004; Saotome et al., 2008), los resultados muestran un constante incremento en los eventos de fusión a lo largo del tiempo. Los ratios y dinámicas de estos eventos en células HEK293T co-transfectadas con mito-PAGFP y Alex3 fueron idénticas a las de células HEK293T control. Experimentos similares en neuronas hipocampales, sobreexpresando Alex3 o una secuencia shRNA, dieron resultados similares, sugiriendo que los niveles de proteína Alex3 no alteran la fusión mitocondrial ni en células HEK293T ni en neuronas.

1.3 Los niveles de proteína de Alex3 regulan el tráfico mitocondrial en neuronas

La regulación del tráfico y dinámica mitocondrial se piensa ser esencial para suplir apropiadamente de energía a las ramas neuronales más distales, y consecuentemente para la correcta neurotransmisión y viabilidad neuronal. Para averiguar si Alex3 está implicado en el transporte mitocondrial en axones, usamos técnicas de live-imaging. Cultivos de neuronas hipocampales fueron transfectados a 4 días *in vitro* (DIV) con

MitDsRed o Alex3-GFP. Después de 2 días, los axones de neuronas vivas fueron identificados y grabados a lo largo de 15 minutos. La motilidad mitocondrial fue cuantitativamente evaluada por medio de kimografías, y la comparación de la motilidad mitocondrial en neuronas control y transfectadas con Alex3-GFP reveló que la sobreexpresión de esta proteína resultaba en una reducción dramática en el porcentaje de las mitocondrias móviles, en ambos sentidos, anterógrado y retrógrado. Además, la velocidad y la distancia media cubierta por cada mitocondria también se mostraron alteradas en las neuronas sobreexpresantes de Alex3-GFP. Los experimentos arriba mencionados apuntan a una implicación de Alex3 en la dinámica y tráfico mitocondrial. Para confirmar esta noción, realizamos experimentos para silenciar la proteína endógena de Alex3. Neuronas hipocampales fueron transfectadas con vectores pLVTHM expresantes de la secuencia shRNAi-Alex3, o una secuencia scrambled control. Posteriormente la motilidad mitocondrial fue cuantitativamente evaluada como arriba. Las neuronas expresantes de Alex3-shRNAi exhibían una motilidad mitocondrial reducida y mitocondrias más pequeñas que las neuronas control. Nuevamente, esta disminución era para el transporte anterógrado y retrógrado. Sin embargo, ni la velocidad ni la distancia cubierta por los movimientos de mitocondrias individuales estaba alterada por el silenciamiento de Alex3 endógena. En conjunto, estos experimentos muestran que los niveles de expresión de Alex3 regulan la motilidad media de las mitocondrias en los axones en neuronas vivas y modulan la velocidad y la distancia cubiertas por estas organelas.

1.4 Alex3 interacciona con las proteínas Miro1/2 y Trak2

El tráfico mitocondrial en neuronas está mediado por los motores kinesina (KIF5) (Hirokawa and Takemura, 2004). Recientemente ha sido encontrado que las Rho GTPasas Miro1 y Miro2, así como el adaptador de kinesina Trak2, unen las mitocondrias a los motores KIF5, permitiendo el transporte mitocondrial en neuronas (Guo et al., 2005; MacAskill et al., 2009a). A continuación, estudiamos si Alex3 formaba parte del complejo de tráfico KIF5/Miro/Trak2. Primero, llevamos a cabo análisis de inmunofluorescencia en células HEK293AD transfectadas. Estas células mostraban una

fuerte colocalización de Alex3 con Miro1, Miro2 y Trak2 mientras que aparentemente no se detectaba colocalización con KIF5C. A continuación, realizamos ensayos de co-inmunoprecipitación en células HEK293AD transfectadas con los cDNAs de Alex3-GFP y o Miro1-myc o Miro2-myc. Miro1 y Miro2 con el epítopo myc fueron detectados por WB en lisados inmunoprecipitando con anticuerpos anti-GFP. A la inversa, inmunoprecipitaciones con el anticuerpo anti-myc (Miro1-2) revelaron la presencia de la proteína Alex3-GFP. No hubo co-inmunoprecipitación cuando las células fueron transfectadas con el cDNA de Miro1/2-myc o Alex3-GFP solos. Experimentos similares mostraron que Alex3-GFP co-inmunoprecipitaba con la proteína Trak2-myc in células transfectadas. En contraste, no detectamos co-inmunoprecipitación de Alex3-GFP con KIF5C-myc o con KIF5-A o KIF5-B. Estos datos indican que Alex3 interacciona directamente con las proteínas Miro1-2/Trak2, por lo tanto sugiriendo que esta proteína está implicada en el complejo de tráfico de KIF5/Miro/Trak2.

Para determinar si los seis dominios similares a armadillo eran requeridos para la interacción con estas proteínas, generamos un constructo N-terminal (1-106) sin estos 6 dominios armadillo. Experimentos de co-inmunoprecipitación en células HEK293T transfectadas mostraron que este mutante de la proteína Alex3 no co-inmunoprecipitaba con las proteínas Trak2 o Miro2, por lo tanto indicando que la región C-terminal que contiene los dominios armadillo es requerida para esta interacción.

Estudios recientes han mostrado evidencias que el complejo Miro/Trak2 interacciona con los motores kinesinas de forma dependiente de Ca^{2+}, en el que el Ca^{2+} se une a las proteínas Miro y desencadena el desacoplamiento del complejo a los microtúbulos, permitiendo así el arresto mitocondrial (Macaskill et al., 2009b; Wang and Schwarz, 2009). Testamos así si la asociación de Alex3 con el complejo de tráfico era también dependiente de Ca^{2+}. La presencia de 2mM Ca^{2+} reduce de forma clara la interacción de Alex3 con Miro1,2 y Trak2 (Figura 25d,e). Resulta interesante que la co-transfección de Alex3-GFP con un cDNA de un mutante de Miro1-myc al que le faltan los “EF hand”, dominios responsables para la unión de Ca^{2+}, bloquea la regulación de la interacción de Miro1/Alex3 por Ca^{2+}, reforzando así la idea que la interacción entre estas dos proteínas es regulada por los niveles de Ca^{2+}. Para corroborar estos hallazgos, realizamos experimentos adicionales usando proteína purificada GST-Miro1 y realizamos pull-downs

con extractos de lisados de cerebro (Macaskill et al., 2009b). Estos experimentos confirmaron la interacción de las proteínas Alex3/Miro1, así como la regulación de esta interacción por Ca^{2+}, y la dependencia de los dominios "EF hand" en la proteína Miro1 para la regulación del complejo por Ca^{2+}. En conjunto, los datos mostrados arriba demuestran que Alex3 pertenece al complejo de tráfico mitocondrial KIF5/Miro1-2/Trak2 y que la interacción de Alex3/Miro1 requiere bajas concentraciones de Ca^{2+}.

2. Armc10/SVH, gen ancestro del cluster Armcx, también regula las dinamicas mitocondriales en neuronas y interacciona con el complejo Miro/Trak2 y Mitofusinas.

2.1 Expresión neuronal de la proteína Armc10/SVH y localización celular

La proteína Armc10 posee 6 dominios armadillo, un dominio transmembrana en el extremo N-terminal (aa 7-29), un probable lugar de cleavage (aa 30-36) y una secuencia flanqueante con una alta basicidad en uno de los extremos de su región transmembrana similar a las que poseen las proteínas Tom20 y Bcl-w, la cual predice una posible localización en la membrana mitocondrial externa (Rapaport, 2003).

La expresión del gen Armc10 ha sido caracterizada por estar ampliamente distribuida en varios tejidos, incluyendo placenta, hígado, riñón, corazón y cerebro En este estudio, el patrón regional y celular del inmunomarcaje de la proteína Armc10 fue estudiado en secciones de ratón adulto, resultando la proteína Armc10 ampliamente expresada en la mayoría de las regiones especialmente en el hipocampo, corteza y cerebelo. Resulta interesante destacar que estas marcas resultaron ser mayoritariamente nucleares, lo cual concuerda con la presencia de putativas señales de exportación nuclear (NES) (Zhou et al., 2007).

Debido a que estudios previos habían señalado una posible localización mitocondrial de la proteína Armc10 (Pagliarini et al., 2008) se realizaron ensayos de inmunofluorescencia en células HEK293T y cultivos neuronales de hipocampo, que corroboraron la predominante localización mitocondrial de la proteína Armc10 endógena. En conjunto estos datos muestran una localización bimodal (mitocondrial y nuclear) parecida a la de la proteína Alex3, y también muestra amplias similitudes con las proteínas localizadas en el

cluster Armcx, lo que apunta a que pueda tener funciones similares en el sistema nervioso.

2.2 Los niveles de proteína de Alex3 regulan la agregación y el tráfico mitocondrial en neuronas

Debido a las similitudes en los patrones de expresión y localización de las proteínas Armc10 y Alex3, resultó interesante demostrar si la proteína Armc10, ancestro del cluster Armcx, estaba también implicada en la regulación de la agregación y transporte mitocondrial. Para ello, hicimos uso de un vector codificante para la proteína Armc10 murina, que mostró nuevamente una localización mitocondrial tras trasfeccion de células HEK293T. También encontramos que el 88% de las células sobreexpresantes de la proteína Armc10 muestran fenotipos anormales, variando entre fenotipos fuertemente agregados (29% aggregated) en los que había un gran y único agregado en la zona perinuclear y fenotipos intermedios (49% altered), lo cual puede indicar un papel similar en la regulación de la agregación mitocondrial en línea celular.

Para investigar si la proteína Armc10 está también implicada en el transporte mitocondrial en axones, cultivos de neuronas hipocampales fueron transfectadas a 4DIV con MitDsRed o Armc10-GFP y después de 2 días, axones de neuronas vivas fueron identificados y grabados a lo largo de 15 minutos y la motilidad mitocondrial cuantificada por medio de kimografías. En los cultivos control, alrededor de un 30% de mitocondrias presentaban movilidad a lo largo de los 15 minutos de grabación, mientras que el resto de mitocondrias permanecían estacionarias. Por el contrario, el transporte mitocondrial en las neuronas transfectadas con la proteína Armc10-GFP mostraban una disminución significativa del transporte mitocondrial en ambos sentidos, anterógrado y retrógrado, aunque a diferencia de los resultados previos observados con la proteína Alex3, ni la velocidad ni la distancia recorrida por mitocondria resultaron afectadas.

Para confirmar la noción de que la proteína Armc10 también regula el tráfico mitocondrial en neuronas, se realizaron experimentos de silenciamiento de la proteína endógena, transfectando los cultivos neuronales con una secuencia específica para la región C-terminal de Armc10 y presente en todas sus isoformas o una secuencia control

scrambled. Las neuronas expresantes del shRNAi para Armc10 eran viables y morfológicamente normales. Nuevamente, las neuronas silenciadas para Armc10 presentaban una reducción en la motilidad y tráfico mitocondrial en ambos sentidos, y nuevamente ni la velocidad ni la distancia recorrida por mitocondria se mostraron alteradas por el silenciamiento. En conjunto, estos datos muestran que los niveles de la proteína Armc10, al igual que los de Alex3, regulan la motilidad de las mitocondrias en cultivos hipocampales de neuronas.

2.3 Armc10 interacciona con Miro/Trak2 y Mitofusina1/2

Finalmente, para confirmar si la regulación del tráfico mitocondrial por parte de la proteína Armc10 es similar al producido por Alex3, investigamos la posible interacción del ancestro del cluster Armcx, Armc10, con el complejo KHC/Miro/Trak2, regulador del trafico mitocondrial en neuronas. Para ello, se llevaron a cabo ensayos de co-inmunoprecipitación en células HEK293T transfectadas con Armc10-GFP y las proteínas Miro2, Trak2 o KIF5C fusionadas al epítopo myc. Alex3 se detectó interaccionar con las proteínas Miro2 y Trak2, mientras no fue posible detectar interacción entre Alex3 y KIF5. En conjunto, estos datos demuestran que el ancestro del cluster Armcx, Armc10, también interacciona con el complejo Miro/Trak2, de forma similar a la que lo hace la proteína Alex3.

Puesto que las proteínas responsables de la fusión mitocondrial, Mitofusina1 o Mitofusina2, interactúan con el complejo Miro2//Trak2 (Misko et al., 2010), llevamos a cabo ensayos de co-inmunoprecipitación en células HEK293AD transfectadas con los cDNAs de Alex3-GFP y o Mitofusina1-myc o Mitofusina2-myc, encontrando que Alex3 interactúa con las dos Mitofusinas.

3. Las proteínas Alex3 y Armc10 regulan la proliferación y la diferenciación celular en la médula espinal de pollo.

3.1 La sobreexpresión de la proteína Alex3 inhibe la vía de señalización de Wnt

La proteína Alex3 posee seis dominios armadillo, que se encuentran en varias proteínas de la vía de Wnt, entre ellas β-catenina (Lopez-Domenech et al., 2012). Para testar un posible papel de Alex3 en la vía de Wnt, usamos un sistema *in vivo*, llevando a cabo ensayos funcionales de electroporación en la médula espinal de pollo. Para ello se realizaron ensayos de transactivación génica por electroporación en los que cotransfectamos el sistema TOP/FLASH-Luciferasa junto con diferentes combinaciones de Alex3 y otros vectores control. Estos estudios mostraron que la expresión de Alex3 reduce sensiblemente la transcripción dependiente de TCF, tanto la endógena del sistema, como la inducida por sobre-expresión de β-catenina o Wnt3a, indicando que Alex3 cumple un papel regulador por inhibición de la vía.

3.2 La sobreexpresión de las proteínas Alex3 y Armc10 no afecta el patrón dorso-ventral de la médula espinal de pollo

Las proteínas Wnt (en concreto Wnt1 y Wnt3a) actúan como señales dorsalizantes en el control de la expresión de marcadores de progenitores neurales, de forma que la sobre-expresión de estos factores en el tubo neural causa la expansión de marcadores dorsales, tal como Pax6 o Pax7, a expensas de marcadores ventrales, como Olig2 o Nkx2.2 (Alvarez-Medina et al., 2008; Machon et al., 2003). Puesto que Alex3 actúa como inhibidor de la vía de Wnt, quisimos comprobar el efecto funcional de las sobreexpresiones de las proteínas Alex3 y Armc10 sobre el patrón dorso-ventral del tubo neural. Electroporaciones de cDNA codificantes para Alex3 o Armc10 en médula de pollo no indujeron cambios en la distribución de marcadores tanto dorsales cuanto ventrales, sugiriendo que la sobre-expresión de estas proteínas no afecta el patterning en los estadios de desarrollo analizados.

3.3 Armc10/SVH se expresa en la médula espinal de pollo y localiza en mitocondrias

Puesto que el cluster Armcx es específico de mamíferos euterios, quisimos caracterizar la expresión del único ortólogo presente en pollo: el gen Armc10/SVH, que presenta una fuerte homología con Armc10 de ratón. A través de hibridaciones in situ de embriones en

estadio HH19 de desarrollo, mostramos que el gen Armc10/SVH está expresado preferentemente en regiones dorsales del tubo y débilmente en la placa del suelo; en estadios más avanzados de desarollo (HH24), la expresión del gen Armc10/SVH sigue detectándose en los progenitores dorsales, en la placa del suelo y también aparece en motoneuronas ventrales. Llevando a cabo el análisis de *inmunohistoquímica* detectamos que la proteína endógena de pollo Armc10/SVH colocaliza con el marcador mitocondrial COXIV. Para analizar la función de las proteínas de interés, electroporamos los DNAs recombinantes de Alex3, del mutante Alex3Δ(1-12) (deletreado en la región N-terminal que lleva la señal de localización mitocondrial) o de Armc10, en el tubo neural de pollo. A Después de 24 horas de la electroporacion, llevamos a cabo el análisis de *inmunohistoquímica* y detectamos que Alex3 y Armc10 colocalizan ambas con el marcador mitocondrial COXIV, mientras que el mutante Alex3Δ(1-12) presenta una marca difusa en el citosol y en el núcleo.

3.4 Alex3 promueve diferenciación neuronal

La vía de señalización de Wnt juega un papel importante en el mantenimiento de los precursores neurales durante el desarrollo de la médula espinal, y la inhibición de esta vía es necesaria para la diferenciación neuronal (Chenn and Walsh, 2002; Zechner et al., 2003). Debido a que Alex3 actúa como inhibidor de la vía de Wnt, quisimos averiguar si Alex3 o Armc10 podrían estar implicados en la diferenciación neural en médula de pollo. Nuestros resultados mostraron que las células electroporadas con Alex3 se encontraban localizadas mayoritariamente en la zona del manto y tan solo unas pocas células se podían detectar en la región ventricular, difiriendo significativamente del caso control y sugiriendo que Alex3 podría actuar promoviendo diferenciación. Este fenotipo no se detectó en médulas electroporadas con Alex3Δ(1-12) o Armc10. Para confirmar el papel de Alex3 como promotor de diferenciación neuronal, analizamos la expresión del marcador de diferenciación neuronal Tuj-1 en médulas electroporadas con Alex3 y encontramos que la mayoría de las células electroporadas expresaban también el marcador Tuj-1, difiriendo sensiblemente del caso control.

3.5 Las proteínas Alex3 y Armc10 son reguladores negativos del ciclo celular

La progresión de los precursores neurales a través del ciclo celular y el equilibrio proliferación-diferenciación están regulados por la vía de señalización de Wnt/β-catenina y pueden ser fácilmente analizadas en la médula espinal de pollo (Chenn and Walsh, 2002; Zechner et al., 2003). Tras electroporacion de los constructos expresantes Alex3, Alex3Δ(1-12) o Armc10, analizamos el efecto de dicha overexpressión 24 horas posterior a la electroporación, sirviéndonos de anticuerpos dirigidos contra la fosfo-histona H3 (PH3, marcador de la fase M del ciclo) o la bromodesoxiuridina (BrdU, marcador de la fase S, previamente inyectado en el tubo 40 minutos antes de la análisis). Se encontró una disminución significativa en la proliferación en los casos de pCIGAlex3 y pCIGArmc10, lo cual indica que tanto la proteína Alex3 *full-length* como la proteína Armc10 son reguladores negativos del ciclo celular.

Discusión y Conclusiones

En este trabajo se muestra principalmente el papel de dos genes: Amcx3, miembro del cluster Armcx en el cromosoma X, y Armc10, ancestro del cluster que puede presentar características que han perdurado en los genes Armcx. Las proteínas Alex3 y Armc10 presentan localización bimodal (en mitocondria y núcleo) y aquí describimos que estas proteínas, altamente expresados en el tejido nervioso, regulan la agregación, dinámica y tráfico mitocondrial en neuronas y están implicadas en eventos clave del desarrollo de la médula espinal de pollo.

El tráfico y dinámica mitocondrial son especialmente importantes en neuronas donde el correcto posicionamiento de estas organelas se ha visto esencial para la viabilidad neuronal y la neurotransmisión. Datos recientes han mostrado que la dinámica mitocondrial neuronal (transporte y fusión-fisión de membranas) está altamente coordinado y controlado por las Kinesinas, las GTPasas Mitofusina 1-2 y Miro1-2, y la proteína adaptadora Trak2 (Misko et al., 2010; Saotome et al., 2008; Verstreken et al., 2005). La sobreexpresión de las proteínas Armcx3 y Armc10 se ha visto provocar la agregación y/o tethering mitocondrial tanto en neuronas como células HEK293, dando

lugar a la formación de un clúster en la zona perinuclear. Estas proteínas podrían regular la agregación mitocondrial por un mecanismo todavía desconocido, que es probable que implique la interacción con otras proteínas que controlan el tethering y agregación, incluyendo Miro1/2 y Mitofusina1/2 (Santel et al., 2003), con las cuales demostramos una interacción directa mediante ensayos de inmunoprecipitación. Aunque Alex3 favorece la aproximación y tethering mitocondrial y este proceso debería facilitar la fusión (Hoppins and Nunnari, 2009), nosotros fuimos incapaces de encontrar evidencias de una implicación de la proteína Alex3 en la fusión mitocondrial; es posible que se requiera alguna señal para la correcta fusión de las membranas, posiblemente a través de la activación de las mitofusinas. Es por ello, que no nos es posible descartar una posible implicación de Alex3 en los procesos de fusión/fisión aunque sea de manera indirecta.

En neuronas, se cree que la agregación y tethering mitocondrial sirve para anclar estas organelas en localizaciones específicas que requieren una alta demanda de energía y unos requerimientos de tamponamiento de Ca^{2+} (Chang and Reynolds, 2006; MacAskill and Kittler, 2010). El fenotipo observado por la sobreexpresión de las proteínas Alex3 y Armc10 es similar al observado después de una disfunción de las proteínas reguladores del tráfico y la dinámica de estas organelas, tales como Miro, Mfn, Pink1 o Trak2, lo cual sugiere que la alteración de los procesos de dinámica mitocondrial darían lugar a agregación (Huang et al., 2007; Liu and Hajnoczky, 2009; MacAskill and Kittler, 2010; Weihofen et al., 2009). Alex3 y Armc10, codifican para unas proteínas que interaccionan con el complejo KIF5/Miro/Trak2, que controla la dinámica mitocondrial en neuronas de forma dependiente de Ca^{2+}. Nuestros experimentos de inmunoprecipitación muestran que tanto Alex3 como Armc10 interaccionan directamente con las GTPasas Miro y con el adaptador de kinesina Trak2. Sin embargo, fuimos incapaces de encontrar una interacción directa con el motor de kinesina KIF5. Esta Resulta importante que, la interacción de Alex3 (y posiblemente de Armc10) con las proteínas Miro/Trak2, requiere bajas concentraciones de Ca^{2+}, ya que la presencia de Ca^{2+} disminuye dramáticamente la interacción. Además, la mutación en el dominio EF-hand (sensor de calcio) de la proteína Miro1 anula esta dependencia de Ca^{2+}, indicando por lo tanto que los cambios conformacionales producidos por el Ca^{2+} en las proteínas Miro (Macaskill et al., 2009b; Nelson and Chazin, 1998; Wang and Schwarz, 2009) son mecanismos esenciales que

regulan la interacción entre Alex3 y el complejo Miro/Trak2. Así, mientras que bajas concentraciones de Ca^{2+} pueden favorecen la formación de los complejos KIF5/Miro/Trak2/Alex3, los incrementos en el Ca^{2+} intracelular rápidamente desacoplan tales complejos (incluyendo a Alex3), por lo tanto deteniendo el tráfico mitocondrial.

La noción que Alex3 (y posiblemente Armc10) interacciona con el complejo Miro/Trak2 (e indirectamente con KIF5) cuando las mitocondrias son móviles a bajas concentraciones de Ca^{2+} (Macaskill et al., 2009b; Wang and Schwarz, 2009) es reforzada por nuestros hallazgos del silenciamiento de Alex3 y Armc10 endógeno en neuronas, que da lugar a una marcada disminución en los porcentajes de las mitocondrias móviles, similarmente a lo que ha sido observado en las perdidas de función de Miro/Trak2 (Brickley and Stephenson, 2011; Macaskill et al., 2009b; Saotome et al., 2008). La observación que el silenciamiento de Alex3 y Armc10 no afectan a la velocidad de las pocas mitocondrias móviles presentes sugiere un mecanismo en las proteínas Armcx/Armc10 favorecerían la formación de los complejos KIF5/Miro/Trak2 (y por lo tanto aumentando el tráfico mitocondrial). Sin embargo, estas proteínas están improbablemente implicadas en la regulación de la actividad motora de la kinesina por ella misma. Nosotros consideramos nuestros hallazgos en la sobreexpresión de Alex3, en las que ambas, el porcentaje y la velocidad de las mitocondrias móviles fueron reducidas, proveen mayores evidencias de la implicación fisiológica de esta proteína en el tráfico mitocondrial, posiblemente al desregular o reclutando componentes del complejo (actuando como un dominante negativo). En conjunto con nuestros datos bioquímicos, los presentes estudios funcionales proponen un modelo en el que las proteínas Alex3 y Armc10 son reguladores positivos del tráfico mitocondrial, interaccionando directamente con los complejos Miro/Trak2. Además, como se muestra para el complejo KIF5/Miro/Trak2 (Macaskill et al., 2009b; Wang and Schwarz, 2009), el incremento de la actividad neuronal que conlleva a incrementos en Ca^{2+} es probablemente la causa del desensamblaje del complejo y del arresto mitocondrial en los lugares de neurotransmisión activa, completando por lo tanto los requerimientos bioenergéticos de la transmisión neuronal.

Debido al control transcripcional (Mou et al., 2009; Zhou et al., 2007) y la presencia de 6 dominios similares a armadillo, los genes Armcx/Armc10 pueden

funcionalmente interaccionar con la vía de Wnt/β-catenina. Las proteínas Wnt han sido involucradas en multitud de procesos del desarrollo de varios tejidos. Entre ellos la vía de señalización por Wnts actúa de forma clave durante el desarrollo de la médula espinal. Debido a su bien conocida estructura anatómica y a la sencilla tratabilidad experimental, la médula espinal ha sido extensivamente usada como modelo experimental para conocer los mecanismos de acción de los morfógenos. Las proteínas Wnt1 y Wnt3a están expresadas en regiones dorsales del tubo neural, actuando en conjunto con otras proteínas de señalización (como Shh, BMPs y FGFs) regulando procesos de patterning, proliferación y diferenciación durante el desarrollo (Alvarez-Medina et al., 2008; Le Dreau and Marti, 2012; Megason and McMahon, 2002).

Puesto que el cluster Armcx es específico de mamíferos euterios, quisimos caracterizar la expresión del único ortólogo presente en pollo: el gen Armc10/SVH, que encontramos expresado preferentemente en regiones dorsales del tubo, en la placa del suelo y en motoneuronas ventrales. Para averiguar si Alex3 puede estar actuando en la vía de Wnt/β-catenina, realizamos ensayos de luciferasa, electroporando en medulas de pollo un constructo expresante Alex3. Nuestros resultados demuestran que la sobreexpresión de Alex3 reduce sensiblemente la transcripción dependiente de TCF, tanto la endógena del sistema, como la inducida por sobre-expresión de β-catenina o Wnt3a, en médula de pollo. Esto indica que Alex3 cumple un papel regulador por inhibición de la vía de Wnt/β-catenina. A este efecto no se corresponde una del patterning dorsoventral en los estadios de desarrollo analizados.

Otro aspecto importante del desarrollo del tubo neural es la orquestación muy coordinada del balance entre proliferación y diferenciación de los progenitores, donde la señalización de Wnt/β-catenina juega un papel crucial, manteniendo los precursores neuronales proliferando (Chenn and Walsh, 2002; Zechner et al., 2003).

En este estudio se encontró que en médulas de pollo electroporadas con Alex3, las células electroporadas (GFP^+) se encontraban principalmente en la región del manto del tubo neural, lo que sugiere que Alex3 pueda promover diferenciación neuronal. Por otra parte, se encontró que en médulas de pollo electroporadas con Alex3, la mayoría de las células electroporadas eran Tuj-1 positivas, produciendo un aumento significativo en el porcentaje de células $Tuj\text{-}1^+/GFP^+$ con respecto a los embriones de control. Este

dato confirmó que Alex3 actúa promoviendo la diferenciación, coherentemente con su papel de inhibidor de la vía Wnt/β-catenina. Es importante destacar que esta función es específica para Alex3 y no se encontró para la proteína Armc10, proporcionando una divergencia funcional en el contexto del desarrollo de la médula espinal. Otro dato interesante es que el efecto de la sobreexpresión Alex3 en la promoción de la diferenciación neuronal requiere la localización mitocondrial de Alex3. Este dato lleva a especular que Alex3 podría retener a mitocondria algún factor nuclear necesario para la activación TCF/LEF, conduciendo a la inhibición de la vía de señalización Wnt/β-catenina y por lo tanto promoviendo la diferenciación neuronal. Un mecanismo similar fue descrito por Mou et al., que sugirieron una cascada de señalización entre la mitocondria y el núcleo a través del complejo Sox10/Alex3. Este grupo propuso que Alex3 modula la actividad transcripcional de Sox10 reteniéndolo a las mitocondrias, donde Sox2 podría someterse a modificaciones post traduccionales que pueden resultar en un aumento de la actividad transcripcional, una vez transportado en el núcleo (Mou et al., 2009).

Otro resultado importante de nuestro estudio indica que tanto Alex3 que Armc10 son reguladores negativos del ciclo celular, y que la localización mitocondrial de Alex3 se requiere para llevar a cabo esta función. Este efecto podría actuarse mediante la promoción de una salida temprana del ciclo celular, afectando la la duración del ciclo celular, o alterando el equilibrio entre las 3 modalidades de división de los precursores neuronales (PP, PN, NN).

En conjunto, nuestros datos sugieren que Alex3 está involucrado tanto en la regulación negativa del ciclo celular (posiblemente promoviendo la salida del ciclo celular) que en la inducción de la diferenciación de precursores neuronales; esta doble acción se refleja en la distribución lateral de las células que sobreexpresan Alex3 en la zona del manto.

Por otro lado, Armc10 sólo está implicada en la regulación negativa del ciclo celular (posiblemente sólo afectando la duración del ciclo celular). Estas diferencias entre los efectos de la sobreexpresión de Alex3 y Armc10 en procesos llave del desarrollo de la médula espinal, evidencian las divergencias funcionales entre las dos proteínas, sugiriendo que Alex3 puede haber adquirido funciones adicionales respecto a Armc10, ancestro filogenético del cluster Armcx.

Los datos reportados en este estudio, que describen los efectos de la sobreexpresión de Alex3 sobre el desarrollo de la médula espinal, son coherentes con el papel de Alex3 como inhibidor de la vía Wnt/β-catenina. Sin embargo, no hay pruebas suficientes para sostener que estos efectos sobre el ciclo celular de los progenitoras y la diferenciación neuronal se logran mediante la inhibición de la vía Wnt/β-catenina y otros experimentos son necesarios para apoyar esta hipótesis.

A falta de desarrollar un mecanismo molecular que describa en detalle la participación de Alex3 en respuesta a los morfógenos Wnt, nuestros datos sugieren que la vía de señalización de Wnt puede estar regulando procesos llave del desarrollo a través de las proteínas mitocondriales Alex3 y Armc10.

INTRODUCTION

1.- Mitochondrial Dynamics

1.1 - Introduction: Mitochondrial Dynamics

Mitochondria are large organelles whose main role in eukaryotic cells is ATP production, cytosolic calcium buffering and regulation of apoptosis. They consist of an outer membrane and a densely folded inner membrane (MacAskill and Kittler, 2010). ATP is produced along the inner membrane though oxidative phosphorylation, a reaction in which ATP is formed from carbon substrates as a result of the transfer of electrons from $FADH_2$ o NADH to O_2 via a series of carriers (Duchen, 2004). This transfer creates an electrochemical gradient across the mitochondrial membrane termed proton motive force, used to power ATP synthase as well to accumulate cytosolic calcium. This ability to undertake calcium buffering can play important roles in many cell types, and especially in neuronal signaling, as calcium serves as an important secondary messenger. Mitochondria also play an important role in apoptosis: cellular stress can result in the release of cytochrome c from the mitochondrial matrix, which then activates a caspase signaling cascade resulting in apoptosis (Danial and Korsmeyer, 2004).

Once thought to be solitary and rigidly structured, mitochondria are now appreciated to constitute a population of organelles that fuse and divide, move throughout the cell, and undergo regulated turnover. These dynamic processes regulate mitochondrial function by enabling mitochondrial recruitment to critical subcellular compartments, content exchange between mitochondria, mitochondrial shape control, mitochondrial communication with the cytosol and mitochondrial quality control (Chen and Chan, 2009). As a result, mitochondria can ready adapt to changes in cellular requirements, whether due to physiological or environmental imperatives. The disruption of mitochondrial dynamics leads to cell dysfunction (Millecamps and Julien, 2013).

1.2 - Mitochondrial transport in neurons

Neurons are polarized cells that consist of three distinct structural and functional domains: the cell body (soma), a long axon and thick dendrites with many branches and elaborate dendritic arbors. Along those regions mitochondria are not uniformly distributed (Hollenbeck and Saxton, 2005): areas with high demands for ATP contain

more mitochondria than other cellular domains, including pre- and post- synaptic domains, the axon initial segment, nodes of Ranvier and growth cones (Sheng and Cai, 2012). Although the biogenesis of mitochondria can occur locally within the axon, it is thought that most new mitochondria are generated in the soma and that dysfunctional mitochondria also return to the soma for degradation by the autophagy-lysosomal system. Thus the position of mitochondria in neurons must be controlled on rapid timescales to match changes in synaptic input, requiring specialized mechanisms to transport mitochondria from the soma to their destination and to ensure that they remain stationary in high energy demand regions to support several neuronal functions.

1.2.a - Mechanisms of mitochondrial transport in neurons

Several studies applying time-laps imaging of live cultured neurons and *in vivo* studies in genetically engineered mice have revealed the complex nature of mitochondrial transport along neuronal processes (Kang et al., 2008; Miller and Sheetz, 2006; Misgeld et al., 2007).

In mature cultured neurons, only one-third of axonal mitochondria are mobile and the remaining 65-80% are stationary (Kang et al., 2008). Saltatory and bidirectional movements result in mean mitochondrial velocities between 0.1 and 1.4 μm per second (MacAskill et al., 2009a; Morris et al., 1995). Differences between mitochondrial velocity parameters reported by several investigations are mainly due to the method of analysis, the direction of mitochondrial transport measured, the cellular compartment, the neural type or the marker used for labeling mitochondria.

The moving mitochondria move in neurons bidirectionally, frequently changing direction, pausing or switching to persistent docking (Hollenbeck and Saxton, 2005; Kang et al., 2008; Miller and Sheetz, 2006; Misgeld et al., 2007).

Three major protein groups are involved in transporting mitochondria in neurons: (1) cytoskeletal proteins, (2) molecular motors, and (3) a host of adaptors and scaffolding proteins that mediate the interactions between motors, cargos and the cytoskeleton (Chang and Reynolds, 2006; Sheng and Cai, 2012); (Table1).

Protein	*Role*	*Organism(s)*
KIF5	Microtubule motor	Drosophila melanogaster and mammals
KIF1Bα	Microtubule motor	Mammals
KLP6	Microtubule motor	Mammals
Dynein–dynactin	Microtubule motor	D. melanogaster and mammals
MIRO	KIF5 receptor	D. melanogaster and mammals
Milton	KIF5 adaptor	D. melanogaster
TRAKs (OIP106, GRIF1)	KIF5 adaptor	Mammals
Syntabulin	KIF5 adaptor	Mammals
FEZ1	KIF5 adaptor	Mammals
RANBP2	KIF5 adaptor	Mammals
APLIP1	KIF5 adaptor	D. melanogaster
Syntaphilin	Static anchor	Mammals
Mitofusins	MIRO–TRAK regulator	Mammals
Tau	Microtubule stability	Mammals
MAP1B	Microtubule stability	Mammals
Myosin XIX	Actin motor	Mammals
Myosin V	Actin motor	D. melanogaster neurons
Myosin VI	Actin motor	D. melanogaster neurons
WAVE1	Actin polymerization	Mammals

Table 1: Molecular motor–scaffold proteins and regulators of mitochondrial transport
APLIP1, APP-like-interacting protein1; FEZ1, fasciculation and elongation protein-ζ1; KIF, kinesin superfamily protein; MAP1B, microtubule-associated protein 1B; MIRO, Mitochondrial rho; RANBP2, RAN-binding protein 2; WAVE1, WASP family verprolin homologous protein 1. Adapted from Sheng & Cai, 2012.

The majority of long distance mitochondrial transport is via motor proteins moving mitochondria along microtubules, whereas the actin cytoskeleton is more important for anchoring mitochondria and for short range movements (Hirokawa and Takemura, 2004; Morris et al., 1995).

Microtubules are formed from the polymerization of α- and β-tubulin and are arranged in a polarized manner with plus and minus ends. Kinesin superfamily proteins (KIFs) and cytoplasmic dynein are the main microtubule-based motor proteins, requiring ATP hydrolysis to guaranteeing the transport of mitochondria as well other membranous

organelles or cargoes (Hirokawa and Takemura, 2004). They transport mitochondria towards the microtubule plus-ends and minus-ends respectively. Axonal microtubules are uniformly arranged so that their minus ends are directed towards the soma and their plus ends are directed distally (Hirokawa and Takemura, 2004; Martin et al., 1998). Thus, in the axons, cytoplasmic dynein motors are responsible for returning mitochondria to the soma, whereas kinesin motors of the KIF5 family drive anterograde mitochondrial transport to distal axonal region and synaptic terminals (Fig.1). As dendritic microtubules exhibit mixed polarity in the proximal regions, KIFs and dynein motors can drive cargo transport in either an anterograde or retrograde direction depending on microtubule polarity (Fig.1).

In presinaptic terminals, growth cones and dendritic spines, actin filaments form the major cytoskeletal architecture and myosin motors probably mediate short range movement along actin filaments (Fig.1). Motile mitochondria can also be recruited to stationary pools via dynamic interactions between the docking receptor syntaphilin and microtubules or actin-based anchoring machinery (Fig.1).

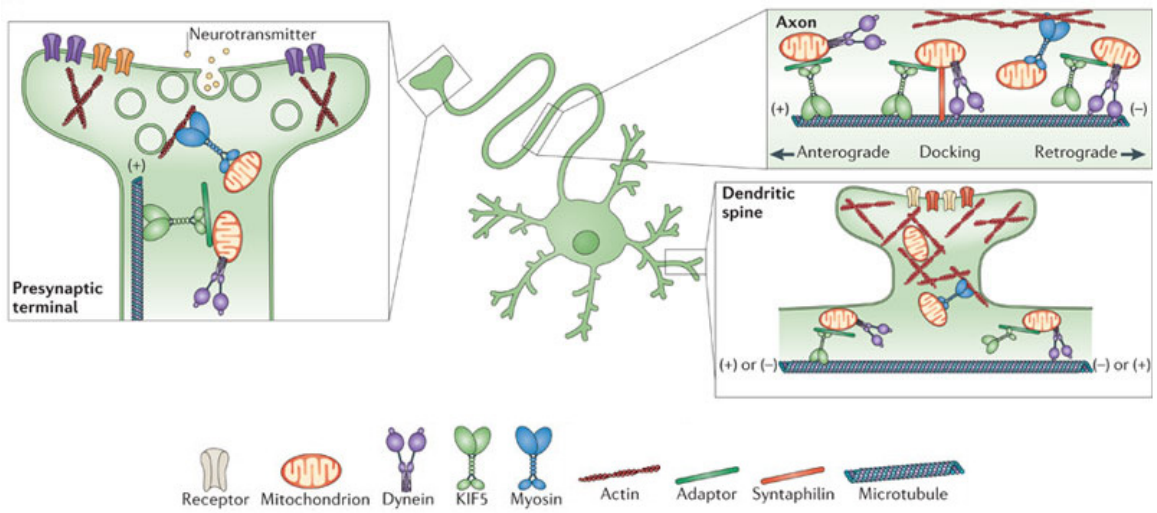

Figure 1: Mitochondrial transport in neurons. Simplified representation of a peripheral neuron showing the cell body that gathers signals from presinaptic neurons. Adapted from Sheng & Cai, 2012.

1.2.b - Anterograde Mitochondrial transport

Kinesins and anterograde mitochondrial transport

Human kinesin superfamily members (KIF) is a large family currently containing at least

45 different genes in human and mouse (Hirokawa and Takemura, 2004), classified into 14 families.

The members of the kinesin-1 family, collectively known as KIF5, contain two kinesin heavy chains (KHCs) and two kinesin light chains (KLCs) (Hirokawa and Takemura, 2004). Each KHC contains an amminoterminal motor domain that has ATPase activity and binds directly to microtubules, whereas its carboxy-terminal cargo-binding domain mediates an association with a KLC or directly interacts with cargoes or cargo adaptors, such as mitochondrial adaptor proteins. KIF5 proteins have a key role in microtubule plus end-directed (anterograde) mitochondrial transport in axons, whereas in dendrites, where microtubule polarity is mixed, it is involved in both anterograde and retrograde transport.

In mammals, there are three forms of KIF5 motors, KIF5A, B and C. KIF5B was the first to be discovered and is present in almost all cell types. KIF5A and C are neuron-specific motors (Hirokawa and Takemura, 2004; Kanai et al., 2000). How these three motors divide cargoes between them and whether they are functionally redundant remains unclear.

Deletion of KIF5B in non-neuronal mouse cells blocks transport of mitochondria to the periphery resulting in their perinuclear clustering (Tanaka et al., 1998). Mutating KIF5 in Drosophila (in which only one KIF5 isoforms is found) severely disrupts anterograde mitochondrial transport along axons even if it does not abolish it entirely, suggesting that other kinesin motors are also involved (Pilling et al., 2006). In cultured rat primary hippocampal neurons, expression of dominant negative KIF5 construct disrupts mitochondrial trafficking in axons (Cai et al., 2005) while function-blocking antibodies to KIF5 block bi-directional mitochondrial trafficking along mixed polarity microtubules in dendrites (MacAskill et al., 2009a).

Kinesin motors could either be attached directly to the lipid bilayer of the mitochondrial membrane, or they could be attached via adaptor proteins that themselves can bind lipids or have transmembrane domains. Recently, significant advances have been made in identifying the molecular machinery that links mitochondria to the KIF5 motors for transport.

Motor Adaptors

The first studies aimed to identify motor adaptor proteins associated with KIF5 and involved in mitochondrial transport were conducted in *Drosophila,* and identified Milton

as a mitochondrion-specific motor protein linker that is needed for movement of mitochondria into the axon (Brickley et al., 2005). *Milton* mutants form normal synapses, but their axons and terminals are devoid of mitochondria (Gorska-Andrzejak et al., 2003; Stowers et al., 2002). Milton colocalizes and co-purifies with mitochondria but not with other organelles. Since the initial identification of Milton, two mammalian kinesin binding orthologues, TRAK1 and TRAK2 (also known as OIP106 and OIP98/Grif-1, respectively), have been identified (Brickley et al., 2005).

Functional similarities and differences have emerged between Milton and TRAKs. In Drosophila, Milton acts as an essential bridging molecule necessary to link mitochondria to kinesin motors (Glater et al., 2006; Wang and Schwarz, 2009). Knocking-down TRAK1 or expressing dominant-negative TRAK1 mutants in hippocampal neurons results in impaired mitochondrial mobility in axons (Brickley et al., 2005).

Roles for Milton other than mitochondrial trafficking have not been identified, and Milton fly mutants do not appear to have defects in the trafficking of other cargo such as synaptic vesicles (Stowers et al., 2002). Thus, Milton appears to be a specific mitochondrial trafficking adaptor. In contrast, TRAK proteins (which Exhibit 33.5% and 35.3% similarity to Milton for rat TRAK1 and TRAK2, respectively) might have evolved other functions and trafficking roles within the cell, as they also regulate intracellular transport of other cargo and organelles including endosomes and ion channels (Grishin et al., 2005; Webber et al., 2008; Wennerberg and Der, 2004).

Milton is linked indirectly with KIF5 through the interaction with the atypical GTPase Miro (mitochondrial rho), that is present in mitochondrial outer membrane (Fig.2). Deletion of dMiro in Drosophila, or depletion of Miro1 in cultured hippocampal neurons, significantly reduces the number of moving mitochondria (Fransson et al., 2006; Guo et al., 2005; MacAskill et al., 2009a). In

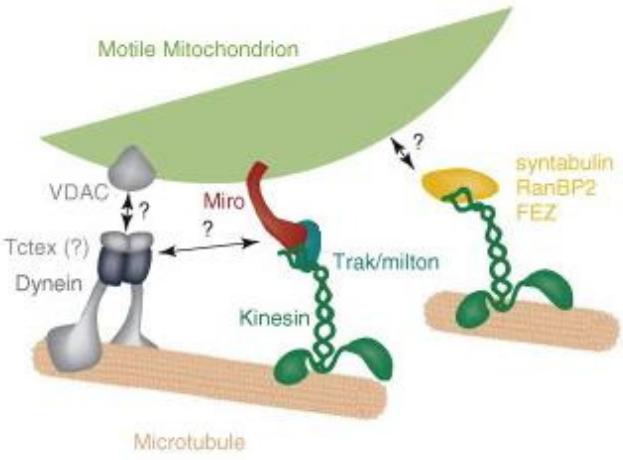

Figure 2: The machinery of mitochondrial transport. Mitochondrial transport along microtubules is mediated by dynein and kinesin motor proteins in cooperation with various adaptor proteins. Adapted from MacAskill et al., 2009.

mammalian two Miro orthologues (Miro1 and Miro2) have been identified. They have a carboxyl terminal transmembrane domain that sits in the outer mitochondrial membrane and two GTPase domains flanked by two EF hand calcium binding domains, required for signalling control over mitochondrial transport (Fransson et al., 2003; Fransson et al., 2006). TRAKs bind to the first GTPase domain of Miros (Fransson et al., 2006).

In hippocampal neurons Miro1 acts as the major mitochondrial acceptor site for TRAK2 and the MIRO1-TRAK2 complex has been shown to be a key regulator of mitochondrial transport (Macaskill et al., 2009b). Elevating Miro1 levels enhances the recruitment of TRAK2 to mitochondria and facilitates mitochondrial transport (Macaskill et al., 2009b).

Syntabulin, FEZ1 and RanBP2 are also implicated in kinesin-dependent transport of mitochondria (Fig.2).

Syntabulin interacts directly with KIF5 isoforms and attaches to outer mitochondrial membrane via its C-terminal domains (Cai et al., 2005). Depletion of syntabulin or blocking of syntabulin-KIF5 interaction, impair mitochondrial trafficking reducing anterograde transport along axons in cultured hippocampal neurons (Cai et al., 2005).

The kinesin adaptor FEZ1 is a brain-specific protein implicated in mitochondrial transport in hippocampal neurons and in the transport of mitochondria into the tips of growing neurites in NGF-stimulated PC12 neuroblastoma cells (Fujita et al., 2006; Ikuta et al., 2007). Knocking down FEZ1 using RNA interference reduces anterograde mitochondrial transport into the tips of growing neurites of both hippocampal neurons and PC12 cells (Fujita et al., 2006; Ikuta et al., 2007).

RanBP2 is a large scaffold protein associated with nucleocytoplasmic transport, protein biogenesis, mitosis and trafficking that interacts directly with KIF5B and KIF5C (but not KIF5A) in brain and retina (Cai et al., 2004) and regulates mitochondrial transport in non-neuronal cells, where inhibition of its interaction with KIF5B or KIF5C causes perinuclear clustering of mitochondria (Cho et al., 2007). However, little is known regarding any potential role this protein might have in regulating mitochondrial trafficking in nerve cells.

Whether syntabulin, FEZ1 or RanBP2 bind directly to the outer mitochondrial membrane or are recruited via interactions with a mitochondrial receptor protein such as Miro remains unclear.

Why do neurons require multiple KIF5 adaptors to mediate mitochondrial transport? One attractive hypothesis is that KIF5 motors physically attach to their transport cargoes via

different adaptor complexes, thus allowing neurons to regulate mitochondrial transport through separate mechanisms in response to different physiological signals.

1.2.c - Retrograde Mitochondrial transport

Cytoplasmic dynein has a key role in microtubule minus end-directed retrograde mitochondrial transport in axons, whereas in dendrites, where microtubule polarity is mixed, it is involved in transporting mitochondria to both the periphery and the cell body. Cytoplasmic dynein is formed by two dynein heavy chains (DHCs) and several dynein intermediate chains (DICs), dynein light intermediate chains (DLICs) and dynein light chains (DLCs) (Karki and Holzbaur, 1999).

There are very few dynein heavy chains functioning as motors, but this relative simplicity is increased by large numbers of accessory proteins, including light chains and dynactin (a multisubunit complex necessary for dynein activity) that allow selectivity between dynein motors and different cargoes (Hirokawa et al., 2009).

Even if the model by which dyneins link to organelle membrane-associated proteins via their light and intermediate chains is largely accepted, the mechanism that link dynein to mitochondria are not well characterized. For example the question whether the dynein motor complex associates with mitochondrial membranes directly or indirectly via a linkage by unidentified dynein adaptor still remains opened. Tctex1, a dynein light chain capable of supporting dynein-mediated transport, has been shown to interact with the voltage-dependent, anion-selective channel (VDAC) localized to the outer mitochondrial membrane, suggesting a possible linkage for mitochondria to dynein motors (Schwarzer et al., 2002); (Fig.2).

Dynactin, a large 11-subunit complex, binds directly to cytoplasmic dynein and to microtubules, enhancing the processivity of the dynein motor or regulating its interaction with cargo(King and Schroer, 2000). Both dynein and dynactin were found associated with purified mitochondria from Drosophila brains and mutations in dynein heavy chain genes dramatically alter axonal mitochondrial transport, affecting retrograde transport velocity and run length (Pilling et al., 2006). However, an in vivo analysis showed that dynactin has a crucial role in regulating and/or coordinating the bidirectional motility of membrane organelles and is not required to link dynein to membranes (Pilling et al., 2006).

An interesting feature of dynein-mediated transport is that it also requires kinesin function, perhaps because kinesin must transport dynein to the periphery of cells. This might also be due to direct regulatory functions of kinesin or kinesin associated proteins on dynein function (Hirokawa and Takemura, 2004; Hollenbeck and Saxton, 2005; Pilling et al., 2006; Susalka et al., 2000; Susalka and Pfister, 2000).

In this direction, a recent work demonstrating that Miro in flies also plays a role in regulating retrograde (presumed dynein-dependent) mitochondrial transport in axons (Russo et al., 2009), raising the possibility that the kinesin adaptor also regulates dynein mediated transport of mitochondria (and raising the possibility that Miro is also the adaptor recruiting dynein motors to these organelles). However, a direct interaction between Miro and dynein has not been demonstrated.

1.2.d - Regulation of mitochondrial transport in neurons

Synaptic activity-dependent regulation

Mitochondrial trafficking dynamics are directly correlated with the levels of neuronal activity, such as synaptic activity or action potential signalling (Pilling et al., 2006). Mitochondria are transported and retained to activated synapses in response to two intracellular signals that control their velocity and their recruitment to stationary pools.

The first signalling pathway involves the detection of ATP and ADP levels: mitochondrial movement is increased in areas where there are high concentrations of ATP (supporting to move mitochondria away from areas where the ATP concentration is high), whereas increases in ADP levels inhibit movement (locally recruiting mitochondria to areas of energy need) (Mironov, 2007). This mechanism might exist to facilitate the recruitment of mitochondria to neuronal subdomains undergoing higher levels of synaptic transmission, which have higher requirements for ATP and/or calcium buffering.

The second signaling pathway involves alteration in intracellular calcium concentrations: increases in dendritic calcium (e.g. via opening of NMDA receptors, which are calcium-permeable glutamate receptors activated during synaptic activity) can also stop mitochondrial movement during high-frequency transmission at a single or a few synapses, allowing recruitment of mitochondria to the base of single spines (the spiny protrusions where most excitatory synapses are formed) (Li et al., 2004; Macaskill et al., 2009b).

As in dendrites, calcium entry in axons (e.g. upon application of a calcium ionophore or via opening of voltage sensitive calcium channels during action potential firing), also stops mitochondria (Chang and Reynolds, 2006; Wang and Schwarz, 2009), providing a potential mechanism for activity-dependent recruitment of mitochondria to presynaptic terminals (Chang and Reynolds, 2006; Wang and Schwarz, 2009) necessary for energy supply required for vesicle trafficking and refilling (Verstreken et al., 2005).

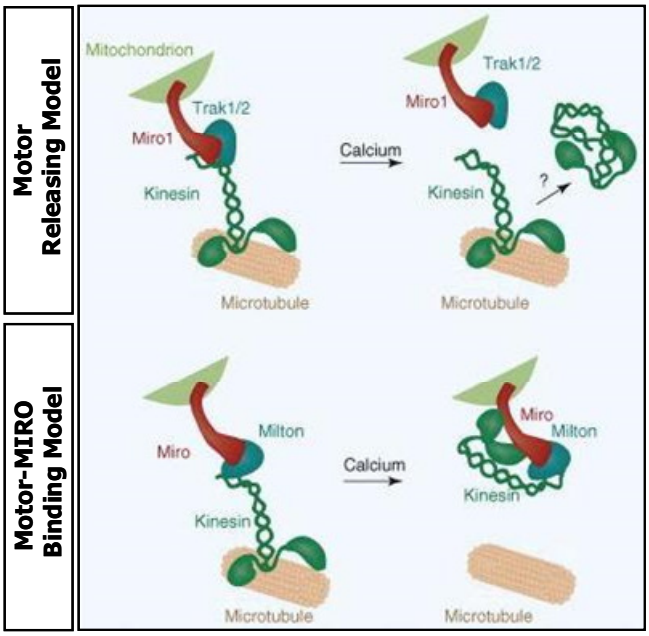

Figure 3: Molecular mechanisms of mitochondrial stopping on synaptic activity. Schematic representation of "Motor Releasing Model" and "Motor-Miro Binding Model". Adapted from MacAskill and Kittler, 2010.

Several papers showed that the EF hand domains of Miro are the calcium sensor that mediates this calcium-dependent mitochondrial stopping. In fact, the calcium-induced cessation of mitochondrial mobility was effectively abolished in neurons expressing mutant Miro EF hands that cannot bind calcium (Macaskill et al., 2009b). Two mechanisms have been proposed for how this occurs (Fig.3). Under basal conditions KIF5 is bound to mitochondria trough the interaction of its C-terminal domain with TRAK2, which in turn binds Miro1/2 at mitochondrial surface. In the "Motor Releasing Model", calcium binding to Miro1/2 inhibits a direct interaction between Miro and KIF motors, resulting in uncoupling of mitochondria from the transport machinery and possible deactivation of the motors (Macaskill et al., 2009b); in the "Motor-Miro Binding Model", at high calcium levels the motor domain of kinesin unbinds microtubules and flips up to bind directly to Miro on the mitochondria, uncoupling mitochondria from the microtubule transport pathway (Wang and Schwarz, 2009). Additional work is needed to solve the differences between these two models.

Neuronal signaling-mediated regulation

Several evidences are emerging about the docking effect of NGF (Nerve Growth Factor, a growth factor that is important for neuronal differentiation and survival), that has been shown to cause axonal mitochondrial arrest in dorsal ganglion neurons, in an actin-based mechanism (Chada and Hollenbeck, 2004).

Axonal mitochondrial transport can also be regulated by activation of the serotonin receptor 5-HT1A receptor subtype and by dopamine 1 receptors, both promoting axonal transport of mitochondria in cultured rat hippocampal neurons by increasing the activity of the protein kinase Akt, and consequently decreasing glycogen synthase kinase (GSK3β) activity (Chen et al., 2007; Chen et al., 2008). In contrast, dopamine acting on dopamine 2 receptors has the opposite effect, inhibiting mitochondrial movement in hippocampal neurons via the same AKT- GSK3β signaling cascade (Chen et al., 2008). Nevertheless, the molecular targets of the AKT- GSK3β signaling pathway are not clear.

Regulation of mitochondrial transport by microtubule associated proteins

Phosphorylation of microtubule-associated proteins (MAPs) such as tau and MAP1b by GSK3b (or other kinases) can alter their binding to microtubules and their microtubule stabilizing ability (Sang et al., 2001; Scales et al., 2009). MAP1b and tau are mainly axon-targeted MAPs and contribute to the regulation of the axonal transport of membrane organelles, including mitochondria (Stamer et al., 2002).

Overexpressing tau in neuroblastoma cell lines, primary cortical neurons and retinal ganglion neurons, selectively inhibits kinesin-driven anterograde mitochondrial transport. In these experiments, dynein-mediated retrograde transport became dominant and mitochondria accumulated in the soma instead of being delivered to neuronal processes (Dubey et al., 2008; Stamer et al., 2002; Stoothoff et al., 2009). These studies suggest that tau preferentially competes with kinesin motors for binding to microtubules because mitochondrial transport velocity was not altered when tau is overexpressed (Trinczek et al., 1999). Interestingly, loss (in Tau -/- mice) or partial reduction (in Tau +/- mice) of tau expression in mutant neurons prevented amyloid-β-mediated defects in mitochondrial transport (Vossel et al., 2010), suggesting that the role of amyloid-β in inhibiting axonal mitochondrial mobility is dependent on tau expression levels.

Moreover, overexpression of GSK3β in cultured neurons results in an increase in the number of axonal motile mitochondria, and the effects of GSK3 β overexpression on

mitochondrial trafficking are abolished in Tau (−/−) neurons, thereby indicating that the effects of this kinase are mediated by its action on the modification of Tau (Llorens-Martin et al., 2011).

Thus, signaling pathways (e.g. GSK3b activity) might converge on indirect regulators of motor protein activity to globally regulate microtubule-based transport.

1.2.e - Mitochondrial transport and quality control

Mitochondria have multiple quality control mechanisms at the molecular, organelle and cellular levels, to limit mitochondrial damage and ensure mitochondrial integrity. The molecular level of defense is supported by the proteolytic system. Molecular chaperons and ATP-dependent proteases in the matrix and inner membrane of mitochondria degrade damaged proteins, stabilize misfolded proteins (thus preventing their aggregation) and/or brake up protein aggregates (and thereby promote proteolysis) (de Castro et al., 2010). In addition, the cytosolic ubiquitin-proteasome system can also participate in the quality control of mitochondrial proteins (Tatsuta and Langer, 2008). At the organelle level, fusion and fission processes act to protect the cell against mitochondrial damage. Fusion between damaged mitochondria and healthy mitochondria provide repair from the damn, as the contents of healthy and dysfunctional mitochondria are mixed (Braun and Westermann, 2011; Chen and Chan, 2009; Chen et al., 2003). Fission sequesters mitochondria that have become irreversibly damaged or are fusion-incompetent and results in their subsequent elimination by autophagy. At the cellular level, the elimination of the whole damaged mitochondria is provided by mitophagy, the autophagy-mediated degradation of mitochondria (Baker et al.; Karbowski and Youle, 2004; Shutt et al., 2012). Mitophagy requires the specific labeling of damaged mitochondria and their subsequent recruitment into isolation membranes, and this can occur through two mechanisms. First, outer mitochondrial membrane proteins such as NIP3-like protein X (NIX) in mammalian cells, bind to LC3 on the isolation membranes, which mediated the sequestration of damaged mitochondria into autophagosomes (Youle and Narendra, 2011). Second, when mitochondria is damaged by losing their membrane potential, the mitochondrial Parkinson disease (PD) protein PINK1 recruits the E3 ubiquitin ligase Parkin from the cytosol to dysfunctional mitochondria where it ubiquitinates mitochondrial proteins for proteosomal degradation and promotes the engulfment of mitochondria by autophagosomes. During this process, mitochondrial dynamics are

shifted toward fission over fusion, partly due to proteasomal degradation of Mitofusin proteins (Gegg et al., 2010; Gegg and Schapira, 2010; Tanaka, 2010; Tanaka et al., 2010). Miro has recently been found to interact with PINK1, linking Miro function to pathological changes in mitochondrial function in stroke and PD. The interaction with the protein kinase PINK1, a regulator of mitochondrial morphology and function, is particularly intriguing because it raises the possibility that Miro is a substrate of PINK1 and hence under the control of PINK1-dependent phospho-regulation, although there is no direct evidence for this.

1.3 - Mitochondrial fusion and fission

When mitochondria are viewed in live cells, it becomes immediately apparent that their morphologies are far from static. In many eukaryotic cell types, mitochondria not only continuously move along cytoskeletal tracks, but also frequently fuse and divide. These concerted activities control mitochondrial morphology and its intracellular distribution and determine the cell type-specific appearance of the network (Detmer and Chan, 2007b).

The antagonistic and balanced activities of the fusion and fission machineries shape the mitochondrial compartment, and the dynamic behaviour of mitochondria allows the cell to respond to its ever-changing physiological conditions. A shift towards fusion favours the generation of interconnected mitochondria, whereas a shift towards fission produces numerous mitochondrial fragments (Fig.4).

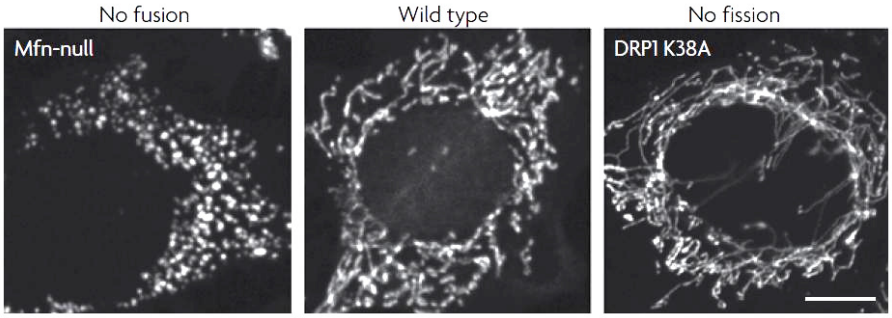

Figure 4: Mitochondrial length, size and connectivity are determined by the relative rates of mitochondrial fusion and fission. In wild-type cells mitochondria form tubules of variable length. In the absence of mitochondrial fusion (for example, in Mfns-null cells) unopposed fission results in fragmented mitochondria. Conversely, decreased fission (for example, in DRP1 K38A cells, which express a dominant-negative form of DRP1) results in elongated and highly interconnected mitochondria. Scale bar 10 μm. Adapted from Detmer and Chan, 2007.

The large mitochondrial networks that are generated by fusion are beneficial in metabolically active cells, in which they contribute towards energy production. In contrast, in quiescent cells mitochondria are frequently present as numerous morphologically and functionally distinct small spheres or short rods (Collins et al., 2002).

Unlike the reticular networks seen in neuronal cell bodies (Eldering et al., 2004; Popov et al., 2005), mitochondria in axons are discrete bean-shaped organelles, ranging from ~ 100 nm to several micrometers long (Pilling et al., 2006). Although the different lengths within this range do not correlate with differing run velocities or other behavior in Drosophila neurons (Pathak et al., 2010; Pilling et al., 2006; Russo et al., 2009), extremely long axonal mitochondria that are generated by gross perturbation of fission and fusion do not move (Amiri and Hollenbeck, 2008).

These observations suggest that appropriately balanced mitochondrial fission and fusion generates discrete mitochondria that are suitable for transport over long distances, providing one explanation for cross-talk between transport and fission–fusion processes. Conversely, perhaps transport supports fission–fusion dynamics in axons.

Research on mitochondrial fusion and fission gained much attention in recent years, as it is important for our understanding of many biological processes, including the maintenance of mitochondrial functions or apoptosis.

Mitochondrial fission and fusion processes are both mediated by large guanosine triphosphatases (GTPases) of the dynamin family that are well conserved between yeast, flies, and mammals (Hoppins et al., 2007). Their combined actions divide and fuse the two lipid bilayers that surround mitochondria. Although the proteins that are involved in mitochondrial fission and fusion are being discovered, the mechanism for the synchronized splitting and melding of the two membrane systems remains vague.

1.3.a - Regulation of Mitochondrial Fusion: Proteins Involved in Mitochondrial Fusion in Mammalian Cells

Mitochondrial fusion is mediated by the conserved dynamin-related GTP proteins Mitofusins (Mfn1 and Mfn2) and optic dominant atrophy 1 (OPA1) (Chen and Chan, 2010; Zhang et al.). In yeast, Mfns and Opa1 counterparts are termed Fzo1p and Mgm1p, respectively.

Fusion requires the apposition of two adjacent organelles, followed by the fusion of the mitochondrial membranes of adjacent tubules. Mfn1 and Mfn2 form homo- and heterocomplexes with each other, and seem to be in equilibrium between conformations that dinstribute them on the outer mitochondrial membrane evenly and those that concentrate into foci at sites of mitochondrial fission and fusion (Chen et al., 2003; Koshiba et al., 2004), (Fig.5).

The N-terminal GTPase domain of Mfn1 is required for fusion activity and is orientated towards the cytosol. It is anchored in the OMM by two hydrophobic domains (Fig.5). The C-terminal coiled-coil domain also faces the cytosol, where it coordinates the docking of mitochondria to one another through antiparallel binding to the C-terminal coiled-coil domains of Mfn1 or Mfn2 molecules on adjacent mitochondria (Liesa et al., 2008).

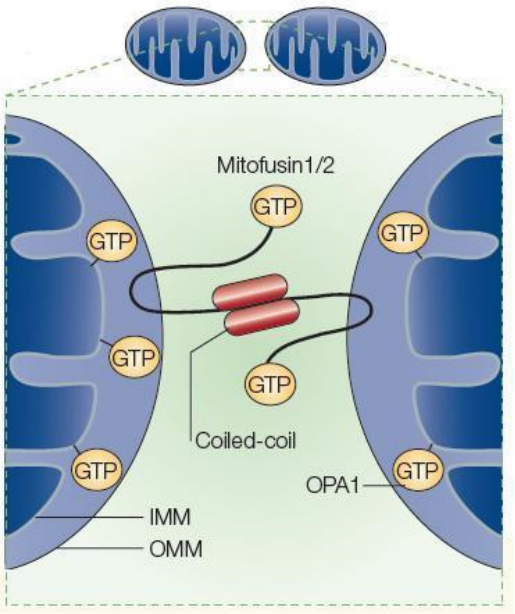

Figure 5: Schematic cross-sections through fusing mitochondria. The two mitochondria dock through interaction of juxtaposed mitofusins's coiled-coil domain protruding from outer mitochondrial membrane (OMM), whereupon OPA1, which is anchored partially on the inner mitochondrial membrane (IMM), participates in the membrane fusion process.
Adapted from Youle and Karbowski, 2005.

Mfn1 mediates tethering of mitochondria more efficiently than Mfn2, and requires GTP hydrolysis for this function (Ishihara et al., 2004). Loss of either Mfn1 or Mfn2 impairs mitochondrial fusion rates and consequently shortens mitochondrial length.

Mammalian OPA1 was originally discovered as the product of the gene that is mutated in the most common form of hereditary blindness, dominant optic atrophy, which results from retinal ganglion cell death (Alexander et al., 2000; Delettre et al., 2000).

OPA1 is located between the inner and outer mitochondrial membranes, closely associated with the inner membrane (Fig.5). It possesses a mitochondrial targeting sequence mediating the mitochondrial import, a transmembrane helix anchoring the protein to the mitochondrial inner membrane and two predicted coiled coils. It interacts with Mfns to form intermembrane protein complexes that couple the fusion of outer membranes to that of inner membranes (Cipolat et al., 2004; Olichon et al., 2003; Song et

al., 2003).

Loss of OPA1 expression causes mitochondrial fragmentation whereas ectopic OPA1 expression can induce mitochondrial fusion that requires Mfn1 but not Mfn2 (Cipolat et al., 2004). The analysis of OPA1 function is complicated by the differential expression of eight splice variants in different cell types (Cipolat et al., 2004; Olichon et al., 2003).

How OPA1, Mfn1 and Mfn2 function in membrane fusion and remodelling beyond the membrane attachment step remains unknown. In vitro reconstitution of mitochondrial fusion will undoubtedly lead to more molecular insights in the future. This study (which uses isolated mitochondria that contain different colored markers) has already revealed that both OMM and IMM fusion events require GTP hydrolysis and that IMM fusion requires a membrane potential gradient (Meeusen et al., 2004).

Due to the strong interconnection between mitochondrial dynamics, it is not surprising that mitochondrial transport along neuronal processes is particularly important for the fusion events. In Mfn1- or Mfn2- null mouse embryonic fibroblast (MEFs), mitochondria lose directional movement and appear to move randomly in the cytosol, suggesting that they are detached from microtubules (Chen et al., 2003). Deleting Mfn2 or expressing mutant form of Mfn2 in neurons resulted in longer pauses and slower anterograde and retrograde movements (Baloh et al., 2007; Misko et al.); motor neurons derived from transgenic mice with mutant Mfn2 showed a decreased number of mitochondria within their highly branched dendrites (Chen and Chan, 2010). Mfn2 was found to interact with the mouse Miro/Milton complex, regulating axonal mitochondrial transport (Misko et al.). Therefore, mitochondrial transport may directly affect mitochondrial morphology by regulating the fusion and fission machinery. Conversely, deficiency of mitochondrial fusion or fission impairs mitochondrial mobility and distribution, due possibly to an alterated mitochondrial respiration or a defective association in the mitochondrial transport complex.

1.3.b - Regulation of Mitochondrial Fission: Proteins Involved in Mitochondrial Fusion in Mammalian Cells

Mitochondrial fission is mediated by FIS1 and the evolutionarily conserved dynamin-related GTPase, Drp1 in mammals and Dnm1p in yeast (Kageyama et al., 2012).

FIS1 is anchored in the OMM by a single hydrophobic domain with two tandem tetratrico-peptide repeat motifs facing the cytosol, which mediate protein–protein interactions between FIS1 and other proteins (Suzuki et al., 2005), (Fig.6). FIS1 is located diffusely throughout the OMM and is thought to recruit DRP1 from the cytosol, where DRP1 predominantly localizes, to punctuate foci on the OMM. Therefore Drp1 assembles into spiral filaments around mitochondria tubules and these spirals have been proposed to constrict mitochondrial tubules trough conformational changes, driven by Drp1 and Dnm1p-mediated GTP hydrolysis (Ford et al.; Fukushima et al., 2001; Mears et al., 2011; Yoon and McNiven, 2001). Interestingly, it has been suggested that tubules of the endoplasmic reticulum (ER) wrap around and squeeze mitochondria at the early stage of division, prior to assembly of Drp1 filaments onto mitochondria (Friedman et al., 2011). ER tubules constrict mitochondria to a diameter comparable to Dnm1/Drp1 helices to facilitate their recruitment and assembly to complete fission. After the completion of mitochondrial fission, Drp1 spirals likely disassemble from mitochondria to allow several rounds of mitochondrial fission (Friedman et al., 2011).

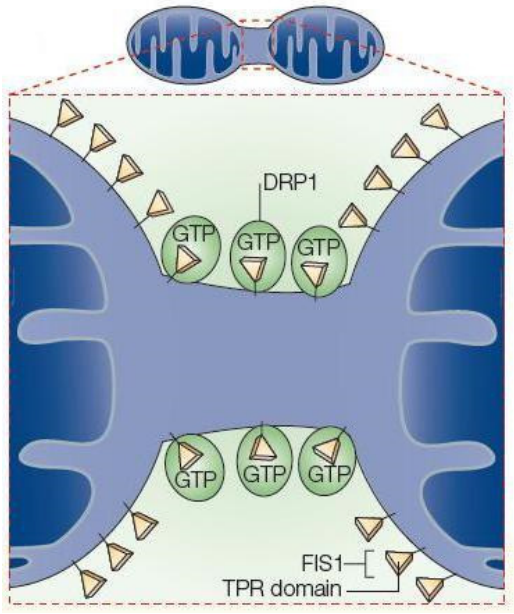

Figure 6: Schematic cross-sections through dividing mitochondria.
FIS1 circumscribing the outer mitochondrial membrane recruits the large GTPase DRP1 through its tetratrico-peptide repeats (TPR), which subsequently coalesces into foci at mitochondrial scission sites.
Adapted from Youle and Karbowski, 2005.

Due to the strong cross-talk between transport and fission-fusion processes, it is not surprising that mitochondrial fission defects result in alterations in the mitochondrial transport and distribution and vice versa: in cultured hippocampal neurons, defects in Drp1-mediated mitochondrial fission result in the accumulation of mitochondria in the cell body and in reduced dendritic mitochondrial content (Li et al., 2004); inhibition of the mitochondrial fission Drp1 (Labrousse et al., 1999) also greatly reduces the number of mitochondria in fly synaptic terminals (Verstreken et al., 2005). This suggests that it

may not be possible for the mitochondria present in fission-deficient neurons to be efficiently transported to distal neuronal processes.

Conversely, loss of Miro function causes mitochondrial fragmentation (Fransson et al., 2006; Macaskill et al., 2009b; Saotome et al., 2008) and overexpression of either Miro or Milton can enhance mitochondrial fusion (Fransson et al., 2006; Koutsopoulos et al., 2010; Saotome et al., 2008). Moreover, disruption of dynein function increases the formation of highly branched mitochondrial structures by controlling the recruitment of Drp1 (Varadi et al., 2004).

1.3.c - Mitochondrial Dynamics and Mitochondrial Function

Mitochondrial fusion and fission are required to maintain a functional mitochondrial population in the cell. Defects in mitophagy may lead to impairment of mitochondrial respiratory function in Drp1-null neurons, and in HeLa cells depleted for Drp1, likely due to oxidative damage on mitochondrial components (Kageyama et al., 2012; Parone et al., 2008). Impaired respiration can lead to further increases in the production of reactive oxygen species (ROS), and it is therefore difficult to pinpoint the primary target. In addition, respiratory defects due to mitochondrial fission deficiency are highly dependent on cell type, likely due to basal levels of ROS and contribution of other quality control mechanisms (Itoh et al., 2012).

Fibroblasts that lack both Mfn1 and Mfn2 have reduced respiratory capacity, and individual mitochondria show great heterogeneity in shape and membrane potential (Stowers et al., 2002).

How does fusion protect mitochondrial function? It is probable that a primary function of mitochondrial fusion is to enable the exchange of contents between mitochondria. An essential component of mitochondrial function is mitochondrial DNA (mtDNA), which is organized into

compact particles termed nucleoids. The mtDNA genome encodes essential subunits of the respiratory complexes I, III and IV, and is therefore essential for oxidative phosphorylation. When mitochondrial fusion is abolished, a large fraction of the mitochondrial population loses mtDNA nucleoids, and therefore may fail to assemble electron transport chain complexes because several subunits of the electron transport chain complex are encoded in mtDNA (Legros et al., 2004).

Moreover, pancreatic β cells that lack Opa1 show similar defects, with an even greater

reduction in respiratory capacity, but contain normal amounts of mtDNA, suggesting that the role of mitochondrial fusion in the maintenance of mtDNA may also depend on cell type (Zhang et al., 2011).

In addition to mtDNA, it is also possible that other components, such as substrates, metabolites or specific lipids, can be restored in defective mitochondria by fusion. Further studies will determine whether content exchange is the primary function of mitochondrial fusion. The importance of mitochondrial fusion in development and disease might be a consequence of this function (Detmer and Chan, 2007a).

1.3.d - Mitochondrial Dynamics and Cell Proliferation

Several data are emerging about morphological changes of mitochondria during the cell cycle (Lee et al., 2007; Mitra et al., 2009), identifying rapid changes in mitochondrial morphology at different stages of the cell cycle. In M phase, fragmented mitochondria localize to opposite telomeres of daughter mitochondria; in G0 both filamentous and fragmented mitochondria occur, whereas in G1–S phases mitochondria form a giant tubular network with tubular elements undergoing fission and fusion (Mitra et al., 2009); (Fig.7).

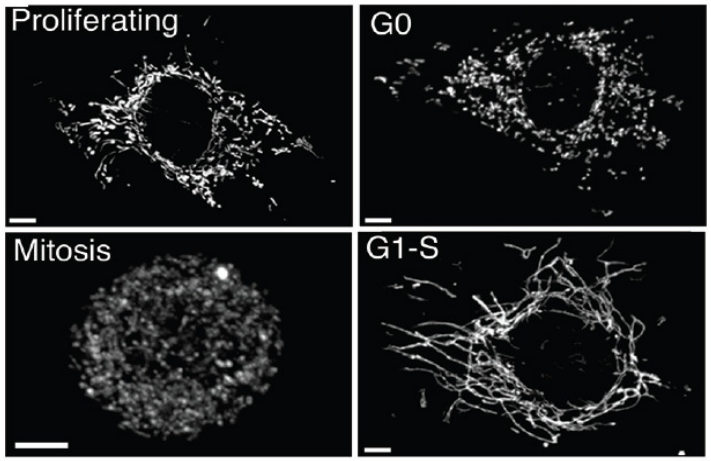

Figure 7: Formation of a giant mitochondrial network during G1-to-S transition. 3D projection images of rat kidney cells stably expressing red fluorescent protein targeted to the mitochondrial matrix, showing mitochondrial distribution in proliferating cells or cells arrested at different cell cycle stages. Scale bars: 5 μm. Adapted from Kasturi Mitra et al., 2009.

The giant voluminous mitochondrial network at G1-S could serve several cellular functions such as efficient distribution of mitochondrial DNA in the continuous matrix (in order to guarantee the appropriate segregation of the organelles and mtDNA into daughter cells during proliferation), enhancement of mitochondrial ATP to compensate for reduced glycolytic ATP during G1-S, and cell protection against apoptosis at this crucial cell cycle stage (Arciuch et al., 2009).

Several lines of evidence support the view that Mfn2 exerts a regulatory role on the cell cycle (Chen et al., 2004). Mfn2 overexpression in vascular smooth muscle cells (VSMCs) causes growth arrest characterized by an increased number of cells in G0/G1 stage and a reduction of cells in S or G2/M phases (Chen et al., 2004). The mechanism proposed by which Mfn2 causes cell cycle arrest involves binding and sequestration of Ras, thereby inhibiting the downstream Raf-MEK1/2- ERK1/2 signaling pathway (Liesa et al., 2009). However, it is still unknown whether the effects of Mfn2 are universal in different cell types.

Another protein involved in mitochondrial regulation of cell cycle is Cyclin E, the Cyclin responsible for G1–S phase progression. Mitra et al., (Mitra et al., 2009) demonstrated that inducing mitochondrial hyperfusion by acute inhibition of Drp1 leads to buildup of Cyclin E and initiation of replication in serum starved cells at G0. Regulation of Cyclin E levels by hyperfused mitochondria at G1-S could explain why knockouts of Mfns phenocopy the effects of Cyclin E knockouts.

1.3.e - Mitochondrial Dynamics and Apoptosis

Cell die trough different mechanisms, such as apoptosis and necrosis, which are interconnected but distinct in terms of cellular morphology and caspase requirements. Mitochondrial dynamics are involved in both cell death processes, given that mitochondria undergo common morphological changes during early stages of apoptosis and necrosis: the filamentous mitochondrial reticulum becomes fragmented, consistent with an excess of fission events. The role of mitochondrial fragmentation in necrosis remains to be determined, but it is likely different from that in apoptosis. During apoptosis, mitochondria play an active role initiating cell death by releasing the proapoptotic factor cytochrome *c*. In contrast, during necrosis, mitochondrial fragmentation may serve as a means to decrease mitochondrial energy production to elicit efficient cell death.

In apoptotic cells excessive fission of mitochondria occurs almost simultaneously with outer membrane permeabilization and cytochrome c release. The pro-apoptotic Bcl-2 family member Bax regulates mitochondrial outer membrane permeabilization during apoptosis. Following extensive cellular stress or damage, Bax translocates to mitochondria and accumulates in concentrated foci that colocalize with Drp1 and mitofusins (Sheridan and Martin, 2010). This process mediates pore formation in mitochondrial outer membranes, which facilitates the release of cytochrome *c* and others

pro-apoptotic factors from mitochondria, and subsequent downstream caspase activation (Sheridan and Martin, 2010).

Inhibition of mitochondrial fission by Drp1 knock-down delays cytochrome c release, indicating that mitochondrial fission participates in Bax-mediated permeabilization of the outer mitochondrial membrane (Suen et al., 2008). The link may be that Bax is activated to oligomerize and release cytochrome c by membrane hemifusion intermediates that are formed during mitochondrial fission (Montessuit et al., 2010). Intriguingly, Bcl-2 family members also participate in mitochondrial fission and fusion in non-apoptotic cells: BAX and BAK double-knockout cells have fragmented mitochondria due to reduced mitochondrial fusion, although the extent of this effect depends on the experimental system (Brooks et al., 2007; Karbowski and Youle, 2004). Little is known about how BAX and BAK mediate their effects on mitochondrial morphology, but BAX influences Mfn2 distribution on the mitochondrial outer membrane and BAK associates with Mfn1 and Mfn2 (Brooks et al., 2007).

In conjunction with mitochondrial outer membrane permeabilization, remodelling of the cristae membranes is required for the rapid and efficient release of cytochrome c, which is mainly localized to cristae compartments (Goldstein et al., 2000; Scorrano et al., 2002). OPA1 appears to regulate the diameter of cristae junctions and therefore regulates cytochrome c release (Scorrano et al., 2002). Overexpression of OPA1 blocks cytochrome c release following the induction of apoptosis by maintaining narrow cristae junctions (Cipolat et al., 2006; Frezza et al., 2006). Drp1 has also been proposed to play a part in cristae remodelling during apoptosis (Germain et al., 2005; Minauro-Sanmiguel et al., 2005).

1.4 - Mitochondrial dynamics and Neurodegeneration

Neurodegenerative diseases are a heterogeneous group of disorders characterized by gradually progressive, selective death of neuronal subtypes. Prototypical examples include Alzheimer disease, Parkinson disease, and Huntington disease, resulting in motor impairment, memory loss, cognitive deficits, emotional alterations and behavioral problems.

The major risk factors include old age, environmental factors (toxins) and genetic mutations in a variety of genes. Due to the phenotypic diversity of neurogenerative

disorders, the study of disease-linked mutations provide key clues about the molecular mechanisms involved in the pathology and have therefore been studied intensively over the last decades. For instance, the study of mutations causing familiar Parkinson disease (PD) shed light on several cellular and molecular mechanisms that contribute to the neurodegenerative processes, such as mitochondrial dysfunction.

The role of impaired mitochondrial function is recognized as an important factor contributing to the pathogenesis of neurodegenerative disorders, involving not only defects in mitochondrial bioenergetics, but also mitochondrial transport, quality control, fusion, fission and turnover.

1.4.a - Alzheimer disease

Alzheimer disease (AD) is the leading cause of dementia, affecting more than 24 million people worldwide. AD patients demonstrate progressive memory loss and decline in cognitive functions as well as behavioral and psychological symptoms, including confusion, irritability and aggression, depression and anxiety. AD is characterized by progressive brain atrophy, particularly in the hippocampus and cortex. Two major pathological features have been observed in postmortem brains from AD patients: neurofibrillary tangles and extracellular amyloid plaques composed chiefly of beta-amyloid generated through the proteolytic cleavage of amyloid precursor protein (APP).

Mitochondrial dysfunction is a prominent feature of Alzheimer's disease (AD) neurons, in particular concerning to alteration in mitochondrial localization, transport and fission.

In autoptic samples from patients with sporadic AD axonal swelling containing several organelles and especially mitochondria were found in the nucleus basalis of Meynert, probably originating from defects in axonal trafficking; in fact the formation of these vesicles was mediated by the expression of Kinesin-1 (Stokin et al., 2005). An altered balance in mitochondrial fission and fusion is likely an important mechanism leading to mitochondrial and neuronal dysfunction in AD brain.

In AD brain protein levels of OPA1, Mfn1, and Mfn2 were significantly reduced whereas levels of Fis1 were significantly increased (Wang et al., 2009a). AD mitochondria displayed elongated shapes which form collapsed perinuclear aggregates (Wang et al., 2008). Moreover, β-amyloid protein can localize to mitochondria causing a cytotoxic effect generated by the production of nitric oxide that leads to activation of Drp1 activity. In fact, enhanced levels of S-nitrosylated Drp1 lead to an enhanced Drp1 dimerization,

triggering mitochondrial fission, synaptic loss, and neuronal damage (Barsoum et al., 2006; Cho et al., 2009; Nakamura et al., 2010).

Among the mitochondrial metabolic defects in the AD brain we can find general changes in glucose consumption, increased oxidative stress, and Ca^{2+} deregulation, causing increased oxidative damage, leading to cellular energy supply failure and impairing the neuronal survival (Santos et al., 2010).

1.4.b - Parkinson disease

Parkinson disease (PD) is the second most common neurodegenerative disease in humans, resulting from the loss of dopaminergic cells in the substantia nigra. The four primary symptoms of PD are tremor, rigidity, bradykinesia and postural instability or impaired balance and coordination. ~ 90% of PD cases are sporadic, but ~ 10% are familial and genetic analysis hve identified a number of PD-associated genes, among them several genes associated with mitochondrial function. Recent studies in flies and vertebrate suggest that the integrity of two genes involved in familial forms of PD, Parkin and PINK1, is essential for mitochondrial morphology and integrity.

Parkin is a cytosolic E3 ubiquitin ligase ubiquitously expressed; Pink1 is a mitochondrial serine/threonine-protein kinase. They are both involved in the control of mitochondrial turnover by autophagy (mitophagy): Parkin translocates from the cytosol to the mitochondria in response to a fall in mitochondrial membrane potential (Narendra, 2008), through a process that requires PINK1 activity (Lee et al., 2010; Narendra et al., 2010).

Moreover it is known that PINK1 interacts with Miro-Milton complex (Weihofen et al., 2009), can phosphorylate Miro and activate its proteasomal degradation in a parkin-dependent manner (Wang et al., 2011). Consistent with this data, it was shown that altered activities of PINK1 cause aberrant mitochondrial transport (Liu et al., 2012). The implication of PINK1/Parkin pathway in the regulation of mitochondrial transport machinery results noteworthy considering that dysfunctions of this process could contribute to the loss of dopaminergics neurons, the cardinal feature of PD, as well as the peripheral neuropathy symptom associated with particular *PINK1* or *Parkin* mutations.

Genetic studies in flies suggest that Pink1 and Parkin act to promote mitochondrial fission and/or inhibit fusion (Deng et al., 2008; Yang et al., 2008) by downregulating Mfn proteins and OPA1 (Deng et al., 2008; Yang et al., 2008; Yu et al., 2011). It has been demonstrated that Parkin ubiquitylates Mfn proteins promoting mitochondrial

fragmentation and probably mitophagy (Chan et al., 2011; Gegg and Schapira, 2010; Tanaka et al., 2010).

LRRK2 is another related gene of PD-familial observed to be associated with mitochondria, and capable of modulating normal mitochondrial integrity and functions under certain conditions.

LRRK2 is a multidomain protein containing a kinase and a GTPase domain (Biosa et al., 2013), mainly present in the cytoplasm, with partial localization to mitochondria. It is associated with membranes, such as mitochondria, endoplasmic reticulum, and synaptic vesicles (Houten and Auwerx, 2004). Autosomal dominant mutations in LRRK2 are associated with both familial and late-onset PD and the G2019S is the most common mutations of LRRK2 (Okamoto et al., 2009). It has been reported that Parkinson's disease patients with the G2019S mutation in LRRK2, exhibited reduced mitochondrial membrane potential and total intracellular ATP levels accompanied by increased mitochondrial elongation and interconnectivity (Mortiboys et al., 2010). Interestingly, it has been demonstrated that Parkin protects against LRRK2-induced neurotoxicity in vivo (Ng et al., 2009).

From the above discussion, it is clear that mitochondrial dysfunction is a key event underlying PD pathogenesis and PD-associated genes related to mitochondrial homeostasis have a profound influence on mitochondrial function.

1.4.c - Charcot-Marie-Tooth type 2A (CMT2A)

Charcot-Marie-Tooth disease (CMT) is an inherited neurological disorders and its classification in several main types was performed on the basis of electrophysiological properties and histopathology. The axonal form of this disorder is referred to as Charcot-Marie-Tooth type 2A disease (CMT2A), an autosomal dominant peripheral in which the axons of the longest sensory and motor nerves are selectively affected. Mutations in Mfn2 are the most commonly identified cause of this pathology and they include both mutations producing Mfn2 proteins with an improved ability to promote the mitochondrial fusion and mutations producing Mfn2 proteins able to induce mitochondrial fusion (Detmer and Chan, 2007b). It is not surprising considering that Mfn2 has a role also in mitochondrial trafficking, and the destruction of this function could lead to peripheral axonal degeneration (Baloh et al., 2007).

1.4.d - Aurosomal Dominant Optic Atrophy (ADOA)

Mutations in OPA1 cause the most common form of optic atrophy, autosomal dominant optic atrophy (ADOA), characterized by progressive blindness and degeneration of retinal ganglion cells and the optic nerve. Down-regulation of OPA1 in HeLa cells leads to fragmentation of the mitochondrial network, dissipation of the mitochondrial membrane potential and a drastic disorganization of the cristae. These events are followed by cytochrome c release and caspase-dependent apoptotic nuclear events (Olichon et al., 2003).

A new set of mutation in OPA1 results in "ADOA-plus" phenotypes characterized by mtDNA instability, deafness, and movement disorders in addition to traditional ADOA symptoms (Amati-Bonneau et al., 2008; Delettre et al., 2000; Hudson et al., 2008).

2.- Armcx/Armc10 gene family

2.1 - Armcx/Armc10 family: genetic evolution and gene expression

Armcx genes belong to a recently described family localized on the X chromosome and characterized by the possession of *Arm* domains in their sequences.

Three members of the this protein family were initially described as putative tumor-suppressor genes, as their expression is reduced in several epithelial-derived carcinomas, including lung, prostate, colon and pancreas cancers (Kurochkin et al., 2001). Due to these features the proteins were called Alex1-3 (Arm-containing protein Lost in Epithelial cancers linked to the X chromosome). In 2005 Winter and Ponting described in the Xq22.1-q22.2 region (2.3MB), identifying three previously unrelated protein-coding gene families, BEX (Brain expressed X-linked), WEX (Wwbp5-like X-linked), and GASP (G-protein-coupled receptor-associated sorting protein), which have been the product of multiple gene duplication and large protein coding sequence diversification specific to eutherian (placental) mammals. They showed that these paralogous genes originated from a common ancestor gene that underwent multiple events of gene conversion acting on both 5'UTR sequences and coding sequences; in particular, their 5'UTRs are highly similar and exhibit a recent ancestry, whereas the protein coding sequences are more distantly related, representing the main divergent point for the gene sequences.

The GASP family includes 10 genes which official names are: Gprasp1 and Gprasp2, Bhlhb9, Armcx 1-6 and Armc10 (Table 2).

Close to these genes we also found the Armcx6-like pseudogene, located up-stream Armcx6 sequence and the Armc10-like pseudo gene, located on 3th chromosome in human (Table 1). The Armc10-like genetic structure consist in one unique codifying exon which sequence is identical to Armc10 one, except for two small regions (34 and 25 amminoacids), corrsponding to Armc10 exon 2 and 6 (Abu-Helo and Simonin, 2010; Simonin et al., 2004).

Oficial Name	*Synonymus*	*Chromosome Reagion (Homo sapiens)*	*Gene ID*
Armc10	Gasp8, SVH	7(q22.1)	83787
Armc10-like	Gasp8 isoform 5	3	100510677
Armcx1	Gasp7, Alex1	X(q22.1-q22.2)	51309
Armcx2	Gasp9, Alex2	X(q22.1-q22.2)	9823
Armcx3	Gasp6, Alex3	X(q22.1-q22.2)	51566
Armcx4	Gasp4	X(q22.1-q22.2)	100131755
Armcx5	Gasp5	X(q22.1-q22.2)	64860
Armcx6	Gasp10	X(q22.1-q22.2)	54470
Armcx6-like	Gasp10Ψ	X(q22.1-q22.2)	653354
Gprasp1	Gasp1, Per1	X(q22.1-q22.2)	9737
Gprasp2	Gasp2	X(q22.1-q22.2)	114928
Bhlhb9	Gasp3, p60TRP	X(q22.1-q22.2)	80823

Table 2: GASP gene family: official name, synonymous, location on chromosome region and gene ID. Adapted from (Abu-Helo and Simonin, 2010).

All these genes are localized in the X chromosome (human Xq22.1-Xq22.2 and mouse X56/57cM), with the sole exception of the Armc10/SVH gene, which mapped to the 7th human and the 5th mouse chromosome.

All Armcx-coding sequences are contained in a single exon, whereas the Armc10 is a typical, multi-exon-containing gene, with the coding sequence split in at least eight exons (Abu-Helo and Simonin, 2010; Simonin et al., 2004). Four Armc10 splicing variants have been described: Svh A, -B, -C, -D (Huang et al., 2003).

The Armcx cluster, formed by Armcx1-6 and Armcx6-like pseudogene, originated in early Eutherian evolution by retrotransposition of an Armc10 mRNA, and then by consecutive tandem duplication events in a rapidly evolving region of the Xq chromosome, which also includes the Armcx-related G-protein coupled receptor Gasp1-3 genes (Lopez-Domenech et al., 2012).

The Armcx genes are almost ubiquitously expressed (Kurochkin et al., 2001; Simonin et al., 2004). Some studies point out their expression in the urogenital system: Armcx2 is

highly expressed during testis development, whereas is little expressed during ovarian development (Smith et al., 2005); Armcx3 expression is enriched in the initial segment of epididymis (Hsia and Cornwall, 2004).

Neverthless, the greates expression of these genes, such as for the BEX and WEX ones, was found in brain, suggesting that these eutherian specific genes are possible candidates for the adaptive evolution of neocortex, a region of the forebrain which has evolved considerably in mammals (Simonin et al., 2004).

The precise time-point for the genesis of the Armcx cluster, when key innovations of the mammalian group took place, namely the origin of a well-developed placenta, or the increase in complexity of the CNS and the enlargement of the neocortex, suggest that this cluster has functions related to the above processes. Hence, the origin of the Armcx cluster may well have been linked to the enlargement of the neocortex, since marsupials are devoid of the Armcx cluster but have a primitive placenta.

2.2 - Armcx/Armc10 proteins: sub-cellular localization

Armcx/Armc10 proteins belong to a new family whose composition and function has been emerging in the last years. They all have a highly conserved C-terminal domain (DUF463) consisting of up to 6 armadillo or armadillo-like tandem repeats (Fig.8). In contrast the N-terminal region is unrelated among members and is highly variable in length and sequence, although various members share several common features, such as an N-terminal signal peptide with a potential transmembrane domain, a putative mitochondrial targeting sequence and a nuclear localization signal (Fig.8).

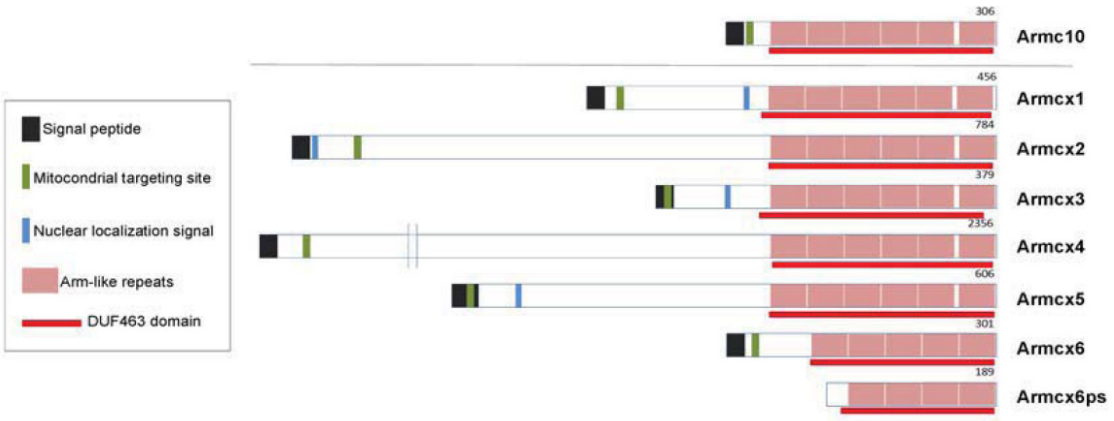

Figure 8: Schematic representation of the Armc10/Armcx proteins. They all have a highly conserved C-terminal domain (DUF463). The N-terminal region includes an N-terminal signal

peptide with a potential transmembrane domain, nuclear localization signals and putative mitochondrial targeting.
Adapted from López-Doménech et al., 2012.

Another important feature that can give clues to shine a light on the Armcx/Armc10 proteins function is their subcellular localization. Data coming from several and independent works carried out during the last ten years contribute to add useful informations about this topic. The subcellular distribution of several Armcx has been studied either in transfected cells or in cells or organs endogenously expressing them (Abu-Helo and Simonin, 2010).

Gasp1 was found to be mostly located in the cytoplasm (Bartlett et al., 2005; Kiyama et al., 2006; Martini et al., 2007; Matsuki et al., 2001; Tappe-Theodor et al., 2007; Whistler et al., 2002). When co-expressed in COS-7 cells (that do not express endogenous Gasp1) with Period-1, Gasp1 was translocated to the nucleus (Matsuki et al., 2001). In PC12 cells (that do not express endogenous Gasp1), a minor fraction of Gasp1 was found in cell nuclei and this fraction increased upon nerve growth factor (NGF) treatment (Kiyama et al., 2006).

Expression of endogenous Gasp2 has been studied in neuroblastoma cells SH-SY5Y cells, where it has been found localized in the cytoplasm and cell membranes of undifferentiated cells, and in newly formed neurite-like extensions of retinoic acid-induced differentiated cells (Horn et al., 2006); moreover it has been identified as a nuclear phosphoprotein from Hela cells, indicating that it can also be localized into the cell nucleus (Beausoleil et al., 2004).

Gasp3 overexpressed in PC12 cells was mainly expressed into cytoplasm, although it could also be detected into nucleus of some cells (Heese et al., 2004).

Alex3 was found exposed on the outer-surface of mitochondria, co-localizing with the mitochondrial marker protein Cox IV in OBL1 cells (Mou et al., 2009). All splicing variants of Armc10, when overexpressed in QSG-7701 cells (that endogenously express Armc10), were localized in the cytoplasm (associating with the endoplasmic reticulum) and nuclear envelope (Huang et al., 2003).

Epitope-tagged Armcx2 transfected in testicular Leydig cells (displaying endogenous expression of this protein), was detected in discrete membrane structures within the cytoplasm, but not specifically localizing with either endoplasmic reticulum or perinuclear Golgi apparatus (Smith et al., 2005).

A great contribution in the field of subcellular localization of Armcx/Armc10 proteins comes from our study (Lopez-Domenech et al., 2012) in which HEK293AD cells were transfected with cDNAs encoding full-length Armcx1, 2, 3, and 6 protein, showing a strong colocalization with the mitochondrial marker MitoTracker (Fig.9) and demonstrating that the Armc10/Armcx cluster encodes for a family of proteins targeted to mitochondria.

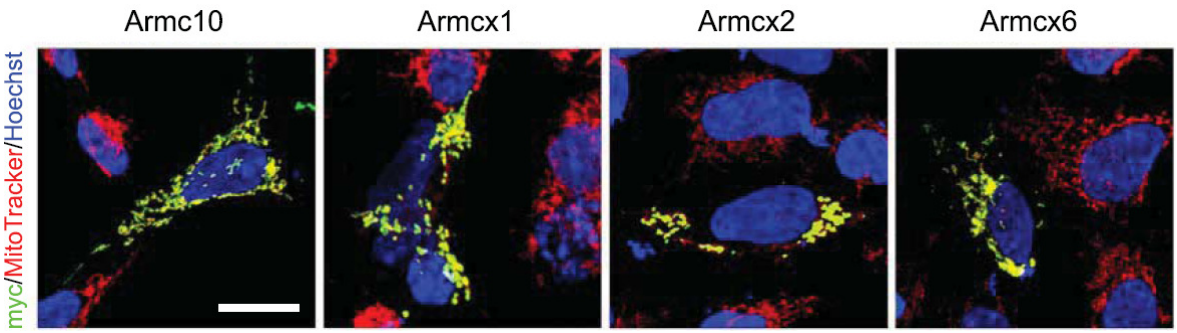

Figure 9: **Subcellular localization of Armcx proteins.** Mitochondrial targeting of Armc10, Armcx1, Armcx2 and Armcx6 proteins after transfection of Myc-tagged cDNAs in HEK293AD cells. Mitochondria were stained with the mitochondrial marker MitoTracker (red) and nuclei were stained with Hoechst (blue). Scale bars: 10 µm. Adapted from López-Doménech et al., 2012.

2.3 - Armcx/Armc10: proteins function

Little is known about Armcx/Armc10 proteins function, even if several studies point to their implications in at least two different cellular activities.

2.3.a - Modulation of the activity of G -protein coupled receptors (GPCRs)

GPCRs constitute a large protein family of receptors that sense molecules outside the cell and activate inside signal transduction pathways and, ultimately, cellular responses. The ligands that bind and activate these receptors include light-sensitive compounds, pheromones, hormones, and neurotransmitters, and vary in size from small molecules to peptides to large proteins. When a ligand binds to the GPCR it causes a conformational change in the GPCR, which allows it to act as a guanine nucleotide exchange factor (GEF). The GPCR can then activate an associated G-protein by exchanging its bound GDP for a GTP (Abu-Helo and Simonin, 2010).

Gprasp1 is the most described gene that has been related to the G-protein coupled receptors (GPCR). Near 30 GPCR has been described to interact with Gprasp1 protein

being implicated in the postendocytic sorting and degradation by lysosomes of these receptors, including the D2 dopamine receptor (Bartlett et al., 2005), delta opioid receptor (Whistler et al., 2002), D3 dopamine receptor (Thompson and Whistler, 2007), cannabinoid 1 receptor (Bartlett et al., 2005); (Tappe-Theodor et al., 2007) and GPR55 (Ritter and Hall, 2009).

Very recently GASP-1 knockout mice have been generated (Boeuf et al., 2009). GASP-1 KO animals are healthy and had no gross abnormalities. Moreover, targeted deletion of Gprasp1 did not alter the overall brain architecture or the general behavior of mice in home cage conditions.

GASP-1 KO and wild-type (WT) mice were tested for sensitization to the locomotor effects of cocaine. Following sustained cocaine administration, acute and sensitized cocaine-locomotor effects were analyzed, resulting attenuated in KO mice. Moreover, a decrease in the percentage of animals that acquired cocaine self-administration was observed in GASP-1-deficient mice, which was associated with pronounced down-regulation of dopamine and muscarinic receptors in the striatum (Kargl et al., 2011). These data indicate that GASP-1 participates in acute and chronic behavioural responses induced by cocaine and are in agreement with a role of GASP-1 in postendocytic sorting of GPCRs. However, in contrast to the previous studies, these data suggest that upon sustained receptor stimulation GASP-1 stimulates recycling rather than receptor degradation.

Gasp2 also has been related to GPCRs, since it is able to interact with D2 dopamine receptor, β-1 and β-2 adrenergic receptors and calcitonin receptor (Simonin et al., 2004); (Thompson and Whistler, 2007). All together these date indicate that this function could be present on other Armcx/Armc10 proteins.

2.3.b - Transcriptional Regulation

There are several lines of evidence suggesting that different members of the GASP family could be implicated in the modulation of transcription. The first one came from the shared nuclear localization signal (Mathis et al., 2010) and their putative subcellular localization into nuclear compartment, at least for some members or under particular physiological conditions.

Matsuki et al. (2001) demonstrated that GASP-1 can interact with Period-1 and that co-expression of both proteins in the same cells promotes the targeting of GASP-1 to the

nucleus. In a second study, the same group showed that NGF treatment of PC12 cells caused a nuclear translocation of Gasp1 (Kiyama et al., 2006). Moreover, NGF rescue of PC12 cells from apoptotic cell death was diminished in cells transfected with GASP-1 siRNA. Again, although there was no direct demonstration, these data suggest that, upon NGF-mediated nuclear translocation, GASP-1 can modulate transcription thus protecting cells from apoptosis (Kiyama et al., 2006).

Gasp3 has been officially named bHLH-B9 due to the presence in its sequence of a putative basic helix-loop-helix motif characteristic of the family of bHLH transcription factors. When transfected in CHO cells, Gasp3 was detected mainly in the cytoplasm, but also in the nucleus of some cells (Heese et al., 2004). On the other hand, Gasp3 knock-down PC12 cells were slightly more sensitive to apoptosis induced by serum withdrawal. Moreover, Suwanwela et al. identified Gasp3 as a novel gene involved into chondrocyte development (Suwanwela et al., 2010).

As for Gasp1, these data suggest a possible involvement of Gasp3 in transcriptional modulation but there is still no direct demonstration of any transcriptional activity or direct interaction with DNA or other bHLH transcription factors.

Experimental data suggesting an implication of Armcx3 in the modulation of transcription are much stronger. As indicated above, Armcx3 has been shown to be localized in the outer membrane of mitochondria where it can interact with the transcription factor, Sox10 (Mou et al., 2009). Moreover, overexpression of Armcx3 was shown to increase the amount of Sox10 in the mitochondrial fraction, and transactivation of the gene promoters for the Acetylcholine receptor α3 and β4 subunits was enhanced by Armcx3. Mou and collaborators proposed that the interaction between Armcx3 and Sox10 within the cytoplasm could lead to post-translational modifications of Sox10 that may result in an increased transcriptional activity once transported into the nucleus (Mou et al., 2009). This study is particularly interesting since Sox10 has been implicated in several processes of central nervous system development, including differentiation (Herbarth et al., 1998), and specification of neural crest-derived sensory neurons (Carney et al., 2006; Elworthy et al., 2003; Elworthy et al., 2005).

The isoform B of Armc10 has been shown to accelerate cell growth when overexpressed in a normal liver cell line (QSG-7701), and inhibition of this isoform in hepatoma cells induces cell apoptosis (Huang et al., 2003; Zhou et al., 2007). Furthermore, this induction of apoptosis was shown to be dependent on p53, and a direct interaction between both

proteins was demonstrated. Finally, Zhou et al. showed that this isoform inhibits the transcriptional activity of p53 in cell lines, although the molecular mechanism modulating this regulation needs to be clarified (Zhou et al., 2007).

In conclusion, several data suggest that Gasp1 and Gasp3 could be involved in the modulation of transcription via their targeting to the cell nucleus, while Armcx3 and Armc10 have been convincingly shown to modulate transcription through their interaction with transcription factors.

2.3.c - Alex3 function in mitochondria: preliminary data

To gain insight into the functional role of Alex proteins, several experiments were performed previously by our group. We confirmed Alex3 mitochondrial localization by immunofluorescence analysis and immunogold electron microscopy performed in transfected HEK293AD cells (Fig.10a-b).

To study the role of endogenous Alex3 protein in neurons, we examined its subcellular distribution in cultured hippocampal neurons (Fig.10c-e). Again, these cells exhibited strong cytosolic Alex3 signals, which colocalized with the mitochondrial network in cell bodies, axons and dendrites. In addition, Alex3 signals were distributed throughout the cytosol. These signals showed strong colocalization with the actin cytoskeleton, particularly in neurites and growth cones. Finally, many neurons exhibited Alex3-immunostaining in nuclei. We thus conclude that endogenous Alex3 protein is localized in at least three neuronal pools and compartments: mitochondria, nucleus and cytosol.

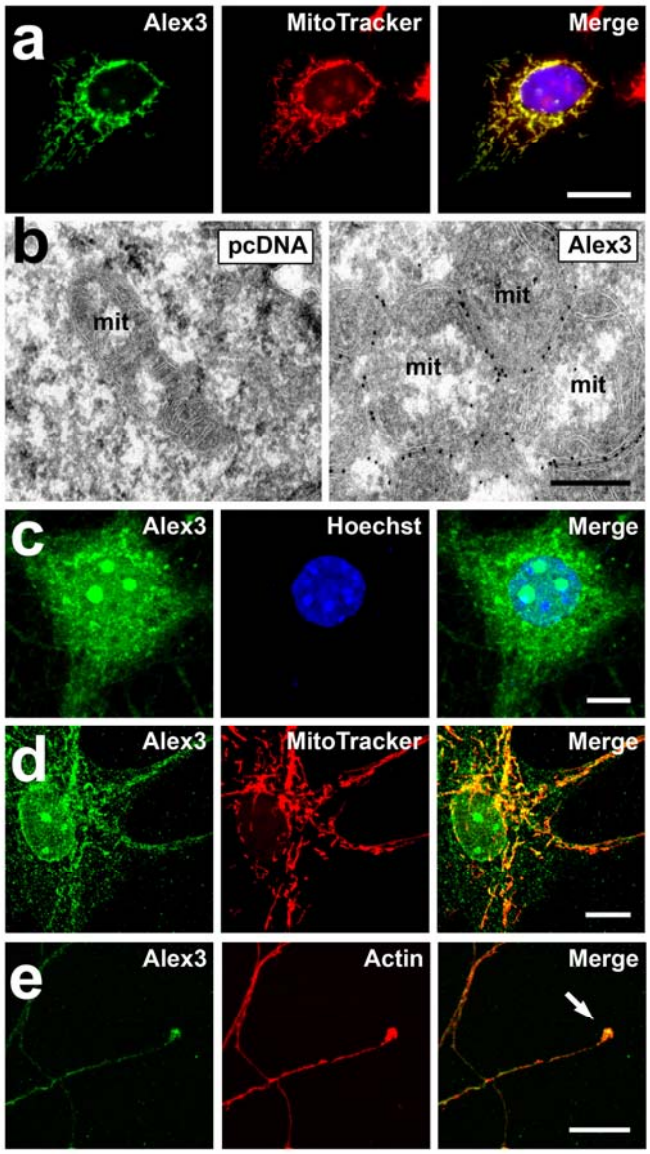

Figure 10: Alex3 subcellular localization in HEK293AD and hippocampal neurons at 15 DIV. (a) Confocal images showing that Alex3 (green) colocalizes with mitochondria in HEK293AD cells; cells were stained with MitoTracker. (b) Electron microscopy images of HEK293AD cells transfected with an empty vector or with an Alex3 expression vector, illustrating Alex3 localization (gold particles) around mitochondria (mit). (c-e) Immunolocalization of Alex3 protein in cultured hippocampal neurons at 15 DIV. Endogenous Alex3 shows a heterogeneous distribution. Alex3 (green) localizes in nuclei, as shown by colabelling with the nuclear marker Hoechst (blue) (c); in cytoplasm, which shows a punctate pattern that corresponds to the mitochondrial compartment stained with MitoTracker (red) (d); and in the cytosol, colocalizing with Actin staining (red), particularly in growth cones (arrow) (e). Scale bars: 15 µm (a), 0.02 µm (b) and 5 µm (c-e). DIV = days *in vitro*.
Adapted from López-Doménech et al., 2012.

Moreover, we identify the protein regions required for mitochondrial targeting, showing that the N-terminal sequence of Alex3 is necessary and sufficient to target the Alex3 protein to the mitochondrial network (Lopez-Domenech et al., 2012). In fact, deletion of the first 12 aminoacids at N-terminal of the protein (GFP-Alex3Δ1-12 fusion protein) abolishes mitochondrial targeting and, interestingly, led to nuclear localization of the mutant form (Fig.11).

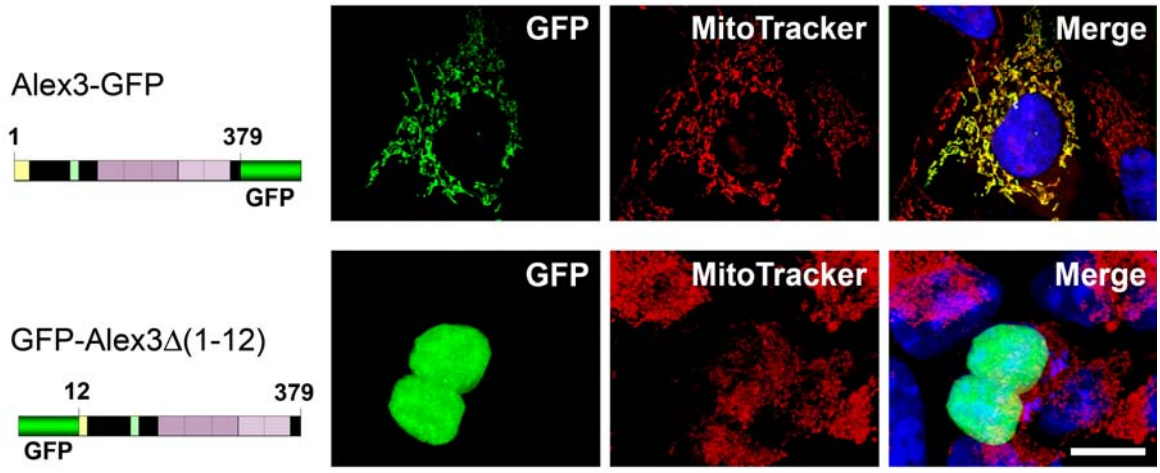

Figure 11: Alex3 N-terminal tail is necessary to target Alex3 to mitochondria. HEK293AD cells were transfected with full-length Alex3-GFP or C-terminal deletion mutant Alex3Δ(1-12). Alex3Δ(1-12) abolishes mitochondrial localization and leads to nuclear localization. (Nuclei were stained with Hoechst). Scale bar: 10μm. Adapted from López-Doménech et al., 2012.

To study whether Alex3 proteins regulate the bioenergetic mitochondrial state or Ca^{2+} handling, we performed several experiments, concluding that Alex3 protein is not involved in mitochondrial respiration, DNA copy number determination, mitochondrial membrane potential regulation, or Ca^{2+} homeostasis and handling in mitochondria (Lopez-Domenech et al., 2012).

During the above experiments, we noted that cells transfected with Alex3 (as well as Alex1, 2, 6 and Armc10) exhibited altered mitochondrial networks. In particular, HEK293AD cells transfected with Alex3 presented abnormal, aggregated-like mitochondrial networks: 33% showed strongly aggregated phenotypes, in which virtually all the mitochondria were concentrated in large, single aggregates near the nucleus; the 55% showed variable and intermediate degrees of clustered and aggregated mitochondria, in which these organelles were often aggregated in several clusters; the remaining 12% showed a normal phenotype (Fig.12a,c).

In similar way, hippocampal cultures transfected with Alex3 also presented alterated mitochondrial network: 23% of neurons displayed mitochondria completely aggregated in peri-nuclear clusters; 62% of neurons displayed intermediate phenotypes with mildly aggregating mitochondria; the remaining 15% showed a normal phenotype (Fig.12a,b). Electron microscopy analysis of Alex3-transfected hippocampal neurons confirmed that Alex3 leads to the aggregation of mitochondria in both the cell bodies and neuritis (Lopez-Domenech et al., 2012). Taken together, the above data suggest that the

Armc10/Armcx gene cluster (and particularly Armcx3) encodes for proteins involved in mitochondrial aggregation and dynamics.

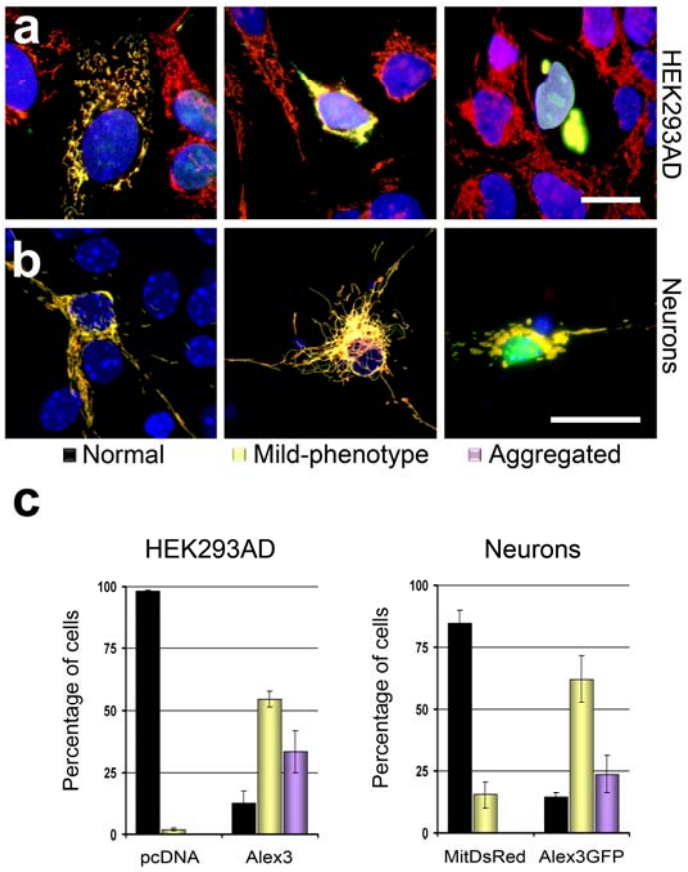

Figure 12: Alex3 overexpression severely alters mitochondrial morphology and distribution, leading to a perinuclear clustering and aggregation. Overexpression of Alex3 in HEK293AD (**a**) or Alex3-GFP in 12 DIV hippocampal neurons (**b**) induce severe alterations in the morphology and distribution of the mitochondrial net when compared with the expression of a control vector (pcDNA in HEK293AD or MitDsRed in neurons). Scale bars: 15 µm. (**c**) Quantification and graphical representation (mean ± standard deviation) of the above mentioned subpopulations of Alex3 or ALEX3-GFP-overexpressing cells.
Adapted from López-Doménech et al., 2012.

2.4 - Armcx/Armc10 genes implications in neurodegeneration and cancer

The involvement of Armcx/Armc10 genes in disorders and pathologies is not yet well know, but several data show their implication in both neurodegenerative diseases and cancer.

2.4.a - Armcx/Armc10 genes implications in neurodegenerative disorders

The expression of several Armcx/Armc10 genes has been found altered in subsets of neurodegenerative disorders.

GPRASP1 was identified as a new binding partner of Ataxin7, a component of chromatin-remodeling complex implicated in Spinocerebellar ataxias 7, possibly contributing to the pathophysiology of this disease (Abu-Helo and Simonin, 2010).

In a study by Piton et al. (2010), the GPRASP2 gene was identified as a genetic factor whose non-synonymous rare variants could predispose to Autism spectrum disorder and

schizophrenia. GPRASP2 and Armcx4 expression were found highly deregulated in sporadic Parkinson disease and both were included in a list of 892 genes that are considered to form the core of the diseased Parkinsonian metabolic network (Moran and Graeber, 2008). Moreover GPRASP2 can interact with the Huntington's disease protein huntingtin (htt) and the two proteins colocalize in SH-SY5Y cells, raising the possibility that htt and GASP2 could interact in neurons (Kahle et al., 2010).

The Bhlhb9 transcript is down-regulated in the brain of AD subjects, suggesting an involvement in cellular survival control (Heese et al., 2004). Furthermore, using a transgenic mouse model overexpressing Bhlhb9, Mishra et al. demonstrated that Bhlhb9 protein modulates the phosphorylation and proteolytic processing of amyloid precursor protein (App), promoting neurosynaptogenesis and increasing synaptic connections and plasticity. They propose a neuroprotective role for Bhlhb9, of putative interest for treatment of Alzheimer disease (Mishra et al., 2011).

2.4.b - Armcx/Armc10 genes implications in cancer

Armadillo domains form a versatile platform for interaction with many protein partners and have been found in a wide range of proteins related to the Wnt/ β-catenin signaling (Tewari et al.). Several alterations in Wnt signaling pathway are implicated in tumorigenesis, for this reason it has attracted considerable attention at several molecular levels.

Strong evidences support an implication of Armcx/Armc10 genes in tumorigenesis and cancer. Amcx1 and Armcx2 were initially described as genes lost in human lung, prostate, colon, pancreas, and ovarian carcinomas and also in cell lines established from different human carcinomas (Kurochkin et al., 2001). The low mRNA expression of those genes led the authors to propose a possible role as tumor suppressors in epithelial tissue.

Moreover, the overexpression of Alex1 seems to play a negative role in human colorectal tumorigenesis, as it suppress the anchorage-dependent and independent colony formation of human colorectal carcinoma cell lines (Iseki et al., 2012).

Furthermore, Armcx1 has been found repressed in adenocarcinomas induced by targeted expression of the serine threonine kinase c-Raf (Mishra et al., 2011) and the hypermethylation of its promoter has been identified as biomarkers for diagnosis of ovarian cancer (Gloss et al., 2011).

The expression of Armcx2 has been found increased in a set of patients with fragile X

syndrome, in which cancer incidence is lower than in the general population, indicating that it may act as potential protector for cancer development (Tuszynski et al., 2011). Bhlhb9 has been also proposed as tumor suppressor, since the hypermetilation of CpG island in the Bhlhb9 promoter, resulting in a silenced gene expression, has been found in the colorectal cancer cell line HCT-116 (Rosales-Reynoso et al., 2010).

Another link between Armcx/Armc genes and tumorigenesis comes from studies about the transcriptional regulation of Armcx genes. It was found that Armcx1 expression is regulated by the Wnt/β-catenina signalling in a CRE-dependent manner; furthermore mutation of a cyclic AMP response element (CRE) and an E-box impaired the basal activity of Armcx1 promoter in colorectal and pancreatic cancer cell lines (Iseki et al., 2012); these data suggest that Alex1 might act as a negative regulator of cell proliferation promoted by aberrant activation of Wnt/β-catenina pathway.

Another link between Armcx/Armc genes and tumorigenesis comes from studies about the transcriptional regulation of Armcx genes. It was found that Armcx1 expression is regulated by the Wnt/β-catenina signalling in a CRE-dependent manner; furthermore mutation of a cyclic AMP response element (CRE) and an E-box impaired the basal activity of Armcx1 promoter in colorectal and pancreatic cancer cell lines (Iseki et al., 2012); these data suggest that Alex1 might act as a negative regulator of cell proliferation promoted by aberrant activation of Wnt/β-catenina pathway. Moreover, Armcx3 and Armcx2 are downregulated in XX gonad, where mesonephric cell migration and testis vascular development are inhibited by Wnt4 signaling (Krig et al., 2007), suggesting a redoundant role in gonad development.

An increased expression of several Armcx/Armc cluster genes (Armcx5, Gprasp2 y Bhlhb9) has been correlated with a propensity to develop metastasis from neck squamous-cell carcinoma (Rickman et al., 2008).

Gpraps1 has been also proposed as a potential biomarker in breast cancer (Rohrbeck and Borlak, 2009) since it has been found in sera of patients with early stage disease but absent in sera of normal patients.

The B isoform of Armc10 transcript has been proposed to play a pivotal role in hepatocarcinogenesis; it was identified as up-regulated in the clinical hepatocellular carcinoma and its overexpression in Human liver cell line QSG-7701 induces an accelerated growth rate and tumorigenicity in nude mice, whereas inhibition of SVH-B in hepatoma cell line BEL-7404 induces apoptosis (Huang et al., 2003).

In summary, some genes belonging to Armcx/Armc10 gene family have been described as tumor suppressor, other ones have been showed accelerate tumorigenicity; taken together these data sustain the strong implication of Armcx/Armc10 genes in cancer, suggesting that the function of each gene can change depending to the cellular context or tissue.

3. – Early Development of Neural Tube

3.1 - Introduction

During gastrulation, the invagination of the developing embryo (which starts out as a single sheet of cells) produces the three germ layers: the outer layer, or ectoderm; the middle layer, or mesoderm; and the inner layer, or endoderm (http://www.ncbi.nlm.nih.gov/books/NBK10993/). Gastrulation defines the midline and the anterior-posterior axes of all vertebrate embryos as well.

One key consequence of gastrulation is the formation of the notochord, a distinct cylinder of mesodermal cells that extends along the midline of the embryo from anterior to posterior level. The notochord forms from an aggregation of mesoderm that invaginates and extends inward from a surface indentation called the primitive pit, which subsequently elongates to form the primitive streak. As a result of these cell movements during gastrulation, the notochord defines the embryonic midline (Placzek, 1995; Purves, 2001) (Fig13.a).

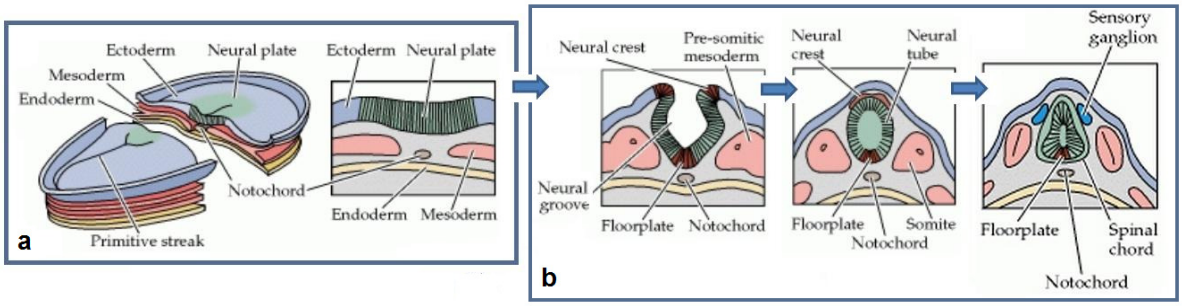

Figure 13: Initial Formation of mammalian Nervous System: Gastrulation and Neurulation. (a) Schematic dorsal view of the embryo at late gastrulation (left); Midline cross section through the embryo at the same stage (right). (b) Sections through the embryo at different stages of neurulation. Adapted from Purves et al., 2001.

The notochord sends inductive signals to the overlying ectoderm that cause a subset of neuroectodermal cells to differentiate into neural precursor cells. During this process, called neurulation, the midline ectoderm containing these cells thickens into a distinct columnar epithelium called the neural plate, that begins to fold on itself, forming the neural groove and ultimately the neural tube (Fig13.b).

The mesoderm adjacent to the tube then thickens and subdivides into structures

called somites, the precursors of the axial musculature and skeleton. As development continues, the neural tube adjacent to the somites becomes the rudimentary spinal cord, and the neural crest gives rise to sensory and autonomic ganglia (the major elements of the peripheral nervous system). Finally, the anterior ends of the neural plate (anterior neural folds) grow together at the midline and continue to expand, eventually giving rise to the brain (Fig13.b).

Different regions of the neural plate have different characteristics as a result of caudal regression of the organizer (Hensen's node in chick). Thus, the neural plate is organized in the anterior-posterior direction and this regionalization is in part controlled by Wnt signalling (Nordstron et al., 2002), ending up with two structural and functionally different structures: a rostral or cephalic region (where the brain will form) and a caudal region (giving rise to the spinal cord). Togheter with antero-posterior cell specification processes, changes in shape of the neural tube take place. In the cephalic region, the wall of the tube grows to create a series of swellings and contrsictions that define the various brain compartments, while the neighbor caudal region, the developing spinal cord, remains as a simple tube that elongates concomitantly to caudal body axis extension (although transient segments are visible).

3.2 - Dorsoventral patterning of spinal cord

When the neural tube first forms, its walls are composed by bipolar shaped cells spanning the entire width of the tube, forming a typical pseudostratified epithelium. At this stage, the majority of the cells proliferate defining the germinal neuroepithelial layer known as the Ventricular Zone (VZ). This is a rapidly dividing cell population, in which the nuclei are located at different relative positions according to the cell cycle. DNA synthesis (S phase) occurs while the nucleus is at the outside edge of the tube, and mitosis (M phase) occurs on the luminal side of the cell layer (Fig.14). Shortly after neural tube closure, scattered neural precursors stop dividing and detach from the apical luminal side of the tube. As a consequence, these postmitotic cells begin to differentiate and move basally through the neural epithelium. The region of the neural tube peripheral to the neuroepithelial cells and where postmitotic cells accumulate and terminally differentiate into both neurons and glia is called Mantle Zone (MZ) (Boudler Commitee et al., 1970).

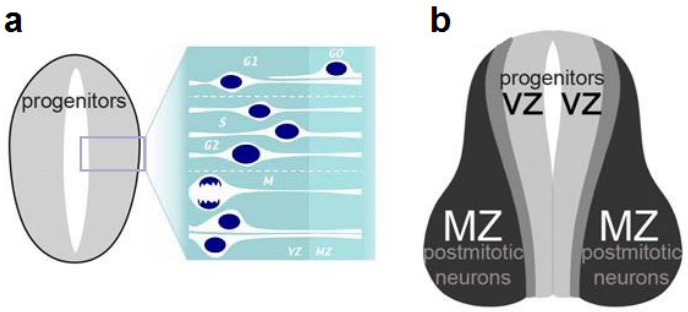

Figure 14: Regionalization of the developing spinal cord. (A) Transverse section of an early neural tube showing precursors cell cycle dynamics. (B) Schematic representation of a late spinal cord section showing the basic anatomical distribution of mitotically active (ventricular zone, VZ) and postmitotic (marginal zone, MZ) cell populations.

During development, the distinct neuronal subtypes will emerge in a precise spatial order from progenitor cells arrayed along the dorsal-ventral axis of the neural tube (Fig.15.a), and this pattern of neurogenesis is controlled by secreted signals that pattern neural progenitor cells into spatially discrete domains (Briscoe et al., 2000; Guillemot, 2007; Ruiz i Altaba, 1994) (Fig.15.b). Although the roof plate and floor plate do not directly participate in neurogenesis, these groups of cells form important embryonic organizing centers that provide the inductive signals necessary to specify the spatial coordinates of a precursor cell along the DV axis (Fig.15.a). Selective removal of the roof plate results in the loss of the most dorsal interneurons (Lee et al., 2000), while deleting the notochord results in the loss of ventral phenotypes (Van Straaten and Hekking, 1991) .

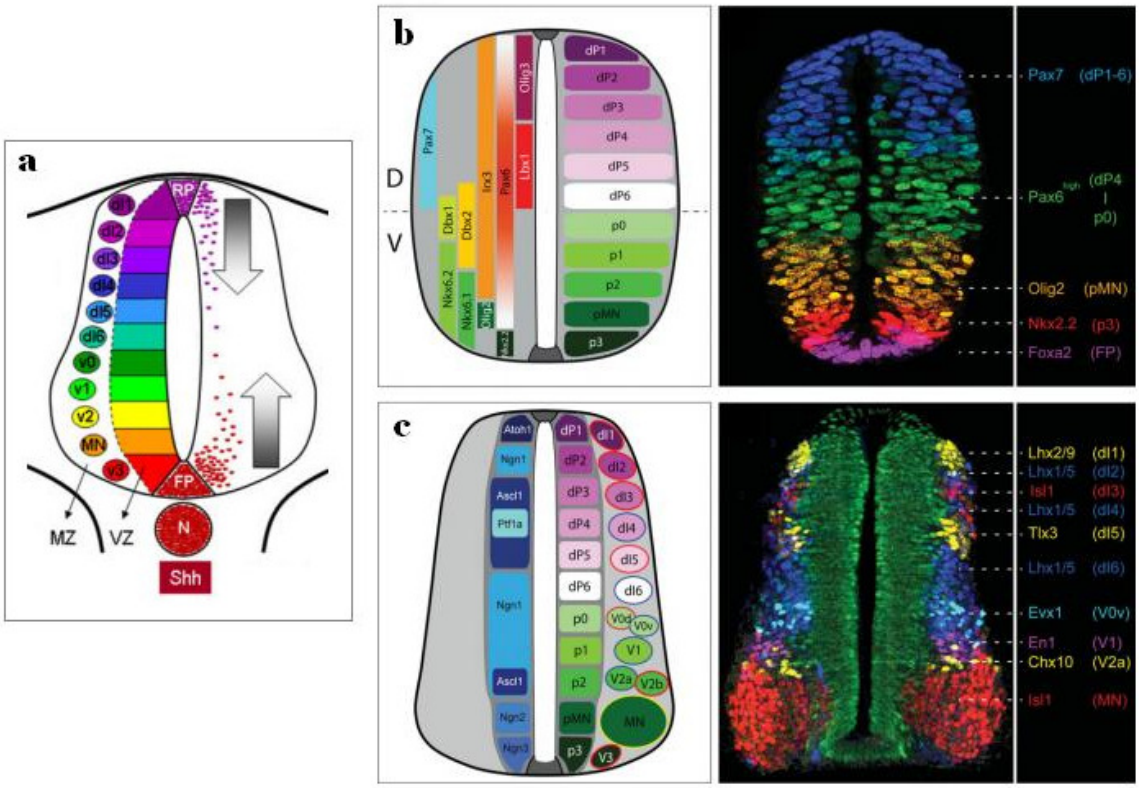

Figure 15: Diagram of transverse section of the developing spinal cord. (**a**) The lumen of the neural tube is surrounded by a layer of proliferative progenitor cells (VZ) that eventually differentiate into postmitotic neurons distributed laterally (MZ). Different subtypes of progenitors and their postmitotic derivates are distributed in a specific order along the dorso-ventral axis. This patterning is established by the action of s Shh gradient, secreted from the notochord (N) and the floor plate (FP), and Wnts and Bmps gradients, produced by the roof plate (RP). (**b,c**) Specification of neuronal fates resulting from expression of several combination of transcription factor along dorso-ventral axis, at two subsequent chicken spinal cord developmental stages. Adapted from Le Dreau and Martí, 2012.

Many classes of secreted factors have been implicated in the acquisition of spinal cord phenotype: BMP and Wnt signals secreted from the roof plate and the overlying ectoderm initiate the patterning of the dorsal neural tube (Lee and Jessell, 1999; Roelink, 1996), whereas the secretion of Shh from the notochord and floor plate has a key role in establishing ventral neuronal fates (Briscoe et al., 2000; Chiang et al., 1996; Ericson et al., 1996), (Fig.15.a).

Together these inductive signals regulate the expression patterns of different transcription factors (Pax6, Pax7, Dbx1, Irx3, Nkx2.2 or Olig2 among others) in partially overlapping domains within the ventricular epithelium in which progenitor cells are located (Ericson et al., 1997), (Fig.15.b). The expression profile along the DV axis of these transcriptional regulators controls the genetic network necessary for the anatomical segregation of each

neuronal subtype (Lee et al., 2008), giving rise to sensory neurons in the dorsal spinal cord and visceral or somatic motor neurons in the ventral spinal cord (Lee and Jessell, 1999). Several interneuron populations connect these two populations, forming distinct axonal trajectories and circuits. There are many molecular markers of neuronal populations in the spinal cord that allow us to identify further sub-groups of postmitotic differentiated neurons: the dorsal interneurons are subdivided into 6 groups (dI1-6), while ventral neurons are divided into 5 groups of interneurons and motoneurons (v0,v1,v2,MN, v3; Fig.15.c).

3.3 - Cell specification along the dorsoventral axis: Shh signaling

3.3.a - Canonical Shh Signalling

The differentiation of the ventral cell types is triggered by signals provided initially by an axial mesodermal cell group, the notochord, and later by floor plate cells (Patten et al., 2003; Placzek, 1995). The main signalling activities of the notochord and floor plate are mediated by a secreted protein, Sonic hedgehog (Shh) (Patten and Placzek, 2000), diffunding form a ventral (high) to dorsal (low) expression gradient (Marti et al., 1995; Roelink et al., 1995).

Canonical Shh signaling occurs via a derepression mechanism involving the multiple-pass transmembrane receptor Patched (Ptch) and the G-protein-coupled receptor-like molecule Smoothened (Smo). In the absence of Shh, Ptch represses Smo activity. Shh binding to Ptch relieves this repression, allowing Smo to translocate to the primary cilium where it activates intracellular signaling pathways. This activation of Smo ends in transcriptional activity, via its regulation of Gli transcription factors that can activate or repress Shh target genes (Marti and Bovolenta, 2002).

In vertebrates, three Gli transcription factors (Gli1 – Gli3) have been described, all of which are expressed in the developing neural tube (Jacob and Briscoe, 2003; Lee et al., 1997; Ruiz i Altaba, 1994; Wilson and Stoeckli, 2012). While Gli2 and Gli3 both have transcriptional activator and repressor activities, Gli1 is solely a transcriptional activator (reviewed by Ruiz i Altaba *et al*., 2007). Each Gli family member responds differently to Shh. In the absence of Shh, Gli2 is fully degraded, while Gli3 is converted (via proteolytic processing of its C-terminus) to a repressor of transcription (Gli3R). When Shh is present, Gli1 expression is induced and proteolysis of Gli2 and Gli3 is inhibited,

allowing full-length activator forms of Gli proteins to be accumulated. The Gli transcriptional activators then induce the expression of Shh pathway target genes (Aza-Blanc et al., 2000; Dai et al., 1999; Pan et al., 2006; Ruiz i Altaba, 1994).

3.3.b - Shh defines cell fate in the ventral spinal cord

Ectopic expression of Shh in vivo and in vitro can induce the differentiation of floor plate cells, motor neurons and ventral interneurons (Ericson et al., 1996; Marti et al., 1995; Roelink et al., 1995). Conversely, elimination of Shh signalling from the notochord by antibody blockade in vitro (Ericson et al., 1996; Marti et al., 1995; Roelink et al., 1995) or through gene targeting in mice (Chiang et al., 1996), prevents the differentiation of floor plate cells, motor neurons and most classes of ventral interneurons (Chiang et al., 1996; Pierani et al., 1999).

Progressive two- to three-fold changes in Shh concentration generate five molecularly distinct classes of ventral neurons from neural progenitor cells *in vitro* (Ericson et al., 1997). Moreover, the position of generation of each of these neuronal classes *in vivo* is predicted by the concentration of Shh required for their induction *in vitro*. Neurons generated in progressively more ventral regions of the neural tube require correspondingly higher concentrations of Shh for their specification (Ericson et al., 1997). Although these findings support the idea that the position of a progenitor cell within a ventral-to-dorsal gradient of Shh signalling activity directs its differentiation into specific neuronal subtypes, they pose the problem of how neural progenitor cells interpret graded Shh signals. Recent studies have provided evidence that a group of homeodomain proteins expressed by ventral progenitor cells act as intermediary factors in the interpretation of graded Shh signalling (Ericson et al., 1997; Pierani et al., 1999). These transcription factors are subdivided into two groups, termed class I (Pax7, Dbx1, Dbx2, Pax6, Irx3) and II (Nkx2,2, Nkx6.1) proteins, on the basis of their mode of regulation by Shh signaling (Briscoe et al., 2000). The class I proteins are constitutively expressed by neural progenitor cells, and their expression is repressed by Shh signaling, whereas neural expression of the class II proteins requires exposure to Shh (Briscoe et al., 2000; Ericson et al., 1996; Pabst et al., 2000; Vallstedt et al., 2001). Due to the Shh mediated regulation of their expression, progenitor domains are delimitaded by the ventral boundaries of each class I protein and by dorsal boundaries of each class II (Fig.16). The combinatorial expression profile of these two classes of homeodomain proteins defines five cardinal

progenitor cell domains within the ventral neural tube (Fig.16a-c).

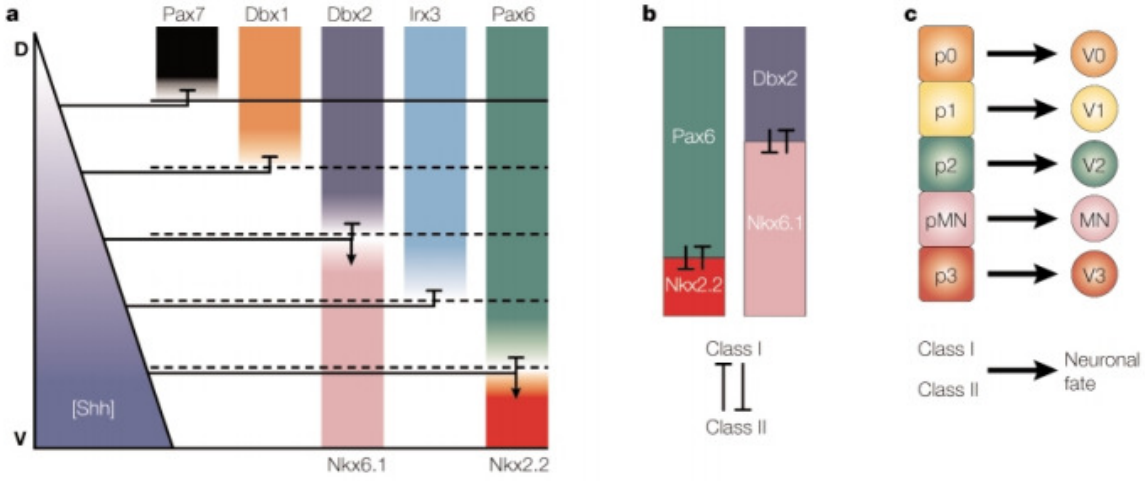

Figure 16: Shh-mediated ventral neural patterning. (**a**) Shh mediates the repression of class I homeodomain proteins (Pax7, Dbx1, Dbx2, Irx3 and Pax6) and the induction of expression of class II proteins (Nkx6.1 and Nkx2.2) at different threshold concentrations. (**b**)The pairs of homeodomain proteins that abut a common progenitor domain boundary (Pax6 and Nkx2.2; Dbx2 and Nkx6.1) repress each other's expression. (**c**) Shh signalling defines five progenitor domains in the ventral neural tube and the relationship between neural progenitor (p) domains and the positions at which post-mitotic neurons are generated along the dorso-ventral axis of the ventral spinal cord.
Adapted from Jessell TM, 2000.

How do these homeodomain proteins convert a gradient of extracellular Shh signalling activity into discrete progenitor domains? This feature is achieved through selective cross-repressive interactions between the complementary pairs of class I and class II homeodomain proteins that abut the same progenitor domain boundary (Briscoe et al., 2000) (Fig17.b). Such interactions seem to have three main roles. First, they establish the initial dorsoventral domains of expression of class I and class II proteins. Second, they ensure the existence of sharp boundaries between progenitor domains. Third, they help to relieve progenitor cells of a requirement for Shh signaling, consolidating progenitor domain identity.

Although manipulation of Shh signaling changes the pattern of class I and class II gene expression in predictable fashion (Briscoe et al., 2001), it remains unclear how graded Shh signaling controls the early steps of differential gene expression in the ventral neural tube.

3.4 - Cell specification along the dorsal axis: Wnt β-catenin signaling

3.4.a - Canonical Wnt Signaling

The Wnt family consists of a group of proteins acting in multiple signaling pathways, binding to cell surface receptors to activate signaling cascades (Ille and Sommer, 2005; Kohn and Moon, 2005; Montcouquiol et al., 2006). Wnt proteins can activate signaling cascades, including the canonical Wnt signaling pathway, the Wnt/PCP pathway and the Wnt/Calcium pathway. Each of these pathways, although distinct, appears to be transduced initially through Dishevelled (Dvl), a cytoplasmic multi-functional protein.

In the canonical Wnt pathway (Fig.18), transcriptional activity is regulated by β-catenin, a bifunctional protein that either regulates gene expression, when translocated to the nucleus, or acts as a linker between surface receptors and the cytoskeleton. In particular, Wnt signal integration remains enigmatic due to the complexity of the signal transduction mechanism, which includes numerous, dynamic molecular components (Wodarz and Nusse, 1998).

In the canonical pathway, in absence of Wnt signaling, β-catenin is part of a complex containing GSK-3β, Axin, adenomatous polyposis coli (APC) tumor suppressor protein and CK1. In this complex, beta-catenin is phosphorylated by GSK-3β leading to its ubiquitination and subsequent proteosomal degradation. Upon Wnt stimulation to Frizzeled receptor and Lrp5/6 co-receptor, Dvl blocks the formation of the protein complex and beta-catenin phosphorylation with its subsequent degradation does not occur. The accumulation of free β-catenin results in its nuclear translocation (Yost et al., 1996). In the nucleus, β-catenin binds to the transcription factors TCF/LEF (Behrens et al., 1996; Hart et al., 1999), leading to transcriptional activation of multiple target genes such as c-myc and Cyclin-D1 (Fig.17).

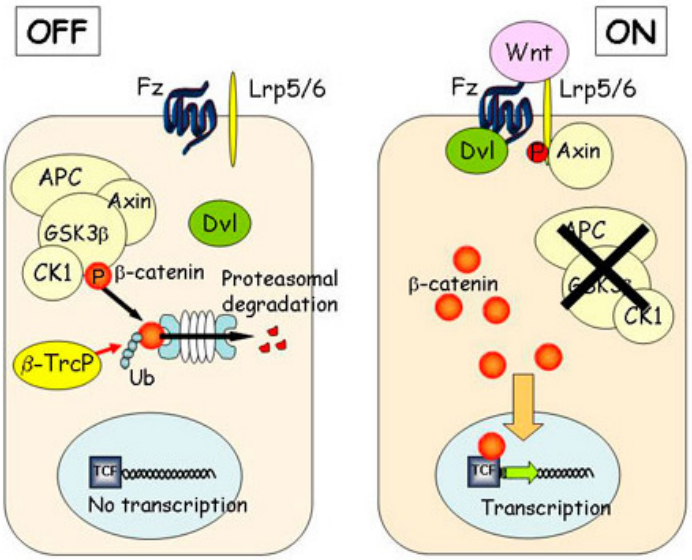

Figure 17: The canonical Wnt pathway. Canonical Wnt pathway is initiated by binding of Wnt ligands to Frizzled receptor and LRP5/6 co-receptor. The key mediator of the canonical Wnt pathway is β-catenin, whose half-life depends to the activity of a complex containing axin, APC, GSK3β and CK1. In the absence of Wnt, β-catenin is sequentially phosphorylated by CK1 and GSK3β leading to proteasomal degradation. Members of the TCF/LEF family remain inactivated in the nucleus. Following Wnt stimulation, the complex disgregates and unphosphorylated β-catenin accumulates and subsequently translocates to the nucleus, where it acts as a transcriptional co-activator for TCF/LEF target genes like Cyclin D1 and c-myc.

Although this model provides a framework for understanding the Dvl/Axin relationship in the context of canonical Wnt signaling, there is evidence that other proteins are associated with this complex and can potentiate Dvl/Axin-mediated Wnt signaling as well (Chen et al., 2006; Ding et al., 2008). Thus, a more complete understanding of the dynamics and constituents of the Dvl/Axin complex is necessary to fully understand the processes that control canonical Wnt signaling.

3.4.b - Wnt defines cell fate in the dorsal spinal cord

Several lines of evidence support the idea that Wnts are involved in dorsoventral patterning of the neural tube. Muroyama and colleagues demonstrated that Wnt1/Wnt3a double mutant mice show reduced numbers of the most dorsal (dI1–dI3) interneurons, and a compensatory increase in intermediate interneurons (Muroyama et al., 2002). Similarly, expression of the secreted Wnt antagonist Dickkopf in zebrafish resulted in the loss or reduction of dorsal progenitor cell types (Bonner et al., 2008). Disruption of β-catenin also results in patterning defects in the dorsal neural tube: expression of a constitutively active form of β-catenin results in ectopic expression of

Olig3, a bHLH transcription factor that is essential for the correct specification of dI1–dI3 neurons (Teo et al., 2006), while the conditional loss of β-catenin in neural progenitors prevents Olig3 expression (Zechner et al., 2007).

Further experiments in chick embryos suggested that Wnt/β-catenin not only induces dorsal cell types but also inhibits ventral cell types (Alvarez-Medina et al., 2008). Ectopic activation of Wnt/β-catenin in the chick neural tube expanded the expression domains of dorsal markers such as Pax6 and Pax7, but also inhibited the expression of ventral makers such as Olig2 and Nkx2.2. Conversely, inhibition of the Wnt/β-catenin pathway by expression of dominant-negative Tcf not only repressed the expression of dorsal cell subtypes but also resulted in an expansion of the ventral markers (Alvarez-Medina et al., 2008). Taken together, the results suggest a model in which the secretion of Wnt1/Wnt3a from the dorsal neural tube simultaneously induces dorsal cell types and repressing ventral cell types.

The activation of β-catenin appears to antagonize the activity of Shh in neural tube patterning and it can actuate following several mechanisms: (i) Wnt/β-catenin acts indirectly on patterning by affecting other signaling molecules downstream of Shh, such as the Glis; and (ii) Wnt/β-catenin directly regulates patterning molecules that oppose those of Shh/Gli, acting in parallel to Bmp-mediated patterning of the dorsal neural tube (Ulloa and Marti, 2010).

3.5 - Growth in neural tube

The CNS develops from neuroepithelial progenitor cells that generate a large variety of differentiated neuronal and glial progeny (Bystron et al., 2008; Donovan and Dyer, 2005). Neural progenitors (NPCs) can undergo three distinct models of divisions during development of the vertebrate CNS (Franco and Muller, 2013): self-expanding symmetric proliferative (PP, generating two daughters with identical progenitor potential), self-renewing asymmetric (PN, generating at least one cell with a more restricted potential than the parental cell), and self-consuming neurogenic (NN, generating two cells committed to differentiation) (Farkas and Huttner, 2008).

The mechanisms controlling the balance between these different modes of division and the global balance between proliferation and differentiation are not yet understood, but it is emerging, from studies performed in mammalian cerebral cortex, that a determinant

key is the length of the different phases of NPCs cell-cycle. Particularly, Calegari and Huttner proposed the ‘‘cell cycle length model’’, which suggested that lengthening G1 alone is sufficient to induce neuroepithelial cell differentiation (Calegari and Huttner, 2003). According to this model, cell fate determinant(s) may, or may not, induce a cell fate change of neural progenitors depending on whether or not the length of G1 provides enough time for the cell fate determinant-produced effect(s) to become effective. In essence, a relatively long G1 may allow the switch to neurogenesis, while a short G1 may not (Calegari and Huttner, 2003). A more recent study showed that cell-cycle regulation of NPCs involved alteration not only in G1-phase but also in S-phase duration. The length of these cell-cycle phases seems to be differentially linked to NPCs proliferation versus differentiation, with G1-phase lengthening being associated with the transition to a more differentiated NCP type, and maintenance of a long S-phase with NPC expansion (Arai et al., 2011). However, we are still far from understanding the determinants playing a role in cell cycle changes.

Progression through the cell cycle is driven by cyclin-dependent kinases (CDK) and their activating Cyclin (CCN) partners. Specific combinations of CDK/Cyclin heterodimers allow progression through specific phases of the cell cycle. CDK/Cyclin activity is suppressed by interaction with two main groups of inhibitor proteins belonging to the INK4 and CIP/Kip families. The rate of cell cycle progression is determined by the relative abundance of these positive and negative regulators. The importance of this process also lies in the coordination of proliferation, fate specification, and differentiation (Dehay and Kennedy, 2007; Ulloa and Briscoe, 2007).

The G1 phase is positively regulated by the action of three Cyclin D proteins, which link extracellular mitogenic signals to the core cell cycle machinery (Lobjois et al., 2004), driving the cell into S fase. In addition to their positive cell-cycle control function, Cyclin Ds have been implicated in a number of other cellular activities (Fu et al., 2004). Interestingly, recent studies have proposed that several Cyclins can modulate progenitors fate in a manner independent from their function in cell cycle progression, as reported for Cyclin D1 in promoting neurogenesis in the embryonic murine spinal cord (Lukaszewicz and Anderson, 2011). Moreover, these cell cycle regulators can directly participate in the transcriptional regulation of factor essential for stem cells identity: for istance, Cyclin D1 was reported to bind to regulatory regions of genes belonging to Id family and Notch signaling pathway (Bienvenu et al., 2010) or repress the basic Helix-loop-helix

transcription factor BETA2/NeuroD (Ratineau et al., 2002).
These results point ut to the notion that cell cycle regulation and cell fate decision are not also simply coordinated, but share commun regulators and are extremely linked also at molecular level.

3.6 - Wnt canonical pathway involvement in neuronal differentiation and cell proliferation

In the last years several evidences about the Wnt-dependent control of neuronal differentiation and NPCs proliferation during CNS development have been accumulated. Loss- and gain of function analysis for the β-catenin locus, performed in mouse, showed that after ablation of β-catenin, the tissue mass of the spinal cord and several brain areas (including cerebral cortex and hippocampus) are reduced, the neural precursor population is not maintained and neural differentiation is promoted (Machon et al., 2003; Zechner et al., 2003). Conversely, the chick spinal cord or the brains from mice that express activated β-catenin have an enlarged mass with an increased population of neuronal precursors (Megason and McMahon, 2002; Zechner et al., 2003). Moreover, in cultured embryonic stem cells, the enhancement of β-catenin signaling following RA treatment, significantly increases the numbers of neurons generated (Otero et al., 2004). More recent studies showed that inhibition of Wnt/β-catenin pathway promotes neuronal differentiation in the intermediate zone of the dorsal neural tube and is mediated by Smad6 (Xie et al., 2011). Wnt/β-catenin signal thus seems essential for the maintenance of proliferation of neuronal progenitors, controlling the size of the progenitor pool, and impinging on the decision of neuronal progenitors to proliferate or differentiate.
In the nucleus, in the absence of the Wnt signal, TCFs act as repressors of Wnt target genes. Following Wnt stimulation, stabilized β-Catenin into the nucleus can act as a TCF co-activator (Logan and Nusse, 2004), acting on the genes containing functional TCF binding sites. Among them we found two main regulators of G1/S cell cycle transition: Cyclin D1 (Shtutman et al., 1999; Tetsu and McCormick, 1999) and c-Myc (He et al., 1998).
Transcriptional activation of Cyclin D1 through the β-catenin/TCF pathway also occurs in the developing neural tube, suggesting that Wnt signaling positively regulates cell cycle progression and negatively regulates cell cycle exit of spinal cord precursors, in

part through transcriptional regulation of Cyclin D1 (Megason and McMahon, 2002; Panhuysen et al., 2004).

It is also important to considerate also the interplay between Wnt and Shh pathway in regulating neural progenitor proliferation. In fact, Cyclin D1 is also a transcriptional target of the canonical Shh pathway (Cayuso et al., 2006; Shtutman et al., 1999; Tetsu and McCormick, 1999). In the developing neural tube, the Wnt family members that regulate mitogenic activity (Wnt1 and Wnt3a) are mainly expressed dorsally (Megason and McMahon, 2002), while Shh is expressed ventrally (Marti et al., 1995). These opposing expression patterns suggest a simplistic model for the control of proliferation, in which these pathways act in parallel on distinct subpopulations of neural precursor cells (i.e. Wnt dorsally and Shh ventrally). However, the loss of either Wnt or Shh leads to cell cycle arrest and to a uniform tissue reduction throughout the dorsoventral axis of the neural tube (Alvarez-Medina et al., 2009; Cayuso et al., 2006), arguing against this simplistic model. Another possibility is that the two pathways act in the same cells, by controlling the activity or transcription of different regulators of cell cycle progression.

Recent studies in chicken support this idea (Alvarez-Medina et al., 2009; Ulloa and Briscoe, 2007). By *in vivo* gain- and loss-of-function experiments, Alvarez-Medina and colleagues showed that the expression of Tcf3/4 in the neural tube depends on Shh activity, thus linking Shh signaling to the canonical Wnt/β-catenin transcription pathway (Alvarez-Medina et al., 2009). In the absence of Tcf3/4, canonical Wnt signaling could not activate mitogenic target genes, including Cyclin D1, leading to arrest of the cell cycle at G1. Thus, Wnt and Shh activities are integrated to control Cyclin D1 expression and the subsequent progression through the G1 phase of the cell cycle (Fig.18).

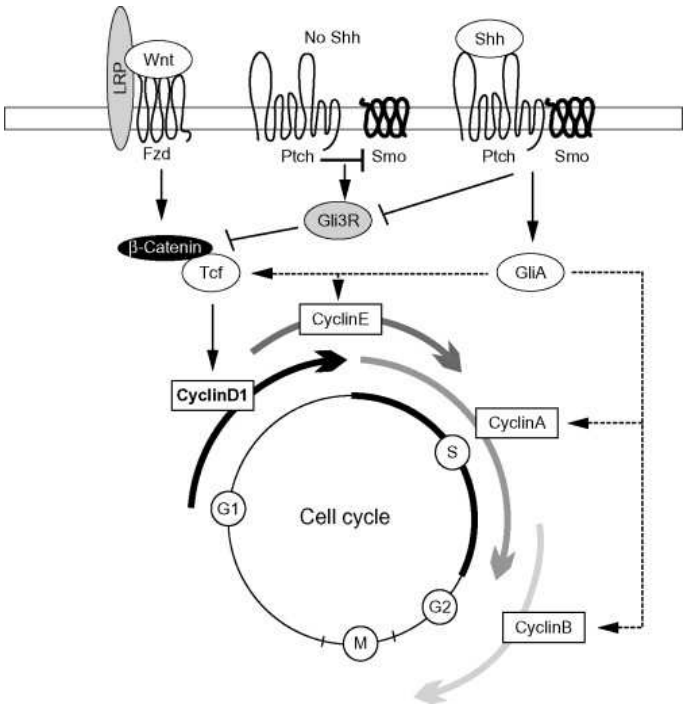

Figure 18: Summary of Wnt and Shh activities in the regulation of cell cycle progression in neuroepithelial cells. CyclinD1 is induced downstream of Wnt and Shh signaling, promoting the G1/S transition of the cell cycle. However, the Wnt signaling response relies on Shh-induced Tcf expression, thus linking the two pathways in the control of neural progenitor proliferation. In the absence of Shh, Gli3R also inhibits the activity of β-catenin. Shh can also induce other Cyclin genes independently of Wnt to control later stages of cell cycle progression.
Adapted from Alvarez-Medina et al., 2009.

Another level of interaction between the Wnt and Shh signaling pathways in the regulation of proliferation has been proposed by Ulloa and colleagues: they found that the loss of Shh signaling reduced the responsiveness of neural cells to canonical Wnt signaling (Ulloa and Briscoe, 2007). When Shh is absent, the transcriptional repressor form of Gli3 (GliR) is generated. Gli3R can physically interact with β-catenin in vitro, inhibiting its transcriptional activity by a mechanism currently unknown (Alvarez-Medina et al., 2009; Hallikas et al., 2006).

Shh and Wnt pathway also have independent roles in cell proliferation. For example, Shh has been shown to activate cell cycle genes promoting the transition from G1 to G2 (including Cyclin A, Cyclin B, and Cyclin E), suggesting that Shh signaling, but not Wnt/β-catenin signaling, also regulates late cell cycle progression (Alvarez-Medina et al., 2009; Megason and McMahon, 2002). Thus, in addition to their integrated activities, the modulation of different transcription factors also allows Wnt and Shh to regulate distinct mechanisms that control cell proliferation in the neural tube.

3.7 - Wnt target genes

Over recent years, a vast number of candidate Wnt target genes have been identified by several techniques; summarizing the data from microarray studies independent from cell

type or organism and sorting out all duplicates yielded 1886 candidates genes, which are differentially expressed in cells with activated Wnt pathway (Hallikas et al., 2006; Huang et al., 2005; Morkel et al., 2003; Sansom et al., 2007; Schwartz et al., 2003; Taneyhill and Pennica, 2004; Ziegler et al., 2005; Zirn et al., 2005).

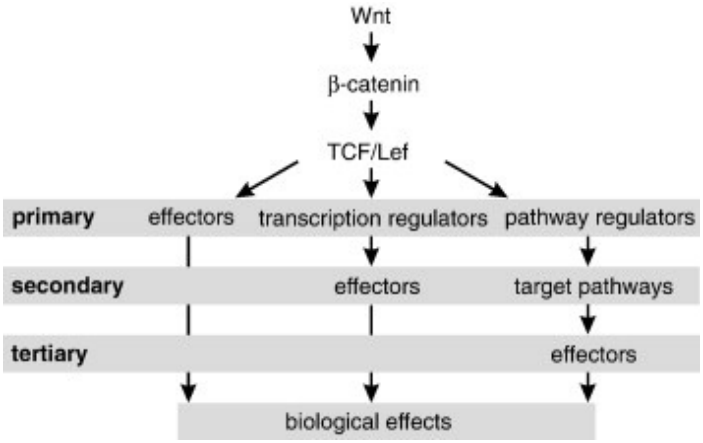

Figure 19: The three levels of the Wnt targetome. TCF/Lef activates the primary level of the targetome including effectors, transcription regulators and pathway regulators. At the secondary level either effectors or target pathways are located. The tertiary level comprises targets of the target. Adapted from Vlad et al., 2008.

The biological effects of the Wnt pathway are mediated via the regulation of direct (primary) and indirect (secondary or tertiary) target genes (Fig.19).

As an example, the transcription factor c-myc regulates the c-myc interacting zinc finger protein-1 (MIZ-1), which is able to inhibit the expression of the indirect target p21WAF1.s. These targets can be understood as regulators or amplifiers of the original signal. Thus, three levels of the Wnt targetome can be distinguished (Fig.19).

In order to identify pathways affected by Wnt signaling, Vlad et al. allocated the genes which have been identified in microarray studies as differentially expressed by using the software package Pathway Assist (Stratagene) (Vlad et al., 2008). Potential Wnt targets are involved in at least 36 different pathways controlling apoptosis, inflammation, proliferation and metabolism (Tab.3).

Target pathway	*Function*
G-protein-MAPK activation, CREB signalling, EGF signalling, ERK-PI3K (collagen) signalling, erythropoietin signalling, hedgehog signalling, JAK-STAT signalling, MAPK signalling, NGF signalling, PDGF signalling, PTEN signalling, SAPK-JNK signalling, VEGF signalling, Wnt signalling (calcium)	**Proliferation**
ACH-R apoptosis signalling, anti-apoptotic pathway, CD40L signalling, death receptor signalling, FAS signalling, mitochondrial apoptosis control, NF-κB signalling, p53 signalling, PTEN signalling	**Apoptosis**
AKT signalling, p38 signalling, p53 signalling, Rb signalling	**Cell cycle**
Regulation of myogenesis	**Differentiation**
Insulin signalling, lipid signalling	**Metabolism**
IFNα signalling, IL-1 and IL-6 signalling, IL-2 signalling, IL-3 signalling, TGFβ signalling, toll-like receptor signalling	**Inflammation, immune response**
Integrin signalling	**Cell adhesion**

Table 3. Pathways and corresponding functions affected by genes which are differentially expressed in cells with activated Wnt pathway. Adapted from Vlad et al., 2008.

In the same study it has been proposed a selection of target genes (collected from *http://www.stanford.edu/rnusse/pathways/targets.htm*) implicated in a large variety of biochemical functions (Tab.4); the diversity of the biochemical functions reflect the variety of different biological effects of the Wnt pathway, including activation of cell cycle progression and proliferation, inhibition of apoptosis, regulation of embryonic development, cell differentiation, cell growth and cell migration.

Function	*Target genes*	*Trend*
Cell cycle kinase regulators	Cyclin D1	Up
	p21	Down
Cell adhesion proteins	Claudin-1, connexin-30, connexin-43, L1CAM, Nr-CAM	Up
	E-cadherin, periostin	Down
Receptors	CD44, Dfz3, EGF, Fz7, receptor, Met, Ret, retinoic acid receptor gamma, Stra6	Up
	Arrow/LRP, Dfz2, Fz	Down
Factor synthases	COX2, NOS2	Up
Hormones, growth factors	Gastrin, BMP4, CCN1/Cyr61, Dickkopf-1, Dll1, Eda, endothelin-1, EphB/ephrin-B, FGF18, FGF20, FGF4, FGF9, follistatin, IGF-I, IGF-II, IL-6, IL-8, jagged 1, nanog, proglucagon, proliferin-2, proliferin-3, s-FRP, Stra6, TNF family 4-1BB ligand, VEGF, wingful/notum, wingless, WISP-1, WISP-2, Xnr3	Up
	BMP4, osteocalcin, RANK, wingless	Down
Transcription regulators	c-Myc, brachyury, Cdx1, Cdx4, c-jun, dharma/bozozok, engrailed-2, FoxN1, fra-1, Id2, Irx3, ITF-2, LEF-1, mBTEB2, MITF/nacre, movo, myogenic bHLH, neurogenin 1, Pitx2, PTTG, Runx2, SALL4, Sox2, SOX9, TCF-1, twin, Twist, Ubx	Up
	Hath1, nanog, Ubx, Six3, SOX9	Down
Proteases, protease inhibitors, protease receptors	CD44, MMP-7, MMP-26, stromelysin-1, survivin, uPAR	Up
Matrix proteins	Fibronectin, keratin, versican	Up
GTPase, GTPase regulator	Tiam, Wrch-1	Up
Others	Axin-2, MDR1, nemo, siamois, β-TRcP, twin	Up

Table 4. List of selected target genes from Wnt homepage (http://www.stanford.edu/rnusse/pathways/targets.htm), with corresponding biochemical functions and regulation trend. Adapted from Vlad et al., 2008.

In cancer cells with mutationally activated Wnt pathway, at least 20 target genes activate proliferation: c-Myc, Cyclin D1, c-jun, fra-1, EphB/ephrin-B, FGF18, Hath1, Met, c-Myc

binding protein, Id2, FGF9, FGF20, Stra6, Twist, WISP, surviving, Pituitary Tumor Transforming Gene (PTTG), TNF family 41BB ligand, VEGF and endothelin-1 (Vlad et al., 2008).

The large number of target genes affected for each process no had to be surprising considering that the induction of a complex effect needs a critical number of active proteins; as an example the up- or down-regulation of more than 570 genes is necessary for the progression through one round of the cell cycle (Cooper and Shedden, 2003). Moreover, a complex process like proliferation must be regulated at several stages; for the cell cycle progression, the activation of Cyclin D1 induces G0/G1 transition, but additional mechanisms like down-regulation of p21 and inactivation of the anaphase promoting complex are necessary for G1/S transition. Finally, a cell cycle control ensured by more than one pathway and several genes opens additional possibilities for modifying the final outcome. Thus, target pathways might be considered as functional elongation of the Wnt cascade downstream of the TCF/Lef level.

3.8 - The Chicken Model System

To study the role of Armcx/Armc10 family in neural development we have selected the chicken embryo as experimental model. The chick embryo provides an excellent model system for studying the development of higher vertebrates wherein growth accompanies morphogenesis. It is a simple *in vivo* model that can be genetically manipulated in an easy way by in ovo electroporation: electroporating DNA plasmids allows to obtain transient and mosaic embryos and use them in gain or loss of function in vivo assays with single cell resolution in a time and space controlled manner (Krull, 2004; Voiculescu et al., 2008).

During neural tube development, neural progenitors proliferate to generate sufficient neural precursors for the construction of nervous system. At the same time, these progenitor cells are taking important cell fate decisions. All these processes can be easily monitored using specific molecular markers, therefore making the chicken an ideal and efficient model for study proliferation and differentiation in spinal cord development. However, the rate of development can be affected by a range of factors, including the specific breed, the temperature of incubation, the delay between laying and incubation, raising the need to generate a standardized staging system based on morphology rather

than chronological age. Viktor Hamburger and Howard L. Hamilton created a morphological system for staging chick development: the Hamburger–Hamilton stages (HH) is a series of 46 developmental stages, starting from laying of the egg and ending with a newly hatched chick (Hamburger and Hamilton, 1992) (Fig.20).

Figure 20: Normal stages of chick embryonic development. Morphological system for staging chick development, created in 1951 by Hamburger and the Hamburger–Hamilton (HH stages). The 46 developmental steps start from laying of the egg and end with a newly hatched chick. Adapted from "Developmental dynamics 195, 231-72", 1992.

At HH10-12 (10-13 somites), the neural folds creates a partially closed system with a lumen into which it is easy to inject DNA constructs *in ovo*. At this stage the tube is most formed by uncommitted progenitor populations, whose fate can be altered by ectopic manipulations.

Starting from 18-24 hours after electroporation (HH16-18) the effects of the ectopic DNA on proliferation can be detected by immunohistochemical techniques o flow cytometry analysis.

By stage HH14 (23 somites) around 12% of the neural progenitors have exited the cell cycle and have started to differentiate at the marginal zone (Wilcock et al., 2007); from stages HH14 to HH24 neural differentiation is more active, while gliogenesis has not yet started (Wilcock et al., 2007). Starting from 48 hours after electroporation (stage HH22-24) possible effects of the ectopic manipulation resulting in changes in neural differentiation, can be detected using pan-neuronal markers, to identify neurons and discerning morphological characteristics.

AIM OF STUDY

Based on existing information we propose to get insight into the mitochondrial function of Armcx/Armc10 encoding proteins and investigate their possible involvement in neural development processes. In particular, the aim of my thesis work has been to characterize the function of Armcx3 and Armc10 genes in mitochondrial dynamics and in the spinal cord development, pursuing the following specific objectives:

1. To get insight into the cellular and molecular function of Alex3 protein in mitochondrial dynamics using as models both cell lines and neuronal primary cultures.

2. To extend the study to Armc10 protein, from which the whole Armcx cluster evolved, looking at possible functional divergences.

3. To investigate the role of Alex3 and Armc10 in an in vivo physiological model of neural development: the chicken spinal cord.

METHODS

Plasmid vectors

Alex3 3′-UTR was found in a Substractive Hybridization library (Garcia-Frigola et al., 2004) and the full sequence was obtained by screening a P0 mouse brain cDNA library (Stratagene). For the generation of Alex3-GFP and Alex3Δ(1-12), Alex3 was amplified with high fidelity Pfu (Stratagene) and a BamHI restriction site was introduced by using appropriate primers for insertion in pEGFP-C1 or pEGFP-N3 vectors. All the constructs generated were sequenced with BigDye-Terminator v3.1 (Applied Biosystems). shRNAi sequences were designed against the Alex3 mRNA sequence using siRNA primer designer software v1.51 (Promega) and subcloned into pVLTHM vector (Tronolab) through MluI/ClaI (New England Biolabs) digestion. The sequence of the selected shRNAi-Alex3 is 5'-cgcgtccccggctttaattgtcctaaatttcaagagaatttaggacaattaaagccttttttggaaat-3'; the sequence of the scrambled shRNAi-control is 5'-cgcgtccccgcagctttaattgctctgggtaataatattcatattacccagagcaattaaagctgctttttggaaat-3'. The expression vectors Miro1-myc, Miro2-myc, Miro1ΔEF-myc, KIF1C-myc, and Trak2-myc were obtained as described in MacAskill et al. (2009). The mitochondrial targeted Aequorin was previously described (Manjarres et al., 2008). Mito-PAGFP was described in Karbowski et al. (2009). Mitochondrial-targeted DsRed (MitDsRed) was a gift from Antonio Zorzano (IRB, Barcelona). GST-Miro1 and GST-Miro1ΔEF were kindly provided by Josef Kittler (UCL, London). Mitofusin1-myc and Mitofusin2-myc were kindly provided by Luca Scorrano (University of Padova). pCIG empty vector (Megason and McMahon, 2002), Wnt3a and β-cateninCA (Tetsu and McCormick, 1999) were kindly provided by Elisa Martì (IBMB, Barcelona). The following DNAs were inserted into pCIG: full coding mouse Alex3 and Armc10, Alex3Δ(1-12).

Animals

OF1 embryos and postnatal mice (Iffra Credo, Lyon, France) were used. The mating day was considered embryonic day 0 (E0) and the day of birth postnatal day 0 (P0). Animals were anesthetized with 4% halothane prior to sacrifice.

Eggs from White-Leghorn chickens were incubated at 38.5°C in an atmosphere of 70% humidity and staged according to Hamburger and Hamilton (HH) (Hamburger and Hamilton, 1951).

Chick embryos were electroporated with plasmid DNA at 3µ µg/µl in H_2O with 50 ng/ml Fast Green, as reported in Cayuso et al., 2006. Transfected embryos were allowed to

develop to the specific stages, then dissected, fixed and processed for immunohistochemistry or in situ hybridization.

In situ hybridization

Whole mount mice in situ hybridization was performed in E10 embryos, which were fixed, dehydrated and rehydrated in a methanol series (25 – 100%), and permeabilized with 10 μg/μl Proteinase K (Garcia-Frigola et al., 2004).

Whole mount chicken in situ hybridization was performed fixing the embryos overnight at 4°C in 4% paraformaldehyde in PB, rinsed and processed for whole-mount RNA in situ hybridization following standard procedures using specific probes for chick Armc10/SVH. Hybridization was revealed by alkaline phosphatase-coupled anti-digoxigenin Fab fragments (Boehringer Mannheim). Hybridized embryos were postfixed in 4% paraformaldehyde, rinsed in PBT and vibratome sectioned (45 μm).

Immunohistochemistry

Chicken embryos were fixed 2-4 hours at 4°C in 4% PFA in PB, washed in PBS and vibratome sectioned (45 μm). The obtained sections were permeabilized in PB Triton X-100 0.1% and blocked with blocking buffer (1% fetal bovine serum, Roche Diagnostics).

For BrdU detection, chicken embryos were fixed over night at 4°C; sections obtained by vibratome were permeabilized in PB Triton X-100 1%, incubated in 2 N HCl for 30 minutes followed by 0.1 M $Na_2B_4O_7$ (pH 8.5) rinses, further PBT rinses and blocked in blocking buffer. Immunostaining was performed following standard procedures (Lobjois et al., 2008). To label the sections, the following antibodies were used: rabbit anti-Alex3 (1:300, obtained as described in Lopez-Domenech et al., 2012) rabbit anti-GFP (1:500, Invitrogen), rabbit anti-PH3 (1:500, Millipore), rat anti-BrdU (1:500, AbD Serotec), rabbit anti-Armc10/SVH (1:200, Abcam), mouse anti-COXIV (1:500, Invitrogen), mouse anti-Pax7 (1:500, DSHB), mouse anti-Nkx2.2 (1:500, DSHB), mouse anti-Nkx6.1 (1:500 DSHB), mouse anti-Tuj-1 (1:500, Sigma-Aldrich), mouse anti-HuC/D (1:500, Invitrogen), rabbit anti-Sox2 (1:500, Invitrogen). Alexa488-, Alexa562- and Alexa660-conjugated secondary antibodies were purchased from Invitrogen, Carlsbad, CA. After staining, sections were mounted in Mowiol, photographed using a Leica SPE Confocal microscope, and processed with Adobe Photoshop CS3. Cell counting was carried out on pictures obtained from at least four different chick embryos per experimental condition.

In vivo luciferase-reporter assay

Transcriptional activity assays of β-catenin/Tcf pathways were performed in vivo. Chick embryos were electroporated at HH stage 11-12 with the indicated DNAs cloned into pCIG or with empty pCIG vector as control; together with a TOPFLASH luciferase reporter construct containing synthetic Tcf-binding sites (Korinek et al., 1998) and a renilla-luciferase reporter construct carrying the CMV immediate early enhancer promoter (Promega) for normalization. Embryos were harvested after 24 hours incubation *in ovo* and GFP-positive neural tubes were dissected and homogenized with a douncer in Passive Lysis Buffer. Firefly- and renilla-luciferase activities were measured by the Dual Luciferase Reporter Assay System (Promega).

Cell culture and transfection

HEK293AD cells were used for all the experiments. Cells were cultured in DMEM medium supplemented with 10% Fetal Bovine Serum (FBS), 2mM glutamine, 120 μg/ml Penicillin and 200 μg/ml Streptomycin and were maintained at 37ºC in the presence of 5% CO_2. Upon confluence, cells were trypsinized and plated at the desired density. After 24 h cells were transfected using Lipofectamin™ (Invitrogen), following manufacturer's instructions, and using a 1:1 DNA ratio when two constructs were transfected. For immunoprecipitation or immunocytochemistry assays, an empty vector was used to balance transfected DNA when required. Cells were processed as required, 24-48 h after transfection.

Generation of HEK293AD stable cell lines

HEK293AD cells stably expressing Alex3GFP or GFP were generated by transfection with Alex3 or pEGFP-C1 vectors, expressing also geneticin resistance. Cells were kept in selective media containing 0.9 mg/ml geneticin until colonies development. About 12 colonies for plate were picked and Alex3GFP or GFP expression was analyzed for each colony by fluorescence and western blot analysis in order to choose the better clone.

Neuronal primary culture and transfection

E16 mouse brains were dissected in PBS containing 0.6% glucose and the hippocampi were dissected out. After trypsin (Invitrogen, Carlsbad, CA) and DNase treatment (Roche

Diagnostics), tissue pieces were dissociated by gentle sweeping. Cells were then counted and seeded onto 0.5 mg/ml poly-L-lysine (Sigma-Aldrich)-coated coverslips (for immunocytochemistry) or 35-mm *Fluorodish* plates (World Precision Instruments, Inc) for live-imaging in neurobasal medium (Gibco) containing 2mM glutamax, 120 µg/ml Penicillin, 200 µg/ml Streptomycin and B27 supplement (Invitrogen, Carlsbad, CA), and were maintained at 37ºC in the presence of 5% CO_2. Cells were cultured for between 7 and 15 days. Transfection of neurons was carried out at 10-12 DIV for immunocytochemistry experiments and at 4 DIV for live-imaging, using Lipofectamine 2000 (Invitrogen), following the manufacturer's instructions, and using a 1:3 DNA ratio when transfection of two constructs was required. Cells were processed 24-48 h after transfection.

Immunocytochemistry

HEK293AD cells or neurons were fixed for 15 min in 4% paraformaldehyde. After fixation, cells were permeabilized with Triton X-100 0.1% in PBS and blocked with blocking buffer (10% fetal bovine serum (Roche Diagnostics), 0.2 M glycine, 0.1% Triton X-100 and 0.05% Deoxicolic acid in PBS-2% gelatin) for 1 h at room temperature. To label the cells, the following antibodies or dyes were used: rabbit anti-Alex3 (1:300, HEK293AD; 1:100, neurons; obtained as described in Lopez-Domenech et al., 2012), rabbit anti-GFP (1:500, Invitrogen), mouse anti-myc (1:500, Santa Cruz) and Phalloidin-TRITC (1:1000, Sigma-Aldrich), rabbit-PH3 (1:500, Millipore), rat-BrdU (1:500, AbD Serotec) in blocking buffer for 2 h and with the corresponding secondary antibodies labelled with fluorocromes (Alexafluor 546 or 488, Invitrogen, Carlsbad, CA). Nuclei were stained with the specific dye Hoechst-33342. When necessary, mitochondria labelling was carried out by incubation with the mitochondrion-selective dye, MitoTracker Orange CM-H2TMRos (1:2000, Molecular Probes, Invitrogen) in culture medium for 30 min at 37ºC prior to cell fixation, or by incubation with bromodeoxyuridine (BrdU), 0.5 µg/µl BrdU 40 minutes prior to fixation. All samples were then mounted on Mowiol.

Live-imaging and quantification of axonal transport of mitochondria

HEK293AD cells and hippocampal neurons were seeded onto Poly-L-lysine-coated *Fluorodish* plates (World Precision Instruments, Inc), transfected with Alex3-GFP,

MitDsRed or Mito-PAGFP and filmed 24 to 48 h after using a Leica TCS SP2 confocal microscope (Leica Microsystems) equipped with a 63x immersion oil objective. All the cultures were kept at 37ºC using a heating insert on the microscope stage and an incubating chamber allowing circulation of a controlled CO_2 (5%)-air heated mixture for the control of pH. For mitochondrial aggregation in transfected HEK293AD cells, time-lapse series of image stacks composed of 10 images (512x512 px) were taken every 5 min over 6 h using Leica Confocal Software (Leica Microsystems). Movies were generated at 10 frames per second. For mitochondrial fusion analyses in HEK293T cells, time-lapse series of image stacks composed of 7 images (512x512 px) were taken every 6 sec over 15 min. Movies were generated at 7 frames per second. For measurements of axonal mitochondrial transport, axonal processes in transfected neurons were identified following morphological criteria, and directionality was determined for each axon. Axonal mitochondria were registered with an additional digital zoom of 1.7x. Time-lapse series of image stacks composed of 5 images (512x512 px) were taken every 6 sec during 15 min. All 151 images obtained were processed mainly with Leica Confocal Software. Further image processing, analysis and video compilation (10 frames per second) and edition was done with ImageJ software (version 1.43K, NIH, USA). Kymographs were generated with MetaMorph Software (Molecular Devices - MDS Analytical Technologies). In overexpression experiments, 42 axons were registered and analyzed in each condition while in silencing experiments 22 axons per group were recorded. In all cases a mitochondrion was considered motile when it moved more than 0.5 μm during 1 min of recording. Distances and speeds of retrograde and anterograde transport were measured separately from the corresponding kymographs (De Vos et al., 2007), and no tracking-plugging was used. ImageJ software was used to quantify mitochondrial length. The first frame recorded of each video was digitally processed and thresholded (using Yi algorithm), and the longest distance between any two points along the selection boundary (Feret's parameter) was measured for all mitochondria. To ensure equal relevance between axons, independently of the number of mitochondria displayed, an average length was calculated for each neuron and then the mean was calculated between axons. For the analysis of the length distribution of the population of mitochondria, all the mitochondria measured in a group were considered together, independently of the neuron to which they belonged, and were compared with the other conditions.

Protein cell extracts and Western blot

HEK293AD cells were obtained and lysed in Laemmli Buffer (LB) at 98ºC for 5 min. Brain extracts were obtained by homogenization in lysis buffer (50 mM HEPES; 150 mM NaCl; 1,5 mM $MgCl_2$; 1 mM EGTA; 10% glycerol; 1% Triton X-100; protease inhibitor cocktail (Roche Diagnostics Gmbh), 1 mM NaF, 0.5 M sodium pyrophosphate and 200 mM ortovanadate). 20 µg of protein for each sample was loaded and run in polyacrylamide gels at 100 V. Transfer to nitrocellulose membranes was performed in 120 mM glycine, 125 mM Tris, 0.1% SDS, and 20% methanol at 35 V o.n. Membranes were then blocked in 5% powder milk in TBS and incubated with primary antibodies anti-Alex3 (1:2000, obtained as described in Lopez-Domenech et al., 2012), rabbit anti-Armc10/SVH (1:800, Abcam), rabbit anti-GFP (1:1000, Invitrogen), mouse anti-myc (1:2000, Santa Cruz Biotechnologies) or mouse anti-KHC (1:1000, Millipore). Mouse anti-actin was used as a loading control (1:1000, Chemicon, Temecula, CA). Secondary antibodies coupled to HRP were used diluted 1:2500 in TBS containing 5% powder milk. Labelling was visualized with ECL plus (Amersham Pharmacia Biotech).

Immunoprecipitation

HEK293AD cells were lysed using a buffer containing 50 mM Tris-HCl pH7.5; 150 mM NaCl; 1.5mM $MgCl_2$; 5 mM EDTA; 1% Triton-100; 10% glycerol; protease inhibitor cocktail (Roche Diagnostics Gmbh); 1 mM NaF; 0.5 M sodium pyrophosphate and 200 mM ortovanadate. 500 µg of total protein per sample was used for the immunoprecipitation assays. Homogenates were incubated with anti-GFP (1:500, Invitrogen), anti-myc (1:500, Santa Cruz Biotechnology), at 4ºC o.n overnight. All the assays were performed using protein G-Sepharose beads (Sigma-Aldrich) for 2 h at 4ºC. In the assays performed in the presence of Ca^{2+}, EDTA and EGTA were omitted from the lysis buffer and Ca^{2+} was added to a final concentration of 2 mM. After incubation with protein G-Sepharose, samples were washed five times in washing buffer (10 mM Tris-HCl pH8, 500 mM NaCl, 1 mM EDTA, 1 mM EGTA, 1% Triton X-100, 0.5% NP-40) in which EDTA and EGTA were again substituted by 2 mM Ca^{2+} when required. LB was added to the beads and they were then boiled at 98ºC for 5 min. Proteins were then analyzed by SDS-PAGE and WB.

In vitro GST pull-down

GST-fusion proteins were produced in *E. coli* and purified as described previously (Kittler et al., 2006). Brain lysates (5 mg of total protein, adult brain) were solubilized in a buffer containing 50mM HEPES, 125 mM NaCl, 1% Triton, 2 mM EDTA, 1 mM PMSF, and antipain, pepstatin, and leupeptin at 10 mg/ml. Solubilized material was ultracentrifuged and the supernatant (solubilized protein) was exposed to 20 mg brain lysate with varying concentrations of [Ca^{2+}]. Bound material was washed five times in the above buffer before elution with SDS sample buffer. WB was carried as described above.

Mitochondrial fusion analysis

Intensity correlation analyses were performed against red (photobleached MitDsRed) and green (photoactivated mito-PAGFP) fluorescence images using ImageJ software. PDM (Product of the Differences from the Mean) images from the (+,+) products were obtained and the total intensity of the cell was used to calculate the mitochondrial fusion rate, as described in Lopez-Domenech et al., 2012.

Gene Chip array sample preparation

HEK293AD cells overexpressing GFP were grown in selective culture media containing 0.9 mg/ml geneticin. Total RNA from subconfluent cell cultures was isolated using RNAeasy kit (Qiagen). RNA quality was verified by running samples on an Agilent Bioanalyzer 2100, and samples of sufficient quality were profiled on Affymetrix HG-U219 chips in collaboration with the "Functional genomics" Facility at IRB (Institute for Research in Biomedicine).

Microarray studies were performed using triplicate RNA samples for each condition. Preparation of complementary RNA, array hybridizations and scanning were done following manufacturer's protocols. Laser scansion generated digitized image data files and CEL files (oe53.ga.cel, oe49.ga.cel, oe45.ga.cel, gfp-47.ga.cel, gfp-43.ga.cel, gfp-51.ga.cel, corresponding to each triplicate condition), that were used for the subsequent statistical analysis.

Gene Chip array data analysis

CEL files were processed with RMAexpress to normalize the chip values and obtain

logarithmic expression values for each probe. The setup for RMAexpressed included a background adjusting, a quantile normalization and summarization of the expression values using median polish.

The obtained expression file was loaded into MeV 4.8. A hierarchical clustering (HCL) was performed to analyze the replicates. Pearson correlation was used to cluster the samples, with an average linkage clustering method. On the basis of the clustering, the data from gfp-43.cel was excluded from further analyses.

The SAM (Significance Analysis of Microarray) test was used to identify differentially expressed genes between control (gfp chips) and overexpressed line (oe chips). Significant genes were selected by setting a p-value < 0.05 and a q-value <0.05 as threshold. The q-values were calculated by using a permutation test (100 tests). S0 was calculated using Tusher et al method (Proc. Natl. Acad. Sci. USA., 98:5116–5121, 2001.). A hierarchical tree was constructed from all significant genes using Pearson correlation and an average linkage clustering.

Reactome tools, *http://www.reactome.org/ReactomeGWT/entrypoint.html*, were used to identify specific pathways among the up- and down-regulated genes according to web-site instructions.

Statistical analysis

Data were analyzed with the Igor Pro (WaveMetrics) and Origin 5.0 (Microcal Software) using the Student´s *t* test or the Mann–Whitney–Wilcoxon (MWW) test for non-parametric data. Minimal statistical significance was fixed at $p<0.05$. In figures, * indicates $p<0.05$, ** $p<0.01$ and *** $p<0.001$.

RESULTS

1. - The Eutherian Armcx genes regulate mitochondrial dynamics in neurons: in depth analysis of Armcx3 protein function

1.1 Expression pattern of Armcx transcripts and neuronal expression of Alex3 protein

The Armcx cluster is formed by Armcx1-6 and Armcx6-like pseudogene, originated in early Eutherian evolution by retrotransposition of an Armc10 mRNA, and then by consecutive tandem duplication events in a rapidly evolving region of the Xq chromosome (Lopez-Domenech et al., 2012).

We analysed the expression of several Armcx genes during embryonic development: at embryonic stage E10, Armc10 and Armcx3-6 genes were highly expressed in the developing neural tissues, neural crest derivatives and hind limbs, in addition to other tissues that were specific for each gene (Fig.21).

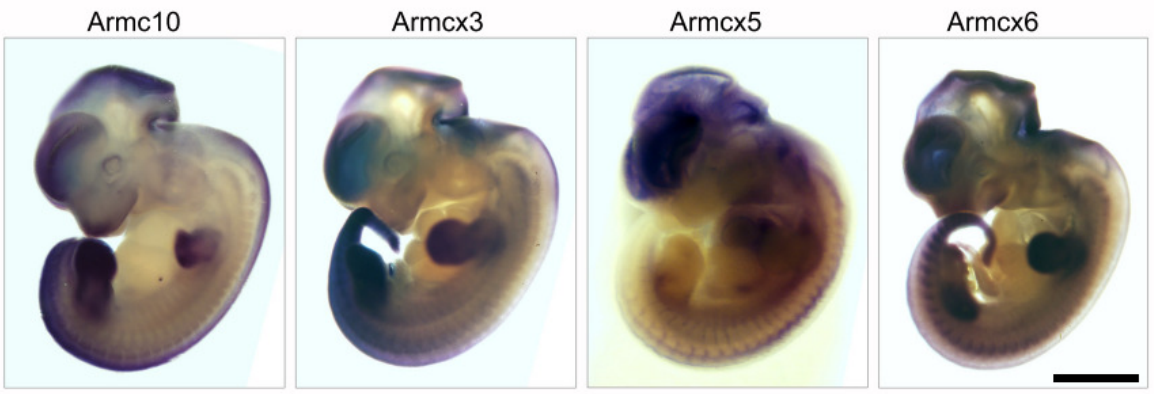

Figure 21: Expression pattern of Armc10 and Armcx3,5,6 transcripts in murine embryos aged E10. In toto in situ hybridization. Note the labeling of many neural structure including the brain, as well as of other tssues, including the hindlimbs, and neural crest derivates. Scale bar: 2mm.

To get insight into the function of Armcx3 in neural tissues, Alex3 protein expression was examined by immunohistochemistry in mouse brain from E16 until adulthood. Thus, at developmental stages, the Alex3 protein showed wide expression in different regions of brain, resulting prominent in laminar structures such as cerebral cortex, hippocampus, olfactory bulb, Purkinje cell layer and granular layer in the cerebellum (Fig.22a,d). Global Alex3 expression decreases during development and in the adulthood, holding over in these laminar structures (Fig.22b-c and Fig.22d-f).

The immunoistochemical analysis showed a bimodal localization of Alex3 protein depending to the brain structure. In most developing neurons Alex3 signal is prominent in

nuclei although it was present also in cytoplasm (Fig.22g). Starting from adult the protein arises cytoplasmatic localization in two neuronal populations: the Purkinje cells and the neurons located into hypotalamic nucleus (Fig.22h).

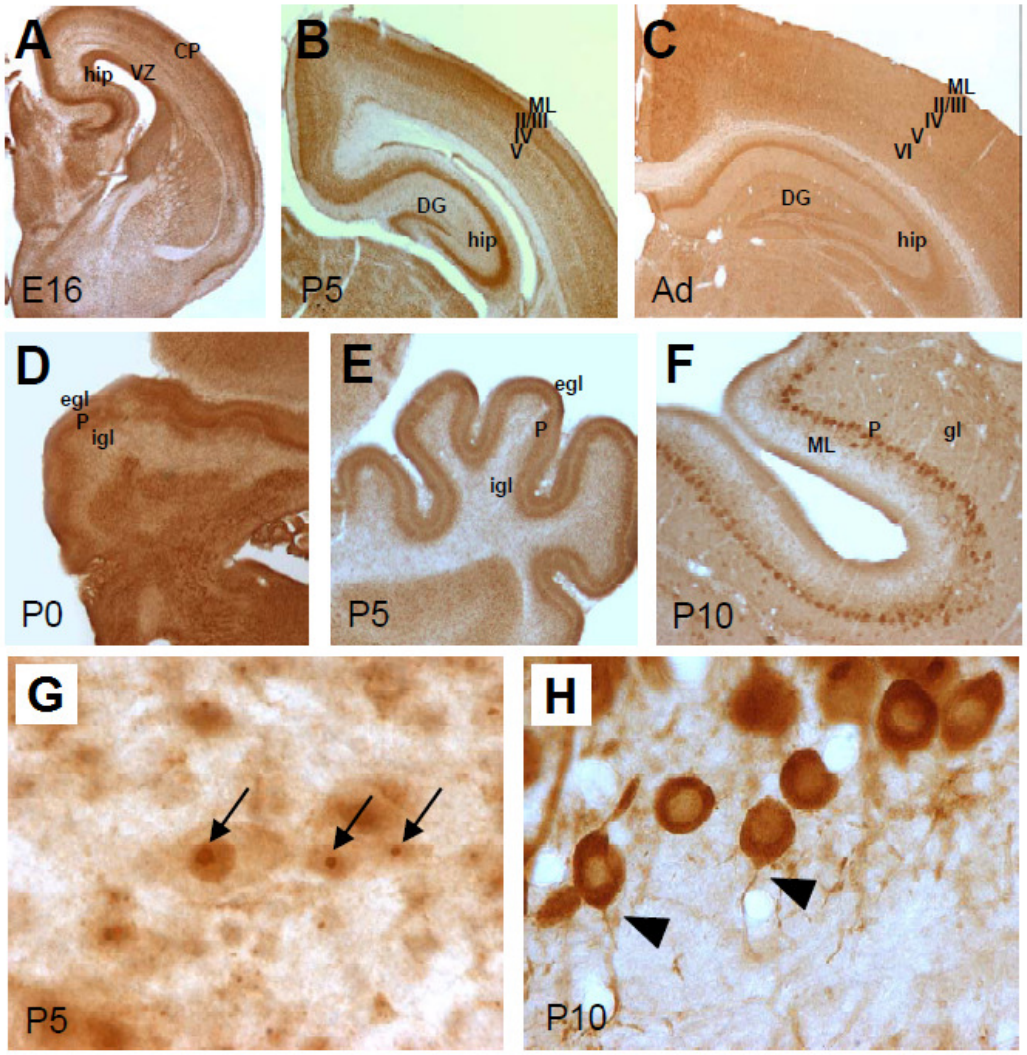

Figura 22: Alex3 protein expression. Alex 3 expression in hippocampus and cortex (**a-c**) and cerebellum (**d-f**) in several developmental stages and in the adulthood. **(g)** Mesencephalic nucleus of P5 mouse brain in which Alex3 has nuclear localization. **(h)** Purkinje cells of P10 mouse brain in which Alex3 has cytosolic localization.
Abbreviations: Ad: Adult; hip, hippocampus; VZ: ventricular zone; ML: molecular layer; DG: Dentate Gyrus; I,II,III,IV,V y VI: neocortical layers; igl, inner granular layer; egl, external germinal layer; gl, granular layer; P: Purkinje cell layer; P 0-5-10: post-natal 0-5-10.

1.2 Alex3 interacts with Mitofusins without altering mitochondrial fusion

Alex3 overexpression leads to mitochondrial aggregation in 293AD cells and neurons, suggesting an involvement in regulation of mitochondrial dynamics (Lopez-Domenech et

al., 2012). Previous date obtained by electronic microscopy showed that Alex3 transfected neurons displayed large aggregates of mitochondria in the cell bodies in which individual mitochondria, surrounded by Alex3-immunorective end product, appeared clearly identifiable. Examination of neurites of these transfected neurons also showed the presence of elongated aggregated mitochondria. These results indicate that Alex3 overexpression leads to mitochondrial aggregation and tethering, rather than increasing mitochondrial fusion (Lopez-Domenech et al., 2012).

However mitochondrial tethering is the first step requiring for mitochondrial fusion and is mediated by Mitofusin proteins (Mfn1 and Mfn2), located at the outer mitochondrial membrane (Huang et al., 2005). We tested by co-immunoprecipitation assay if Alex3 could be able to interact with Mfn1 and Mfn2. HEK293AD cells were co-transfected with Alex3-GFP and Mfn1-myc or Mfn2-myc; cell lysates were immunoprecipitated with anti-GFP or anti-myc antibodies and a faint co-immunoprecipitation was detected in both cases (Fig. 23).

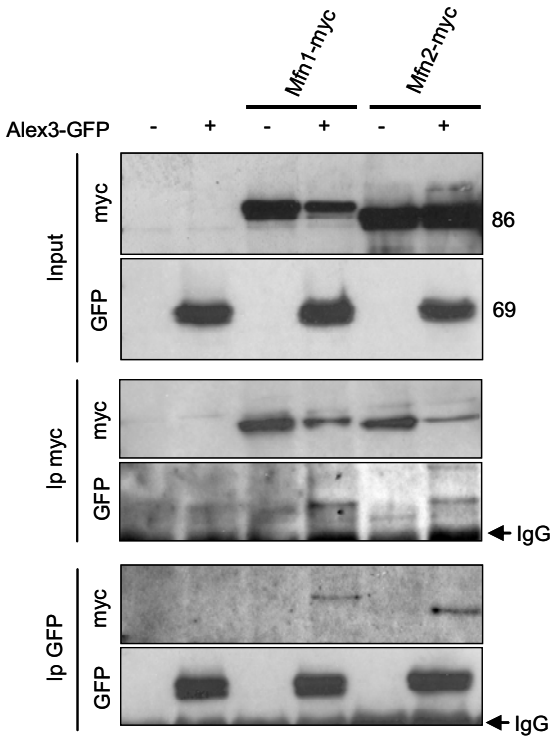

Figure 23: Alex3 interacts with Mitofusin1 and Mitofusin2. HEK293AD cells were transfected with Alex3-GFP and Mfn1-myc or Mfn2-myc. Immunoprecipitation with anti-myc antibodies revealed co-association of Mfn1-myc and Mfn2-myc with Alex3-GFP. The reverse immunoprecipitation with anti-GFP antibodies confirmed interaction with Mfn1-myc and Mfn2-myc.

To directly test whether Alex3 regulates mitochondrial fusion, we took advantage of a photoactivable mito-PAGFP version (Karbowski and Youle, 2004). HEK293AD cells transfected with mito-PAGFP were photoactivated and video recorded over 15 min, and the rates of mitochondrial fusion were analysed (Fig. 24a). In agreement with previous

studies (Gomes et al., 2011; Karbowski and Youle, 2004; Saotome et al., 2008), we observed a constant increase in mitochondrial fusion events over time. The rate and dynamics of these events in cells transfected with Alex3 were identical to those in control cells (Fig. 24c). Similar experiments in hippocampal neurons, either overexpressing Alex3 or a shRNA sequence, gave similar results (Fig.24b,d).

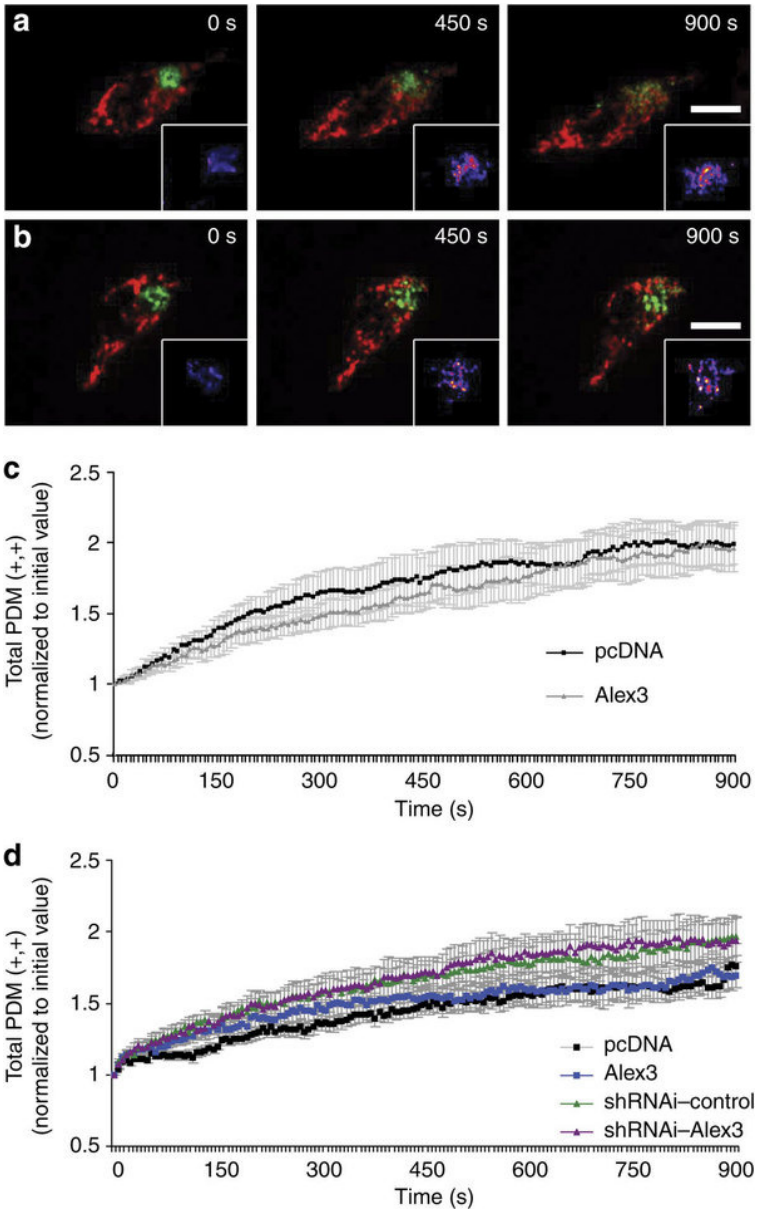

Figure 24: Alex3 protein does not alter mitochondrial fusion. HEK293AD cells were transfected with MitDsRed, mito-PAGFP and pcDNA (**a**), or Alex3 (**b**). Mito-PAGFP was photoactivated, MitDsRed was photobleached at t=0 s, and cells were video recorded over 15 min. Panels in (**a,b**) show the same cell at a range of time points; note the increase in yellow signals representing mitochondrial fusion (insets). The rates of fusion were analysed (**c**) using PDM (+,+) images (shown in boxed areas in (**a,b**)). Eleven cells, corresponding to two independent experiments, were quantified for each group. (**d**) Rates of mitochondrial fusion over time in hippocampal neurons overexpressing Alex3, or a shRNA, demonstrating that Alex3 levels do not alter mitochondrial fusion in neurons. At least eight cells, corresponding to two independent experiments, were quantified for each group. The values show mean±s.e.m. Scale bar: 15 μm.

1.3 Alex3 protein levels regulate axonal transport of mitochondria in hippocampal neurons

Mfn2 was found to interact with the mouse Miro/TRAK2 complex, regulating axonal mitochondrial transport, a process that results essential for neuronal viability (Misko et al., 2010). To address whether Alex3 is involved in mitochondrial transport in axons, we used live-imaging techniques. Cultured hippocampal neurons were transfected at 4 DIV with mitochondrial-targeted DsRed (MitDsRed) or Alex3–GFP. After 2 days, axons were identified and recorded over 15 min (Fig.25). Control neurons exhibited high motility rates for mitochondria, which were transported both in the anterograde and retrograde direction (Fig.25a,b). As described (Hollenbeck and Saxton, 2005), only a fraction of individual mitochondria (about 30%, Fig24.e) moved over the 15-min recording periods, whereas the remaining ones remained stationary. The distance covered in single trafficking events by mitochondria was heterogeneous. While some organelles moved over relatively long distances (more than 100–150 μm), others displaced only a few μm (10–20 μm). The speed at which single mitochondria were transported was also variable (anterograde: average=0.21±0.14 μm per segment; range: 0.07/ 1.03 μm per segment; retrograde: average=0.29±0.15 μm per segment; range 0.07/0.83 μm per segment). Mitochondrial trafficking tended to be more active in the retrograde than in the anterograde direction (Fig.25c).

We recorded only Alex3–GFP-tranfected neurons that displayed an apparently normal distribution of mitochondria in the cell bodies and in axons. In these cultures, Alex3–GFP protein was targeted mainly to mitochondria and virtually all the mitochondrial meshwork displayed Alex3 signals (Fig.24a). We also noted that individual mitochondria were larger in Alex3–GFP-transfected neurons than in control cells (Fig.25a). Examination of video recordings indicated that mitochondrial transport was reduced in these neurons. To confirm this observation, video recordings were represented as kymographs (Miller and Sheetz, 2004) and mitochondrial motility was analysed quantitatively (Fig.25b,e). Overexpression of Alex3–GFP resulted in a dramatic reduction in the percentage of moving mitochondria, in both the anterograde and retrograde directions (Fig.25c). Moreover, the velocity and average distance covered by individual mitochondria was impaired in neurons overexpressing Alex3–GFP (Fig.25c).

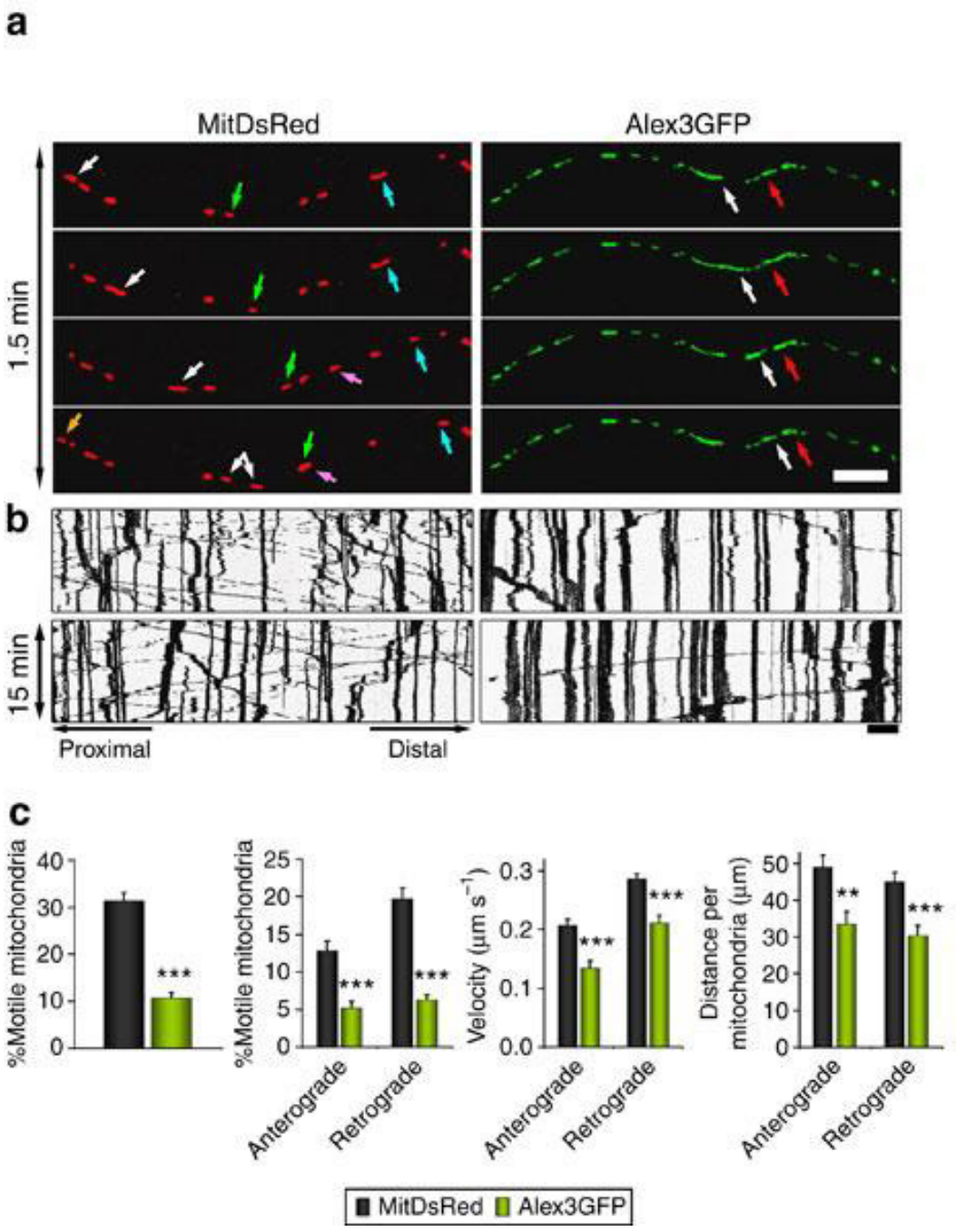

Figure 25: Alex3 overexpression regulates axonal transport of mitochondria in hippocampal neurons. Series of four representative confocal images, taken every 30 s, of live axons overexpressing the mitochondrial-tagged protein MitDsRed or Alex3–GFP fusion protein (**a**). Coloured arrows identify the same mitochondria through the different acquisitions. (**b**) Two representative kymographs showing the full-time acquisition periods (that is, 15 min of movie) in overexpressing experiments. All kymographs are arranged with the distal axonal end to the right. (**c**) Graphical representation of the percentage of motile mitochondria, velocity and distance covered by individual mitochondria measured in kymographs. Data were analysed using the Student's *t*-test and represent the mean±s.e.m of 22–42 axons (neurons) per experimental group, from at least eight independent experiments. ***P<0.001; **P<0.01; *P<0.05 (For individual P see text). Scale bars: 10 μm.

To confirm the involvement of Alex3 in mitochondrial dynamics and trafficking, we performed experiments to knockdown endogenous Alex3 protein. Lentivirus containing different Alex3 specific shRNAi sequences (101, 103,2 01, 302; Fig.26a) were produced and tested for Alex3 silencing together with scrambled vector (402, Fig.26a); one of them (302 shRNA), successfully silencing Alex3 (Fig.26a,b), was selected for perform silencing experiment.

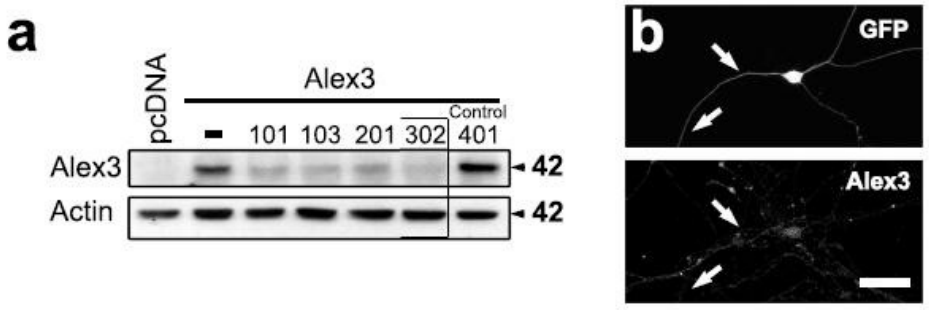

Figure 26: Silencing of Alex3 in transfected HEK293AD cells and in hippocampal neurons. (**a**) HEK293AD cells were transfected with an Alex3 expression construct and pLVTHM containing different Alex3-silencing sequences (101, 103,2 01, 302) and a control scrambled (401) shRNAi. Boxed, 302, shRNAi sequence was selected to perform all silencing experiments. (**b**) Hippocampal neurons transfected with shRNAi 302 and GFP were stained against Alex3 with anti-Alex3 antibody to show the antibody specificity. Note that the neurites from the transfected neuron (arrows) display no immunostaining. Scale bars: 30 μm.

Hippocampal neurons were transfected with pLVTHM vectors expressing shRNAi-Alex3 sequences (Fig.27a,b), or a control scrambled sequence. Neurons expressing shRNAi for Alex3 transcripts were viable and morphologically normal, and they extended normal dendrites and axons (Fig.27a). Alex3–shRNAi-expressing neurons exhibited reduced mitochondrial motility and trafficking and smaller mitochondria than control neurons (Fig.27b,c). This decrease was for anterograde and retrograde transport. However, neither the velocity nor the distance covered by single movements of individual mitochondria was altered by the knockdown of endogenous Alex3 (Fig27.c).

Taken together, these experiments show that Alex3 expression levels regulate the motility of mitochondria in axons in living neurons and modulate both the velocity and distance covered by these organelles.

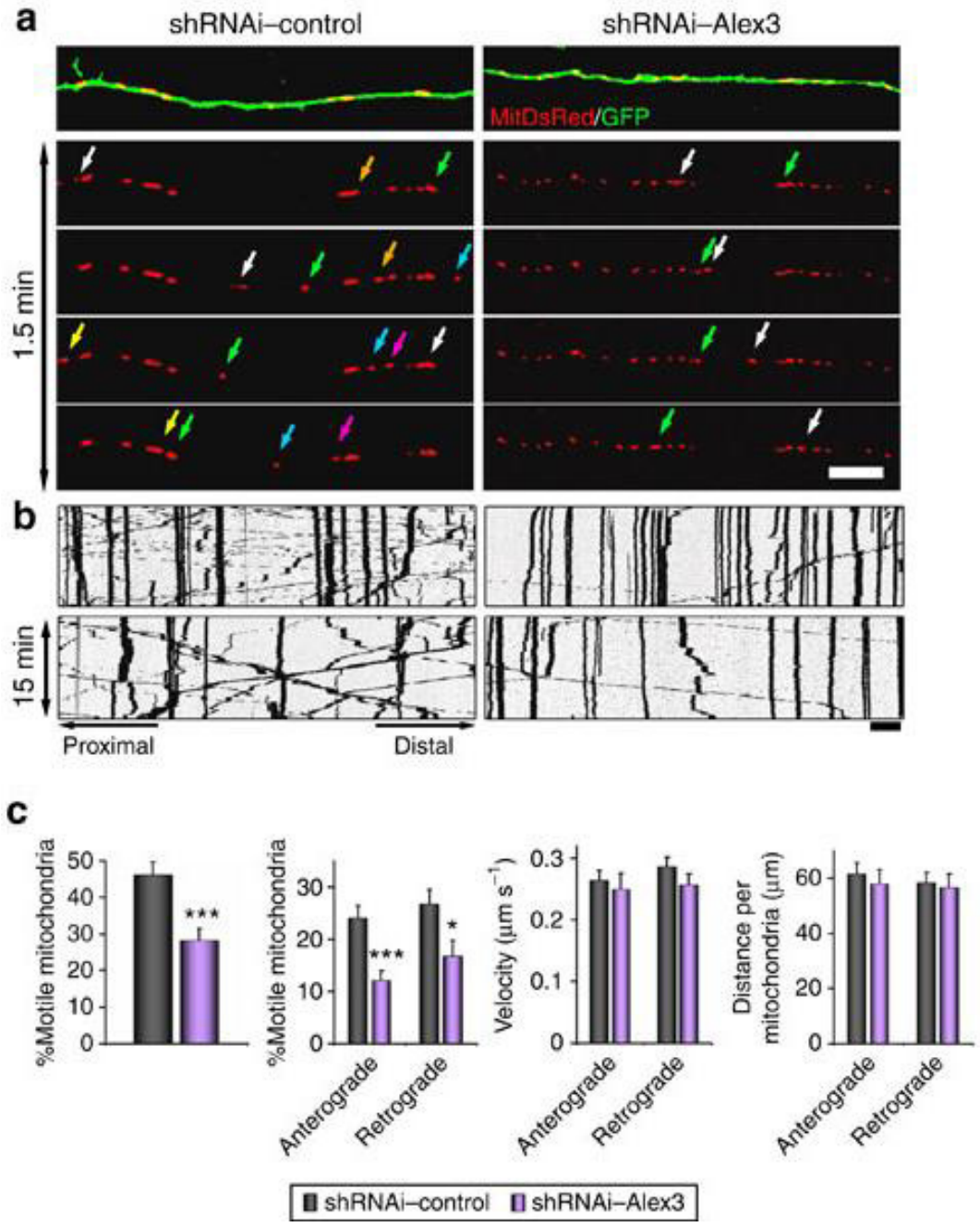

Figure 27: Alex3 silencing regulates axonal transport of mitochondria in hippocampal neurons. Series of four representative confocal images, taken every 30 s, of live axons overexpressing MitDsRed plus a control shRNAi or a specific Alex3 shRNAi. Coloured arrows identify the same mitochondria through the different acquisitions. The upper panel identifies the imaged axon expressing GFP after infection (**a**). Two representative kymographs showing the full-time acquisition periods (that is, 15 min of movie) in silencing experiments. All kymographs are arranged with the distal axonal end to the right (**b**). Graphical representation of the percentage of motile mitochondria, velocity and distance covered by individual mitochondria measured in kymographs for silencing experiments (**c**). Data were analysed using the Student's *t*-test and represent the mean±s.e.m of 22–42 axons (neurons) per experimental group, from at least eight independent experiments. ***P<0.001; **P<0.01; *P<0.05 (For individual P see text). Scale bar: 10 μm.

1.4 Alex3 interacts with Miro and Trak2 proteins and its Arm domains are required for the that interaction

Mitochondrial trafficking in neurons is mediated by Kinesin (KIF5) motors (Hirokawa and Takemura, 2004), by the Kinesin adaptor Trak2 and by the Rho GTPases Miro1 and Miro2 (Guo et al., 2005; MacAskill and Kittler, 2010). We next studied whether Alex3 forms part of the KIF5/Miro/Trak2 trafficking complex. First, immunofluorescence analyses in transfected HEK293AD cells showed strong colocalization of Alex3 with Miro1, Miro2 and Trak2, while no apparent colocalization was detected with KIF5C (Fig.28a-d).

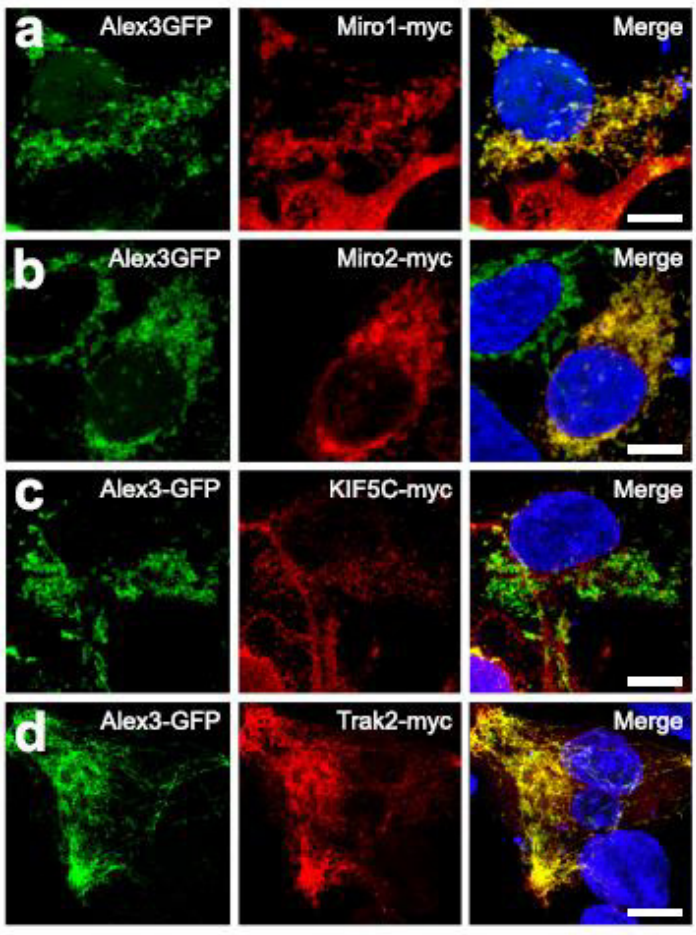

Figure 28: Transfected Alex3-GFP colocalizes with the components of the mitochondrial transport machinery. HEK293AD cells were co-transfected with Alex3-GFP (green) and Miro1-myc (**a**), Miro2-myc (**b**), KIF5C-myc (**c**) and Trak2-myc (**d**) (red) and processed for immunoicitochemistry. Right panels show a merged image where colocalization (yellow) of Alex3-GFP is apparent with Miro1-myc, Miro2-myc and Trak2-myc; Alex3-GFP and KIF5C-myc share low levels of colocalization. Nuclei were stained with Hoecst (blue). Scale bar: 10 μm.

Next, we performed co-immunoprecipitation assays in HEK293AD cells transfected with Alex3–GFP and either Miro1-myc or Miro2-myc cDNAs. Miro1 and Miro2 were detected by WB in lysates immunoprecipitated with anti-GFP antibodies. Conversely, pull-downs with anti-myc antibodies revealed Alex3–GFP protein. No co-immunoprecipitation was detected when cells were transfected with either Miro1/2-myc

or Alex3–GFP DNA alone (Fig.29a). Similar experiments showed that Alex3–GFP was co-immunoprecipitated with Trak2-myc protein (Fig.29c). In contrast, we did not detect co-immunoprecipitation of Alex3–GFP with KIF5C, KIF5A or KIF5B (Fig.29b). These data indicate that Alex3 interacts directly with the Miro1-2/Trak2 proteins, thereby suggesting that this protein is therefore involved in the KIF5/Miro/Trak2 trafficking complex.

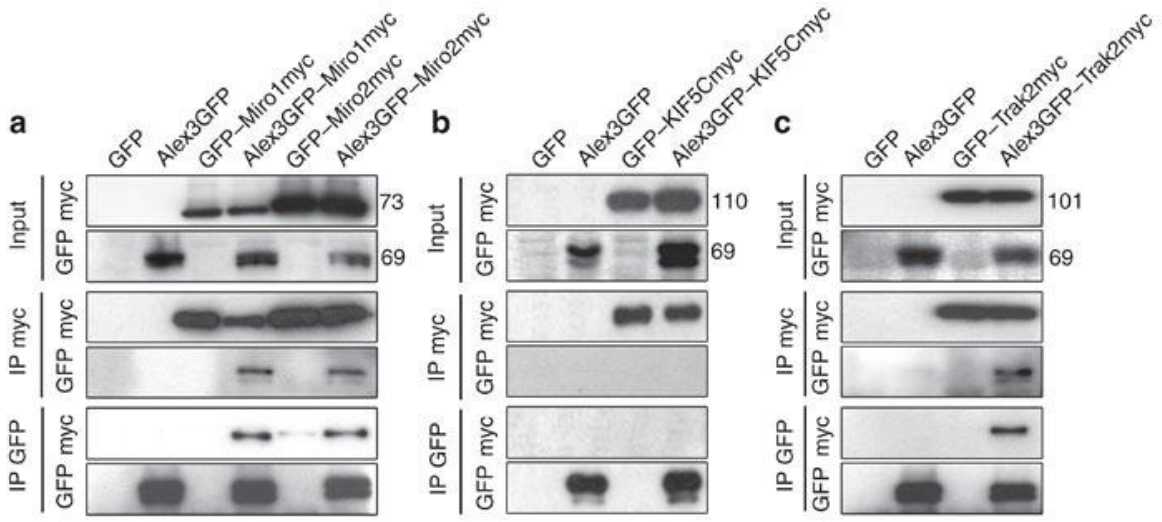

Figure 29: Alex3 is a component of the protein complex responsible for mitochondrial transport. Co-immunoprecipitation of Alex3–GFP with Miro1myc, Miro2myc, KIF5Cmyc or Trak2myc results in the specific interaction of Alex3–GFP with Miro1myc, Miro2myc (**a**) and Trak2myc (**c**) but no interaction is detected between Alex3–GFP and KIF5Cmyc (**b**). A GFP construct was used as control.

To determine whether the Arm-like domains of Alex3 were required for interaction with these proteins, we generated a N-terminus Alex3(1-106) construct lacking the six Arm domains. Co-immunoprecipitation experiments in HEK293T cells showed that this mutant protein did not co-immunoprecipitate with Trak2 or Miro2 proteins (Fig.30a,b), thereby indicating that the Arm-containing C-terminal region is required for this interaction.

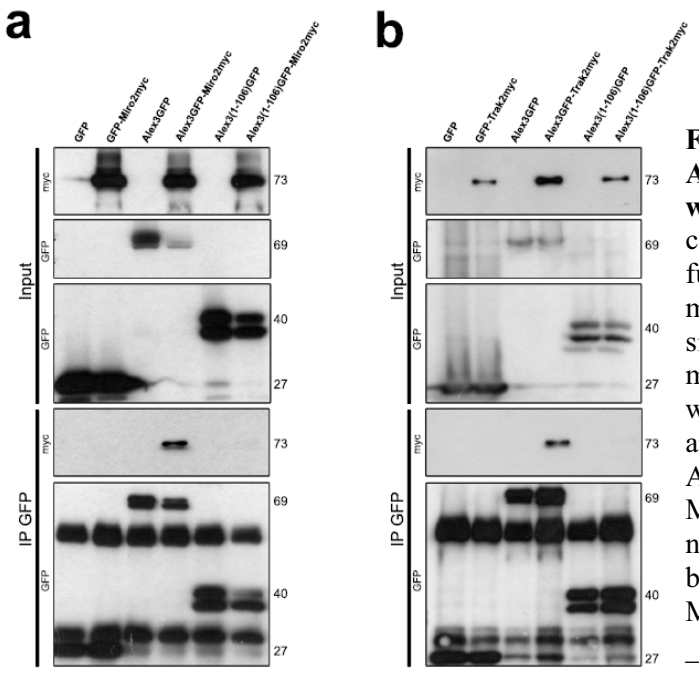

Figure 30: The Arm domains of Alex3 are required for interaction with Miro2 and Trak2. HEK293T cells were co-transfected with full.lenght Alex3-GFP or a deletion mutaln Alex3-GFP(1-106) lacking all six Arm domains, and with Miro2-myc (**a**) or Trak2-myc (**b**); cell lysates were co-immunoprecipitated with anti-GFP antibodies. While full length Alex3 immunoprecipitated with Miro2-myc protein and Trak2 protein, no co-immunoprecipitation was found between Alex3-GFP(1-106) and Miro2-myc or Trak2-myc.

The Miro/Trak2 complex interacts with Kinesin motors in a Ca^{2+}-dependent manner, in which Ca^{2+} binding to Miro proteins triggers the uncoupling of the complex to microtubules, thereby allowing mitochondrial arrest (MacAskill et al., 2009a; Wang and Schwarz, 2009). We thus tested whether the association of Alex3 with the trafficking complex was also Ca^{2+}-dependent. The presence of 2 mM Ca^{2+} markedly reduced the interaction of Alex3 with Miro1, 2 and Trak2 (Fig.31a,d). Interestingly, cotransfection of Alex3–GFP with a Miro1-myc mutant cDNA lacking the EF-hand domain responsible for Ca^{2+} binding blocked the regulation of Miro1/Alex3 interaction by Ca^{2+}, thereby reinforcing the notion that the interaction between these two proteins is regulated by Ca^{2+} levels (Fig.31b). To corroborate these findings, we purified GST-Miro1 protein and performed pull-downs with extracts from brain lysates (MacAskill et al., 2009a). These experiments confirmed the direct interaction of Alex3/Miro1 proteins, as well as the regulation of this interaction by Ca^{2+} and the dependence on the EF-hand domain in Miro1 protein for the regulation of the complex by Ca^{2+} (Fig.31d). Taken together, the above data demonstrate that Alex3 belongs to the KIF5/Miro1-2/Trak2 mitochondrial trafficking complex and that the Alex3/Miro1 protein interaction requires low Ca^{2+} concentrations.

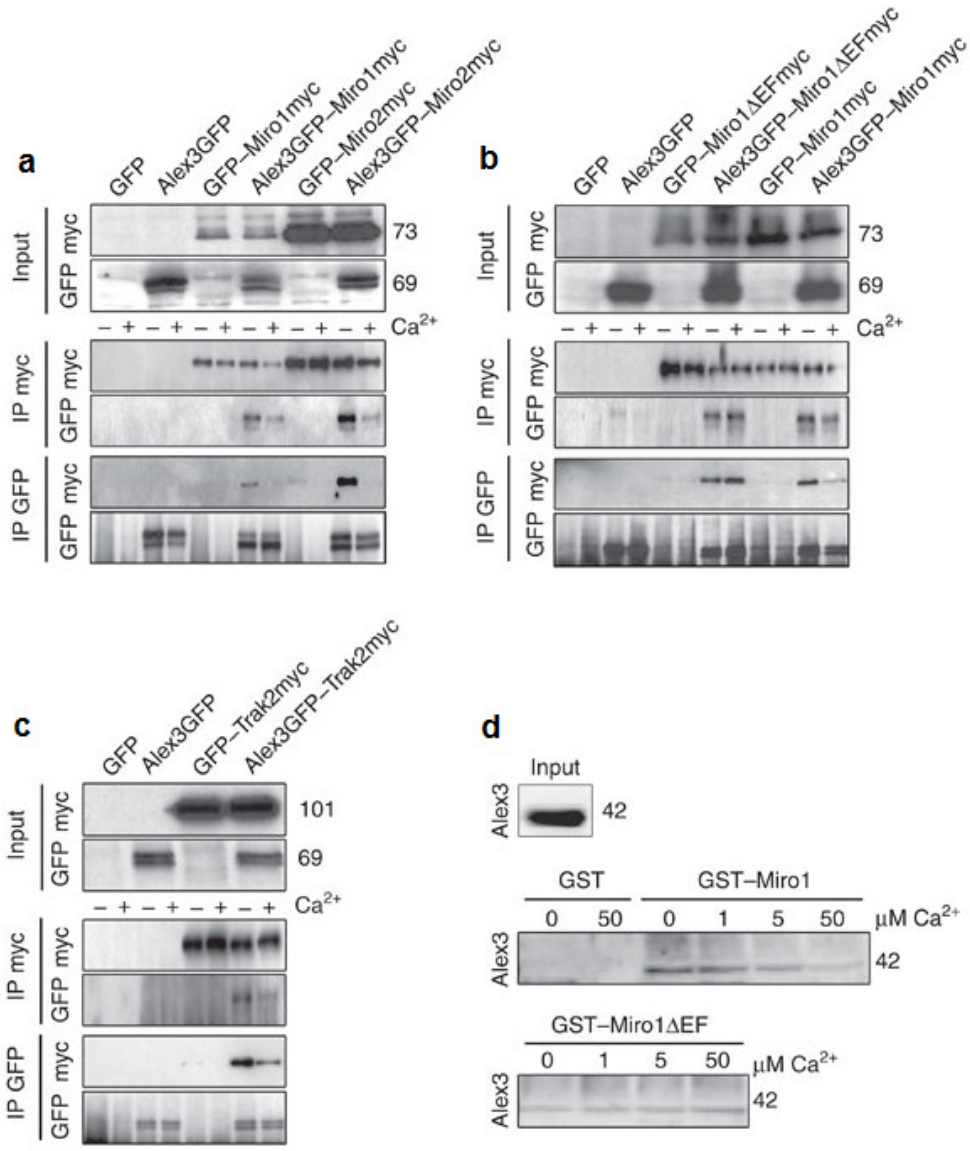

Figure 31: The interaction between Alex3 and the protein complex responsible for mitochondrial transport depends on Ca^{2+} levels. (**a**) The interaction between Alex3–GFP and Miro1myc and Miro2myc is reduced in the presence of 2 mM of calcium. (**b**) When the EF-hand mutant form of Miro1myc is co-expressed with Alex3–GFP, the interaction between the two components is no longer sensitive to Ca^{2+} levels. (**c**) The association between Alex3–GFP and Trak2myc is also dependent on the presence of Ca^{2+}, thereby indicating that the whole complex could be dismantled when Miro1/2 recognizes an increment in Ca^{2+} levels. (**d**) Pull-down assays using purified GST–Miro1 and GST–Miro1ΔEF proteins as bait and showing interaction with Alex3 (in brain lysates) and its dependence on Ca^{2+}concentration (top panel). The lack of the EF-hand domain in Miro-1 protein abolishes Ca^{2+} dependence (bottom panel).

2. - The Armc10/SVH ancestral gene also regulates mitochondrial dynamics in neuron and interacts with Miro/Trak2 complex

2.1 - Neuronal expression and cellular localization of Armc10/SVH protein

In contrast to the Armcx 1-6 proteins, which are encoded by single exons arrayed in a gene cluster in chromosome X (Lopez-Domenech et al., 2012), the mouse Armc10 protein sequence is encoded by 7 exons localized in chromosome 7q11.22 (Huang et al., 2003). It has been proposed that up to 6 isoforms arise from alternative splicing of the Armc10 gene. Of these, 4 have been detected in human hepatocarcinoma cells (Armc10 A-D) (Huang et al., 2003). The Armc10 protein contains a transmembrane domain at the N terminus (aa 7-29), a putative cleavage site (aa 30-36), and also a flanking basic region near the transmembrane region (similar to that found in Tom20 and Bcl-w), which predicts putative targeting to the outer mitochondrial membrane (Rapaport, 2003). Full-length Armc10 (A isoform) contains up to 6 armadillo domains arranged in a DUF634 domain (aa 85-337). The former are partially deleted in some isoforms. The protein also contains nuclear export signals and several potential phosphorylation sites (Fig.31a).

Western blot (WB) experiments revealed that an anti-Armc10 antibody recognized up to 4 bands in untrasfected HEK293T cells (Fig. 32b). These bands corresponded presumably to different Armc10 isoforms. WBs of embryonic and adult brain lysates showed a prominent 31- kDa band, which is likely to correspond to the Armc10 C and/or E isoforms. We analyzed the regional and cellular patterns of protein distribution by immunohistochemistry. Thus, the Armc10 protein showed wide expression both at developmental (E16-P5) and adult (Fig. 32c-g) stages, labelling many neuronal populations. Labelling was prominent in the cerebral cortex, hippocampus, thalamus and cerebellum. In most developing and adult neurons Armc10 signals were prominent in neuronal nuclei and fainter staining was detected in neuronal perikarya and in the neuropile.

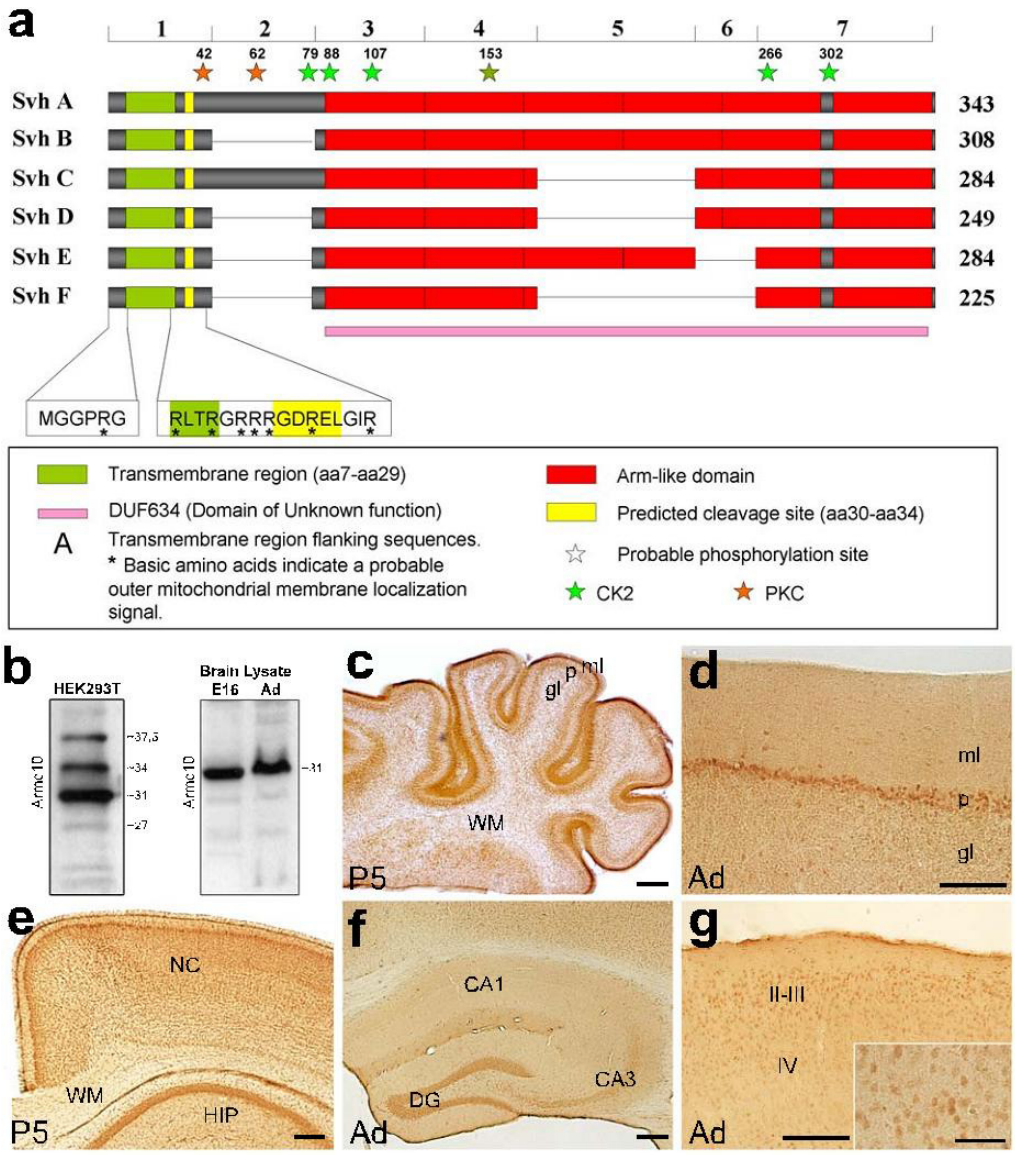

Figure 32. Schematic representation of Armc10 isoforms and expression of Armc10 protein. (**a**) Structure, domains and putative phosphorylation sites of six Armc10 (A-E) isoforms. They all have an N-terminal potential transmembrane region and a predicted cleavage site. The C-terminal domain (DUF634) consists of up of six Arm-like tandem repeats, the distribution of which depends on the alternative splicing pattern of the Armc10 gene (see numbers above representing exons). Stars point to putative phosphorylation sites by CK2 and PKC kinases. (**b**) WB showing that an anti-Armc10 antibody recognizes four Armc10 bands, presumably corresponding to isoforms (37.5, 34, 31 and 27 kDa) in HEK293T cells and one single band, corresponding to isoforms of 31 kDa, in brain lysates from E16 and adult mice. (**c-g**) Coronal sections of P5 and adult mouse brain showing expression pattern of the Armc10 protein in the cerebellum (**c,d**), neocortex (**e,g**) and hippocampus (**f**). Boxed area in (**g**) shows nuclear localization of the Armc10 protein in the neocortex. Abbreviations: Ad: Adult; CA1-CA3: hippocampal regions CA1-CA3; DG: Dentate Gyrus; gl: granular layer; HIP: hippocampus; II-III-IV: neocortical layers; ml: molecular layer; NC: neocortex; p: purkinje cell layer; P5: post-natal 5; WM: White Matter; Scale bars: 100 µm (**c-g**); 50 µm (boxed area in **g**).

To gain insight into the subcellular distribution of endogenous Armc10 protein, we immunostained HEK293T cells and hippocampal primary cultures. These cells exhibited marked co-staining of the Armc10 protein with mitochondrial markers in both cell bodies and neurites (Fig. 33a,b). Faint staining was also visible in the nuclei of cultured neurons (Fig 33b). The above data indicated that, like the Armcx3 protein, Armc10 is widely expressed in the nervous system, where it shows a bimodal localization in mitochondria and the cell nucleus.

2.2 - Armc10 protein regulates mitochondrial aggregation and trafficking.

To examine the role of the Armc10 protein in mitochondrial dynamics, we transfected HEK293T cells and hippocampal neurons with a GFP-tagged Armc10 cDNA. In agreement with the above studies, transfection of Armc10 yielded a preferential localization of this protein in mitochondria (Fig.33c,d). Armcx3 overexpression has been found to lead to mitochondrial aggregation (Lopez-Domenech et al., 2012). To study whether this also held true for the Armc10 protein, we analyzed the mitochondrial phenotypes induced by Armc10-GFP overexpression. In control HEK293AD cells, most control transfected cells (MitDsRed, Fig.33e) displayed a regularly arranged mitochondrial meshwork (as in Fig.33a). In contrast, up to 78% of cells overexpressing Armc10 displayed abnormal mitochondrial phenotypes: while 29% of cells showed strong phenotypes in which mitochondria were aggregated in a single cluster near the cell nucleus (Fig.33d,e), 49% of transfected cells displayed milder degrees of mitochondrial aggregation involving several clusters in which individual mitochondria were still visible (Fig.33c,e).

In contrast, overexpression of Armc10-GFP in cultured hippocampal neurons caused mild mitochondrial aggregation, without leading to severe aggregating phenotypes. Thus, only 33% of transfected neurons displayed mild aggregating phenotypes, with small clusters of mitochondria present in both the cell body and neurites (Fig.33f-h). The differential aggregation phenotypes caused by Armc10 overexpression in HEK293AD cells and neurons support the notion of a differential regulation of mitochondrial dynamics and aggregation in these two cell types.

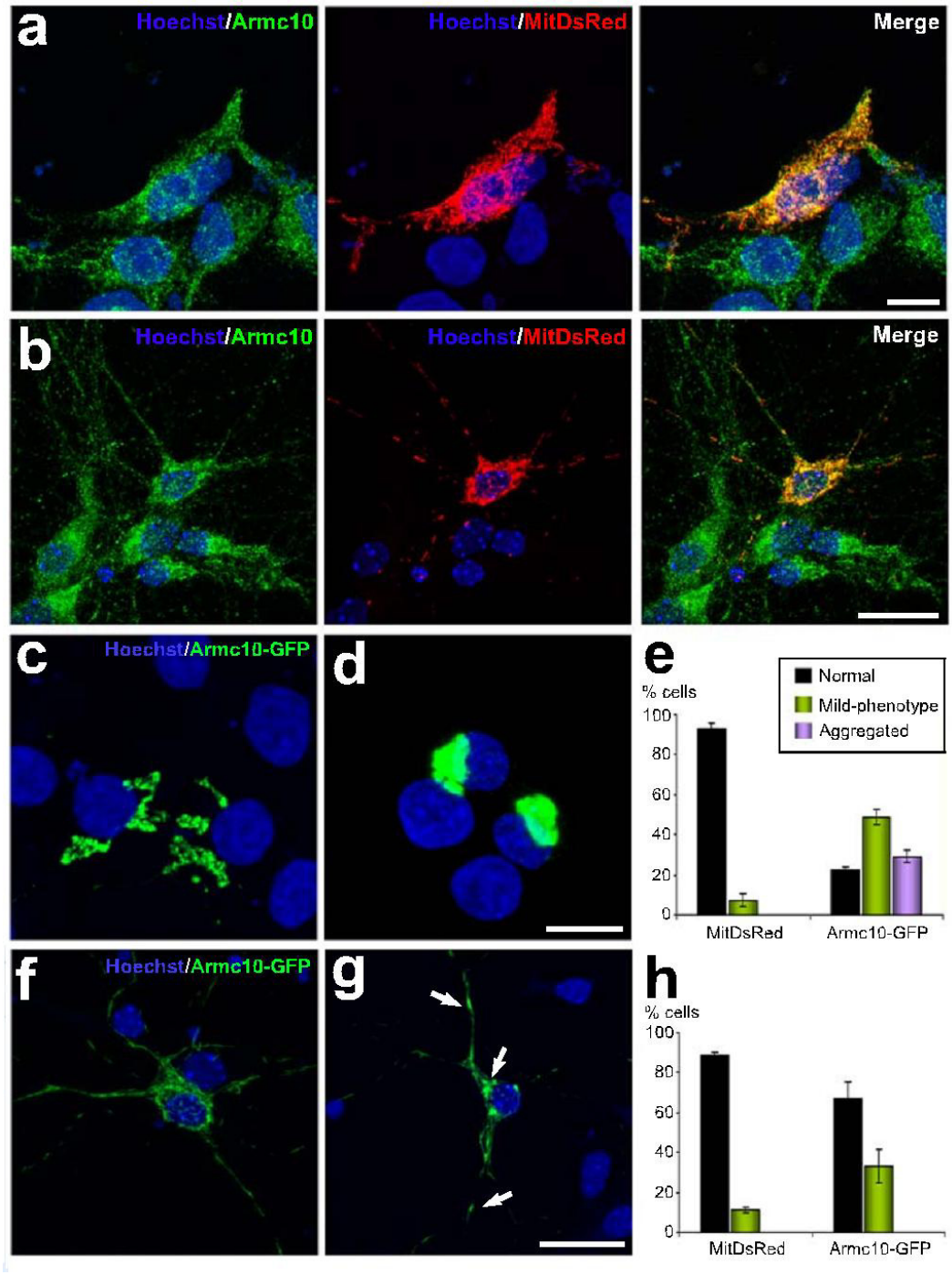

Figure 33. Armc10 co-localizes with mitochondria and its overexpression alters mitochondrial distribution, thus leading to perinuclear aggregation in HEK293AD cells but not in neurons. (**a-b**) Confocal images showing mitochondrial colocalization of endogenous Armc10 (green) with the mitochondrial marker MitDsRed (red) in HEK293AD cells (**a**) and in 6 DIV hippocampal neurons (**b**). (**c-e**) Overexpression of Armc10-GFP in HEK293AD cells induces alterations in the distribution of mitochondria when compared with the expression of MitDsRed control vector. These phenotypes were classified as "normal", "mild" and "aggregated". Examples of HEK293AD cells displaying mild (**c**) and strong (**d**) aggregating mitochondrial phenotypes. (**e**) Histogram illustrating percentages of HEK293T mitochondrial phenotypes after transfection with MitDsRed or Armc10-GFP. (**f-g**) Hippocampal neurons overexpressing an Armc10-GFP cDNA display normal mitochondrial phenotype (**f**) or a mild aggregated phenotype (**g**) with small clusters of mitochochondria in

cell bodies and neurites (arrows). (**h**) Histogram illustrating percentages of hippocampal neurons showing normal and mild phenotypes after transfection with MitDsRed or Armc10-GFP. We counted 62-157 HEK293AD cells and 35-41 neurons per condition. Data represent mean±s.e.m of 3 independent experiments. Nuclei were stained with bisbenzimide (blue). Scale bars: 10 μm (**a,c,d**); 20 μm (**b,f,g**).

To address whether Armc10 protein levels alter mitochondrial trafficking in neurons, we first transfected hippocampal neurons with Armc10-GFP cDNA or with the control vector MitDsRed. Two days later, axons from transfected neurons were identified and recorded over 15 min, and mitochondrial dynamics was quantified using kymographies (Hollenbeck and Saxton, 2005; Lopez-Domenech et al., 2012). Control neurons displayed active mitochondrial trafficking (~30% of mitochondria) in anterograde and retrograde directions (Fig.34a,b). Individual mitochondria moved at an average velocity of ~0.16-0.19 μm/s (for retrograde and anterograde transport, respectively; Fig.34b). Overexpression of Armc10-GFP resulted in a marked decrease in the percentages of motile mitochondria, both in the anterograde and retrograde directions. In contrast, the velocity of the mitochondria that remained motile was unaffected by Armc10 overexpression (Fig.34b). To study the contribution of endogenous Armc10 protein to mitochondrial transport, we designed shRNA sequences corresponding to the C terminal region of Armc10 in order to knockdown all endogenous Armc10 isoforms (Fig.34c). Again, Armc10 downregulation resulted in a percentage of motile mitochondria that was reduced by more than half in the retrograde and anterograde directions of transport, in comparison with control neurons transfected with a scrambled sequence. Interestingly, the velocity of the mitochondria that remained motile was unaffected by the levels of Armc10 protein expression (Fig.34d,e). These findings indicate that Armc10 protein levels regulate mitochondrial trafficking in neurons mainly by controlling the percentage of motile mitochondria.

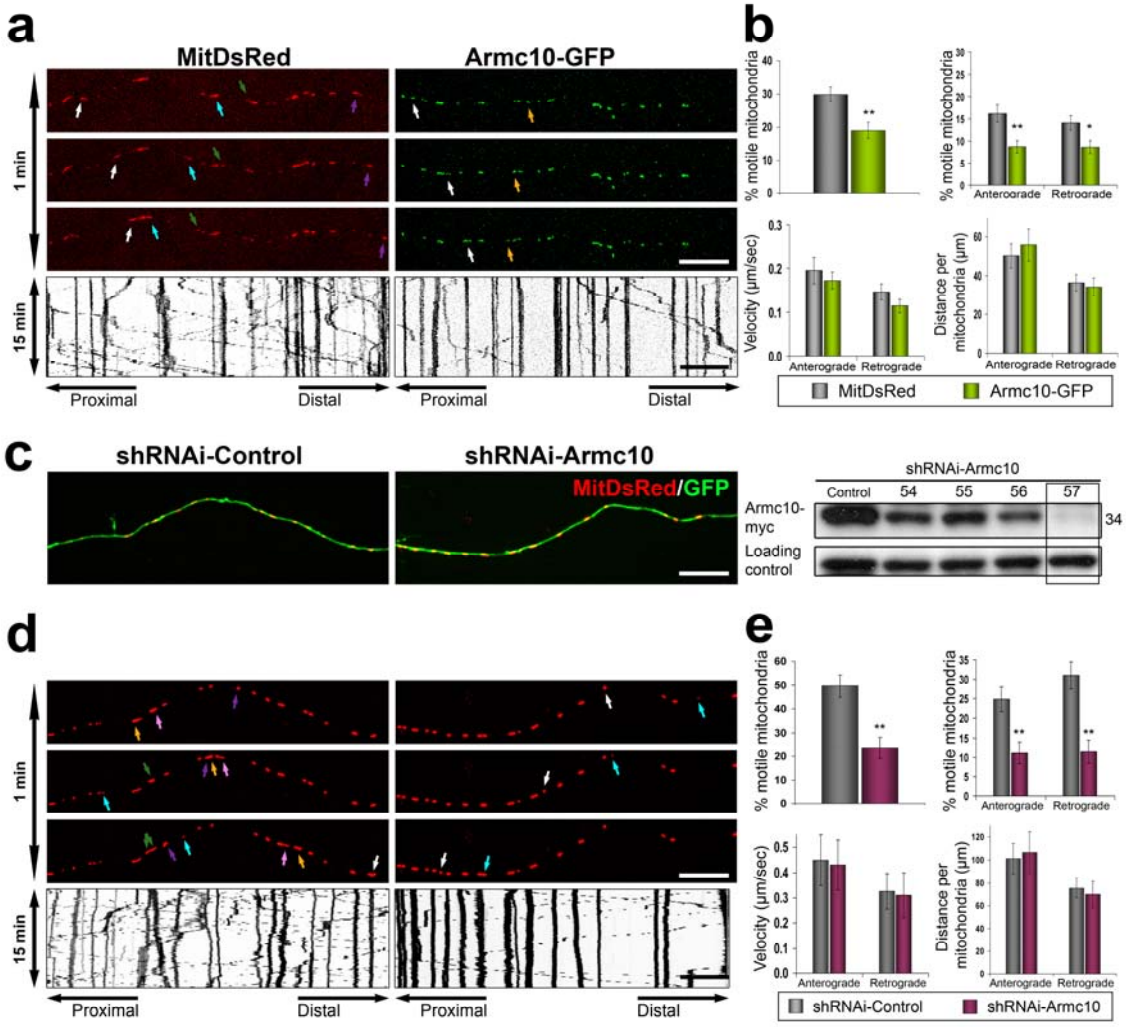

Figure 34: Armc10 protein levels regulate mitochondrial axonal transport in hippocampal neurons. (**a**) Series of three representative confocal images, taken every 30 s, of live axons overexpressing MitDsRed or Armc10–GFP fusion protein. Representative kymographs showing the full-time acquisition periods are shown in lower panels. (**b**) Graphical representation of the percentages of motile mitochondria, and the velocity and distance covered by individual mitochondria measured in kymographs in control and overexpressing neurons. Data represent the mean±s.e.m. (**c**) Examples of axons co-expressing MitDsRed plus an Armc10-specific shRNAi or a control shRNAi. In the right panel HEK293T cells were co-transfected with an Armc10-myc expression construct and pLVTHM, containing several Armc10-specific shRNAi sequences (54, 55, 56, 57) and a scrambled control; cells were lysated and processed for WB with an anti-myc antibody. One Armc10-specific shRNAi sequence (57) dowregulated Armc10 protein expression and was selected to perform the silencing experiments. (**d**) Series of representative confocal images, taken every 30 s, of live axons overexpressing MitDsRed together with an Armc10-specific shRNAi or a control shRNAi. Representative kymographs showing the full-time acquisition periods are shown in lower panels. (**e**) Graphical representation of the percentages of motile mitochondria, and the velocity and distance covered by individual mitochondria measured in kymographs in shRNAi-control and shRNAi-Armc10 overexpressing neurons. Data represent the mean±s.e.m. Scale bars: 10 µm.

2.3 - Armc10 protein interacts with the Miro/Trak2 and Mitofusins

Mitochondrial trafficking in neurons is believed to be controlled by the Kinesin 1 motor protein and by the adaptor and Rho GTPase proteins Trak2 and Miro1-2, respectively (Guo et al., 2005; Pilling et al., 2006; Stowers et al., 2002). We thus studied whether the Armc10 protein interacts with the Kinesin/Miro/Trak2 trafficking complex. Immunofluorescence analyses in transfected HEK293AD cells showed strong colocalization of Armc10 with Miro2 and Trak2, and partial overlapping with KIF5C (Fig.35a). Co-immunoprecipitation experiments in HEK293AD cells transfected with Armc10-GFP and either Miro1-myc or Miro2-myc cDNAs revealed that Miro proteins were detected by WB in lysates immunoprecipitated with anti-GFP antibodies. Conversely, immunoprecipitation with anti-myc antibodies revealed the Armc10-GFP protein. No co-immunoprecipitation was detected when cells were transfected with either Miro1-2-myc or Armc10-GFP DNA alone (Fig.35b and not shown). Co-immunoprecipitation experiments with the mitochondrial adaptor protein Trak2 also revealed co-association with the Armc10 protein (Fig.35b). In contrast, we did not detect co-immunoprecipitation of the Armc10-GFP protein with KIF5C, KIF5A or KIF5B in transfected HEK293AD cells (Fig.35b and not shown).

To support these findings, we performed co-immunoprecipitation assays with adult brain lysates (Fig.35c). The Armc10 protein was found to interact both with Miro1 and Trak2, but not with KHC, the heavy chain of Kinesin 1. The reverse immunoprecipitation, with Trak2 and Miro1 antibodies, also yielded the Armc10 protein (Fig.35c).

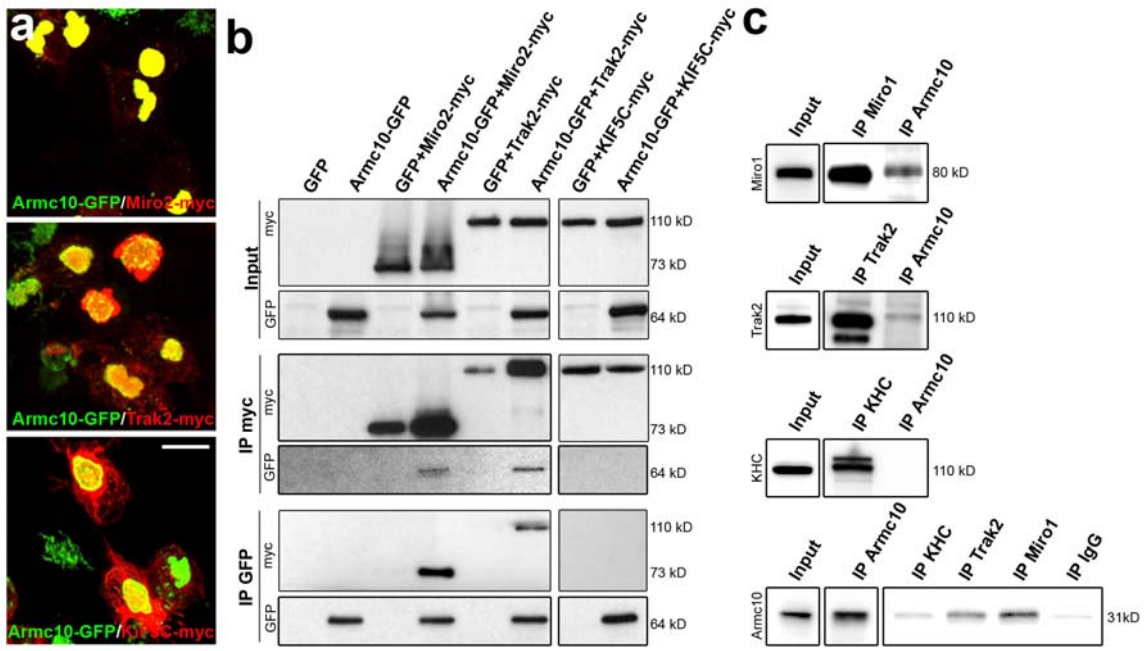

Figure 35: Armc10 colocalizes and interacts with Miro1-2 and Trak2 but not with KIF5C proteins. (**a**) HEK293AD cells were transfected with Armc10-GFP and Miro2-myc, Trak2-myc or KIF5C-myc and processed for immunocytochemistry. Note the high degree of colocalization with Miro2 and Trak2, and partial colocalization with KIF5C. (**b**) Co-immunoprecipitation expreriments in transfected HEK293AD cells. Immunoprecipitation with myc antibodies revealed co-association of Miro2-myc and Trak2-myc with Armc10-GFP protein. The reverse immunoprecipitation with GFP antibodies revealed interaction with Miro2-myc and Trak2-myc proteins. No co-association was observed with KIF5C-myc. (**c**) Immunoprecipitation experiments in adult brain lysates. Immunoprecipitation with Armc10 antibodies reveals co-association with Miro1 and Trak2, but not with KHC (three upper panels). The reverse immunoprecipitation shows interaction of Miro1 and Trak2 with Armc10 (bottom panel). Scale bar: 10 µm.

Recent studies underlines the role of the main actors in mitochondrial fusion process, Mitofusin2 (Mfn2) in regulation of mitochondrial transport. Mfn2 is directly involved in and required for axonal mitochondrial transport, distinct from its role in mitochondrial fusion (Misko et al., 2010). Live imaging of neurons cultured from Mfn2 knock-out mice or neurons expressing Mfn2 disease mutants shows that axonal mitochondria spend more time paused and undergo slower anterograde and retrograde movements, indicating an alteration in attachment to microtubule-based transport systems. Moreover, both Mfn1 and Mfn2 interact with mammalian MIRO proteins and Trak2 (Misko et al., 2010). We thus studied whether Armc10 can also interact with Mitofusin1 and Mitofusin2. Immunofluorescence analyses in transfected HEK293AD cells showed strong colocalization of Armc10 with Mitofusin1 and Mitofusin2 (data not showed). Co-

immunoprecipitation experiments in HEK293AD cells transfected with Armc10-GFP and either Mitofusin1-myc or Mitofusin2-myc cDNAs revealed that Mitofusin proteins were detected by WB in lysates immunoprecipitated with anti-GFP antibodies. The reverse immunoprecipitation, with anti-myc antibodies, also yielded the Armc10 protein. No co-immunoprecipitation was detected when cells were transfected with either Miro1/2-myc or Armc10-GFP DNA alone (Fig.36a). The interaction between Armc10 and Mfn2 was confirmed immunoprecipitating ectopically expressed in HEK293AD Armc10GFP with anti-GFP antibody and detecting endogenous Mfn2 in co-immunioprecipitate with anti-Mitofusin2 antibody (Fig.36b).

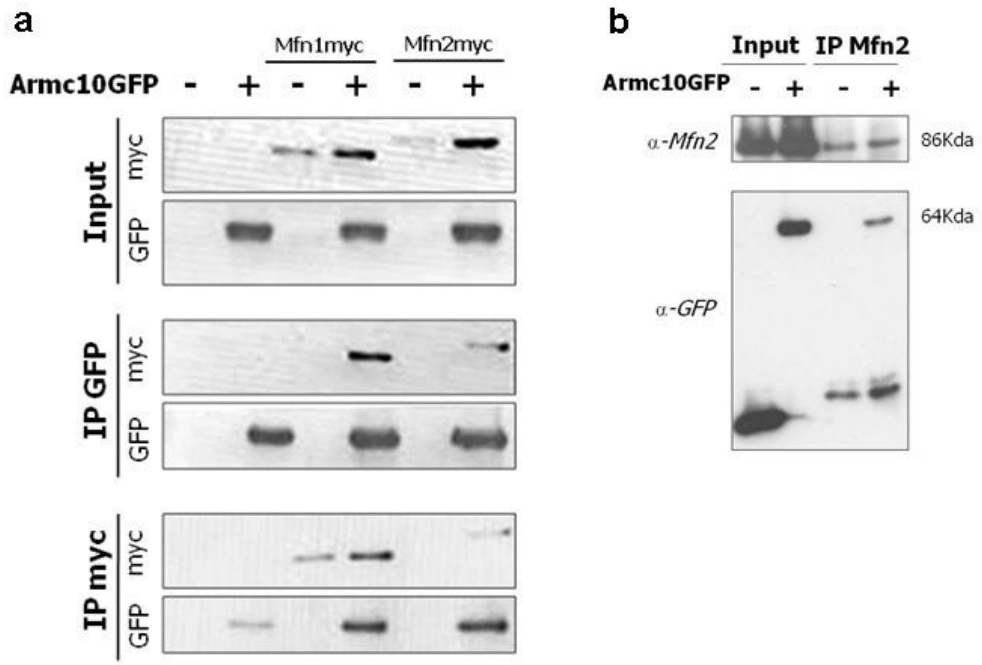

Figure 36: Armc10 interacts with Mitofusin1 and Mitofusin2 (**a**) HEK293AD cells were transfected with Armc10-GFP and Mfn1-myc or Mfn2-myc. Immunoprecipitation with anti-GFP antibodies revealed co-association of Mfn1-myc and Mfn2-myc with Armc10-GFP. The reverse immunoprecipitation with anti-myc antibodies confermed co-association of Armc10-GFP with Mfn1-myc and Mfn2-myc. (**b**) The interaction between Armc10 and Mfn2 was further confirmed transfecting HEK293AD with Armc10-GFP, immunoprecipitating with anti-GFP antibody and detecting endogenous Mfn2 in co-immunoprecipitate by detection with anti-Mfn2 antibody.

3. Alex3 and Armc10 proteins regulate cell proliferation and differentiation

3.1 Alex3 overexpression inhibits Wnt signaling pathway

Alex3 protein sequence contains six Armadillo repeats, found in a wide range of proteins related to the Wnt/ β-catenin signaling. Wnt activation of β-catenin pathway results in the accumulation of β-catenin in the cytosol and ultimately in the nucleus, where it combines with TCF/LEF family of transcription factors to turn on the expression of Wnt target genes. As multiple Wnt proteins have been implicated in key aspects of nervous system development, we investigated a possible involvement of Alex3 in this signaling pathway, using an *in vivo* physiological model: the chicken spinal cord (37a). Luciferase assay was performed evaluating luciferase activity in embryos electroporated with pCIGAlex3 alone, and embryos co-electroporated with pCIGAlex3 and Wnt3a or stable form of β-catenin (β-catenin^{CA}), lacking one of the four phosphorylation sites that mediate axin/adenomatous polyposis coli complex binding and degradation (Tetsu and McCormick, 1999). The results showed that the presence of Alex3 decreases TCF/LEF-transcriptional activity at basal condition (10-folds) as well following Wnt3a (4-folds) or β-catenin^{CA} induction (2.8-folds), indicating that Alex3 substantially acts as an inhibitor of canonical Wnt pathway (Fig.37b).

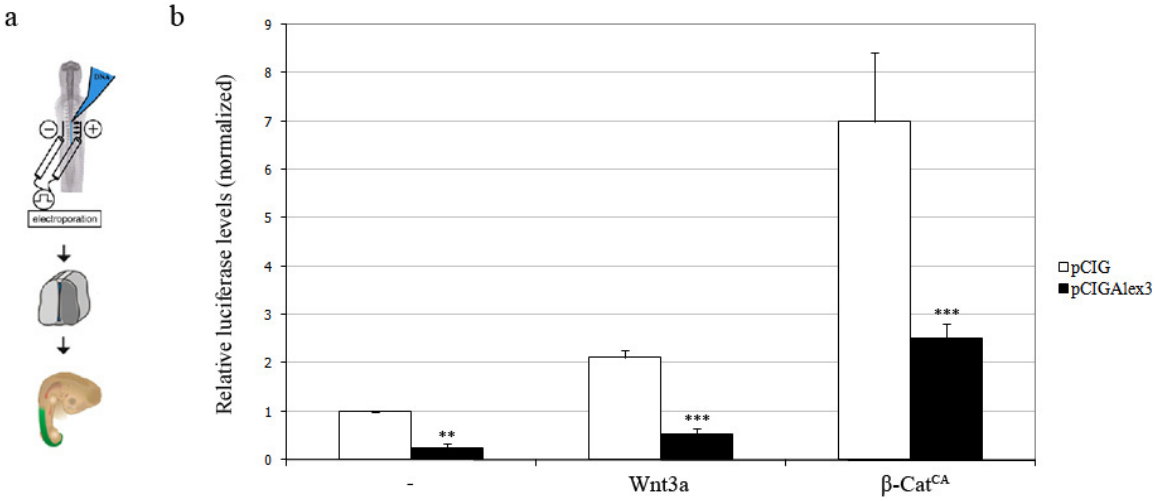

Figure 37: Alex3 inhibits canonical Wnt pathway. (**a**) Schematic representation showing the electroporation in chicken spinal cord. (**b**) Luciferase analysis of the transcriptional activity of pCIGAlex3 alone or in combination with Wnt3a or β-cateninCA on TCF/LEF promoter. Graph shows normalized luciferase units relative to pCIG control. Each bar represents mean ±s.e.m.

3.2 Alex3 and Armc10 overexpression doesn't affect dorso-ventral patterning of spinal cord

Dorso-ventral patterning of the vertebrate nervous system is achieved by the combined activity of morphogenetic signals secreted from dorsal and ventral signaling centers (Ulloa and Briscoe, 2007). Wnt1 and Wnt3a are both expressed in dorsal regions of chicken neural tube, promoting dorsalization and suppressing ventral program (Alvarez-Medina et al., 2008; Muroyama et al., 2002), by signaling through the canonical β-catenin/TCF pathway (Alvarez-Medina et al., 2008).

As we showed that Alex3 acts as an inhibitor of the canonical Wnt/β-catenin pathway, we aimed to test whether Armcx3 and Armc10 genes may be involved in cell fate specification in chicken spinal cord.

For this purpose, we electroporeted pCIGAlex3, pCIGAlex3Δ(1-12) (Alex3 deletion mutant lacking the mitochondrial localization signal located at N-terminal of the protein) or pCIGArmc10 cDNAs, in chick embryos neural tubes (stage HH12). The cDNAs were cloned in a bicistronic vector containing GFP sequence, so that the electroporated cells were GFP positive (GFP^+). As described below (see paragraph 3.4), we detected a differential distribution of the GFP positive cells in pCIGAlex3 embryos respect to the pCIG control.

Twenty-four hours post-electroporation (hPE), the expression of Nkx6.1 and Nkx2.2 (expressed in vivo by ventral CNS progenitors) and Pax7 (expressed in vivo by dorsal CNS progenitors) transcription factors, was analyzed by immunohistochemistry, and no changes were detected in their expression comparing electroporated and no electroporated sides (Fig.38). This result indicates that Alex3 and Armc10 overexpression doesn't affect dorso-ventral patterning of spinal cord.

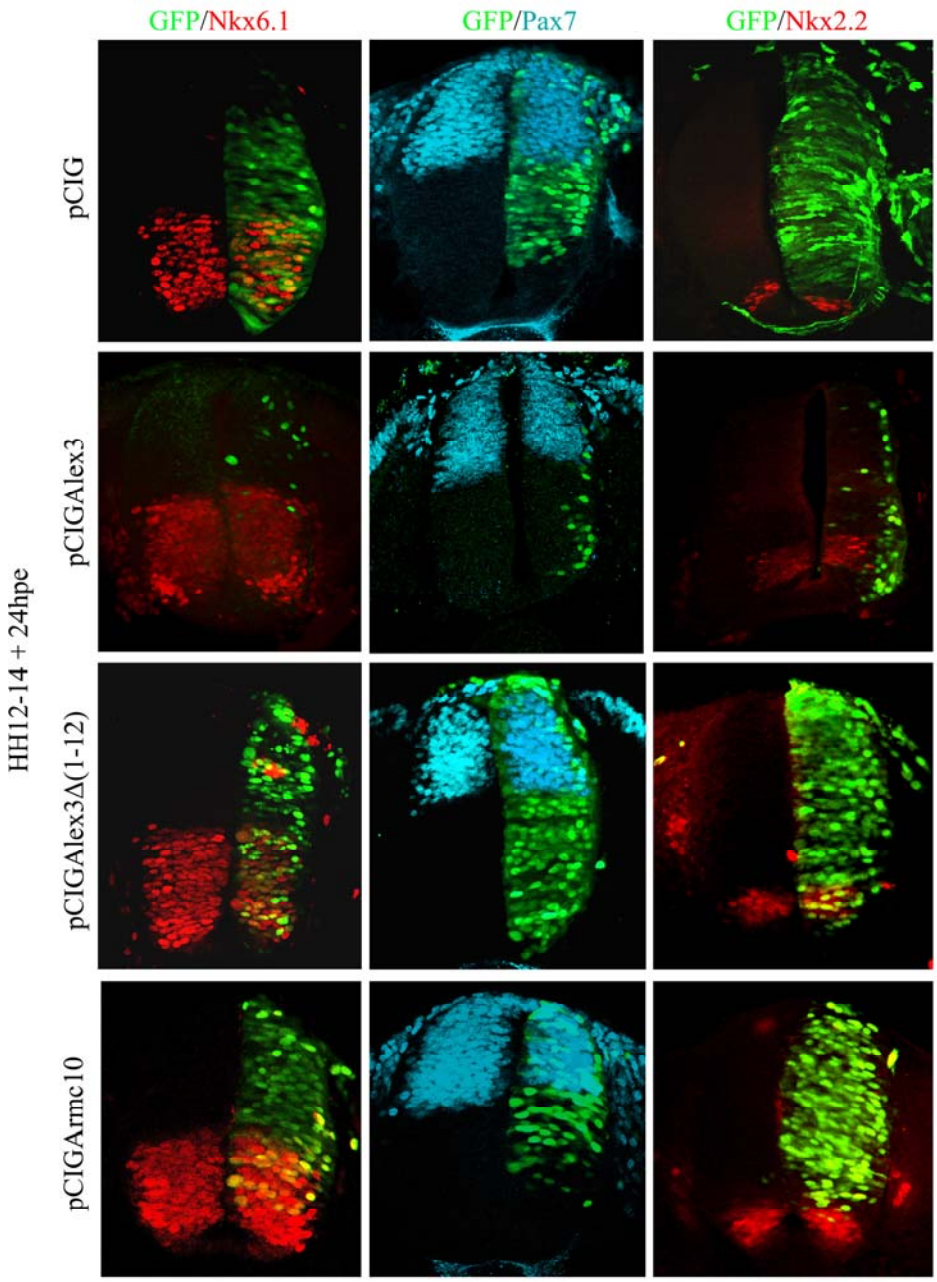

Figure 38: Alex3 and Armc10 overexpression doesn't affect dorso-ventral patterning of spinal cord. Twenty-four hours post-electroporation (24hPE) of empty vector pCIG, pCIGAlex3, pCIGAlex3Δ(1-12) or pCIGArmc10, expression of Nk6.1, Pax7 and Nkx2.2 is not altered. bar: 75 µm.

3.3 Armc10/SVH is expressed in spinal cord and localizes at mitochondria.

As Armcx gene cluster is specific to Eutherian mammals, we first wanted to characterize the expression of the unique gene copy present in chick: the Armc10/SVH gene that shares a strong protein sequence homology with mouse Armc10. We characterized the expression domains of Armc10/SVH by in situ hybridization of HH19 HH24 embryos. By HH19, when newly born neurons rise around 12% of cells in the neural tube (Wilcock

et al., 2007), Armc10/SVH is expressed preferentially in dorsal regions and weakly in floor plate (Fig.39a); by stage HH24, when neural differentiation is more active and gliogenesis has not yet started, Armc10/SVH expression remained in dorsal progenitors and floor plate, and appeared also in ventral motoneurons (Fig.39a).

To get insight into subcellular localization of chicken Armc10 protein in spinal cord, we performed immunohistochemical analysis in HH24 stage embryos, and we found co-localization between Armc10 protein and the mitochondrial marker COXIV (Fig.39b).

To analyze the function of the proteins of interest, we electroporeted the mouse recombinant DNAs pCIGAlex3, pCIGAlex3Δ(1-12) or pCIGArmc10 in the neural tube. The embryos were analyzed 24 hours after electroporation by immunohistochemical analysis, showing that both Alex3 and Armc10 are cytosolic proteins co-localizing with COXIV at mitochondria when overexpressed in chicken spinal cord (Fig.39c-d). Moreover, the deletion mutant pCIGAlex3Δ(1-12) loses mitochondrial localization, showing a diffuse cytosolic and nuclear staining (Figd).

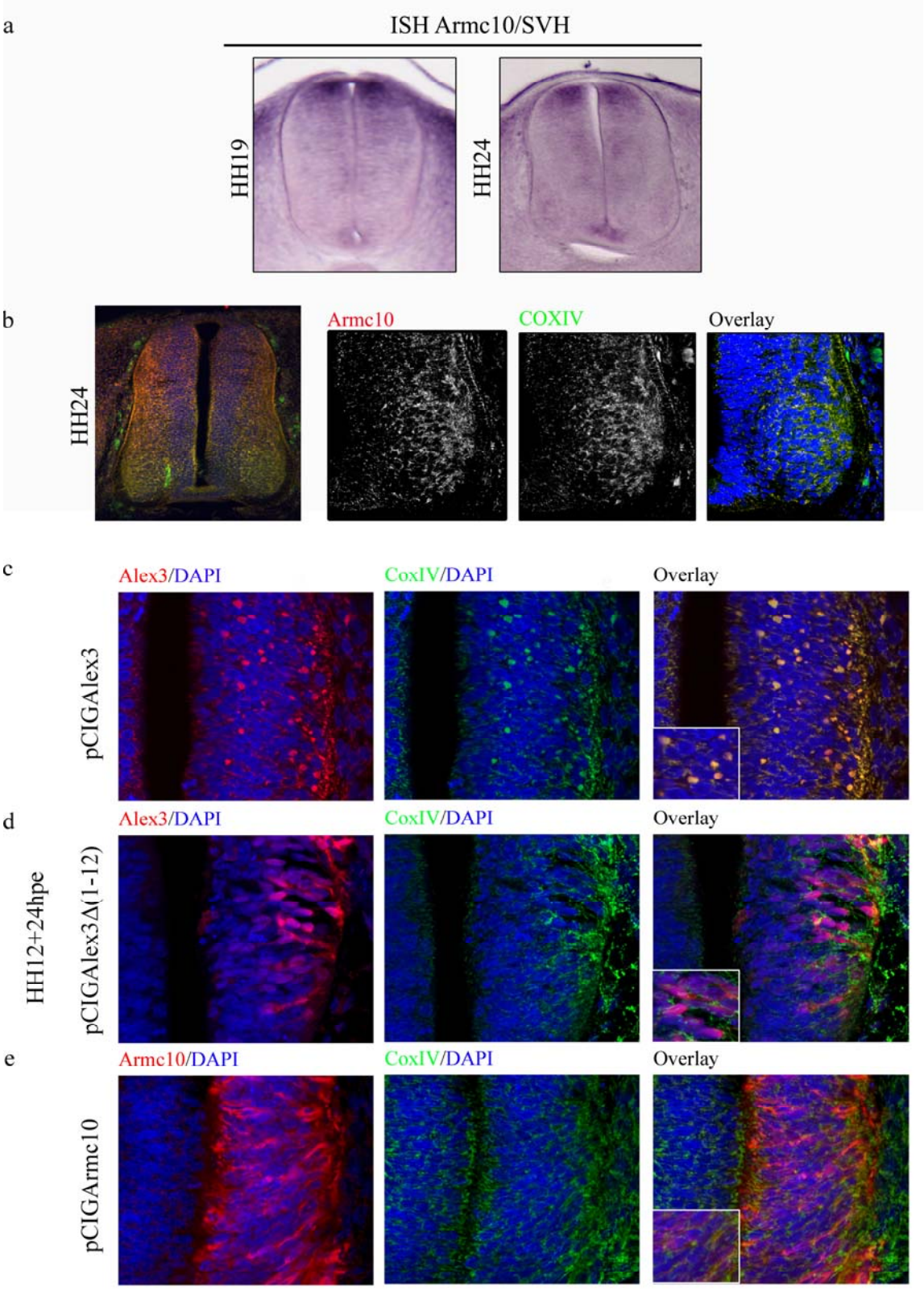

Figure 39: Expression of endogenous Armc10/SVH in spinal cord and subcellular localization of mouse Alex3, Alex3Δ(1-12) and Armc10.
(**a**) Armc10/SVH mRNA in situ hybridization in HH19 and HH24 embryo spinal cord. (**b**) Immunohistochemical analysis of HH24 stage embryo showing co-localization between Armc10 protein (red) and the mitochondrial marker COXIV (green). Nuclei were stained with DAPI (blue).

(**c-e**) pCIGAlex3, pCIGAlex3Δ(1-12) or pCIGArmc10, were electroporated in HH12 neural tube and embryos were analyzed 24 hours after electroporation. Cells were analyzed using antibodies directed against Alex3 (red) or Armc10 (red), mitochondrial marker COXIV (green) and nuclear marker DAPI (blu).

3.4 Full length Alex3 promote neuronal differentiation in chicken spinal cord

Wnt/β-catenin signaling plays a crucial role in maintaining neural precursor cells during spinal cord development and the inhibition of the Wnt/β-catenin pathway is an important prerequisite for neuronal differentiation (Chenn and Walsh, 2002; Zechner et al., 2003). As we showed that Alex3 acts as an inhibitor of the canonical Wnt/β-catenin pathway, we aimed to test whether Armcx3 and Armc10 genes may be involved in neural differentiation in chicken spinal cord.

In the developing spinal cord, neural progenitors reside in the ventricular zone (VZ) and are identified by the expression of pluripotent factors such as Sox2. Neurogenesis is accompanied by lateral migration to the mantle zone (MZ) and the expression of pan-neural markers such as HuC/D. The neuronal differentiation phenotype can be monitored by analyzing lateral distribution of GFP-positive cells in spinal cord of electroporeted embryos.

Embryos electroporated with the empty vector pCIG, pCIGAlex3, pCIGAlex3Δ(1-12) or pCIGArmc10 were analyzed 24 hours (Fig.40) or 48 hours (Fig.41) after electroporation, by staining the neural tubes with the precursors marker Sox2 (delimitating the ventral zone, VZ) and the differentiated neurons marker HuC/D (delimitating the mantle zone, MV); thus we were able to distinguish the VZ to the MZ (Fig.40a; Fig.41a). pCIG cells showed an even distribution through MZ and VZ; pCIGAlex3 cells were mainly at MZ of the neural tube, whereas only few electroporated cells were located at VZ, strongly differing respect to the pCIG control phenotype; pCIGAlex3Δ(1-12) and pCIGArmc10 cells were uniformly distributed between MZ and VZ, likely to the control phenotype. These data are quantified in Figure 40b-c and 41b-c.

The results suggest that full length Alex3, but not Armc10 or Alex3 deletion mutant, acts promoting differentiation.

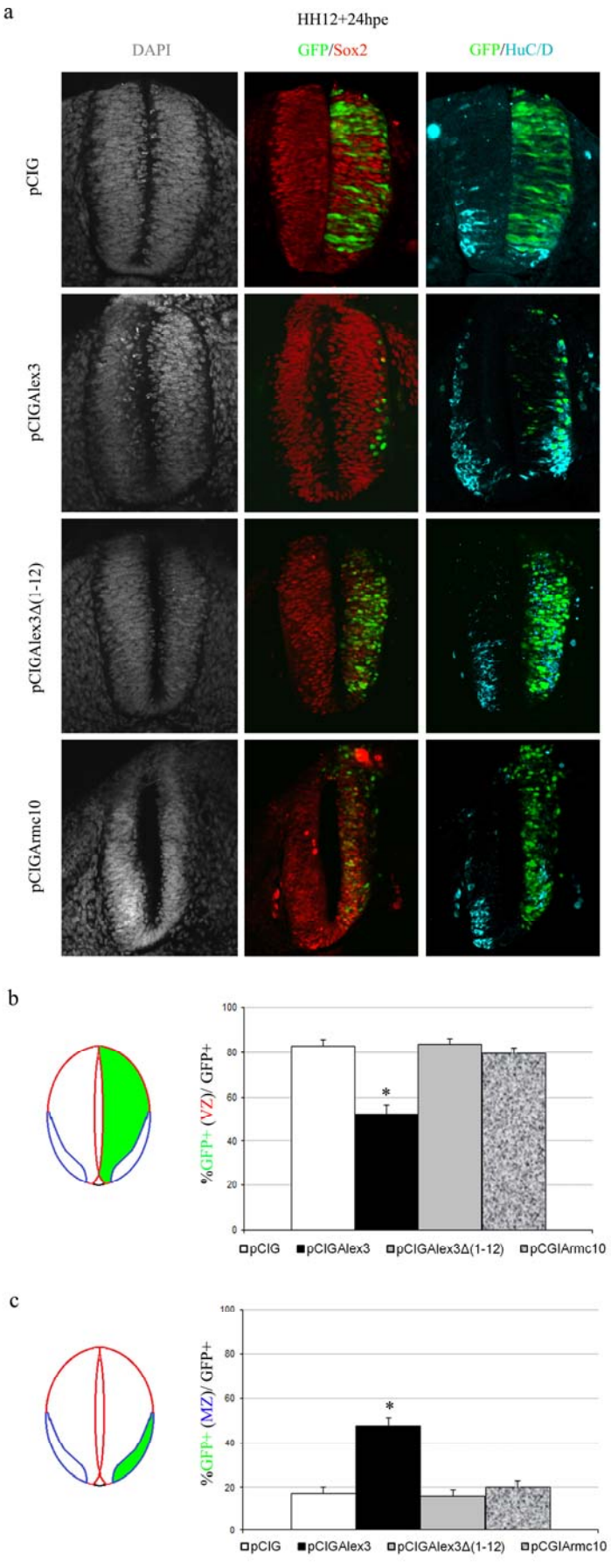

Figure 40: Lateral distribution of GFP-positive cells in pCIGAlex3, pCIGAlex3Δ(1-12) or pCIGArmc10 electroporated embryo. (**a**) HH12 embryos were electroporated in ovo with pCIGAlex3, pCIGAlex3Δ(1-12) or pCIGArmc10, analyzed 24 hours after electroporation and processed for the immunostaining indicated. (**b-c**) Quantification of lateral distribution of GFP^+ cells from the lumen to the mantel zone of the neural tube. Data represent the mean±s.e.m. **P*<0.05.

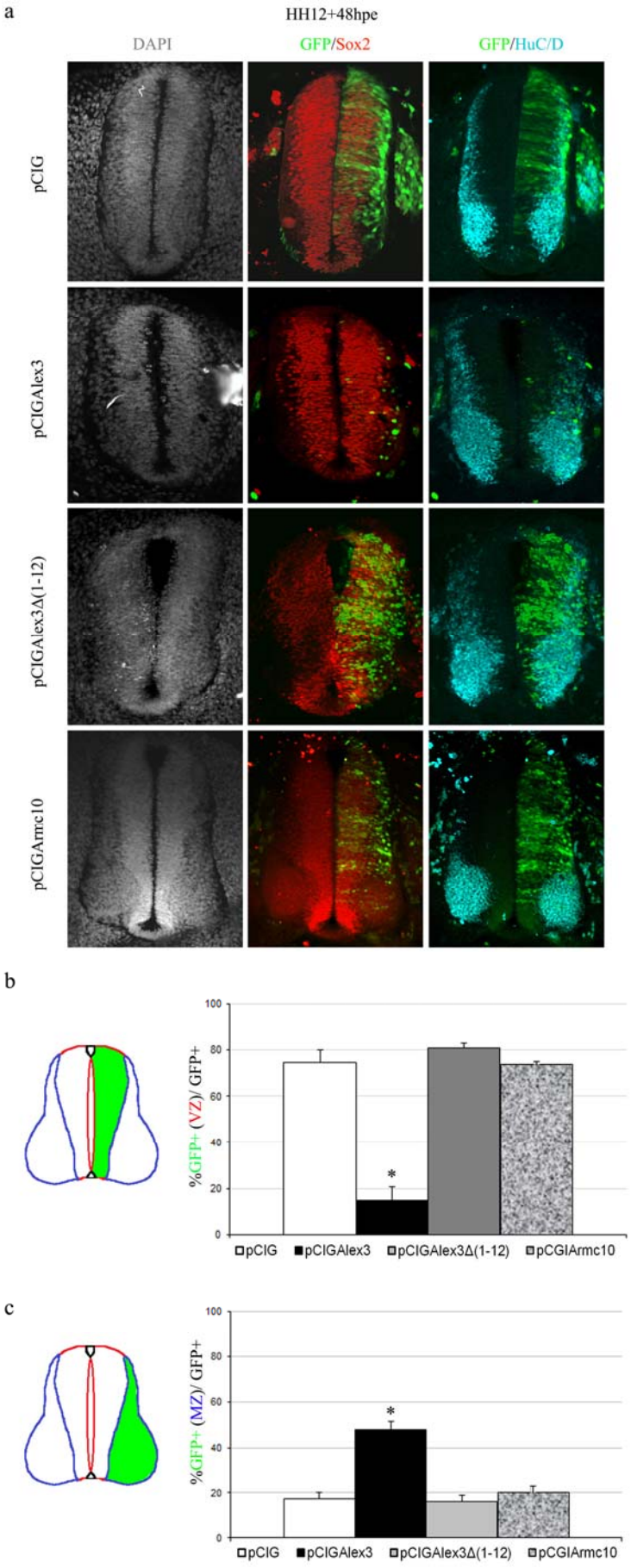

Figure 41: Lateral distribution of GFP-positive cells in pCIGAlex3, pCIGAlex3Δ(1-12) or pCIGArmc10 electroporated embryo. (**a**) HH12 embryos were electroporated in ovo with pCIGAlex3, pCIGAlex3Δ(1-12) or pCIGArmc10, analyzed 48 hours after electroporation and processed for the immunostaining indicated. (**b-c**) Quantification of lateral distribution of GFP^+ cells from the lumen to the mantel zone of the neural tube. Data represent the mean±s.e.m. **P*<0.05.

We tested the hypothesis of full length Alex3 as promoter of neural differentiation analyzing the expression of neuronal differentiation marker Tuj-1 (Neuron-specific class III β-tubulin) in pCIG, pCIGAlex3, pCIGAlex3Δ(1-12) or pCIGArmc10 electroporated embryos, 48 hours after electroporation (Fig.42). We showed that most pCIGAlex3 electroporated cells express Tuj-1 marker, while there are no differences in Tuj-1 expression levels between pCIGAlex3Δ(1-12) or pCIGArmc10 and control pCIG electroporated cells (Fig42.a,c). This data confirm that full length Alex3, but not Armc10, acts promoting differentiation.

We want also measure the size of area in which differentiated cells are located and compare this size of electroporated and control side. In both full length Alex3 and Armc10 electroporated embryos, Tuj-1 positive region of electroporated side has a smaller width respect to control side (Fig.42a,d).

Similarly, in both full length Alex3 and Armc10 electroporated embryos, the HuC/D positive area of electroporated side is smaller respect to control side (Fig.42b.e).

Taken together this data suggest that full length Alex3 overexpression acts promoting differentiation; moreover, the overexpression of both full length Alex3 and Armc10 leads to a decrease in differentiated cell density, maybe acting on precursors cells by promoting an early cell cycle exit or affecting cell cycle length.

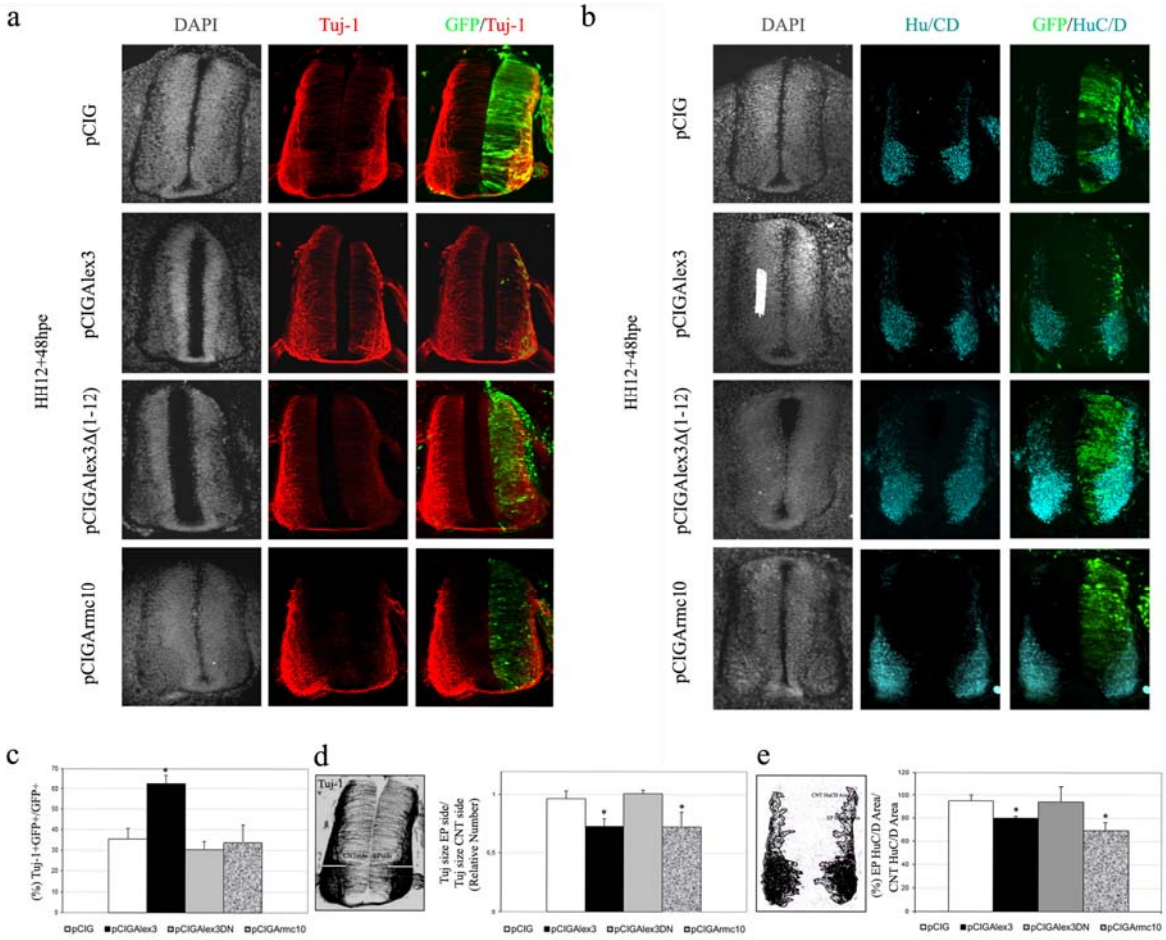

Figure 42: Mitochondrial Alex3 overexpression promote differentiation, while overexpression of both mitochondrial Alex3 and Armc10 lead to a decrease in differentiated cell density. (**a,b**) HH12 embryos were electroporated in ovo with pCIGAlex3, pCIGAlex3Δ(1-12) or pCIGArmc10, analyzed 48 hours after electroporation and processed for the immunostaining indicated. (**c**) Graph showing the percentage of electroporated cells (GFP^+) positive for Tuj-1. (**d**) Graph showing ratio between widths of Tuj marked region in electroporated (EP) and control (CNT) side. (**e**) Graph showing ratio between area of HuC/D marked region in electroporated (EP) and control (CNT) side. Data represent the mean±s.e.m. **P*<0.05.

3.5 Alex3 and Armc10 are involved in cell cycle regulation

To test the hypothesis of a possible involvement of Alex3 and Armc10 in cell cycle progression, we transfected HEK293AD cells with Alex3-GFP, GFP-Alex3Δ(1-12), Armc10-GFP and control GFP constructs and measured the effects of their overexpression on cell proliferation by staining for phospho histone H3 (PH3, M-phase marker) and Bromodeoxyuridine (BrdU, S-phase marker; 2h pulse) after 48 hours from transfection. We found that Alex3 and Armc10 expression cause a reduction in both BrdU and PH3-positive cells.

Quantitative analysis showed that Alex3-GFP and Armc10-GFP significantly decreased HEK293AD cell proliferation; the data were normalized with respect to the GFP control (Fig.43a-b).

Moreover we found that Alex3 mitochondrial localization is necessary to induce this effect on cell cycle progression, since deletion of the first 12 N-terminal amminoacids (containing the mitochondrial localization signal) in Alex3 sequence abolished this phenotype (Fig.43a-b).

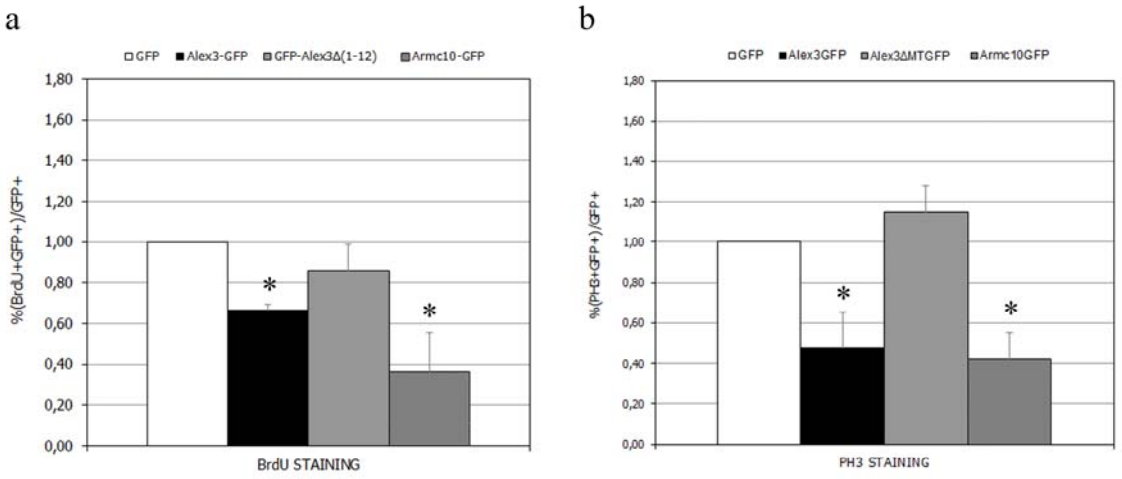

Figure 43: Alex3 and Armc10 overexpression inhibits proliferation of cultured HEK293AD cells. Effect of Alex3-GFP, GFP-Alex3Δ(1-12) and Armc10-GFP on the proliferation of cultured HEK293AD cells. (**a**) Quantitative results of the % of BrdU-labeled transfected HEK293AD cells respect to total transfected cells. (**b**) Quantitative results of the % of PH3-labeled transfected HEK293AD cells respect to total transfected cells.

3.6 Alex3 and Armc10 are negative regulators of cell cycle in chicken spinal cord.

To better investigate the involvement of Alex3 and Armc10 proteins in cell cycle progression we moved to the chick embryo neural tube, as Alex3 was found to act as inhibitor of canonical Wnt pathway in this system. The progression through the cell cycle and the proliferation-differentiation balance are both regulated by Wnt/β-catenin signaling and can be easily analyzed in chicken neural tube.

We analyze the number of GFP^+ cells expressing phospho histone H3 (PH3, M-phase marker) or Bromodeoxyuridine (BrdU, S-phase marker) incorporation after 40-min pulse, in control pCIG, pCIGAlex3, pCIGAlex3Δ(1-12) or pCIGArmc10 electroporated embryos, 24 hours after electroporation (Fig.44).

We found a significant decrease in proliferation in pCIGAlex3 and pCIGArmc10 electroporated embryos (Fig.44c-d), indicating that both full length Alex3 and Armc10 are negative regulator of cell cycle.

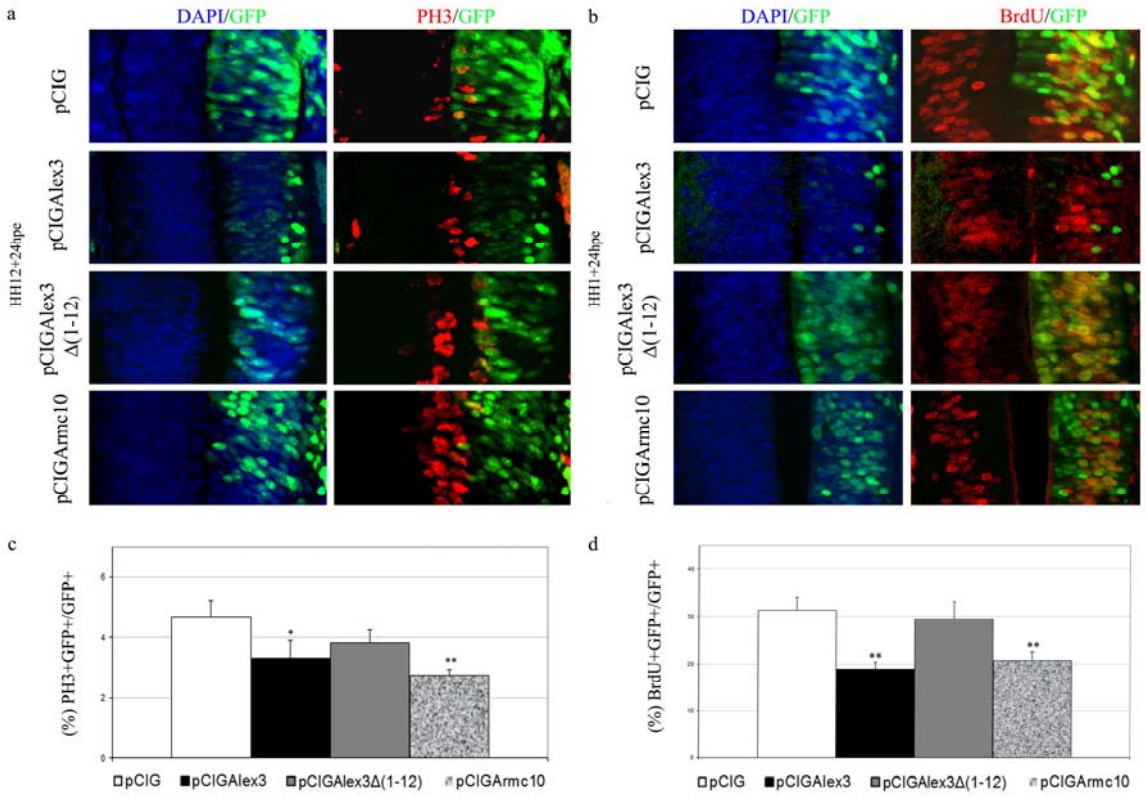

Figure 44. Mitochondrial Alex3 and Armc10 overexpression affect cell cycle progression. (**a-b**) HH12 embryos were electroporated in ovo with pCIGAlex3, pCIGAlex3Δ(1-12) or pCIGArmc10 and analyzed 24 hours after electroporation for PH3 (a) and BrdU (b) staininig. (**c-d**) Graphs showing that percentage of electroporated cells (GFP^+) positive for PH3 (c) or BrDU (d) decrease in pCIGAlex3 and pCIGArmc10 electroporated embryos. Data represent the mean±s.e.m. **P*<0.05.

3.7 - Gene expression profiling of Alex3 stable HEK293AD cell line

Several lines of evidence suggest that Alex3 may be implicated in the modulation of transcription, such as its nuclear localization, the interaction with the transcription factor Sox10 (Mou et al, 2010) and its ability to inhibits TCF/LEF transcriptional activity (Fig.37). A better understanding of the downstream effects of Alex3 overexpression on global gene expression would be helpful to further shade light on the biological processes in which it is involved. For this purpose, we performed a genome wide transcription profiling of HEK293AD cells stably expressing Alex3GFP.

HEK293AD cells stably expressing Alex3GFP protein or GFP as control, were genereted by transfecting these cells with vectors codifying for Alex3GFP or GFP in addition to a geneticin resistance. We kept the cells in selection media containing geneticin until colonies were developed; we picked about 12 colonies for plate. We chose the better Alex3GFP or GFP expressing colonies by immunofluorescence assays and western blot analysis (data not shown).

We used these clones in a genome wide transcription profiling study to identify genes differentially expressed between HEK293Alex3GFP and HEK293GFP cells lines, using Affymetrix HG-U219 Gene Chips. Microarray studies were performed using triplicate RNA samples for each condition. Array image data analysis gave rise to six CEL files (oe53.ga.cel, oe49.ga.cel, oe45.ga.cel, gfp-47.ga.cel, gfp-43.ga.cel, gfp-51.ga.cel), corresponding to each triplicate condition.

The file containing the normalized expression values was loaded into MeV 4.8 for statistical analysis. A hierarchical clustering (HCL) was performed to analyze the replicates quality and, on the basis of the clustering, the data from gfp-43.cel was excluded from further analyses.

The SAM (Significance Analysis of Microarray) test was used to identify significant differentially expressed genes between control ("gfp" chips) and overexpressing cells ("oe" chips). The SAM Graphic indicates the presence of genes differentially regulated between the two conditions (Fig.45a). Specifically 21751 genes (49100 probesets) were discarded as no-significant ($p > 0.05$), whereas 99 genes (114 probesets) were selected using a q-value < 0.05 as threshold. Among them, 96 genes (110 probesets) were downregulated and 3 genes (4 probesets) were found upregulated in Alex3GFP cell line (Tab.5).

A hierarchical tree based on average linkage clustering, was calculated for the up-regulated and down-regulated genes (Fig.45b-c). The results of the clustering highlighted that most of the up-regulated genes were characterized by high basal level of expression in control cells, which was further increased in the overexpression mutant.

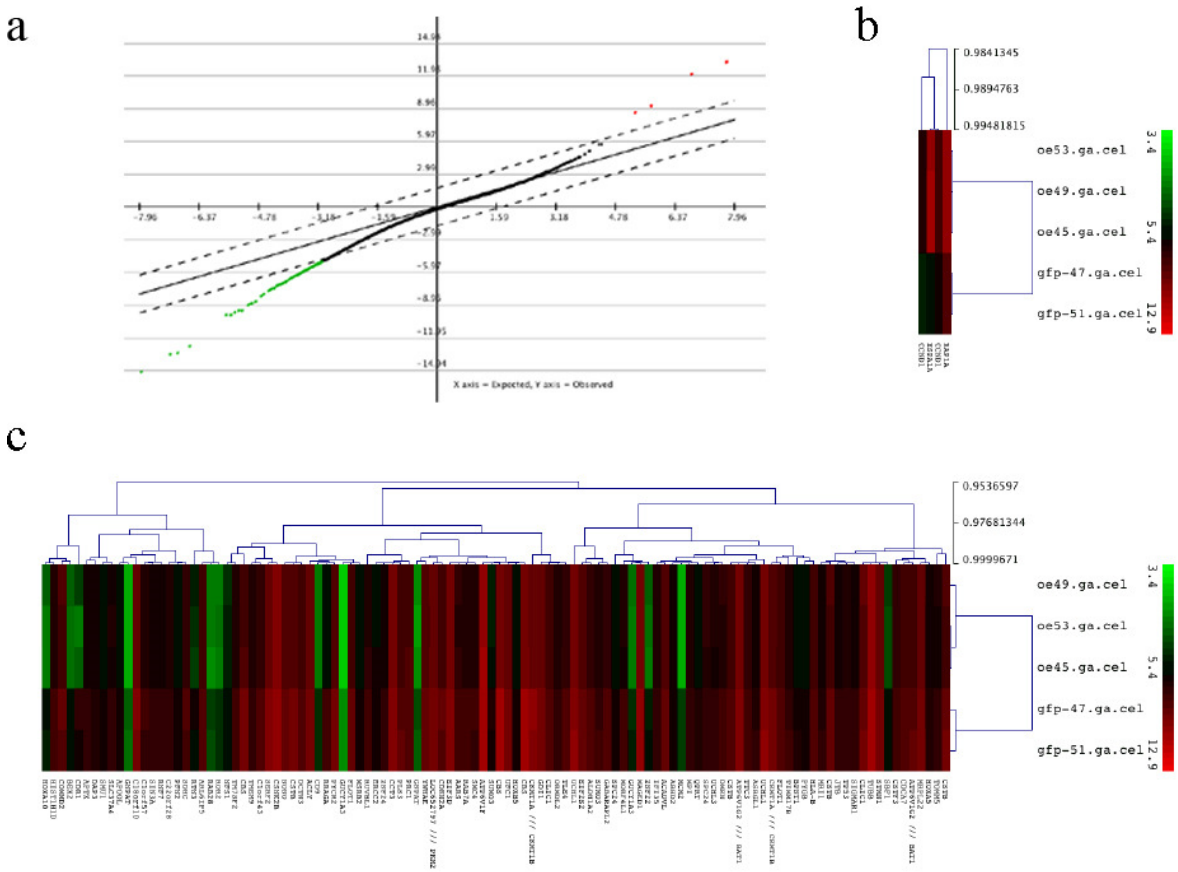

Figure 45: Clustering can illustrate samples relationships. The Significance Analysis of Microarray (SAM) test was used for the selection of genes differentially expressed between control ("gfp" chips) and overexpressed line ("oe" chips). In the SAM Graphic the genes in red correspond to the up-regulated genes, the genes in green are the down-regulated genes, while black dots show gene with no-significant changes (GFPvsAlex3GFP). (**a**). Hierarchical clustering of the significantly upregulated (**a**) or downregulated (**b**) probes for the two replicate groups, HEK293Alex3GFP ("oe") and HEK293GFP ("gfp"), (MeV 4.8 tool). Relative gene expression levels are shown with high expression represented by red and low expression represented in green. Dendrograms include average linkage clustering for the down-reguklates or up-regulated genes.

Up-regulated					
Probesets	**GENE_TITLE**	**GENE_SYMBOL**	**UNIGENE_ID**	**Fold change (Unlogged)**	**q-value (%)**
11721257_at	cyclin D1	CCND1	Hs.523852	2,4752789	0
11751330_a_at	cyclin D1	CCND1	Hs.523852	2,4923828	0
11762533_a_at	RAP1A, member of RAS oncogene family	RAP1A	Hs.190334	3,6232867	0
11757907_x_at	heat shock 70kDa protein 1A	HSPA1A	Hs.274402	29,335287	0
Down-regulated					
Probesets	**GENE_TITLE**	**GENE_SYMBOL**	**UNIGENE_ID**	**Fold change (Unlogged)**	**q-value (%)**
11737481_s_at	cerebellar degeneration-related protein 1, 34kDa	CDR1	Hs.446675	0,22785638	3,872936
11758655_s_at	Ras-related GTP binding A	RRAGA	Hs.723151	0,35218892	0
11744835_s_at	cystathionine-beta-synthase	CBS	Hs.533013	0,3860609	0
11744286_s_at	cystathionine-beta-synthase	CBS	Hs.533013	0,39911732	0
11752656_a_at	cystathionine-beta-synthase	CBS	Hs.533013	0,400407	1,6989
11721798_a_at	SMT3 suppressor of mif two 3 homolog 3 (S. cerevisiae)	SUMO3	Hs.474005	0,44664207	0
11751077_a_at	aldehyde dehydrogenase 1 family, member A2	ALDH1A2	Hs.643455	0,4801666	0
11745016_a_at	chromosome 1 open reading frame 43	C1orf43	Hs.287471	0,4809587	3,9150
11722812_s_at	RAB7A, member RAS oncogene family	RAB7A	Hs.723832	0,48790807	0
11718848_a_at	brain expressed X-linked 2	BEX2	Hs.398989	0,49184987	0
11758318_s_at	cystatin B (stefin B)	CSTB	Hs.695	0,49903056	3,5082
11749409_a_at	dermokine	DMKN	Hs.417795	0,5053733	0
11717916_s_at	creatine kinase, mitochondrial 1A /// creatine kinase, mitochondrial 1B	CKMT1A /// CKMT1B	Hs.425633	0,5080059	3,6753
11743046_a_at	flotillin 1	FLOT1	Hs.179986	0,51632863	0
11742733_x_at	mortality factor 4 like 1	MORF4L1	Hs.374503	0,5254258	4,0929
11736915_at	histone cluster 1, H1d	HIST1H1D	Hs.136857	0,52675784	4,0470
11715991_a_at	minichromosome maintenance complex component 2	MCM2	Hs.477481	0,54395175	0
11715506_a_at	melanoma antigen family D, 1	MAGED1	Hs.5258	0,54544115	1,6989
11759151_at	SPC24, NDC80 kinetochore complex component, homolog (S. cerevisiae)	SPC24	Hs.381225	0,56027585	4,3711
11757287_x_at	cystatin B (stefin B)	CSTB	Hs.695	0,560293	0
11723260_s_at	zinc finger protein 24	ZNF24	Hs.514802	0,566643	0
11756895_a_at	SET binding factor 1	SBF1	Hs.589924	0,567206	0
11736759_s_at	succinate dehydrogenase complex, subunit C, integral membrane protein, 15kDa	SDHC	Hs.444472	0,567508	0
11718293_a_at	cyclin-dependent kinase inhibitor 2A (melanoma, p16, inhibits CDK4)	CDKN2A	Hs.512599	0,56838053	2,81393
11721797_at	SMT3 suppressor of mif two 3 homolog 3 (S. cerevisiae)	SUMO3	Hs.474005	0,56926894	0
11728129_s_at	aprataxin	APTX	Hs.20158	0,57296246	4,7392
11720938_a_at	translocase of inner mitochondrial membrane 17 homolog B (yeast)	TIMM17B	Hs.30570	0,5744171	3,5082
11730293_a_at	SIN3 homolog A, transcription regulator (yeast)	SIN3A	Hs.513039	0,574863	0
11716143_a_at	sigma non-opioid intracellular receptor 1	SIGMAR1	Hs.522087	0,5765314	0
11743578_x_at	translocase of outer mitochondrial membrane 5 homolog (yeast)	TOMM5	Hs.130774	0,5781048	3,6753
11744919_a_at	chromosome 18 open reading frame 10	C18orf10	Hs.436636	0,580632	1,6371
11728661_a_at	GABA(A) receptor-associated protein-like 2	GABARAPL2	Hs.461379	0,581035	0

11715834_x_at	RuvB-like 1 (E. coli)	RUVBL1	Hs.272822	0,582862	4,329123
11720303_s_at	reticulon 3	RTN3	Hs.473761	0,5919385	4,2077
11715305_s_at	homeobox A10	HOXA10	Hs.110637	0,59319234	4,7392
11749391_x_at	quinolinate phosphoribosyltransferase	QPRT	Hs.513484	0,5970813	0
11748279_s_at	transmembrane 7 superfamily member 2	TM7SF2	Hs.31130	0,6032558	3,3767
11745345_x_at	pyrroline-5-carboxylate reductase family, member 2	PYCR2	Hs.654718	0,61012167	0
11716064_a_at	solute carrier family 37 (glucose-6-phosphate transporter), member 4	SLC37A4	Hs.719203	0,6129431	1,6989
11716755_at	ring finger protein 7	RNF7	Hs.134623	0,6152057	3,9580
11719995_a_at	transducin-like enhancer of split 4 (E(sp1) homolog, Drosophila)	TLE4	Hs.444213	0,6174958	0
11757316_a_at	flotillin 1	FLOT1	Hs.179986	0,61778367	0
11715525_a_at	ATPase, H+ transporting, lysosomal 13kDa, V1 subunit G2 /// HLA-B associated transcript 1	ATP6V1G2 /// BAT1	Hs.249227	0,6193295	0
11722137_a_at	guanylate cyclase 1, soluble, alpha 3	GUCY1A3	Hs.24258	0,6201297	2,8139
11715829_at	plastin 3	PLS3	Hs.496622	0,6207649	0
11754056_x_at	cystatin B (stefin B)	CSTB	Hs.695	0,620822	0
11715883_x_at	death associated protein 3	DAP3	Hs.516746	0,6222521	4,0929
11754803_s_at	ubiquitin carboxyl-terminal esterase L1 (ubiquitin thiolesterase)	UCHL1	Hs.518731	0,62278336	0
11757915_s_at	ubiquitin carboxyl-terminal esterase L1 (ubiquitin thiolesterase)	UCHL1	Hs.518731	0,6311897	4,8238
11722977_at	homeobox B5	HOXB5	Hs.654456	0,6312294	0
11724194_s_at	small EDRK-rich factor 2	SERF2	Hs.424126	0,6328649	4,3711
11747744_s_at	creatine kinase, mitochondrial 1A /// creatine kinase, mitochondrial 1B	CKMT1A /// CKMT1B	Hs.425633	0,633066	3,7914
11743149_at	zinc finger protein 22 (KOX 15)	ZNF22	Hs.462693	0,6336687	0
11735108_a_at	dynactin 3 (p22)	DCTN3	Hs.511768	0,6385269	0
11755966_x_at	major histocompatibility complex, class I, B	HLA-B	Hs.130838	0,6385467	0
11744376_a_at	mannose phosphate isomerase	MPI	Hs.75694	0,6430768	0
11751334_x_at	3'(2'), 5'-bisphosphate nucleotidase 1	BPNT1	Hs.406134	0,64708006	4,0929
11733874_a_at	structural maintenance of chromosomes 4	SMC4	Hs.58992	0,6498452	0
11748012_x_at	transmembrane protein 9	TMEM9	Hs.181444	0,65092266	4,1305394
11754365_s_at	receptor tyrosine kinase-like orphan receptor 2	ROR2	Hs.98255	0,6574552	3,8047504
11726125_at	homeobox A5	HOXA5	Hs.655218	0,66072875	4,0929
11720232_at	ubiquitin carboxyl-terminal esterase L3 (ubiquitin thiolesterase)	UCHL3	Hs.162241	0,6637591	0
11738335_x_at	tumor protein p53	TP53	Hs.654481	0,6650947	2,81393
11715621_at	ubiquitin-fold modifier conjugating enzyme 1	UFC1	Hs.301412	0,6677263	0
11715866_x_at	ATPase, H+ transporting, lysosomal 14kDa, V1 subunit F	ATP6V1F	Hs.78089	0,6681031	0
11753251_a_at	jumping translocation breakpoint	JTB	Hs.6396	0,6704726	3,9150
11757405_a_at	methionine sulfoxide reductase B2	MSRB2	Hs.461420	0,6722686	0
11757576_x_at	casein kinase 2, beta polypeptide	CSNK2B	Hs.73527	0,67507905	3,6753373
11715569_at	CD9 molecule	CD9	Hs.114286	0,67522717	0

11743821_x_at	chromosome 1 open reading frame 57	C1orf57	Hs.642715	0,67536247	4,3711
11757612_a_at	asparaginase like 1	ASRGL1	Hs.535326	0,6755648	0
11733107_at	COMM domain containing 2	COMMD2	Hs.591315	0,67724293	3,8047
11753092_s_at	tyrosine 3-monooxygenase/tryptophan 5-monooxygenase activation protein, epsilon polypeptide	YWHAE	Hs.513851	0,6810114	4,092
11719064_a_at	glyceronephosphate O-acyltransferase	GNPAT	Hs.498028	0,6810351	1,6371
11730285_at	smu-1 suppressor of mec-8 and unc-52 homolog (C. elegans)	SMU1	Hs.655351	0,68143904	4,82388
11719664_a_at	GDP dissociation inhibitor 1	GDI1	Hs.74576	0,68244135	3,7914
11716358_s_at	protein regulator of cytokinesis 1	PRC1	Hs.366401	0,68443453	3,0523
11753891_x_at	tubulin, beta	TUBB	Hs.636480	0,6863551	0
11745737_x_at	acyl-CoA dehydrogenase, very long chain	ACADVL	Hs.437178	0,6873732	0
11745595_a_at	methylthioribose-1-phosphate isomerase homolog (S. cerevisiae)	MRI1	Hs.439370	0,6890336	4,1305
11748839_a_at	NFS1 nitrogen fixation 1 homolog (S. cerevisiae)	NFS1	Hs.194692	0,689811	4,8238
11752165_s_at	pyruvate kinase isozymes M1/M2-like /// pyruvate kinase, muscle	LOC652797 /// PKM2	Hs.534770	0,69259316	3,4194
11753705_x_at	stathmin 1	STMN1	Hs.209983	0,6952393	3,4194
11749919_a_at	guanylate cyclase 1, soluble, alpha 3	GUCY1A3	Hs.24258	0,6995833	0
11722009_a_at	chloride intracellular channel 1	CLIC1	Hs.414565	0,69993126	3,2159
11715955_a_at	ADP-ribosylation-like factor 6 interacting protein 5	ARL6IP5	Hs.518060	0,700161	3,6505
11758694_s_at	RAB28, member RAS oncogene family	RAB28	Hs.656060	0,7006859	2,8139
11719065_x_at	glyceronephosphate O-acyltransferase	GNPAT	Hs.498028	0,70442855	4,0020
11715642_s_at	tetratricopeptide repeat domain 3	TTC3	Hs.368214	0,7093346	0
11746316_a_at	alanyl-tRNA synthetase	AARS	Hs.315137	0,7171608	0
11749528_a_at	cell division cycle associated 7	CDCA7	Hs.470654	0,72207946	0
11754857_a_at	mitochondrial ribosomal protein L22	MRPL22	Hs.483924	0,7223607	3,2159
11715808_a_at	phosphorylase, glycogen; brain	PYGB	Hs.368157	0,72241515	4,0319
11757474_x_at	chloride intracellular channel 1	CLIC1	Hs.414565	0,7270369	3,8729
11727579_s_at	cleavage stimulation factor, 3' pre-RNA, subunit 3, 77kDa	CSTF3	Hs.44402	0,72903806	4,2878
11719180_a_at	eukaryotic translation initiation factor 3, subunit D	EIF3D	Hs.55682	0,7296543	3,1050
11736241_a_at	ORM1-like 2 (S. cerevisiae)	ORMDL2	Hs.534450	0,733478	3,2159
11716383_x_at	chaperonin containing TCP1, subunit 3 (gamma)	CCT3	Hs.491494	0,73411417	3,6505
200057_PM_s_at	non-POU domain containing, octamer-binding	NONO	Hs.533282	0,7398309	2,8139
11750082_a_at	excision repair cross-complementing rodent repair deficiency, complementation group 2	ERCC2	Hs.487294	0,7440526	4,3711534
11720620_s_at	ATP citrate lyase	ACLY	Hs.387567	0,7465485	0
11762311_x_at	SPC24, NDC80 kinetochore complex component, homolog (S. cerevisiae)	SPC24	Hs.381225	0,7466945	3,7519
11715527_x_at	ATPase, H+ transporting, lysosomal 13kDa, V1 subunit G2 /// HLA-B associated transcript 1	ATP6V1G2 /// BAT1	Hs.249227	0,75366414	1,6989
11753675_x_at	profilin 2	PFN2	Hs.91747	0,7561549	3,2159

11723916_at	eukaryotic translation initiation factor 2, subunit 2 beta, 38kDa	EIF2S2	Hs.429180	0,7588636	3,5082
11728320_a_at	cystatin B (stefin B)	CSTB	Hs.695	0,7613518	1,6079
11731149_a_at	apolipoprotein O-like	APOOL	Hs.706885	0,7616948	4,2077
11715645_s_at	chromosome 22 open reading frame 28	C22orf28	Hs.474643	0,7691503	4,0929
11733839_s_at	abhydrolase domain containing 2	ABHD2	Hs.122337	0,7917911	3,1595
11719492_s_at	interferon-induced protein 35	IFI35	Hs.632258	0,810749	4,3711

Table 5: SAM (Significance Analysis of Microarray) test was used to identify significant differentially expressed genes between control ("gfp" chips) and overexpressing cell line ("oe" chips). Upregulated and Downregulated probesets are reported together with the corresponding gene, gene symbol, unigene id, fold change and q-value. Significant genes were selected by setting a p-value <0.05 and a q-value <0.05 as threshold. The q-values were calculated by using a permutation test (100 tests).

Functional pathway analysis of the ninety six down-regulated genes was performed using Reactome, a database in which proteins participating in reactions form a network of biological interactions and are grouped into biological pathways (http://www.reactome.org/ReactomeGWT/entrypoint.html). Examples of biological pathways in Reactome include signaling, innate and acquired immune function, transcriptional regulation, translation, apoptosis and classical intermediary metabolism. In Fig.38 we show the five main pathways reported by Reactome analysis. Ten out of ninety six down-regulated-genes belong to metabolic pathways.

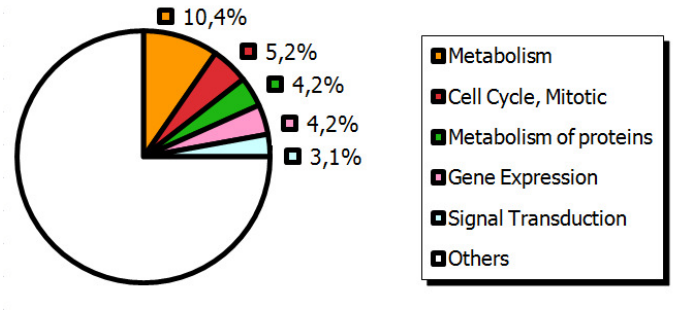

Pathway name	Matching proteins in data	% down-regulated proteins	Gene Symbol
Metabolism	10	10,4	NFS1//TM7SF2//PYGB//ACLY//BPNT1// ACADVL//MRI1//SDHC//QPRT//PKM2//
Cell Cycle, Mitotic	5	5,2	SPC24//MCM2//YWHAE//SMC4//TUBB
Metabolism of proteins	4	4,1	EIF2S2//CCT3//EIF3D//MPI
Gene Expression	4	4,1	TM7SF2//EIF2S2//AARS//CSTF3
Signal Transduction	3	3,1	ATP6V1G2 // BAT1//YWHAE//MAGED1

Figure 46: Pathway analysis for the 96 down-regulated genes in HEK293Alex3GFP vs HEK293GFP cells. The five main pathways reported by Reactome analysis are shown in the graphic and in the table, together with the number of genes included in each category, the percentages respect to the total number of down-regulated genes and the gene symbols.

Among them we found genes involved in *Metabolism*, such as ACADVL, "Very long-chain specific acyl-CoA dehydrogenase", codifying for mitochondrial protein catalyzing the first step of the mitochondrial fatty acid beta- oxidation pathway (Isackson et al., 2013); TM7SF2, "Transmembrane 7 superfamily member 2", involved in the conversion of lanosterol to cholesterol (Bennati et al., 2006); ACLY, "ATP citrate lyase", catalyzing the formation of acetyl-CoA and oxaloacetate (from citrate and CoA) and supporting several important biosynthetic pathways, including lipogenesis and cholesterogenesis (moreover in nervous tissue, ATP citrate-lyase may be involved in the biosynthesis of acetylcholine) (Chypre et al., 2012).

Five out of ninety six down-regulated-genes belong to *Cell Cycle/Mitotic* pathways.

Among them we found: MCM2, “minichromosome maintenance complex component 2”, codifying for a key component of the pre-replication complex, involved in the formation of replication forks and in the recruitment of other DNA replication related proteins (Evrin et al., 2013); SPC24, “spindle pole body component 24 homolog”, codifying for a component of the essential kinetochore-associated NDC80 complex, which is required for kinetochore integrity and the organization of stable microtubule binding sites in the outer plate of the kinetochore during chromosome segregation and spindle checkpoint activity; SMC4, “structural maintenance of chromosomes 4”, a central component of the condensin complex, required for conversion of interphase chromatin into mitotic-like condense chromosomes (Bharadwaj et al., 2004); TUBB, “beta1-tubulin”, forming microtubules together with alfa-tubulin (Wade, 2007).

Four out of ninety six down-regulated-genes belong to *Metabolism of protein* pathway (EIF2S2, “eukaryotic translation initiation factor 2, subunit 2 beta, 38kDa”; CCT3, “chaperonin containing TCP1, subunit 3, gamma”; EIF3D, “eukaryotic translation initiation factor 3, subunit D”; MPI, “mannose phosphate isomerase”) and *Gene expression* pathway (EIF2S2, “eukaryotic translation initiation factor2, subunit 2 beta, 38kDa”; CSTF3, “cleavage stimulation factor, 3’mRNA, subunit 3, 77kDa”; TM7SF2, “transmembrane 7 superfamily member 2”; AARS, “alanyl-tRNA sinthetase”). Finally, three down-regulated-genes belongs to *Signal transduction* pathway (ATP6V1G2/BAT1, “ATPase, H^+ transporting, lysosomal 13kDa, V1 subunit G2/HLA-B associated transcript 1”; MAGED1, “melanoma antigen family D, 1”; YWHAE, “tyrosine 3-monooxygenase/tryptophan 5-monooxygenase activation protein, epsilon polypeptide”).

Moreover, among up-regulated genes we found CCND1, codifying for cyclin D1, belonging to the highly conserved cyclin family, whose members unction as regulators of CDKs (Cyclin-dependent kinase), to contribute to the temporal coordination of each mitotic event (Lew et al., 1991).

Taken together these data indicate that Alex3 overexpression causes changes in global gene expression that involved key processes of cellular physiology, such as metabolic processes or cell cycle progression.

DISCUSSION

A - Armcx/Armc10 gene expression

The Armcx gene cluster (Armcx1-6, Gprasp1-2 y bhlhb9) arose by retrotransposition from a single Arm-containing gene (Armc10), and by subsequent short-range tandem duplications of a rapidly evolving region of the Eutherian X chromosome (Lopez-Domenech et al., 2012).

Armc10 gene sequence has strong similarity to the Armcx genes, but several differences can be found respect with them: i) it maps out of the cluster, to the 7th human and the 5th mouse chromosome; ii) it is a typical, multi-exon-containing gene, with the coding sequence split in at least eight exons (Abu-Helo and Simonin, 2010; Simonin et al., 2004), whereas all Armcx-coding sequences are contained in a single exon; iii) it is present in all vertebrates, whereas all Armcx genes are specific to Eutherian (placental) mammals.

Several Armcx/Armc10 genes were found to be expressed in the brain (Kurochkin et al., 2001), and in this work we further analysed the expression of Armcx/Armc10 genes during embryonic development, confirming their expression in the developing neural tissues, neural crest derivatives and hind limbs, in addition to other tissues that were specific for each gene (Fig.21). The neural expression of Armcx/Armc10 genes, together with their unusual and rapid evolution, is consistent with their involvement in the evolution of innovative brain cortical structures among Eutherian mammals (Lopez-Domenech et al., 2012).

Given that i) the expression of retrotransposed genes depends largely on the regulatory landscape of the insertion site, ii) gene clusters are often maintained to allow the sharing of regulatory sequences, and iii) Armcx gene expression is similar, it was suggested that the Armcx gene cluster is globally regulated (Lopez-Domenech et al., 2012), indicating redundant function for Armcx/Armc10 genes (Coveney et al., 2008). However, the presence of 9 Armcx cluster genes in Eutherian mammals suggests that their proteins can operate under specific physiological conditions, at different developmental stages, in different subcellular compartments or in alternative splicing forms. One example can be provided by the further evidences of neural expression of Alex3 and Armc10 described in this work: looking at the subcellular localization of Alex3 and Armc10 in Purkinje cells we showed that Alex3 is mainly localized at cytosol, whether Armc10 localized at nuclei of these cells, probably carrying out different functions in the same cell type (Fig.22h and Fig.32g).

B - Armcx/Armc10 mitochondrial function

We describe Alex3 and Armc10 as regulator of mitochondrial aggregation, dynamics and trafficking in neurons. This notion has great relevance, given that mitochondrial dynamics are essential for neuronal viability and neurotransmission. Lopez-Domenech et al. showed that Alex3 protein is not involved in mitochondrial respiration, DNA copy number determination, mitochondrial membrane potential regulation, or Ca^{2+} homoeostasis and handling in mitochondria (Lopez-Domenech et al., 2012). This is interesting because often proteins regulating mitochondrial dynamics also participate in these bioenergetic processes (Santel and Fuller, 2001).

As yet shown for Alex3 protein (Lopez-Domenech et al., 2012), Armc10 also causes mitochondrial aggregation and/or tethering in neurons and HEK293 cells (Fig.33). In neurons, these processes are believed to serve to capture mitochondria at specific locations requiring high-energy and Ca^{2+} buffering conditions (Chang and Reynolds, 2006; MacAskill and Kittler, 2010). The mechanism by which Alex3 and Armc10 cause mitochondrial aggregation may involve Mitofusins, as they both interact with Mfn1 and Mfn2 (Fig.23 and Fig.36). Nevertheless, we were unable to find evidence about the involvement of Alex3 protein in mitochondrial fusion (Fig.24). Although Alex3 and Armc10 promote mitochondrial tethering and this process could facilitate mitochondrial fusion (Hoppins and Nunnari, 2009), it is possible that a signal was required for membranes fusion, possibly through Mitofusins activation.

On the other hand, it has been recently shown that Mitofusin2 is directly involved in and required for mitochondrial axonal transport, independently from its role in mitochondrial fusion (Misko et al., 2010). Importantly, both Mitofusin1 and Mitofusin2 interact with mammalian Miro1/Miro2 and Trak2 (Van Straaten and Hekking, 1991). Moreover mitochondrial peri-nuclear aggregation phenotypes have been observed after dysfunction in Miro1/2 and Trak2 proteins, suggesting that alteration of transport results in aggregation (Liu and Hajnoczky, 2009; MacAskill and Kittler, 2010). For this reasons we can suppose that Alex3 and Armc10 cause mitochondrial aggregation and/or tethering independently of a possible role in mitochondrial fusion.

It is interesting to note that the evolutionary appearance of the Armc10 gene in basal chordates coincides with the genomic duplication of mitochondrial dynamics-related genes, including Mitofusins and Miro GTPases (Vlahou et al., 2011). This observation

suggests a coordinated increase in the complexity of the molecular machinery that regulates this process.

Alex3 and Armc10 interact with the KIF5/Miro/Trak2 complex, which controls mitochondrial dynamics in neurons and at least Alex3 fulfill this function in a Ca^{2+}-dependent manner (Fig.29, Fig.21 and Fig.35). Our immunoprecipitation experiments show that Alex3 and Armc10 interact directly with Miro1-2 and Trak2. However, we were unable to find a direct interaction with the Kinesin motor KIF5. Importantly, the interaction of Alex3 with Miro/Trak2 proteins requires low Ca^{2+} concentrations, as the presence of Ca^{2+} dramatically reduced the interaction. Furthermore, mutation of the EF-hand motif in Miro1 protein abolished this Ca^{2+}dependence, thereby indicating that Ca^{2+}-driven conformational changes in Miro proteins (MacAskill et al., 2009a; Nelson and Chazin, 1998; Wang and Schwarz, 2009) are the essential mechanisms that regulate the interaction between Alex3 and the Miro/Trak2complex. Thus, while low Ca^{2+} concentrations may favour the formation of KIF5/Miro/Trak2/Alex3 complex, increases in intracellular Ca^{2+} rapidly uncouple such complex (including Alex3), thereby arresting mitochondrial trafficking.

Our experiments indicate that the C-terminal region of Alex3, containing six Arm domains, is required to interact with Miro protein (Fig.30). However, we do not yet know whether this interaction is mediated directly by these domains, as is the case for other proteins (Tewari et al., 2010), or by other regions included in the C-terminus. It can be interesting mentioned that the protein p115, localized at Golgi membrane, contains armadillo domains mediating the interaction with the GTPase Rab1a, serving as vesicle tethering factor and playing an important role at different steps of vesicular transport (An et al., 2009).

The notion that Alex3 (and possibly also Armc10) interacts with the Miro/Trak2 complex when mitochondria are motile at low Ca^{2+} concentrations (Macaskill et al., 2009b; Wang and Schwarz, 2009) is further supported by our findings that knockdown of Alex3 (such as Armc10) results in a decrease in the percentages of motile mitochondria, similarly to what was observed in Miro/Trak2 loss-of-function (Brickley and Stephenson, 2011; MacAskill et al., 2009a; Saotome et al., 2008). The observation that knockdown of Alex3 and Armc10 do not affect the speed of the few motile mitochondria present suggests a mechanism in which Alex3 and Armc10 favor the formation of KIF5/Miro/Trak2 complexes (thereby enhancing mitochondrial trafficking).

However, Alex3 and Armc10 are unlikely to be involved in regulating the motor activity of Kinesin itself. We consider our overexpression findings, in which both the percentage and velocity of motile mitochondria were reduced, to provide further evidence of the physiological involvement of Alex3 and Armc10 in mitochondrial trafficking, possibly by deregulating and/or recruiting components of the complex (acting as a dominant negative). Together with our biochemical data, the present functional study proposes a model in which Alex3 and Armc10 proteins are positive regulators of mitochondrial trafficking, by interacting directly with Miro/Trak2. Furthermore, as shown for the KIF5/Miro/Trak2 complex (Macaskill et al., 2009b; Wang and Schwarz, 2009), increased neuronal activity leading to increases in Ca^{2+} is likely to cause Alex3/Miro/Trak2 complex disassembly and mitochondrial arrest at active neurotransmission sites, thereby fulfilling the bioenergetic requirements of neuronal transmission.

In conclusion, we described Alex3 and Armc10 as proteins with evolutionarily conserved functions in the regulation of mitochondrial dynamics and transport. However, gene-specific particularities are present: whereas dysregulation (both overexpression and downregulation) of Armc10 protein levels causes marked mitochondrial arrest, we did not find evidence of involvement of the Armc10 protein in the regulation of the velocity of the few mitochondria that remained motile in the two experimental conditions. In contrast, Alex3 protein participates to this regulation. Moreover, Armc10 overexpression induced mitochondrial aggregation in HEK293T cells, but not in hippocampal neurons. Armc10 involvement in fusion/fission processes or in Ca^{2+}-dependent interaction with mitochondrial transport machinery, remains to be further investigated.

These data suggest overlapping but differential levels and mechanism of regulation of mitochondrial dynamics and transport by Alex3 and Armc10 proteins and probably by the whole Armcx cluster.

Further studies are needed to ascertain whether the novel Armc10/Armcx gene family of mitochondrial proteins described herein contributes to the pathophysiology of neurological diseases, which often bear mutations or functional dysregulation in proteins controlling mitochondrial trafficking in neurons (Chen and Chan, 2009; Han et al., 2011).

C - Nuclear function of Armcx/Armc10 and Wnt signalling pathway

Mitochondria are dynamic organelles playing critical roles in energy production, apoptosis, and intracellular signaling (Finkel and Holbrook, 2000; Wallace, 2005). Not surprisingly, changes in mitochondrial number, distribution and activity are highly regulated depending to cell requirement and to the developmental stage (Nagata, 2006; Wallace, 2005).

Although mitochondria contain their own genome encoding 13 subunits involved in electron transport, the vast majority of the estimated 1000–1500 mitochondrial proteins are nuclear encoded (Johnson et al., 2007; Pagliarini et al., 2008). Mitochondrial biogenesis requires a sophisticated transcriptional program capable of responding to the energetic demands of the cell by coordinating expression of both nuclear and mitochondrial encoded genes (Scarpulla, 2002).

Moreover, nuclear gene expression can be influenced by signals coming from mitochondria, a process called retrograde communication (Liao and Butow, 1993; Liu and Butow, 2006; Parikh et al., 1987; Poyton and McEwen, 1996), so that the regulation of mitochondrial activity depends on a bidirectional flow of informations. The retrograde signaling could be realized by the translocation of some mitochondrial proteins to the cytoplasm, and/or into the nucleus (Cannino et al., 2007).

In skeletal mammalian myoblasts and in human pulmonary carcinoma cells, mitochondrial retrograde signaling seems to occur through cytosolic $[Ca^{2+}]i$ changes (Amuthan et al., 2002; Biswas et al., 1999). The alteration of mitochondrial membrane potential ($\Delta\Psi$) reduces mitochondrial Ca^{2+} uptake and, in turn, it reduces ATP availability, causing reduction of calcium efflux into storage organelles or outside the cells. Increased cytosolic Ca^{2+} concentration in turn activates calcineurin, and related factors such as Ca^{2+}-dependent kinases, causing the activation of different nuclear transcription factors (Butow and Avadhani, 2004).

In summary, the control of mitochondrial biogenesis and function requires a variety of well-orchestrated regulatory mechanisms, and a continuous nuclear-mitochondrial communication allows the cell to respond to changes in functional state of mitochondrial in both physiological and pathological conditions (Butow and Avadhani, 2004; Cannino et al., 2007; Finley and Haigis, 2009; Liu and Butow, 2006).

In this work we characterize the function of Alex3 and Armc10 proteins, both targeted to mitochondria and controlling the distribution and dynamics of these organelles in

HEK293AD cells and hippocampal neurons. The mitochondrial localization of Alex3 and Armc10 was previously described (Mou et al., 2009), consistent with the presence of a putative mitochondrial targeting signal in their sequences. Moreover it was demonstrated that Alex3 is located in the outer-surface of mitochondria (Mou et al., 2009), with its C-terminal (containing the Arm domains) exposed to the cytosol.

However, Alex3 and Armc10 localization is not restricted to mitochondrial compartment. All splicing variants of Armc10, when overexpressed in QSG-7701 cells were localized in the cytoplasm and nuclear envelope (Huang et al., 2003); we also showed that endogenous Armc10 also localized at nuclei (Fig.32g and Fig.33b) This data is consistent with the study of Zhou et al., where Armc10-B isoform was described to regulate transcription though interaction with p53 (Zhou et al., 2007).

In addition to putative mitochondrial targeting sequences, Alex3 contains a nuclear localization signal and has nuclear localization in neurons (Fig.10 and Fig.22g). Moreover, the deletion of the first 12 aminoacids at N-terminal of Alex3 sequence (where putative mitochondrial targeting signal is located), abolishes mitochondrial targeting and, interestingly, led to nuclear localization of the mutant form (Fig.11). The observation is consistent with a previous study showing interaction of Alex3 with the transcription factor Sox10 and enhancement of its transcriptional activity by Alex3 (Mou et al., 2009).

On the other hand we showed that chicken endogenous Armc10 protein and mouse Alex3 or Armc10 proteins (ectopically expressed in chicken spinal cord), also localize at mitochondria (Fig.39). Moreover, the deletion of the first 12 aminoacids at N-terminal of Alex3 sequence, also abolishes mitochondrial targeting in chicken spinal cord cells, without restrict Alex3 localization at nuclear compartment, but causing a diffuse cytosolic and nuclear localization. This data suggest that the mechanisms regulating Alex3 localization between nucleus and mitochondria may be organism- or tissue-specific.

Taken together, these observations support that *Armcx* genes have biological functions in two compartments (namely, mitochondria and nucleus), as has been shown for other proteins, including Sox10, DISC1 and HDAC1 (Atkin et al., 2011; Kim et al., 2010; Sawamura et al., 2008). Finally, because of their transcriptional control (Mou et al., 2009) and the presence of six Arm domains, *Armcx*/*Arm10* genes may functionally interact with the Wnt/β-catenin pathway, (as showed in 3.1 and discussed below). The observation that the lack of the N-terminal region targets Alex3 to the nucleus and the existence of a putative starting codon at the first internal methionine (aa 38) raise the

possibility of alternatively translated isoforms acting selectively at the mitochondria or in the nucleus.

Our data suggest that the Armc10/Armcx gene cluster encodes a new protein family that may act as a shuttle between the mitochondrial and nuclear compartments. They may act, in response to certain stimuli or physiological conditions, regulating mitochondrial transport and/or tethering in order to promote the renewal/replacement of dysfunctional mitocondria, in a quality-control mechanism (Tatsuta and Langer, 2008).

Nevertheless, the exact function carried out by Alex3 and Armc10 following re-localization to nucleus or mitochondria, the mechanism by which they can translocate to/from nucleus and the conditions activating that translocation, are still far to be understood.

In order to find a molecular pathway in which Alex3 may carry out its function during development, we alight on its protein structure: the whole Armcx/Armc10 cluster codify for proteins containing six Armadillo repeats, found in a wide range of proteins related to the Wnt/β-catenin signaling, such as β-catenin or Adenomatous polyposis coli (APC).

Wnt proteins are important mediators of intercellular communication, and the signaling by members of the Wnt family of molecules is crucial for normal embryonic development in various systems, including the nervous system. They can influence tissue organization and growth by functioning locally, in an autocrine manner or on immediately adjacent cells, and can also act at a distance, by generating a gradient across a tissue.

The role of Wnt signaling in the development and maturation of the vertebrate nervous system includes the control of cell proliferation, differentiation, cell migration, axonal guidance, axon remodelling, dendrite morphogenesis and synapsis formation (Carmona-Fontaine et al., 2008; Chenn and Walsh, 2002; Hirabayashi et al., 2004; Lyuksyutova et al., 2003; Matthews et al., 2008; Salinas, 1999; Salinas and Zou, 2008).

These processes are extremely expensive in terms of energy and need an appropriate mitochondrial distribution and functionality to fulfill local energy requirement or Ca^{2+} buffering (Hollenbeck and Saxton, 2005; Morris and Hollenbeck, 1993). Little is known about signaling pathways involved in the regulation of these processes, and few studies suggest molecular link between Wnt/β-catenin pathway and mitochondrial function. For instance, it was described that the activation of Wnt signaling by Wnt-3a results in

significant increase in mitochondrial biogenesis (An et al., 2010; Yoon et al., 2010) and in reduction in organelle membrane injury and apoptosis (Deng et al., 2009; Wang et al., 2009b). Moreover, it was described that the proinflammatory mediator Leukotriene D(4), implicated in the pathology of chronic inflammation and cancer, causes translocation of β-catenin to the mitochondria, triggering a cellular increase in NADPH dehydrogenase activity, ATP/ADP ratio and in the transcription of mtDNA (Mezhybovska et al., 2009). Another link between Wnt/β-catenin pathway and mitochondrial function cames from APC, localizing at several cell compartments (Henderson, 2000; Nathke, 2006; Neufeld et al., 2000a; Neufeld et al., 2000b). In particular, truncated APC mutants preferentially accumulate at mitochondria and regulate accumulation of Bcl-2, contributing to the survival and proliferation of cancer cells (Brocardo et al., 2008). The truncated APC mutants shuttle more dynamically than full-length APC and could potentially transport specific factors (*e.g.*, Bcl-2) from the nucleus to the mitochondria to extend tumor cell survival. More recently, Qian et al. (Qian et al., 2010) confirmed the localization of APC at mitochondria and showed that caspase-cleaved shortened forms of APC bound to the protein hTID-1 at mitochondria. hTID-1 is a regulator of apoptosis, and APC was shown to bind two distinct hTID-1 isoforms (40 and 43 kDa) that can differentially affect apoptosis.

Probably the stronger contribution to the understanding of the link between Wnt/β-catenin pathway and mitochondrial function/dynamics comes from unpublished data collected in our lab. This data indicate that the mitochondrial aggregation phenotypes induced by Alex3 overexpression in HEK293 cells is attenuated by treatment with several Wnts, trough Wnt-induced Alex3 degradation. Moreover, while the Wnt canonical pathway did not alter the pattern of mitochondrial aggregation induced by Alex3, Wnt/PKC non-canonical pathway regulated both Alex3 protein levels and Alex3-induced mitochondrial aggregation. Wnt/PKC non-canonical pathway probably acts trough Alex3 de-phosphorylation, targeting Alex3 protein to a proteasome-independent degradation pathway. These data links non-canonical Wnt signaling cascade to various and convergent functions of mitochondrial biology, including the regulation of mitochondrial aggregation, dynamics and trafficking, trough Alex3 protein levels regulation (Serrat et al., submitted).

Taken together this data led us to speculate that Alex3 (but also the whole Armcx cluster) could play a role in regulation of mitochondrial dynamics or function during

neural development by regulating Wnt/β-catenin signaling pathway. Using the chicken spinal cord as physiological model, we found that Alex3 overexpression decreases TCF/LEF-transcriptional activity at basal condition and following Wnt3a or β-catenin^{CA} induction, indicating that Alex3 substantially acts as an inhibitor of canonical Wnt/β-catenin pathway (Fig.37).

D - Function of Armcx/Armc10 during spinal cord development

Wnt/β-catenin signaling pathway plays a pivotal role in spinal cord development, for instance regulating patterning of neural tube, promoting the proliferation of dorsal spinal progenitor cells and inducing the differentiation of dorsal spinal neurons. For this reason we questioned if Alex3 and Armc10 could be involved in some of these developmental processes.

As the Armcx gene cluster is specific to Eutherian mammals, we first wanted to characterize the expression of the unique gene copy present in chick: the Armc10/SVH gene that shares a strong protein sequence homology with mouse Armc10. Armc10/SVH is expressed in a dorsal to ventral gradient (highest dorsally) in mitotically active neural precursors and weakly in floor plate (Fig.39a) at early stage HH19. This expression pattern is maintained at the later stage (HH24), when Armc10/SVH transcripts appeared also in ventral motoneurons, suggesting a possible role for Armc10/SVH in the control of differentiation program progression.

The expression of Armc10/SVH in a dorso-ventral gradient resembles the expression of the mitogenic Wnt proteins (composed principally of Wnt1 and Wnt3a) across the ventricular zone of the neural tube (Megason and McMahon, 2002). In vertebrates, morphogenesis of the developing neural tube is achieved by the counteracting activities of morphogenetic signaling gradients. Wnt1 and Wnt3a mRNA are co-expressed in highly restricted dorsal domain (Alvarez-Medina et al., 2008; Megason and McMahon, 2002). However, *in vivo* reporter-gene analysis predicted canonical Wnt signaling to be active in dorsal two-thirds of the developing mous (Maretto et al., 2003) and chick (Alvarez-Medina et al., 2008; Megason and McMahon, 2002) spinal cord, suggesting a broader function for Wnts. In particular, within the forming spinal cord, the dorso-ventral gradient of Wnt signaling (composed principally of Wnt1 and Wnt3a) has been proposed to organize the growth of neural progenitors (Alvarez-Medina et al., 2008; Megason and

McMahon, 2002), promoting G_1 to S progression and negatively regulating cell differentiation by inhibiting cell cycle exit.

Neural tube patterning

Even if Wnts have primarily been considered as mitogenic signals for neural cells (Dickinson et al., 1994; Machon et al., 2003), several studies indicate that Wnt signaling plays an additional and crucial role in patterning the neural tube (Alvarez-Medina et al., 2008; Lee and Deneen, 2012; Yu et al., 2008). Overexpression of a stabilized form of β-catenin results in prominent changes in progenitor gene expression along the dorso-ventral axis, in both mouse (Yu et al., 2008) and chick (Alvarez-Medina et al., 2008) spinal cord: the expression patterns of dorsal markers such as Pax7 or intermediate markers such as Pax6 are shifted ventrally at the expense of ventral progenitors marker such as Nkx6.1, Olig2 and Nkx2.2. Moreover, the expansion of the territory of dorsal progenitors results in the increased generation of dorsal neuronal subtypes with the concomitant loss of ventral motor neurons (Duchen, 2004).

We showed that Alex3 acts as an inhibitor of the canonical Wnt/β-catenin pathway in chicken spinal cord (Fig.37), then we expected to find an alteration in the expression pattern of dorsal and ventral markers following overxpression of Alex3 (or Armc10). Surprisingly, we didn't find any changes in the expression of ventral marker Nkx6.1 or the dorsal marker Pax7. We can suppose that the inibition of Alex3 is not so strong as to induce changes in patterning, at least at the analyzed developmental stage (HH12+24hPE).

Proliferation and differentiation in neural tube

Another important aspect of neural tube development is the requirement of a highly coordinated orchestration of progenitors cell proliferation and differentiation. In developing chick spinal cord, cells located at ventricular zone (VZ) are proliferative neural progenitor cells, which progressively initiate the expression of proneural genes (such as Mash1 and Neurogenins) in response to region-specific neurogenic signals. Proneural genes drive neuronal progenitor cells to produce postmitotic neurons that migrate into mantle zone (MZ).

Wnt/β-catenin signaling plays a crucial role in maintaining neural precursor cells during spinal cord development. Overexpression of constitutively activated β-catenin promotes

neural precursor proliferation (Chenn and Walsh, 2002). Conversely, knockout of β-catenin inhibits neural precursors proliferation and promotes neuronal differentiation (Zechner et al., 2007). Thus, inhibition of the Wnt/β-catenin pathway is an important prerequisite for neurogenesis and neuronal differentiation.

In this study we found that in Alex3 electroporated chicken spinal cord, Alex3 (GFP^+) electroporated cells are mainly located at MZ of the neural tube, suggesting that Alex3 may promote neural differentiation.

Moreover, we found that in Alex3 electroporated embryos, most Alex3 electroporated cells were Tuj-1 positive, producing a significant increase in the percentage of Tuj-1^+/GFP^+ cells with respect to the control embryos. This data confirmed that full length Alex3 acts to promote differentiation and is coherent with its role of Wnt/β-catenin pathway inhibitor. Importantly, this function is specific for Alex3 and was not found for the Armc10 protein, providing a functional divergence in the context of spinal cord development.

Another interesting data is that the effect of Alex3 overexpression in promoting neuronal differentiation requires the mitochondrial localization of Alex3, given that pCIGAlex3Δ(1-12) deletion mutant overexpression doesn't induce any changes in electroporated cells distribution neither in Tuj-1 expression levels in GFP^+ cells.

This data leads to speculate that mitochondrial Alex3 could retain at mitochondria same nuclear factor necessary for TCF/LEF activation, leading to the Wnt/β-catenin signaling pathway inhibition and thus promoting differentiation. According with this mechanisms, the deletion mutant pCIGAlex3Δ(1-12) shouldn't be able to inhibit Wnt/β-catenin signaling pathway. A similar mechanism was described by Mou et al., suggesting a novel signaling cascade between the mitochondria and the nucleus through a Sox10/Alex3 protein complex. They propose that Alex3 modulates the transcriptional activity of Sox10 retaining it to mitochondria, where it could undergo post-translational modifications resulting in an increased transcriptional activity once transported into the nucleus (Mou et al., 2009). However, we cannot yet sustain that the effect of Alex3 overexpression on neuronal differentiation is achieved by inhibition of Wnt/β-catenin pathway and further experiments are required to support this intriguing hypothesis.

Our data also showed that overexpression of both full length Alex3 and Armc10 (but not the overexpression of pCIGAlex3Δ(1-12) mutant) causes a decrease in differentiated cell density (Fig.42d and 42e). Further analysis revealed a reduction in proliferation of

neural progenitors after the overexpression of full length Alex3 and Armc10 (Fig.44). These results indicate that both Alex3 and Armc10 are negative regulators of cell cycle, and that mitochondrial localization of Alex3 is required to carry out this function, even if we don't yet know if Alex3/Alrmc10 overexpression acts on precursor cells cell cycle by promoting an early cell cycle exit, or affecting cell cycle length, or altering the balance between the 3 modes of division in neural precursors (PP, PN, NN). However, we can explain the reduction in the total number of neurons generated as consequence of the negative regulation on cell cycle.

Taken together, our data suggest that full length Alex3 is involved in both negative cell cycle regulation (possibly promoting cell cycle exit) and induction of differentiation in neural precursors; this double action would be reflected in lateral distribution of full length Alex3 overexpressing cells at mantle zone.

On the other hand, Armc10 is only involved in negative cell cycle regulation (possibly just affecting cell cycle length) and for this reason we find Armc10 overexpressing cells uniformly distributed between MZ and VZ. However, the effects of overexpression of both constructs result in a reduction of differentiated cells density in the electroporated side of neural tube. These differences between Alex3 and Armc10 overexpression effects on spinal cord developmental processes highlight functional divergences between the two proteins, suggesting that Alex3 may have acquired additional function respect to Armc10, phylogenetic ancestor of the whole Armcx gene cluster.

The data collected in this study, describing Alex3 overexpression effects on spinal cord development, are coherent with the inhibitor function of Alex3 on Wnt/β-catenin pathway. However there is not sufficient evidence to sustain that these effects on progenitor cell cycle and neuronal differentiation are achieved by inhibition of Wnt/β-catenin pathway and further experiments are required to support this hypothesis.

E - Downstream effects of Alex3 overexpression: candidate genes involved

To shade light on the biological processes in which Alex3 can be involved (trough regulation of mitochondrial dynamics, regulation of Wnt/β-catenin pathway or new and different activity) we carried out a genome-wide analysis of changes in mRNA levels subjecting HEK293AD cells stably expressing Alex3GFP to microarray analysis. HEK293AD cells are human embryonic kidney cell line and were used in our studies to analyze the Alex3 function in mitochondrial dynamics, together with primary mouse

hippocampal neurons. They express all the molecular elements belonging to Wnt canonical and non-canonical signaling cascade, and studies performed by our groups confirmed that Alex3 acts as an inhibitor of TCF/LEF-transcriptional activity both at basal level and after β-catenin or Wnt3a activation in this cell type, similarly to in chicken spinal cord. Our results indicate that Alex3 overexpression causes changes in global gene expression that involved key processes of cellular physiology.

Alterations in mRNA levels were found mainly for genes involved in metabolism and cell cycle regulation. In mitochondria, energy can be obtained from glucose or glycogen through anaerobic glycolysis and from oxidation of carbohydrates and fatty acids. The common metabolic product of sugars and fats is acetyl-CoA, which enters the Krebs cycle. Oxidation of one molecule of acetyl-CoA results in the reduction of three molecules of NAD and one of FAD. These reducing equivalents flow down a chain of carriers through a series of oxidation-reduction events. The released energy “charges” the inner mitochondrial membrane, converting the mitochondrion into a veritable biological battery. This oxidation process is coupled to ATP synthesis from ADP and inorganic phosphate (Pi), catalyzed by mitochondrial ATPase.

Several genes involved in these pivotal metabolic processes showed downregulated mRNA levels in HEK293ADAlex3 cells. Among them we found genes codifying for mitochondrial proteins, such as *ACLY* (ATP citrate synthase) or *ACADVL* (Very long-chain specific acyl-CoA dehydrogenase, mitochondrial), both involved in acetyl-CoA methabolism (Isackson et al., 2013); genes codifying for cytosolic proteins involved in glycolysis or glycogen degradation, such as *PYGB* (Glycogen phosphorylase, brain form) or *PKM2* (Pyruvate kinase muscle isozyme); *SDHC* (Succinate dehydrogenase complex subunit C) encoding one of four nuclear-encoded subunits that comprise succinate dehydrogenase, also known as mitochondrial complex II, key enzyme complex of the tricarboxylic acid cycle and aerobic respiratory chains of mitochondria (Ishii, 2007); *QPRT* (Quinolinate phosphoribosyltransferase) encoding a key enzyme in catabolism of quinolinate, (an intermediate in the tryptophan-nicotinamide adenine dinucleotide pathway), acting as a most potent endogenous exitotoxin to neurons, (elevation of quinolinate levels in the brain has been linked to the pathogenesis of neurodegenerative disorders such as epilepsy, Alzheimer's disease, and Huntington's disease) (Kincses et al., 2010).

As Alex3 overexpression causes strong alteration in mitochondrial distribution and dynamics is not surprising that it could affect bioenergetics processes, as described for many proteins involved in mitochondrial dynamics regulation, through a direct mechanism or by modulating the transcriptional activity resulting from some signaling cascade (Duarte et al., 2012; John et al., 2005; Park et al., 2010; Santel and Fuller, 2001). Surprisingly, data obtained in our lab suggested that Alex3 protein is not involved in mitochondrial respiration, DNA copy number determination, mitochondrial membrane potential regulation, or Ca^{2+} homoeostasis and handling in mitochondria (Lopez-Domenech et al., 2012).

As Alex3 overexpression was found to reduce proliferation in both HEK293AD cells line and in vivo in chicken spinal cord, the more interesting data obtained by microarray analysis, certain concerns genes involved in cell cycle regulation.

Alteration in mRNA levels were observed for two genes involved in S-phase entrance: *YWHAE* (Tyrosine 3-monooxygenase/tryptophan 5-monooxygenase activation protein, epsilon polypeptide) and *MCM2* (minichromosome maintenance complex component 2), both downregulated in HEK293ADAlex3GFP, consistently with the inhibitory activity of Alex3 on cell cycle.

YHWAE belongs to the 14-3-3 family of proteins which mediate signal transduction by binding to phosphoserine-containing proteins and which were first identified as abundant brain proteins. Depending on their interaction with specific protein effectors, 14-3-3 proteins participate in many vital regulatory processes, such as DNA replication, cell cycle regulation, signal transduction pathways, exocytosis, cell adhesion and neuronal plasticity (Aitken, 2006; Zannis-Hadjopoulos et al., 2008). 14-3-3 proteins are involved in DNA replication of eukaryotes through binding to the cruciform DNA that forms transiently at the replication origins at the onset of S phase. The involvement of 14-3-3 proteins in the regulation of initiation of DNA replication may be mediated by their interaction with several initiator proteins. Recent proteomic studies suggest that 14-3-3 proteins are involved in DNA replication through their interaction with components of the prereplication (pre-RC) complex, among them the replication factor C, the histones HJ4 and H2B, and the minichromosome maintenance (MCM) proteins (Zannis-Hadjopoulos et al., 2008).

MCM2, codifies for a key component of the pre-replication complex in late mitosis (Bell et al., 2002) and forms a complex with MCM4, 6, and 7, regulating the

helicase activity of the complex (Zannis-Hadjopoulos et al., 2008). Several subunits of the MCM hexameric complex are phosphorylated and it is thought that phosphorylation activates the intrinsic MCM-DNA helicase activity, thus allowing formation of active replication forks. Cdc7, Cdk2, and ataxia telangiectasia and Rad3-related kinases regulate S-phase entry and S-phase progression and are known to phosphorylate the MCM2 subunit (Masai and Arai, 2000; Montagnoli et al., 2008).

beta1-tubulin was also found downregulated in HEK293ADAlex3GFP and this data can be associated with the state of resting cells more that the state of dividing cell. In fact, the total cellular tubulin content increases as the cells progress towards mitosis, and whereas alpha-tubulin isotype and gamma-tubulin transcripts were found to be expressed at constant levels throughout the cell cycle, some of the beta-tubulin isotypes transcripts were found to be more highly expressed in dividing then in resting cells (Dumontet et al., 1996).

As the interphase array of microtubules, focused on the centrosome, is necessary for a variety of important cellular processes, its integrity could be necessary for the cell to progress through G1. In this regard, many studies contain data regarding the impact of microtubule cytoskeleton alteration on G1 progression for a variety of mammalian cell lines (Uetake and Sluder, 2007). Almost all report that alterations of the microtubule cytoskeleton lead to a G1 arrest in a variable and often high proportion of the cell populations, particularly for cell lines expected to have an intact p53 pathway (Uetake and Sluder, 2007). Then, a *beta1-tubulin* downregulation can be easily associated to a cell cycle negative regulation.

Moreover, the downregulation of *beta1-tubulin* in HEK293ADAlex3GFP allows speculating a link between Alex3 overexpression and alteration of mitochondrial trafficking, independently of its function in KHC/Miro/Trak2 complex, at least in pathological conditions. As microtubules are fundamental to the morphology of neurons, defects in tubulin genes are likely to cause neuronal diseases (Jaglin and Chelly, 2009; Poirier et al., 2010; Tischfield et al., 2010) or induce very severe neurological symptoms, such as peripheral neuropathy and loss of axons in many kinds of brain neurons (Tischfield et al., 2010). Recent analysis of b-tubulin mutants showed that the punctiform mutation E410K and D417H, found in patients suffering of various neurological symptoms (such as loss of axons in the central nervous system, fibrosis of extraocular muscles and peripheral neuropathy), affect the microtubule binding of axonal-

transport KIFs. In addition, these mutations disrupt axonal transport of vesicles and mitochondria in cells derived from the central and peripheral nervous systems. Moreover, in vivo knockdown of KIF1Bb obtained by in utero electroporation of microRNA in E14 brains, induced axonal defects in the brain, similarly to phenotypes associated to E410K and D417H electroporated brains (Niwa et al., 2013). Nevertheless, in physiological conditions, regulation of mitochondrial transport has never been linked to regulation of beta-tubulin levels. Not surprisingly, microtubule-based transport id known to be regulated through microtubule-associated proteins, such as tau and MAP1b that in turn, alter their binding to microtubules and their microtubule stabilizing ability (Sang et al., 2001; Scales et al., 2009).

Other genes belonging to Cell Cycle pathway were found downregulated in HEK293ADAlex3GFP: *SMC4*, (structural maintenance of chromosomes 4) and *SPC24*, (spindle pole body component 24 homolog). SMC4 is a central component of the condensin complex, required for conversion of interphase chromatin into mitotic-like condense chromosomes (Bharadwaj et al., 2004); SPC24 is an essential component for kinetochore targeting of the NDC80 complex, the key microtubule-binding element of the kinetochore, directly interacting with microtubules and required for the organization of stable microtubule binding sites in the outer plate of the kinetochore during chromosome segregation and spindle checkpoint activity (Foley and Kapoor, 2013).

The majority of alterations in mRNA levels detected by microarray analysis were found for downregulated genes and just 3 genes were found upregulated in in HEK293ADAlex3GFP. Among them, we point out on CyclinD1, a key protein that promote proliferation in G1 phase of cell cycle, linking extracellular mitogenic signals to the core cell cycle machinery (Lobjois et al., 2004; Sherr et al., 2005).

At first glance this data seems quite contradictory with our results concerning Alex3 function in regulation of proliferation in HEK293AD cells, or in proliferation/differentiation balance in chicken spinal cord. Moreover, Wnt/β-catenin pathway is known to control the growth of dorsal region of the closing neural tube, in part through transcriptional regulation of CyclinsD1 and D2 (Megason and McMahon, 2002), so the inhibition of TCF/LEF transcriptional activity observed in Alex3 overexpressing cells shouldn't result in an increase of CyclinD1 transcript.

Nevertheless recent studies have proposed that several Cyclins can modulate progenitors fate in a manner independent from their function in cell cycle progression. Interestingly,

forced expression of either CyclinD1 or CyclinD2 in the chick spinal cord was observed to be qualitatively compatible with terminal motoneuron differentiation (Chiang et al., 1996). Moreover, Cyclin D1 was recently described promote neurogenesis in the embryonic murine spinal cord in a cell-cycle-indipendent manner (Lukaszewicz and Anderson, 2011).

However, the exact mechanism by which CyclinD1 can lose its function as cell-cycle promoting factor and acquire pro-neurogenesis features remains to be unraveled. Given that increasing biochemical and molecular evidence indicate that CyclinD1 can regulate transcription (Bienvenu et al., 2010; Fu et al., 2004; Ratineau et al., 2002), it is attractive to think that a transcriptional function underlies its neurogenic influence. Moreover is intriguing to speculate that Alex3 could be a factor contributing to confer to CyclinD1 a pro-neurogenic activity.

Taken together these data indicate that Alex3 overexpression causes changes in global gene expression that involved key processes of cellular physiology, such as metabolic processes or cell cycle progression. However we are still far to identify the cellular and molecular mechanism by which Alex3 (and the whole Armcx/Armc10 cluster gene) act in these processes. To achieve this goal it is essential to clarify Armcx/Armc10 function in nervous system development.

CONCLUSIONS

1. - Armcx/Armc10 genes are highly expressed in the developing neural tissues.

2. - Alex3 and Armc10 exhibit bimodal localization in mitochondria and cell nucleus.

3. - Both Alex3 and Armc10 interact with Mitofusin1 and Mitofusin2 and at least Alex3 overexpression or silencing doesn't affect mitochondrial fusion-fusion balance.

4. - As yet shown for Alex3 protein, Armc10 also causes perinuclear aggregation and/or tethering of mitochondria.

5. - Alex3 and Armc10 overexpression or silencing in hippocampal neurons affects mitochondrial distribution and trafficking.

6. - Alex3 and Armc10 interact with Kinesina/Miro/Trak2 complex, which controls mitochondrial dynamics in neurons. At least Alex3 fulfills this function in a Ca^{2+}-dependent manner, given that the interaction of Alex3 with Miro/Trak2 proteins requires low Ca^{2+} concentrations.

7. - Alex3 is as an inhibitor of canonical Wnt/β-catenin pathway in chicken spinal cord.

8. - Alex3 is involved in both negative cell cycle regulation and induction of differentiation in neural precursors, while Armc10 is only involved in negative cell cycle regulation. This data suggests that Alex3 may have acquired additional function respect to Armc10, phylogenetic ancestor of the whole Armcx gene cluster.

REFERENCES

Abu-Helo, A., and F. Simonin. 2010. Identification and biological significance of G protein-coupled receptor associated sorting proteins (GASPs). *Pharmacology & therapeutics*. 126:244-250.

Aitken, A. 2006. 14-3-3 proteins: a historic overview. *Seminars in cancer biology*. 16:162-172.

Alexander, C., M. Votruba, U.E. Pesch, D.L. Thiselton, S. Mayer, A. Moore, M. Rodriguez, U. Kellner, B. Leo-Kottler, G. Auburger, S.S. Bhattacharya, and B. Wissinger. 2000. OPA1, encoding a dynamin-related GTPase, is mutated in autosomal dominant optic atrophy linked to chromosome 3q28. *Nature genetics*. 26:211-215.

Alvarez-Medina, R., J. Cayuso, T. Okubo, S. Takada, and E. Marti. 2008. Wnt canonical pathway restricts graded Shh/Gli patterning activity through the regulation of Gli3 expression. *Development*. 135:237-247.

Alvarez-Medina, R., G. Le Dreau, M. Ros, and E. Marti. 2009. Hedgehog activation is required upstream of Wnt signalling to control neural progenitor proliferation. *Development*. 136:3301-3309.

Amati-Bonneau, P., M.L. Valentino, P. Reynier, M.E. Gallardo, B. Bornstein, A. Boissiere, Y. Campos, H. Rivera, J.G. de la Aleja, R. Carroccia, L. Iommarini, P. Labauge, D. Figarella-Branger, P. Marcorelles, A. Furby, K. Beauvais, F. Letournel, R. Liguori, C. La Morgia, P. Montagna, M. Liguori, C. Zanna, M. Rugolo, A. Cossarizza, B. Wissinger, C. Verny, R. Schwarzenbacher, M.A. Martin, J. Arenas, C. Ayuso, R. Garesse, G. Lenaers, D. Bonneau, and V. Carelli. 2008. OPA1 mutations induce mitochondrial DNA instability and optic atrophy 'plus' phenotypes. *Brain : a journal of neurology*. 131:338-351.

Amiri, M., and P.J. Hollenbeck. 2008. Mitochondrial biogenesis in the axons of vertebrate peripheral neurons. *Developmental neurobiology*. 68:1348-1361.

Amuthan, G., G. Biswas, H.K. Ananadatheerthavarada, C. Vijayasarathy, H.M. Shephard, and N.G. Avadhani. 2002. Mitochondrial stress-induced calcium signaling, phenotypic changes and invasive behavior in human lung carcinoma A549 cells. *Oncogene*. 21:7839-7849.

An, J.H., J.Y. Yang, B.Y. Ahn, S.W. Cho, J.Y. Jung, H.Y. Cho, Y.M. Cho, S.W. Kim, K.S. Park, S.Y. Kim, H.K. Lee, and C.S. Shin. 2010. Enhanced mitochondrial biogenesis contributes to Wnt induced osteoblastic differentiation of C3H10T1/2 cells. *Bone*. 47:140-150.

An, Y., C.Y. Chen, B. Moyer, P. Rotkiewicz, M.A. Elsliger, A. Godzik, I.A. Wilson, and W.E. Balch. 2009. Structural and functional analysis of the globular head domain of p115 provides insight into membrane tethering. *Journal of molecular biology*. 391:26-41.

Arai, Y., J.N. Pulvers, C. Haffner, B. Schilling, I. Nusslein, F. Calegari, and W.B. Huttner. 2011. Neural stem and progenitor cells shorten S-phase on commitment to neuron production. *Nature communications*. 2:154.

Atkin, T.A., A.F. MacAskill, N.J. Brandon, and J.T. Kittler. 2011. Disrupted in Schizophrenia-1 regulates intracellular trafficking of mitochondria in neurons. *Molecular psychiatry*. 16:122-124, 121.

Aza-Blanc, P., H.Y. Lin, A. Ruiz i Altaba, and T.B. Kornberg. 2000. Expression of the vertebrate Gli proteins in Drosophila reveals a distribution of activator and repressor activities. *Development*. 127:4293-4301.

Baker, M.J., T. Tatsuta, and T. Langer. Quality control of mitochondrial proteostasis. *Cold Spring Harbor perspectives in biology*. 3.

Baloh, R.H., R.E. Schmidt, A. Pestronk, and J. Milbrandt. 2007. Altered axonal mitochondrial transport in the pathogenesis of Charcot-Marie-Tooth disease from mitofusin 2 mutations. *J Neurosci*. 27:422-430.

Barsoum, M.J., H. Yuan, A.A. Gerencser, G. Liot, Y. Kushnareva, S. Graber, I. Kovacs, W.D. Lee, J. Waggoner, J. Cui, A.D. White, B. Bossy, J.C. Martinou, R.J. Youle, S.A. Lipton, M.H. Ellisman, G.A. Perkins, and E. Bossy-Wetzel. 2006. Nitric oxide-induced

mitochondrial fission is regulated by dynamin-related GTPases in neurons. *The EMBO journal*. 25:3900-3911.

Bartlett, S.E., J. Enquist, F.W. Hopf, J.H. Lee, F. Gladher, V. Kharazia, M. Waldhoer, W.S. Mailliard, R. Armstrong, A. Bonci, and J.L. Whistler. 2005. Dopamine responsiveness is regulated by targeted sorting of D2 receptors. *Proceedings of the National Academy of Sciences of the United States of America*. 102:11521-11526.

Beausoleil, S.A., M. Jedrychowski, D. Schwartz, J.E. Elias, J. Villen, J. Li, M.A. Cohn, L.C. Cantley, and S.P. Gygi. 2004. Large-scale characterization of HeLa cell nuclear phosphoproteins. *Proceedings of the National Academy of Sciences of the United States of America*. 101:12130-12135.

Behrens, J., J.P. von Kries, M. Kuhl, L. Bruhn, D. Wedlich, R. Grosschedl, and W. Birchmeier. 1996. Functional interaction of beta-catenin with the transcription factor LEF-1. *Nature*. 382:638-642.

Bennati, A.M., M. Castelli, M.A. Della Fazia, T. Beccari, D. Caruso, G. Servillo, and R. Roberti. 2006. Sterol dependent regulation of human TM7SF2 gene expression: role of the encoded 3beta-hydroxysterol Delta14-reductase in human cholesterol biosynthesis. *Biochimica et biophysica acta*. 1761:677-685.

Bharadwaj, R., W. Qi, and H. Yu. 2004. Identification of two novel components of the human NDC80 kinetochore complex. *The Journal of biological chemistry*. 279:13076-13085.

Bienvenu, F., S. Jirawatnotai, J.E. Elias, C.A. Meyer, K. Mizeracka, A. Marson, G.M. Frampton, M.F. Cole, D.T. Odom, J. Odajima, Y. Geng, A. Zagozdzon, M. Jecrois, R.A. Young, X.S. Liu, C.L. Cepko, S.P. Gygi, and P. Sicinski. 2010. Transcriptional role of cyclin D1 in development revealed by a genetic-proteomic screen. *Nature*. 463:374-378.

Biosa, A., A. Trancikova, L. Civiero, L. Glauser, L. Bubacco, E. Greggio, and D.J. Moore. 2013. GTPase activity regulates kinase activity and cellular phenotypes of Parkinson's disease-associated LRRK2. *Human molecular genetics*. 22:1140-1156.

Biswas, G., O.A. Adebanjo, B.D. Freedman, H.K. Anandatheerthavarada, C. Vijayasarathy, M. Zaidi, M. Kotlikoff, and N.G. Avadhani. 1999. Retrograde Ca2+ signaling in C2C12 skeletal myocytes in response to mitochondrial genetic and metabolic stress: a novel mode of inter-organelle crosstalk. *The EMBO journal*. 18:522-533.

Boeuf, J., J.M. Trigo, P.H. Moreau, L. Lecourtier, E. Vogel, J.C. Cassel, C. Mathis, P. Klosen, R. Maldonado, and F. Simonin. 2009. Attenuated behavioural responses to acute and chronic cocaine in GASP-1-deficient mice. *The European journal of neuroscience*. 30:860-868.

Bonner, J., S.L. Gribble, E.S. Veien, O.B. Nikolaus, G. Weidinger, and R.I. Dorsky. 2008. Proliferation and patterning are mediated independently in the dorsal spinal cord downstream of canonical Wnt signaling. *Developmental biology*. 313:398-407.

Braun, R.J., and B. Westermann. 2011. Mitochondrial dynamics in yeast cell death and aging. *Biochemical Society transactions*. 39:1520-1526.

Brickley, K., M.J. Smith, M. Beck, and F.A. Stephenson. 2005. GRIF-1 and OIP106, members of a novel gene family of coiled-coil domain proteins: association in vivo and in vitro with kinesin. *The Journal of biological chemistry*. 280:14723-14732.

Brickley, K., and F.A. Stephenson. 2011. Trafficking kinesin protein (TRAK)-mediated transport of mitochondria in axons of hippocampal neurons. *The Journal of biological chemistry*. 286:18079-18092.

Briscoe, J., Y. Chen, T.M. Jessell, and G. Struhl. 2001. A hedgehog-insensitive form of patched provides evidence for direct long-range morphogen activity of sonic hedgehog in the neural tube. *Molecular cell*. 7:1279-1291.

Briscoe, J., A. Pierani, T.M. Jessell, and J. Ericson. 2000. A homeodomain protein code specifies progenitor cell identity and neuronal fate in the ventral neural tube. *Cell*. 101:435-445.

Brocardo, M., Y. Lei, A. Tighe, S.S. Taylor, M.T. Mok, and B.R. Henderson. 2008.

Mitochondrial targeting of adenomatous polyposis coli protein is stimulated by truncating cancer mutations: regulation of Bcl-2 and implications for cell survival. *The Journal of biological chemistry*. 283:5950-5959.

Brooks, C., Q. Wei, L. Feng, G. Dong, Y. Tao, L. Mei, Z.J. Xie, and Z. Dong. 2007. Bak regulates mitochondrial morphology and pathology during apoptosis by interacting with mitofusins. *Proceedings of the National Academy of Sciences of the United States of America*. 104:11649-11654.

Butow, R.A., and N.G. Avadhani. 2004. Mitochondrial signaling: the retrograde response. *Molecular cell*. 14:1-15.

Bystron, I., C. Blakemore, and P. Rakic. 2008. Development of the human cerebral cortex: Boulder Committee revisited. *Nature reviews*. 9:110-122.

Cai, L., H. Huang, S. Blackshaw, J.S. Liu, C. Cepko, and W.H. Wong. 2004. Clustering analysis of SAGE data using a Poisson approach. *Genome biology*. 5:R51.

Cai, Q., C. Gerwin, and Z.H. Sheng. 2005. Syntabulin-mediated anterograde transport of mitochondria along neuronal processes. *The Journal of cell biology*. 170:959-969.

Cai, Q., and Z.H. Sheng. 2009. Mitochondrial transport and docking in axons. *Experimental neurology*. 218:257-267.

Calegari, F., and W.B. Huttner. 2003. An inhibition of cyclin-dependent kinases that lengthens, but does not arrest, neuroepithelial cell cycle induces premature neurogenesis. *Journal of cell science*. 116:4947-4955.

Cannino, G., C.M. Di Liegro, and A.M. Rinaldi. 2007. Nuclear-mitochondrial interaction. *Mitochondrion*. 7:359-366.

Carmona-Fontaine, C., H. Matthews, and R. Mayor. 2008. Directional cell migration in vivo: Wnt at the crest. *Cell adhesion & migration*. 2:240-242.

Carney, T.J., K.A. Dutton, E. Greenhill, M. Delfino-Machin, P. Dufourcq, P. Blader, and R.N. Kelsh. 2006. A direct role for Sox10 in specification of neural crest-derived sensory neurons. *Development (Cambridge, England)*. 133:4619-4630.

Cayuso, J., F. Ulloa, B. Cox, J. Briscoe, and E. Marti. 2006. The Sonic hedgehog pathway independently controls the patterning, proliferation and survival of neuroepithelial cells by regulating Gli activity. *Development*. 133:517-528.

Ciani, L., and P.C. Salinas. 2005. WNTs in the vertebrate nervous system: from patterning to neuronal connectivity. *Nat Rev Neurosci*. 6:351-362.

Cipolat, S., O. Martins de Brito, B. Dal Zilio, and L. Scorrano. 2004. OPA1 requires mitofusin 1 to promote mitochondrial fusion. *Proceedings of the National Academy of Sciences of the United States of America*. 101:15927-15932.

Cipolat, S., T. Rudka, D. Hartmann, V. Costa, L. Serneels, K. Craessaerts, K. Metzger, C. Frezza, W. Annaert, L. D'Adamio, C. Derks, T. Dejaegere, L. Pellegrini, R. D'Hooge, L. Scorrano, and B. De Strooper. 2006. Mitochondrial rhomboid PARL regulates cytochrome c release during apoptosis via OPA1-dependent cristae remodeling. *Cell*. 126:163-175.

Collins, T.J., M.J. Berridge, P. Lipp, and M.D. Bootman. 2002. Mitochondria are morphologically and functionally heterogeneous within cells. *The EMBO journal*. 21:1616-1627.

Cooper, S., and K. Shedden. 2003. Microarray analysis of gene expression during the cell cycle. *Cell & chromosome*. 2:1.

Coveney, D., A.J. Ross, J.D. Slone, and B. Capel. 2008. A microarray analysis of the XX Wnt4 mutant gonad targeted at the identification of genes involved in testis vascular differentiation. *Gene Expr Patterns*. 8:529-537.

Chada, S.R., and P.J. Hollenbeck. 2004. Nerve growth factor signaling regulates motility and docking of axonal mitochondria. *Curr Biol*. 14:1272-1276.

Chan, D.C. 2006. Mitochondria: dynamic organelles in disease, aging, and development. *Cell*. 125:1241-1252.

Chan, N.C., A.M. Salazar, A.H. Pham, M.J. Sweredoski, N.J. Kolawa, R.L. Graham, S. Hess, and D.C. Chan. 2011. Broad activation of the ubiquitin-proteasome system by Parkin is critical for mitophagy. *Human molecular genetics*. 20:1726-1737.

Chang, D.T., and I.J. Reynolds. 2006. Mitochondrial trafficking and morphology in healthy and injured neurons. *Progress in neurobiology*. 80:241-268.

Chen, H., and D.C. Chan. 2004. Mitochondrial dynamics in mammals. *Current topics in developmental biology*. 59:119-144.

Chen, H., and D.C. Chan. 2006. Critical dependence of neurons on mitochondrial dynamics. *Current opinion in cell biology*. 18:453-459.

Chen, H., and D.C. Chan. 2009. Mitochondrial dynamics--fusion, fission, movement, and mitophagy--in neurodegenerative diseases. *Human molecular genetics*. 18:R169-176.

Chen, H., and D.C. Chan. 2010. Physiological functions of mitochondrial fusion. *Annals of the New York Academy of Sciences*. 1201:21-25.

Chen, H., S.A. Detmer, A.J. Ewald, E.E. Griffin, S.E. Fraser, and D.C. Chan. 2003. Mitofusins Mfn1 and Mfn2 coordinately regulate mitochondrial fusion and are essential for embryonic development. *The Journal of cell biology*. 160:189-200.

Chen, H.J., C.M. Lin, C.S. Lin, R. Perez-Olle, C.L. Leung, and R.K. Liem. 2006. The role of microtubule actin cross-linking factor 1 (MACF1) in the Wnt signaling pathway. *Genes & development*. 20:1933-1945.

Chen, K.H., X. Guo, D. Ma, Y. Guo, Q. Li, D. Yang, P. Li, X. Qiu, S. Wen, R.P. Xiao, and J. Tang. 2004. Dysregulation of HSG triggers vascular proliferative disorders. *Nature cell biology*. 6:872-883.

Chen, S., G.C. Owens, K.L. Crossin, and D.B. Edelman. 2007. Serotonin stimulates mitochondrial transport in hippocampal neurons. *Molecular and cellular neurosciences*. 36:472-483.

Chen, S., G.C. Owens, and D.B. Edelman. 2008. Dopamine inhibits mitochondrial motility in hippocampal neurons. *PloS one*. 3:e2804.

Chenn, A., and C.A. Walsh. 2002. Regulation of cerebral cortical size by control of cell cycle exit in neural precursors. *Science (New York, N.Y.* 297:365-369.

Chiang, C., Y. Litingtung, E. Lee, K.E. Young, J.L. Corden, H. Westphal, and P.A. Beachy. 1996. Cyclopia and defective axial patterning in mice lacking Sonic hedgehog gene function. *Nature*. 383:407-413.

Cho, D.H., T. Nakamura, J. Fang, P. Cieplak, A. Godzik, Z. Gu, and S.A. Lipton. 2009. S-nitrosylation of Drp1 mediates beta-amyloid-related mitochondrial fission and neuronal injury. *Science (New York, N.Y.* 324:102-105.

Cho, D.H., T. Nakamura, and S.A. Lipton. 2010. Mitochondrial dynamics in cell death and neurodegeneration. *Cell Mol Life Sci*. 67:3435-3447.

Cho, K.I., Y. Cai, H. Yi, A. Yeh, A. Aslanukov, and P.A. Ferreira. 2007. Association of the kinesin-binding domain of RanBP2 to KIF5B and KIF5C determines mitochondria localization and function. *Traffic (Copenhagen, Denmark)*. 8:1722-1735.

Chong, Z.Z., and K. Maiese. 2004. Targeting WNT, protein kinase B, and mitochondrial membrane integrity to foster cellular survival in the nervous system. *Histology and histopathology*. 19:495-504.

Chypre, M., N. Zaidi, and K. Smans. 2012. ATP-citrate lyase: a mini-review. *Biochemical and biophysical research communications*. 422:1-4.

Dai, P., H. Akimaru, Y. Tanaka, T. Maekawa, M. Nakafuku, and S. Ishii. 1999. Sonic Hedgehog-induced activation of the Gli1 promoter is mediated by GLI3. *The Journal of biological chemistry*. 274:8143-8152.

Danial, N.N., and S.J. Korsmeyer. 2004. Cell death: critical control points. *Cell*. 116:205-219.
de Castro, I.P., L.M. Martins, and R. Tufi. 2010. Mitochondrial quality control and neurological disease: an emerging connection. *Expert reviews in molecular medicine*. 12:e12.
Dehay, C., and H. Kennedy. 2007. Cell-cycle control and cortical development. *Nature reviews*. 8:438-450.
Delettre, C., G. Lenaers, J.M. Griffoin, N. Gigarel, C. Lorenzo, P. Belenguer, L. Pelloquin, J. Grosgeorge, C. Turc-Carel, E. Perret, C. Astarie-Dequeker, L. Lasquellec, B. Arnaud, B. Ducommun, J. Kaplan, and C.P. Hamel. 2000. Nuclear gene OPA1, encoding a mitochondrial dynamin-related protein, is mutated in dominant optic atrophy. *Nature genetics*. 26:207-210.
Deng, H., M.W. Dodson, H. Huang, and M. Guo. 2008. The Parkinson's disease genes pink1 and parkin promote mitochondrial fission and/or inhibit fusion in Drosophila. *Proceedings of the National Academy of Sciences of the United States of America*. 105:14503-14508.
Deng, L., S. Hu, A.R. Baydoun, J. Chen, X. Chen, and X. Cong. 2009. Aspirin induces apoptosis in mesenchymal stem cells requiring Wnt/beta-catenin pathway. *Cell proliferation*. 42:721-730.
Detmer, S.A., and D.C. Chan. 2007a. Complementation between mouse Mfn1 and Mfn2 protects mitochondrial fusion defects caused by CMT2A disease mutations. *The Journal of cell biology*. 176:405-414.
Detmer, S.A., and D.C. Chan. 2007b. Functions and dysfunctions of mitochondrial dynamics. *Nature reviews. Molecular cell biology*. 8:870-879.
Dickinson, M.E., R. Krumlauf, and A.P. McMahon. 1994. Evidence for a mitogenic effect of Wnt-1 in the developing mammalian central nervous system. *Development*. 120:1453-1471.
Ding, Y., Y. Xi, T. Chen, J.Y. Wang, D.L. Tao, Z.L. Wu, Y.P. Li, C. Li, R. Zeng, and L. Li. 2008. Caprin-2 enhances canonical Wnt signaling through regulating LRP5/6 phosphorylation. *The Journal of cell biology*. 182:865-872.
Donovan, S.L., and M.A. Dyer. 2005. Regulation of proliferation during central nervous system development. *Seminars in cell & developmental biology*. 16:407-421.
Duarte, A., C. Poderoso, M. Cooke, G. Soria, F. Cornejo Maciel, V. Gottifredi, and E.J. Podesta. 2012. Mitochondrial fusion is essential for steroid biosynthesis. *PloS one*. 7:e45829.
Dubey, M., P. Chaudhury, H. Kabiru, and T.B. Shea. 2008. Tau inhibits anterograde axonal transport and perturbs stability in growing axonal neurites in part by displacing kinesin cargo: neurofilaments attenuate tau-mediated neurite instability. *Cell motility and the cytoskeleton*. 65:89-99.
Duchen, M.R. 2004. Roles of mitochondria in health and disease. *Diabetes*. 53 Suppl 1:S96-102.
Dumontet, C., G.E. Duran, K.A. Steger, G.L. Murphy, H.H. Sussman, and B.I. Sikic. 1996. Differential expression of tubulin isotypes during the cell cycle. *Cell motility and the cytoskeleton*. 35:49-58.
Eldering, E., W.J. Mackus, I.A. Derks, L.M. Evers, E. Beuling, P. Teeling, S.M. Lens, M.H. van Oers, and R.A. van Lier. 2004. Apoptosis via the B cell antigen receptor requires Bax translocation and involves mitochondrial depolarization, cytochrome C release, and caspase-9 activation. *European journal of immunology*. 34:1950-1960.
Elworthy, S., J.A. Lister, T.J. Carney, D.W. Raible, and R.N. Kelsh. 2003. Transcriptional regulation of mitfa accounts for the sox10 requirement in zebrafish melanophore development. *Development (Cambridge, England)*. 130:2809-2818.
Elworthy, S., J.P. Pinto, A. Pettifer, M.L. Cancela, and R.N. Kelsh. 2005. Phox2b function in the enteric nervous system is conserved in zebrafish and is sox10-dependent. *Mechanisms of development*. 122:659-669.
Ericson, J., J. Briscoe, P. Rashbass, V. van Heyningen, and T.M. Jessell. 1997. Graded sonic

hedgehog signaling and the specification of cell fate in the ventral neural tube. *Cold Spring Harbor symposia on quantitative biology*. 62:451-466.

Ericson, J., S. Morton, A. Kawakami, H. Roelink, and T.M. Jessell. 1996. Two critical periods of Sonic Hedgehog signaling required for the specification of motor neuron identity. *Cell*. 87:661-673.

Evrin, C., A. Fernandez-Cid, J. Zech, M.C. Herrera, A. Riera, P. Clarke, S. Brill, R. Lurz, and C. Speck. 2013. In the absence of ATPase activity, pre-RC formation is blocked prior to MCM2-7 hexamer dimerization. *Nucleic acids research*. 41:3162-3172.

Farkas, L.M., and W.B. Huttner. 2008. The cell biology of neural stem and progenitor cells and its significance for their proliferation versus differentiation during mammalian brain development. *Current opinion in cell biology*. 20:707-715.

Finkel, T., and N.J. Holbrook. 2000. Oxidants, oxidative stress and the biology of ageing. *Nature*. 408:239-247.

Finley, L.W., and M.C. Haigis. 2009. The coordination of nuclear and mitochondrial communication during aging and calorie restriction. *Ageing research reviews*. 8:173-188.

Foley, E.A., and T.M. Kapoor. 2013. Microtubule attachment and spindle assembly checkpoint signalling at the kinetochore. *Nature reviews. Molecular cell biology*. 14:25-37.

Ford, M.G., S. Jenni, and J. Nunnari. The crystal structure of dynamin. *Nature*. 477:561-566.

Franco, S.J., and U. Muller. 2013. Shaping our minds: stem and progenitor cell diversity in the mammalian neocortex. *Neuron*. 77:19-34.

Fransson, A., A. Ruusala, and P. Aspenstrom. 2003. Atypical Rho GTPases have roles in mitochondrial homeostasis and apoptosis. *The Journal of biological chemistry*. 278:6495-6502.

Fransson, S., A. Ruusala, and P. Aspenstrom. 2006. The atypical Rho GTPases Miro-1 and Miro-2 have essential roles in mitochondrial trafficking. *Biochemical and biophysical research communications*. 344:500-510.

Freese, J.L., D. Pino, and S.J. Pleasure. 2010. Wnt signaling in development and disease. *Neurobiology of disease*. 38:148-153.

Frezza, C., S. Cipolat, O. Martins de Brito, M. Micaroni, G.V. Beznoussenko, T. Rudka, D. Bartoli, R.S. Polishuck, N.N. Danial, B. De Strooper, and L. Scorrano. 2006. OPA1 controls apoptotic cristae remodeling independently from mitochondrial fusion. *Cell*. 126:177-189.

Friedman, J.R., L.L. Lackner, M. West, J.R. DiBenedetto, J. Nunnari, and G.K. Voeltz. 2011. ER tubules mark sites of mitochondrial division. *Science (New York, N.Y.*. 334:358-362.

Fu, M., C. Wang, Z. Li, T. Sakamaki, and R.G. Pestell. 2004. Minireview: Cyclin D1: normal and abnormal functions. *Endocrinology*. 145:5439-5447.

Fujita, H., T. Ogino, H. Kobuchi, T. Fujiwara, H. Yano, J. Akiyama, K. Utsumi, and J. Sasaki. 2006. Cell-permeable cAMP analog suppresses 6-hydroxydopamine-induced apoptosis in PC12 cells through the activation of the Akt pathway. *Brain research*. 1113:10-23.

Fukushima, N.H., E. Brisch, B.R. Keegan, W. Bleazard, and J.M. Shaw. 2001. The GTPase effector domain sequence of the Dnm1p GTPase regulates self-assembly and controls a rate-limiting step in mitochondrial fission. *Molecular biology of the cell*. 12:2756-2766.

Garcia-Frigola, C., F. Burgaya, M. Calbet, G. Lopez-Domenech, L. de Lecea, and E. Soriano. 2004. A collection of cDNAs enriched in upper cortical layers of the embryonic mouse brain. *Brain research. Molecular brain research*. 122:133-150.

Gegg, M.E., J.M. Cooper, K.Y. Chau, M. Rojo, A.H. Schapira, and J.W. Taanman. 2010. Mitofusin 1 and mitofusin 2 are ubiquitinated in a PINK1/parkin-dependent manner upon induction of mitophagy. *Human molecular genetics*. 19:4861-4870.

Gegg, M.E., and A.H. Schapira. 2010. PINK1-parkin-dependent mitophagy involves ubiquitination of mitofusins 1 and 2: Implications for Parkinson disease pathogenesis.

Autophagy. 7:243-245.
Germain, M., J.P. Mathai, H.M. McBride, and G.C. Shore. 2005. Endoplasmic reticulum BIK initiates DRP1-regulated remodelling of mitochondrial cristae during apoptosis. *The EMBO journal*. 24:1546-1556.
Glater, E.E., L.J. Megeath, R.S. Stowers, and T.L. Schwarz. 2006. Axonal transport of mitochondria requires milton to recruit kinesin heavy chain and is light chain independent. *The Journal of cell biology*. 173:545-557.
Gloss, B.S., K.I. Patterson, C.A. Barton, M. Gonzalez, J.P. Scurry, N.F. Hacker, R.L. Sutherland, P.M. O'Brien, and S.J. Clark. 2011. Integrative genome-wide expression and promoter DNA methylation profiling identifies a potential novel panel of ovarian cancer epigenetic biomarkers. *Cancer letters*. 318:76-85.
Goldstein, J.C., N.J. Waterhouse, P. Juin, G.I. Evan, and D.R. Green. 2000. The coordinate release of cytochrome c during apoptosis is rapid, complete and kinetically invariant. *Nature cell biology*. 2:156-162.
Gomes, L.C., G. Di Benedetto, and L. Scorrano. 2011. During autophagy mitochondria elongate, are spared from degradation and sustain cell viability. *Nature cell biology*. 13:589-598.
Gorska-Andrzejak, J., R.S. Stowers, J. Borycz, R. Kostyleva, T.L. Schwarz, and I.A. Meinertzhagen. 2003. Mitochondria are redistributed in Drosophila photoreceptors lacking milton, a kinesin-associated protein. *The Journal of comparative neurology*. 463:372-388.
Grishin, S., A. Shakirzyanova, A. Giniatullin, R. Afzalov, and R. Giniatullin. 2005. Mechanisms of ATP action on motor nerve terminals at the frog neuromuscular junction. *The European journal of neuroscience*. 21:1271-1279.
Guillemot, F. 2007. Spatial and temporal specification of neural fates by transcription factor codes. *Development*. 134:3771-3780.
Guo, X., G.T. Macleod, A. Wellington, F. Hu, S. Panchumarthi, M. Schoenfield, L. Marin, M.P. Charlton, H.L. Atwood, and K.E. Zinsmaier. 2005. The GTPase dMiro is required for axonal transport of mitochondria to Drosophila synapses. *Neuron*. 47:379-393.
Hallikas, O., K. Palin, N. Sinjushina, R. Rautiainen, J. Partanen, E. Ukkonen, and J. Taipale. 2006. Genome-wide prediction of mammalian enhancers based on analysis of transcription-factor binding affinity. *Cell*. 124:47-59.
Hamburger, V., and H.L. Hamilton. 1992. A series of normal stages in the development of the chick embryo. 1951. *Developmental dynamics : an official publication of the American Association of Anatomists*. 195:231-272.
Han, X.J., K. Tomizawa, A. Fujimura, I. Ohmori, T. Nishiki, M. Matsushita, and H. Matsui. 2010. Regulation of mitochondrial dynamics and neurodegenerative diseases. *Acta medica Okayama*. 65:1-10.
Han, X.J., K. Tomizawa, A. Fujimura, I. Ohmori, T. Nishiki, M. Matsushita, and H. Matsui. 2011. Regulation of mitochondrial dynamics and neurodegenerative diseases. *Acta medica Okayama*. 65:1-10.
Hart, M., J.P. Concordet, I. Lassot, I. Albert, R. del los Santos, H. Durand, C. Perret, B. Rubinfeld, F. Margottin, R. Benarous, and P. Polakis. 1999. The F-box protein beta-TrCP associates with phosphorylated beta-catenin and regulates its activity in the cell. *Curr Biol*. 9:207-210.
Hatzfeld, M. 1999. The armadillo family of structural proteins. *International review of cytology*. 186:179-224.
He, T.C., A.B. Sparks, C. Rago, H. Hermeking, L. Zawel, L.T. da Costa, P.J. Morin, B. Vogelstein, and K.W. Kinzler. 1998. Identification of c-MYC as a target of the APC pathway. *Science (New York, N.Y*. 281:1509-1512.
Heese, K., T. Yamada, H. Akatsu, T. Yamamoto, K. Kosaka, Y. Nagai, and T. Sawada. 2004.

Characterizing the new transcription regulator protein p60TRP. *Journal of cellular biochemistry*. 91:1030-1042.
Henderson, B.R. 2000. Nuclear-cytoplasmic shuttling of APC regulates beta-catenin subcellular localization and turnover. *Nature cell biology*. 2:653-660.
Herbarth, B., V. Pingault, N. Bondurand, K. Kuhlbrodt, I. Hermans-Borgmeyer, A. Puliti, N. Lemort, M. Goossens, and M. Wegner. 1998. Mutation of the Sry-related Sox10 gene in Dominant megacolon, a mouse model for human Hirschsprung disease. *Proceedings of the National Academy of Sciences of the United States of America*. 95:5161-5165.
Hirabayashi, Y., Y. Itoh, H. Tabata, K. Nakajima, T. Akiyama, N. Masuyama, and Y. Gotoh. 2004. The Wnt/beta-catenin pathway directs neuronal differentiation of cortical neural precursor cells. *Development (Cambridge, England)*. 131:2791-2801.
Hirokawa, N., Y. Noda, Y. Tanaka, and S. Niwa. 2009. Kinesin superfamily motor proteins and intracellular transport. *Nature reviews. Molecular cell biology*. 10:682-696.
Hirokawa, N., and R. Takemura. 2004. Kinesin superfamily proteins and their various functions and dynamics. *Experimental cell research*. 301:50-59.
Hollenbeck, P.J., and W.M. Saxton. 2005. The axonal transport of mitochondria. *Journal of cell science*. 118:5411-5419.
Hollyday, M., J.A. McMahon, and A.P. McMahon. 1995. Wnt expression patterns in chick embryo nervous system. *Mechanisms of development*. 52:9-25.
Hoppins, S., L. Lackner, and J. Nunnari. 2007. The machines that divide and fuse mitochondria. *Annual review of biochemistry*. 76:751-780.
Hoppins, S., and J. Nunnari. 2009. The molecular mechanism of mitochondrial fusion. *Biochimica et biophysica acta*. 1793:20-26.
Houten, S.M., and J. Auwerx. 2004. PGC-1alpha: turbocharging mitochondria. *Cell*. 119:5-7.
Hsia, N., and G.A. Cornwall. 2004. DNA microarray analysis of region-specific gene expression in the mouse epididymis. *Biology of reproduction*. 70:448-457.
Huang, P., C.A. Galloway, and Y. Yoon. 2011. Control of mitochondrial morphology through differential interactions of mitochondrial fusion and fission proteins. *PloS one*. 6:e20655.
Huang, P., T. Yu, and Y. Yoon. 2007. Mitochondrial clustering induced by overexpression of the mitochondrial fusion protein Mfn2 causes mitochondrial dysfunction and cell death. *European journal of cell biology*. 86:289-302.
Huang, R., Z. Xing, Z. Luan, T. Wu, X. Wu, and G. Hu. 2003. A specific splicing variant of SVH, a novel human armadillo repeat protein, is up-regulated in hepatocellular carcinomas. *Cancer research*. 63:3775-3782.
Huang, S., Y. Li, Y. Chen, K. Podsypanina, M. Chamorro, A.B. Olshen, K.V. Desai, A. Tann, D. Petersen, J.E. Green, and H.E. Varmus. 2005. Changes in gene expression during the development of mammary tumors in MMTV-Wnt-1 transgenic mice. *Genome biology*. 6:R84.
Hudson, G., P. Amati-Bonneau, E.L. Blakely, J.D. Stewart, L. He, A.M. Schaefer, P.G. Griffiths, K. Ahlqvist, A. Suomalainen, P. Reynier, R. McFarland, D.M. Turnbull, P.F. Chinnery, and R.W. Taylor. 2008. Mutation of OPA1 causes dominant optic atrophy with external ophthalmoplegia, ataxia, deafness and multiple mitochondrial DNA deletions: a novel disorder of mtDNA maintenance. *Brain : a journal of neurology*. 131:329-337.
Ikuta, J., A. Maturana, T. Fujita, T. Okajima, K. Tatematsu, K. Tanizawa, and S. Kuroda. 2007. Fasciculation and elongation protein zeta-1 (FEZ1) participates in the polarization of hippocampal neuron by controlling the mitochondrial motility. *Biochemical and biophysical research communications*. 353:127-132.
Ille, F., S. Atanasoski, S. Falk, L.M. Ittner, D. Marki, S. Buchmann-Moller, H. Wurdak, U. Suter, M.M. Taketo, and L. Sommer. 2007. Wnt/BMP signal integration regulates the balance between proliferation and differentiation of neuroepithelial cells in the dorsal spinal cord.

Developmental biology. 304:394-408.
Ille, F., and L. Sommer. 2005. Wnt signaling: multiple functions in neural development. *Cellular and molecular life sciences : CMLS*. 62:1100-1108.
Isackson, P.J., K.A. Sutton, K.Y. Hostetler, and G.D. Vladutiu. 2013. Novel mutations in the gene encoding very long-chain acyl-CoA dehydrogenase identified in patients with partial carnitine palmitoyltransferase II deficiency. *Muscle & nerve*. 47:224-229.
Iseki, H., A. Takeda, T. Andoh, K. Kuwabara, N. Takahashi, I.V. Kurochkin, H. Ishida, Y. Okazaki, and I. Koyama. 2012. ALEX1 suppresses colony formation ability of human colorectal carcinoma cell lines. *Cancer Sci*. 103:1267-1271.
Ishihara, N., Y. Eura, and K. Mihara. 2004. Mitofusin 1 and 2 play distinct roles in mitochondrial fusion reactions via GTPase activity. *Journal of cell science*. 117:6535-6546.
Ishii, N. 2007. Role of oxidative stress from mitochondria on aging and cancer. *Cornea*. 26:S3-9.
Itoh, M., N. Nishibori, T. Sagara, Y. Horie, A. Motojima, and K. Morita. 2012. Extract of fermented brown rice induces apoptosis of human colorectal tumor cells by activating mitochondrial pathway. *Phytotherapy research : PTR*. 26:1661-1666.
Jacob, J., and J. Briscoe. 2003. Gli proteins and the control of spinal-cord patterning. *EMBO reports*. 4:761-765.
Jaglin, X.H., and J. Chelly. 2009. Tubulin-related cortical dysgeneses: microtubule dysfunction underlying neuronal migration defects. *Trends in genetics : TIG*. 25:555-566.
John, G.B., Y. Shang, L. Li, C. Renken, C.A. Mannella, J.M. Selker, L. Rangell, M.J. Bennett, and J. Zha. 2005. The mitochondrial inner membrane protein mitofilin controls cristae morphology. *Molecular biology of the cell*. 16:1543-1554.
Johnson, D.T., R.A. Harris, S. French, P.V. Blair, J. You, K.G. Bemis, M. Wang, and R.S. Balaban. 2007. Tissue heterogeneity of the mammalian mitochondrial proteome. *American journal of physiology. Cell physiology*. 292:C689-697.
Kageyama, Y., Z. Zhang, and H. Sesaki. 2012. Mitochondrial division: molecular machinery and physiological functions. *Current opinion in cell biology*. 23:427-434.
Kahle, J.J., N. Gulbahce, C.A. Shaw, J. Lim, D.E. Hill, A.L. Barabasi, and H.Y. Zoghbi. 2010. Comparison of an expanded ataxia interactome with patient medical records reveals a relationship between macular degeneration and ataxia. *Human molecular genetics*. 20:510-527.
Kanai, Y., Y. Okada, Y. Tanaka, A. Harada, S. Terada, and N. Hirokawa. 2000. KIF5C, a novel neuronal kinesin enriched in motor neurons. *J Neurosci*. 20:6374-6384.
Kang, J.S., J.H. Tian, P.Y. Pan, P. Zald, C. Li, C. Deng, and Z.H. Sheng. 2008. Docking of axonal mitochondria by syntaphilin controls their mobility and affects short-term facilitation. *Cell*. 132:137-148.
Karbowski, M., D. Arnoult, H. Chen, D.C. Chan, C.L. Smith, and R.J. Youle. 2004. Quantitation of mitochondrial dynamics by photolabeling of individual organelles shows that mitochondrial fusion is blocked during the Bax activation phase of apoptosis. *The Journal of cell biology*. 164:493-499.
Karbowski, M., and R.J. Youle. 2004. Regulating mitochondrial outer membrane proteins by ubiquitination and proteasomal degradation. *Current opinion in cell biology*. 23:476-482.
Kargl, J., N. Balenga, W. Platzer, L. Martini, J. Whistler, and M. Waldhoer. 2011. The GPCR - associated sorting protein 1 regulates ligand-induced downregulation of GPR55. *British journal of pharmacology*.
Karki, S., and E.L. Holzbaur. 1999. Cytoplasmic dynein and dynactin in cell division and intracellular transport. *Current opinion in cell biology*. 11:45-53.
Kim, J.Y., S. Shen, K. Dietz, Y. He, O. Howell, R. Reynolds, and P. Casaccia. 2010. HDAC1 nuclear export induced by pathological conditions is essential for the onset of axonal damage. *Nature neuroscience*. 13:180-189.

Kincses, Z.T., J. Toldi, and L. Vecsei. 2010. Kynurenines, neurodegeneration and Alzheimer's disease. *Journal of cellular and molecular medicine*. 14:2045-2054.

King, S.J., and T.A. Schroer. 2000. Dynactin increases the processivity of the cytoplasmic dynein motor. *Nature cell biology*. 2:20-24.

Kiyama, A., Y. Isojima, and K. Nagai. 2006. Role of Per1-interacting protein of the suprachiasmatic nucleus in NGF mediated neuronal survival. *Biochemical and biophysical research communications*. 339:514-519.

Kohn, A.D., and R.T. Moon. 2005. Wnt and calcium signaling: beta-catenin-independent pathways. *Cell calcium*. 38:439-446.

Koshiba, T., S.A. Detmer, J.T. Kaiser, H. Chen, J.M. McCaffery, and D.C. Chan. 2004. Structural basis of mitochondrial tethering by mitofusin complexes. *Science (New York, N.Y.* 305:858-862.

Koutsopoulos, O.S., D. Laine, L. Osellame, D.M. Chudakov, R.G. Parton, A.E. Frazier, and M.T. Ryan. 2010. Human Miltons associate with mitochondria and induce microtubule-dependent remodeling of mitochondrial networks. *Biochimica et biophysica acta*. 1803:564-574.

Krig, S.R., V.X. Jin, M.C. Bieda, H. O'Geen, P. Yaswen, R. Green, and P.J. Farnham. 2007. Identification of genes directly regulated by the oncogene ZNF217 using chromatin immunoprecipitation (ChIP)-chip assays. *The Journal of biological chemistry*. 282:9703-9712.

Kroemer, G., B. Dallaporta, and M. Resche-Rigon. 1998. The mitochondrial death/life regulator in apoptosis and necrosis. *Annual review of physiology*. 60:619-642.

Krull, C.E. 2004. A primer on using in ovo electroporation to analyze gene function. *Developmental dynamics : an official publication of the American Association of Anatomists*. 229:433-439.

Kurochkin, I.V., N. Yonemitsu, S.I. Funahashi, and H. Nomura. 2001. ALEX1, a novel human armadillo repeat protein that is expressed differentially in normal tissues and carcinomas. *Biochemical and biophysical research communications*. 280:340-347.

Labrousse, A.M., M.D. Zappaterra, D.A. Rube, and A.M. van der Bliek. 1999. C. elegans dynamin-related protein DRP-1 controls severing of the mitochondrial outer membrane. *Molecular cell*. 4:815-826.

Le Dreau, G., and E. Marti. 2012. Dorsal-ventral patterning of the neural tube: a tale of three signals. *Developmental neurobiology*. 72:1471-1481.

Lee, H.K., and B. Deneen. 2012. Daam2 is required for dorsal patterning via modulation of canonical Wnt signaling in the developing spinal cord. *Developmental cell*. 22:183-196.

Lee, J., K.A. Platt, P. Censullo, and A. Ruiz i Altaba. 1997. Gli1 is a target of Sonic hedgehog that induces ventral neural tube development. *Development*. 124:2537-2552.

Lee, J.Y., Y. Nagano, J.P. Taylor, K.L. Lim, and T.P. Yao. 2010. Disease-causing mutations in parkin impair mitochondrial ubiquitination, aggregation, and HDAC6-dependent mitophagy. *The Journal of cell biology*. 189:671-679.

Lee, K.J., P. Dietrich, and T.M. Jessell. 2000. Genetic ablation reveals that the roof plate is essential for dorsal interneuron specification. *Nature*. 403:734-740.

Lee, K.J., and T.M. Jessell. 1999. The specification of dorsal cell fates in the vertebrate central nervous system. *Annual review of neuroscience*. 22:261-294.

Lee, S., S. Kim, X. Sun, J.H. Lee, and H. Cho. 2007. Cell cycle-dependent mitochondrial biogenesis and dynamics in mammalian cells. *Biochemical and biophysical research communications*. 357:111-117.

Lee, S., B. Lee, K. Joshi, S.L. Pfaff, J.W. Lee, and S.K. Lee. 2008. A regulatory network to segregate the identity of neuronal subtypes. *Developmental cell*. 14:877-889.

Legros, F., F. Malka, P. Frachon, A. Lombes, and M. Rojo. 2004. Organization and dynamics of

human mitochondrial DNA. *Journal of cell science*. 117:2653-2662.
Lew, D.J., V. Dulic, and S.I. Reed. 1991. Isolation of three novel human cyclins by rescue of G1 cyclin (Cln) function in yeast. *Cell*. 66:1197-1206.
Li, F., Z.Z. Chong, and K. Maiese. 2006. Winding through the WNT pathway during cellular development and demise. *Histology and histopathology*. 21:103-124.
Li, Z., K. Okamoto, Y. Hayashi, and M. Sheng. 2004. The importance of dendritic mitochondria in the morphogenesis and plasticity of spines and synapses. *Cell*. 119:873-887.
Liao, X., and R.A. Butow. 1993. RTG1 and RTG2: two yeast genes required for a novel path of communication from mitochondria to the nucleus. *Cell*. 72:61-71.
Liesa, M., B. Borda-d'Agua, G. Medina-Gomez, C.J. Lelliott, J.C. Paz, M. Rojo, M. Palacin, A. Vidal-Puig, and A. Zorzano. 2008. Mitochondrial fusion is increased by the nuclear coactivator PGC-1beta. *PloS one*. 3:e3613.
Liesa, M., M. Palacin, and A. Zorzano. 2009. Mitochondrial dynamics in mammalian health and disease. *Physiological reviews*. 89:799-845.
Liu, S., T. Sawada, S. Lee, W. Yu, G. Silverio, P. Alapatt, I. Millan, A. Shen, W. Saxton, T. Kanao, R. Takahashi, N. Hattori, Y. Imai, and B. Lu. 2012. Parkinson's disease-associated kinase PINK1 regulates Miro protein level and axonal transport of mitochondria. *PLoS genetics*. 8:e1002537.
Liu, X., and G. Hajnoczky. 2009. Ca2+-dependent regulation of mitochondrial dynamics by the Miro-Milton complex. *The international journal of biochemistry & cell biology*. 41:1972-1976.
Liu, Z., and R.A. Butow. 2006. Mitochondrial retrograde signaling. *Annual review of genetics*. 40:159-185.
Lobjois, V., B. Benazeraf, N. Bertrand, F. Medevielle, and F. Pituello. 2004. Specific regulation of cyclins D1 and D2 by FGF and Shh signaling coordinates cell cycle progression, patterning, and differentiation during early steps of spinal cord development. *Developmental biology*. 273:195-209.
Logan, C.Y., and R. Nusse. 2004. The Wnt signaling pathway in development and disease. *Annual review of cell and developmental biology*. 20:781-810.
Lopez-Domenech, G., R. Serrat, S. Mirra, S. D'Aniello, I. Somorjai, A. Abad, N. Vitureira, E. Garcia-Arumi, M.T. Alonso, M. Rodriguez-Prados, F. Burgaya, A.L. Andreu, J. Garcia-Sancho, R. Trullas, J. Garcia-Fernandez, and E. Soriano. 2012. The Eutherian Armcx genes regulate mitochondrial trafficking in neurons and interact with Miro and Trak2. *Nature communications*. 3:814.
Lukaszewicz, A.I., and D.J. Anderson. 2011. Cyclin D1 promotes neurogenesis in the developing spinal cord in a cell cycle-independent manner. *Proceedings of the National Academy of Sciences of the United States of America*. 108:11632-11637.
Lyuksyutova, A.I., C.C. Lu, N. Milanesio, L.A. King, N. Guo, Y. Wang, J. Nathans, M. Tessier-Lavigne, and Y. Zou. 2003. Anterior-posterior guidance of commissural axons by Wnt-frizzled signaling. *Science (New York, N.Y.*. 302:1984-1988.
Llorens-Martin, M., G. Lopez-Domenech, E. Soriano, and J. Avila. 2011. GSK3beta is involved in the relief of mitochondria pausing in a Tau-dependent manner. *PloS one*. 6:e27686.
MacAskill, A.F., T.A. Atkin, and J.T. Kittler. 2010. Mitochondrial trafficking and the provision of energy and calcium buffering at excitatory synapses. *The European journal of neuroscience*. 32:231-240.
MacAskill, A.F., K. Brickley, F.A. Stephenson, and J.T. Kittler. 2009a. GTPase dependent recruitment of Grif-1 by Miro1 regulates mitochondrial trafficking in hippocampal neurons. *Molecular and cellular neurosciences*. 40:301-312.
MacAskill, A.F., and J.T. Kittler. 2010. Control of mitochondrial transport and localization in neurons. *Trends in cell biology*. 20:102-112.

Macaskill, A.F., J.E. Rinholm, A.E. Twelvetrees, I.L. Arancibia-Carcamo, J. Muir, A. Fransson, P. Aspenstrom, D. Attwell, and J.T. Kittler. 2009b. Miro1 is a calcium sensor for glutamate receptor-dependent localization of mitochondria at synapses. *Neuron*. 61:541-555.

Machon, O., C.J. van den Bout, M. Backman, R. Kemler, and S. Krauss. 2003. Role of beta-catenin in the developing cortical and hippocampal neuroepithelium. *Neuroscience*. 122:129-143.

Maretto, S., M. Cordenonsi, S. Dupont, P. Braghetta, V. Broccoli, A.B. Hassan, D. Volpin, G.M. Bressan, and S. Piccolo. 2003. Mapping Wnt/beta-catenin signaling during mouse development and in colorectal tumors. *Proceedings of the National Academy of Sciences of the United States of America*. 100:3299-3304.

Marti, E., and P. Bovolenta. 2002. Sonic hedgehog in CNS development: one signal, multiple outputs. *Trends in neurosciences*. 25:89-96.

Marti, E., R. Takada, D.A. Bumcrot, H. Sasaki, and A.P. McMahon. 1995. Distribution of Sonic hedgehog peptides in the developing chick and mouse embryo. *Development*. 121:2537-2547.

Martin, R., B. Vaida, R. Bleher, M. Crispino, and A. Giuditta. 1998. Protein synthesizing units in presynaptic and postsynaptic domains of squid neurons. *Journal of cell science*. 111 (Pt 21):3157-3166.

Martini, L., M. Waldhoer, M. Pusch, V. Kharazia, J. Fong, J.H. Lee, C. Freissmuth, and J.L. Whistler. 2007. Ligand-induced down-regulation of the cannabinoid 1 receptor is mediated by the G-protein-coupled receptor-associated sorting protein GASP1. *Faseb J*. 21:802-811.

Masai, H., and K. Arai. 2000. Regulation of DNA replication during the cell cycle: roles of Cdc7 kinase and coupling of replication, recombination, and repair in response to replication fork arrest. *IUBMB life*. 49:353-364.

Mathis, C., J.B. Bott, M.P. Candusso, F. Simonin, and J.C. Cassel. 2010. Impaired striatum-dependent behavior in GASP-1-knock-out mice. *Genes, brain, and behavior*.

Matsuki, T., A. Kiyama, M. Kawabuchi, M. Okada, and K. Nagai. 2001. A novel protein interacts with a clock-related protein, rPer1. *Brain Res*. 916:1-10.

Matthews, H.K., L. Marchant, C. Carmona-Fontaine, S. Kuriyama, J. Larrain, M.R. Holt, M. Parsons, and R. Mayor. 2008. Directional migration of neural crest cells in vivo is regulated by Syndecan-4/Rac1 and non-canonical Wnt signaling/RhoA. *Development (Cambridge, England)*. 135:1771-1780.

Mears, J.A., L.L. Lackner, S. Fang, E. Ingerman, J. Nunnari, and J.E. Hinshaw. 2011. Conformational changes in Dnm1 support a contractile mechanism for mitochondrial fission. *Nature structural & molecular biology*. 18:20-26.

Meeusen, S., J.M. McCaffery, and J. Nunnari. 2004. Mitochondrial fusion intermediates revealed in vitro. *Science (New York, N.Y.* 305:1747-1752.

Megason, S.G., and A.P. McMahon. 2002. A mitogen gradient of dorsal midline Wnts organizes growth in the CNS. *Development*. 129:2087-2098.

Mezhybovska, M., Y. Yudina, A. Abhyankar, and A. Sjolander. 2009. Beta-catenin is involved in alterations in mitochondrial activity in non-transformed intestinal epithelial and colon cancer cells. *British journal of cancer*. 101:1596-1605.

Millecamps, S., and J.P. Julien. 2013. Axonal transport deficits and neurodegenerative diseases. *Nature reviews*. 14:161-176.

Miller, K.E., and M.P. Sheetz. 2004. Axonal mitochondrial transport and potential are correlated. *Journal of cell science*. 117:2791-2804.

Miller, K.E., and M.P. Sheetz. 2006. Direct evidence for coherent low velocity axonal transport of mitochondria. *The Journal of cell biology*. 173:373-381.

Minauro-Sanmiguel, F., S. Wilkens, and J.J. Garcia. 2005. Structure of dimeric mitochondrial ATP synthase: novel F0 bridging features and the structural basis of mitochondrial cristae biogenesis. *Proceedings of the National Academy of Sciences of the United States of America*. 102:12356-12358.

Mironov, S.L. 2007. ADP regulates movements of mitochondria in neurons. *Biophysical journal*. 92:2944-2952.

Misgeld, T., M. Kerschensteiner, F.M. Bareyre, R.W. Burgess, and J.W. Lichtman. 2007. Imaging axonal transport of mitochondria in vivo. *Nature methods*. 4:559-561.

Mishra, P.J., L. Ha, J. Rieker, E.V. Sviderskaya, D.C. Bennett, M.D. Oberst, K. Kelly, and G. Merlino. 2011. Dissection of RAS downstream pathways in melanomagenesis: a role for Ral in transformation. *Oncogene*. 29:2449-2456.

Misko, A., S. Jiang, I. Wegorzewska, J. Milbrandt, and R.H. Baloh. Mitofusin 2 is necessary for transport of axonal mitochondria and interacts with the Miro/Milton complex. *J Neurosci*. 30:4232-4240.

Misko, A., S. Jiang, I. Wegorzewska, J. Milbrandt, and R.H. Baloh. 2010. Mitofusin 2 is necessary for transport of axonal mitochondria and interacts with the Miro/Milton complex. *J Neurosci*. 30:4232-4240.

Mitra, K., C. Wunder, B. Roysam, G. Lin, and J. Lippincott-Schwartz. 2009. A hyperfused mitochondrial state achieved at G1-S regulates cyclin E buildup and entry into S phase. *Proceedings of the National Academy of Sciences of the United States of America*. 106:11960-11965.

Montagnoli, A., B. Valsasina, V. Croci, M. Menichincheri, S. Rainoldi, V. Marchesi, M. Tibolla, P. Tenca, D. Brotherton, C. Albanese, V. Patton, R. Alzani, A. Ciavolella, F. Sola, A. Molinari, D. Volpi, N. Avanzi, F. Fiorentini, M. Cattoni, S. Healy, D. Ballinari, E. Pesenti, A. Isacchi, J. Moll, A. Bensimon, E. Vanotti, and C. Santocanale. 2008. A Cdc7 kinase inhibitor restricts initiation of DNA replication and has antitumor activity. *Nature chemical biology*. 4:357-365.

Montcouquiol, M., E.B. Crenshaw, 3rd, and M.W. Kelley. 2006. Noncanonical Wnt signaling and neural polarity. *Annual review of neuroscience*. 29:363-386.

Montessuit, S., S.P. Somasekharan, O. Terrones, S. Lucken-Ardjomande, S. Herzig, R. Schwarzenbacher, D.J. Manstein, E. Bossy-Wetzel, G. Basanez, P. Meda, and J.C. Martinou. 2010. Membrane remodeling induced by the dynamin-related protein Drp1 stimulates Bax oligomerization. *Cell*. 142:889-901.

Moran, L.B., and M.B. Graeber. 2008. Towards a pathway definition of Parkinson's disease: a complex disorder with links to cancer, diabetes and inflammation. *Neurogenetics*. 9:1-13.

Morkel, M., J. Huelsken, M. Wakamiya, J. Ding, M. van de Wetering, H. Clevers, M.M. Taketo, R.R. Behringer, M.M. Shen, and W. Birchmeier. 2003. Beta-catenin regulates Cripto- and Wnt3-dependent gene expression programs in mouse axis and mesoderm formation. *Development*. 130:6283-6294.

Morris, A.A., M.J. Jackson, L.A. Bindoff, and D.M. Turnbull. 1995. The investigation of mitochondrial respiratory chain disease. *Journal of the Royal Society of Medicine*. 88:217P-222P.

Morris, R.L., and P.J. Hollenbeck. 1993. The regulation of bidirectional mitochondrial transport is coordinated with axonal outgrowth. *Journal of cell science*. 104 (Pt 3):917-927.

Mortiboys, H., K.K. Johansen, J.O. Aasly, and O. Bandmann. 2010. Mitochondrial impairment in patients with Parkinson disease with the G2019S mutation in LRRK2. *Neurology*. 75:2017-2020.

Mou, Z., A.R. Tapper, and P.D. Gardner. 2009. The armadillo repeat-containing protein, ARMCX3, physically and functionally interacts with the developmental regulatory factor Sox10. *The Journal of biological chemistry*. 284:13629-13640.

Muroyama, Y., M. Fujihara, M. Ikeya, H. Kondoh, and S. Takada. 2002. Wnt signaling plays an essential role in neuronal specification of the dorsal spinal cord. *Genes & development*. 16:548-553.

Nagata, T. 2006. Electron microscopic radioautographic study on protein synthesis in hepatocyte mitochondria of aging mice. *TheScientificWorldJournal*. 6:1583-1598.

Nakamura, T., P. Cieplak, D.H. Cho, A. Godzik, and S.A. Lipton. 2010. S-nitrosylation of Drp1 links excessive mitochondrial fission to neuronal injury in neurodegeneration. *Mitochondrion*. 10:573-578.

Narendra, D.P., S.M. Jin, A. Tanaka, D.F. Suen, C.A. Gautier, J. Shen, M.R. Cookson, and R.J. Youle. 2010. PINK1 is selectively stabilized on impaired mitochondria to activate Parkin. *PLoS biology*. 8:e1000298.

Nathke, I. 2006. Cytoskeleton out of the cupboard: colon cancer and cytoskeletal changes induced by loss of APC. *Nature reviews. Cancer*. 6:967-974.

Nelson, M.R., and W.J. Chazin. 1998. Structures of EF-hand Ca(2+)-binding proteins: diversity in the organization, packing and response to Ca2+ binding. *Biometals : an international journal on the role of metal ions in biology, biochemistry, and medicine*. 11:297-318.

Nelson, W.J., and R. Nusse. 2004. Convergence of Wnt, beta-catenin, and cadherin pathways. *Science (New York, N.Y.* 303:1483-1487.

Neufeld, K.L., D.A. Nix, H. Bogerd, Y. Kang, M.C. Beckerle, B.R. Cullen, and R.L. White. 2000a. Adenomatous polyposis coli protein contains two nuclear export signals and shuttles between the nucleus and cytoplasm. *Proceedings of the National Academy of Sciences of the United States of America*. 97:12085-12090.

Neufeld, K.L., F. Zhang, B.R. Cullen, and R.L. White. 2000b. APC-mediated downregulation of beta-catenin activity involves nuclear sequestration and nuclear export. *EMBO reports*. 1:519-523.

Ng, C.H., S.Z. Mok, C. Koh, X. Ouyang, M.L. Fivaz, E.K. Tan, V.L. Dawson, T.M. Dawson, F. Yu, and K.L. Lim. 2009. Parkin protects against LRRK2 G2019S mutant-induced dopaminergic neurodegeneration in Drosophila. *J Neurosci*. 29:11257-11262.

Nicholls, D.G., and S.L. Budd. 2000. Mitochondria and neuronal survival. *Physiological reviews*. 80:315-360.

Niwa, S., H. Takahashi, and N. Hirokawa. 2013. beta-Tubulin mutations that cause severe neuropathies disrupt axonal transport. *The EMBO journal*.

Nusse, R. 2001. An ancient cluster of Wnt paralogues. *Trends Genet*. 17:443.

Nusse, R. 2005. Wnt signaling in disease and in development. *Cell research*. 15:28-32.

Nusse, R., and H.E. Varmus. 1982. Many tumors induced by the mouse mammary tumor virus contain a provirus integrated in the same region of the host genome. *Cell*. 31:99-109.

Okamoto, K., N. Kondo-Okamoto, and Y. Ohsumi. 2009. Mitochondria-anchored receptor Atg32 mediates degradation of mitochondria via selective autophagy. *Developmental cell*. 17:87-97.

Olichon, A., L. Baricault, N. Gas, E. Guillou, A. Valette, P. Belenguer, and G. Lenaers. 2003. Loss of OPA1 perturbates the mitochondrial inner membrane structure and integrity, leading to cytochrome c release and apoptosis. *The Journal of biological chemistry*. 278:7743-7746.

Otero, J.J., W. Fu, L. Kan, A.E. Cuadra, and J.A. Kessler. 2004. Beta-catenin signaling is required for neural differentiation of embryonic stem cells. *Development*. 131:3545-3557.

Pabst, O., H. Herbrand, N. Takuma, and H.H. Arnold. 2000. NKX2 gene expression in neuroectoderm but not in mesendodermally derived structures depends on sonic hedgehog in mouse embryos. *Development genes and evolution*. 210:47-50.

Pagliarini, D.J., S.E. Calvo, B. Chang, S.A. Sheth, S.B. Vafai, S.E. Ong, G.A. Walford, C. Sugiana, A. Boneh, W.K. Chen, D.E. Hill, M. Vidal, J.G. Evans, D.R. Thorburn, S.A.

Carr, and V.K. Mootha. 2008. A mitochondrial protein compendium elucidates complex I disease biology. *Cell*. 134:112-123.

Pan, Y., C.B. Bai, A.L. Joyner, and B. Wang. 2006. Sonic hedgehog signaling regulates Gli2 transcriptional activity by suppressing its processing and degradation. *Molecular and cellular biology*. 26:3365-3377.

Panhuysen, M., D.M. Vogt Weisenhorn, V. Blanquet, C. Brodski, U. Heinzmann, W. Beisker, and W. Wurst. 2004. Effects of Wnt1 signaling on proliferation in the developing mid-/hindbrain region. *Molecular and cellular neurosciences*. 26:101-111.

Parikh, V.S., M.M. Morgan, R. Scott, L.S. Clements, and R.A. Butow. 1987. The mitochondrial genotype can influence nuclear gene expression in yeast. *Science (New York, N.Y.* 235:576-580.

Park, Y.U., J. Jeong, H. Lee, J.Y. Mun, J.H. Kim, J.S. Lee, M.D. Nguyen, S.S. Han, P.G. Suh, and S.K. Park. 2010. Disrupted-in-schizophrenia 1 (DISC1) plays essential roles in mitochondria in collaboration with Mitofilin. *Proceedings of the National Academy of Sciences of the United States of America*. 107:17785-17790.

Parone, P.A., S. Da Cruz, D. Tondera, Y. Mattenberger, D.I. James, P. Maechler, F. Barja, and J.C. Martinou. 2008. Preventing mitochondrial fission impairs mitochondrial function and leads to loss of mitochondrial DNA. *PloS one*. 3:e3257.

Parr, B.A., M.J. Shea, G. Vassileva, and A.P. McMahon. 1993. Mouse Wnt genes exhibit discrete domains of expression in the early embryonic CNS and limb buds. *Development (Cambridge, England)*. 119:247-261.

Patapoutian, A., and L.F. Reichardt. 2000. Roles of Wnt proteins in neural development and maintenance. *Current opinion in neurobiology*. 10:392-399.

Pathak, D., K.J. Sepp, and P.J. Hollenbeck. 2010. Evidence that myosin activity opposes microtubule-based axonal transport of mitochondria. *J Neurosci*. 30:8984-8992.

Patten, I., P. Kulesa, M.M. Shen, S. Fraser, and M. Placzek. 2003. Distinct modes of floor plate induction in the chick embryo. *Development*. 130:4809-4821.

Patten, I., and M. Placzek. 2000. The role of Sonic hedgehog in neural tube patterning. *Cellular and molecular life sciences : CMLS*. 57:1695-1708.

Pierani, A., S. Brenner-Morton, C. Chiang, and T.M. Jessell. 1999. A sonic hedgehog-independent, retinoid-activated pathway of neurogenesis in the ventral spinal cord. *Cell*. 97:903-915.

Pilling, A.D., D. Horiuchi, C.M. Lively, and W.M. Saxton. 2006. Kinesin-1 and Dynein are the primary motors for fast transport of mitochondria in Drosophila motor axons. *Molecular biology of the cell*. 17:2057-2068.

Placzek, M. 1995. The role of the notochord and floor plate in inductive interactions. *Current opinion in genetics & development*. 5:499-506.

Poirier, K., Y. Saillour, N. Bahi-Buisson, X.H. Jaglin, C. Fallet-Bianco, R. Nabbout, L. Castelnau-Ptakhine, A. Roubertie, T. Attie-Bitach, I. Desguerre, D. Genevieve, C. Barnerias, B. Keren, N. Lebrun, N. Boddaert, F. Encha-Razavi, and J. Chelly. 2010. Mutations in the neuronal ss-tubulin subunit TUBB3 result in malformation of cortical development and neuronal migration defects. *Human molecular genetics*. 19:4462-4473.

Popov, V., N.I. Medvedev, H.A. Davies, and M.G. Stewart. 2005. Mitochondria form a filamentous reticular network in hippocampal dendrites but are present as discrete bodies in axons: a three-dimensional ultrastructural study. *The Journal of comparative neurology*. 492:50-65.

Poyton, R.O., and J.E. McEwen. 1996. Crosstalk between nuclear and mitochondrial genomes. *Annual review of biochemistry*. 65:563-607.

Prud'homme, B., N. Lartillot, G. Balavoine, A. Adoutte, and M. Vervoort. 2002. Phylogenetic analysis of the Wnt gene family. Insights from lophotrochozoan members. *Curr Biol*.

12:1395.
Purves, D. 2001. Viktor Hamburger 1900-2001. *Nature neuroscience*. 4:777-778.
Qian, J., E.M. Perchiniak, K. Sun, and J. Groden. 2010. The mitochondrial protein hTID-1 partners with the caspase-cleaved adenomatous polyposis cell tumor suppressor to facilitate apoptosis. *Gastroenterology*. 138:1418-1428.
Rapaport, D. 2003. Finding the right organelle. Targeting signals in mitochondrial outer-membrane proteins. *EMBO reports*. 4:948-952.
Ratineau, C., M.W. Petry, H. Mutoh, and A.B. Leiter. 2002. Cyclin D1 represses the basic helix-loop-helix transcription factor, BETA2/NeuroD. *The Journal of biological chemistry*. 277:8847-8853.
Ritter, S.L., and R.A. Hall. 2009. Fine-tuning of GPCR activity by receptor-interacting proteins. *Nature reviews*. 10:819-830.
Rizzuto, R. 2001. Intracellular Ca(2+) pools in neuronal signalling. *Current opinion in neurobiology*. 11:306-311.
Roelink, H. 1996. Tripartite signaling of pattern: interactions between Hedgehogs, BMPs and Wnts in the control of vertebrate development. *Current opinion in neurobiology*. 6:33-40.
Roelink, H., J.A. Porter, C. Chiang, Y. Tanabe, D.T. Chang, P.A. Beachy, and T.M. Jessell. 1995. Floor plate and motor neuron induction by different concentrations of the amino-terminal cleavage product of sonic hedgehog autoproteolysis. *Cell*. 81:445-455.
Rohrbeck, A., and J. Borlak. 2009. Cancer genomics identifies regulatory gene networks associated with the transition from dysplasia to advanced lung adenocarcinomas induced by c-Raf-1. *PloS one*. 4:e7315.
Rosales-Reynoso, M.A., A.B. Ochoa-Hernandez, A. Aguilar-Lemarroy, L.F. Jave-Suarez, R. Troyo-Sanroman, and P. Barros-Nunez. 2010. Gene expression profiling identifies WNT7A as a possible candidate gene for decreased cancer risk in fragile X syndrome patients. *Archives of medical research*. 41:110-118 e112.
Ruiz i Altaba, A. 1994. Pattern formation in the vertebrate neural plate. *Trends in neurosciences*. 17:233-243.
Russo, G.J., K. Louie, A. Wellington, G.T. Macleod, F. Hu, S. Panchumarthi, and K.E. Zinsmaier. 2009. Drosophila Miro is required for both anterograde and retrograde axonal mitochondrial transport. *J Neurosci*. 29:5443-5455.
Salinas, P.C. 1999. Wnt factors in axonal remodelling and synaptogenesis. *Biochemical Society symposium*. 65:101-109.
Salinas, P.C., and Y. Zou. 2008. Wnt signaling in neural circuit assembly. *Annual review of neuroscience*. 31:339-358.
Sang, H., Z. Lu, Y. Li, B. Ru, W. Wang, and J. Chen. 2001. Phosphorylation of tau by glycogen synthase kinase 3beta in intact mammalian cells influences the stability of microtubules. *Neuroscience letters*. 312:141-144.
Sansom, O.J., V.S. Meniel, V. Muncan, T.J. Phesse, J.A. Wilkins, K.R. Reed, J.K. Vass, D. Athineos, H. Clevers, and A.R. Clarke. 2007. Myc deletion rescues Apc deficiency in the small intestine. *Nature*. 446:676-679.
Santel, A., S. Frank, B. Gaume, M. Herrler, R.J. Youle, and M.T. Fuller. 2003. Mitofusin-1 protein is a generally expressed mediator of mitochondrial fusion in mammalian cells. *Journal of cell science*. 116:2763-2774.
Santel, A., and M.T. Fuller. 2001. Control of mitochondrial morphology by a human mitofusin. *Journal of cell science*. 114:867-874.
Santos, R.X., S.C. Correia, X. Wang, G. Perry, M.A. Smith, P.I. Moreira, and X. Zhu. 2010. A synergistic dysfunction of mitochondrial fission/fusion dynamics and mitophagy in Alzheimer's disease. *Journal of Alzheimer's disease : JAD*. 20 Suppl 2:S401-412.
Saotome, M., D. Safiulina, G. Szabadkai, S. Das, A. Fransson, P. Aspenstrom, R. Rizzuto, and G.

Hajnoczky. 2008. Bidirectional Ca2+-dependent control of mitochondrial dynamics by the Miro GTPase. *Proceedings of the National Academy of Sciences of the United States of America*. 105:20728-20733.

Sawamura, N., T. Ando, Y. Maruyama, M. Fujimuro, H. Mochizuki, K. Honjo, M. Shimoda, H. Toda, T. Sawamura-Yamamoto, L.A. Makuch, A. Hayashi, K. Ishizuka, N.G. Cascella, A. Kamiya, N. Ishida, T. Tomoda, T. Hai, K. Furukubo-Tokunaga, and A. Sawa. 2008. Nuclear DISC1 regulates CRE-mediated gene transcription and sleep homeostasis in the fruit fly. *Molecular psychiatry*. 13:1138-1148, 1069.

Scales, T.M., S. Lin, M. Kraus, R.G. Goold, and P.R. Gordon-Weeks. 2009. Nonprimed and DYRK1A-primed GSK3 beta-phosphorylation sites on MAP1B regulate microtubule dynamics in growing axons. *Journal of cell science*. 122:2424-2435.

Scarpulla, R.C. 2002. Transcriptional activators and coactivators in the nuclear control of mitochondrial function in mammalian cells. *Gene*. 286:81-89.

Scorrano, L., M. Ashiya, K. Buttle, S. Weiler, S.A. Oakes, C.A. Mannella, and S.J. Korsmeyer. 2002. A distinct pathway remodels mitochondrial cristae and mobilizes cytochrome c during apoptosis. *Developmental cell*. 2:55-67.

Schwartz, D.R., R. Wu, S.L. Kardia, A.M. Levin, C.C. Huang, K.A. Shedden, R. Kuick, D.E. Misek, S.M. Hanash, J.M. Taylor, H. Reed, N. Hendrix, Y. Zhai, E.R. Fearon, and K.R. Cho. 2003. Novel candidate targets of beta-catenin/T-cell factor signaling identified by gene expression profiling of ovarian endometrioid adenocarcinomas. *Cancer research*. 63:2913-2922.

Schwarzer, C., S. Barnikol-Watanabe, F.P. Thinnes, and N. Hilschmann. 2002. Voltage-dependent anion-selective channel (VDAC) interacts with the dynein light chain Tctex1 and the heat-shock protein PBP74. *The international journal of biochemistry & cell biology*. 34:1059-1070.

Sheng, Z.H., and Q. Cai. 2012. Mitochondrial transport in neurons: impact on synaptic homeostasis and neurodegeneration. *Nature reviews*. 13:77-93.

Sheridan, C., and S.J. Martin. 2010. Mitochondrial fission/fusion dynamics and apoptosis. *Mitochondrion*. 10:640-648.

Sherr, C.J., D. Bertwistle, D.E.N.B. W, M.L. Kuo, M. Sugimoto, K. Tago, R.T. Williams, F. Zindy, and M.F. Roussel. 2005. p53-Dependent and -independent functions of the Arf tumor suppressor. *Cold Spring Harbor symposia on quantitative biology*. 70:129-137.

Shtutman, M., J. Zhurinsky, I. Simcha, C. Albanese, M. D'Amico, R. Pestell, and A. Ben-Ze'ev. 1999. The cyclin D1 gene is a target of the beta-catenin/LEF-1 pathway. *Proceedings of the National Academy of Sciences of the United States of America*. 96:5522-5527.

Shutt, T., M. Geoffrion, R. Milne, and H.M. McBride. 2012. The intracellular redox state is a core determinant of mitochondrial fusion. *EMBO reports*. 13:909-915.

Simonin, F., P. Karcher, J.J. Boeuf, A. Matifas, and B.L. Kieffer. 2004. Identification of a novel family of G protein-coupled receptor associated sorting proteins. *Journal of neurochemistry*. 89:766-775.

Smalley, M.J., and T.C. Dale. 1999. Wnt signalling in mammalian development and cancer. *Cancer metastasis reviews*. 18:215-230.

Smith, C.A., P.J. McClive, and A.H. Sinclair. 2005. Temporal and spatial expression profile of the novel armadillo-related gene, Alex2, during testicular differentiation in the mouse embryo. *Dev Dyn*. 233:188-193.

Song, S., L.J. Wheeler, and C.K. Mathews. 2003. Deoxyribonucleotide pool imbalance stimulates deletions in HeLa cell mitochondrial DNA. *The Journal of biological chemistry*. 278:43893-43896.

Stamer, K., R. Vogel, E. Thies, E. Mandelkow, and E.M. Mandelkow. 2002. Tau blocks traffic of organelles, neurofilaments, and APP vesicles in neurons and enhances oxidative stress.

The Journal of cell biology. 156:1051-1063.
Stokin, G.B., C. Lillo, T.L. Falzone, R.G. Brusch, E. Rockenstein, S.L. Mount, R. Raman, P. Davies, E. Masliah, D.S. Williams, and L.S. Goldstein. 2005. Axonopathy and transport deficits early in the pathogenesis of Alzheimer's disease. *Science (New York, N.Y.* 307:1282-1288.
Stoothoff, W., P.B. Jones, T.L. Spires-Jones, D. Joyner, E. Chhabra, K. Bercury, Z. Fan, H. Xie, B. Bacskai, J. Edd, D. Irimia, and B.T. Hyman. 2009. Differential effect of three-repeat and four-repeat tau on mitochondrial axonal transport. *Journal of neurochemistry*. 111:417-427.
Stowers, R.S., L.J. Megeath, J. Gorska-Andrzejak, I.A. Meinertzhagen, and T.L. Schwarz. 2002. Axonal transport of mitochondria to synapses depends on milton, a novel Drosophila protein. *Neuron*. 36:1063-1077.
Suen, D.F., K.L. Norris, and R.J. Youle. 2008. Mitochondrial dynamics and apoptosis. *Genes & development*. 22:1577-1590.
Susalka, S.J., W.O. Hancock, and K.K. Pfister. 2000. Distinct cytoplasmic dynein complexes are transported by different mechanisms in axons. *Biochimica et biophysica acta.* 1496:76-88.
Susalka, S.J., and K.K. Pfister. 2000. Cytoplasmic dynein subunit heterogeneity: implications for axonal transport. *Journal of neurocytology*. 29:819-829.
Suwanwela, J., C.R. Farber, B.L. Haung, B. Song, C. Pan, K.M. Lyons, and A.J. Lusis. 2010. Systems genetics analysis of mouse chondrocyte differentiation. *J Bone Miner Res*. 26:747-760.
Suzuki, M., A. Neutzner, N. Tjandra, and R.J. Youle. 2005. Novel structure of the N terminus in yeast Fis1 correlates with a specialized function in mitochondrial fission. *The Journal of biological chemistry*. 280:21444-21452.
Tanaka, A. 2010. Parkin-mediated selective mitochondrial autophagy, mitophagy: Parkin purges damaged organelles from the vital mitochondrial network. *FEBS letters*. 584:1386-1392.
Tanaka, A., M.M. Cleland, S. Xu, D.P. Narendra, D.F. Suen, M. Karbowski, and R.J. Youle. 2010. Proteasome and p97 mediate mitophagy and degradation of mitofusins induced by Parkin. *The Journal of cell biology*. 191:1367-1380.
Tanaka, Y., Y. Kanai, Y. Okada, S. Nonaka, S. Takeda, A. Harada, and N. Hirokawa. 1998. Targeted disruption of mouse conventional kinesin heavy chain, kif5B, results in abnormal perinuclear clustering of mitochondria. *Cell*. 93:1147-1158.
Taneyhill, L., and D. Pennica. 2004. Identification of Wnt responsive genes using a murine mammary epithelial cell line model system. *BMC developmental biology*. 4:6.
Tappe-Theodor, A., N. Agarwal, I. Katona, T. Rubino, L. Martini, J. Swiercz, K. Mackie, H. Monyer, D. Parolaro, J. Whistler, T. Kuner, and R. Kuner. 2007. A molecular basis of analgesic tolerance to cannabinoids. *J Neurosci*. 27:4165-4177.
Tatsuta, T., and T. Langer. 2008. Quality control of mitochondria: protection against neurodegeneration and ageing. *The EMBO journal*. 27:306-314.
Teo, R., F. Mohrlen, G. Plickert, W.A. Muller, and U. Frank. 2006. An evolutionary conserved role of Wnt signaling in stem cell fate decision. *Developmental biology*. 289:91-99.
Tetsu, O., and F. McCormick. 1999. Beta-catenin regulates expression of cyclin D1 in colon carcinoma cells. *Nature*. 398:422-426.
Tewari, R., E. Bailes, K.A. Bunting, and J.C. Coates. Armadillo-repeat protein functions: questions for little creatures. *Trends in cell biology*. 20:470-481.
Tewari, R., E. Bailes, K.A. Bunting, and J.C. Coates. 2010. Armadillo-repeat protein functions: questions for little creatures. *Trends in cell biology*. 20:470-481.
Thompson, D., and J.L. Whistler. 2007. Dopamine D(3) receptors are down-regulated following heterologous endocytosis by a specific interaction with G protein-coupled receptor-

associated sorting protein-1. *The Journal of biological chemistry*. 286:1598-1608.
Tischfield, M.A., H.N. Baris, C. Wu, G. Rudolph, L. Van Maldergem, W. He, W.M. Chan, C. Andrews, J.L. Demer, R.L. Robertson, D.A. Mackey, J.B. Ruddle, T.D. Bird, I. Gottlob, C. Pieh, E.I. Traboulsi, S.L. Pomeroy, D.G. Hunter, J.S. Soul, A. Newlin, L.J. Sabol, E.J. Doherty, C.E. de Uzcategui, N. de Uzcategui, M.L. Collins, E.C. Sener, B. Wabbels, H. Hellebrand, T. Meitinger, T. de Berardinis, A. Magli, C. Schiavi, M. Pastore-Trossello, F. Koc, A.M. Wong, A.V. Levin, M.T. Geraghty, M. Descartes, M. Flaherty, R.V. Jamieson, H.U. Moller, I. Meuthen, D.F. Callen, J. Kerwin, S. Lindsay, A. Meindl, M.L. Gupta, Jr., D. Pellman, and E.C. Engle. 2010. Human TUBB3 mutations perturb microtubule dynamics, kinesin interactions, and axon guidance. *Cell*. 140:74-87.
Trinczek, B., A. Ebneth, E.M. Mandelkow, and E. Mandelkow. 1999. Tau regulates the attachment/detachment but not the speed of motors in microtubule-dependent transport of single vesicles and organelles. *Journal of cell science*. 112 (Pt 14):2355-2367.
Tuszynski, G.P., V.L. Rothman, X. Zheng, M. Gutu, X. Zhang, and F. Chang. 2011. G-protein coupled receptor-associated sorting protein 1 (GASP-1), a potential biomarker in breast cancer. *Experimental and molecular pathology*. 91:608-613.
Uetake, Y., and G. Sluder. 2007. Cell-cycle progression without an intact microtuble cytoskeleton. *Curr Biol*. 17:2081-2086.
Ulloa, F., and J. Briscoe. 2007. Morphogens and the control of cell proliferation and patterning in the spinal cord. *Cell cycle*. 6:2640-2649.
Ulloa, F., and E. Marti. 2010. Wnt won the war: antagonistic role of Wnt over Shh controls dorso-ventral patterning of the vertebrate neural tube. *Developmental dynamics : an official publication of the American Association of Anatomists*. 239:69-76.
Vallstedt, A., J. Muhr, A. Pattyn, A. Pierani, M. Mendelsohn, M. Sander, T.M. Jessell, and J. Ericson. 2001. Different levels of repressor activity assign redundant and specific roles to Nkx6 genes in motor neuron and interneuron specification. *Neuron*. 31:743-755.
van Amerongen, R., and R. Nusse. 2009. Towards an integrated view of Wnt signaling in development. *Development (Cambridge, England)*. 136:3205-3214.
Van Straaten, H.W., and J.W. Hekking. 1991. Development of floor plate, neurons and axonal outgrowth pattern in the early spinal cord of the notochord-deficient chick embryo. *Anatomy and embryology*. 184:55-63.
Varadi, A., L.I. Johnson-Cadwell, V. Cirulli, Y. Yoon, V.J. Allan, and G.A. Rutter. 2004. Cytoplasmic dynein regulates the subcellular distribution of mitochondria by controlling the recruitment of the fission factor dynamin-related protein-1. *Journal of cell science*. 117:4389-4400.
Verstreken, P., C.V. Ly, K.J. Venken, T.W. Koh, Y. Zhou, and H.J. Bellen. 2005. Synaptic mitochondria are critical for mobilization of reserve pool vesicles at Drosophila neuromuscular junctions. *Neuron*. 47:365-378.
Vlad, A., S. Rohrs, L. Klein-Hitpass, and O. Muller. 2008. The first five years of the Wnt targetome. *Cellular signalling*. 20:795-802.
Vlahou, G., M. Elias, J.C. von Kleist-Retzow, R.J. Wiesner, and F. Rivero. 2011. The Ras related GTPase Miro is not required for mitochondrial transport in Dictyostelium discoideum. *European journal of cell biology*. 90:342-355.
Voiculescu, O., C. Papanayotou, and C.D. Stern. 2008. Spatially and temporally controlled electroporation of early chick embryos. *Nature protocols*. 3:419-426.
Vossel, K.A., K. Zhang, J. Brodbeck, A.C. Daub, P. Sharma, S. Finkbeiner, B. Cui, and L. Mucke. 2010. Tau reduction prevents Abeta-induced defects in axonal transport. *Science (New York, N.Y.* 330:198.
Wade, R.H. 2007. Microtubules: an overview. *Methods in molecular medicine*. 137:1-16.
Wallace, D.C. 2005. A mitochondrial paradigm of metabolic and degenerative diseases, aging,

and cancer: a dawn for evolutionary medicine. *Annual review of genetics*. 39:359-407.
Wang, X., and T.L. Schwarz. 2009. The mechanism of Ca2+ -dependent regulation of kinesin-mediated mitochondrial motility. *Cell*. 136:163-174.
Wang, X., B. Su, H.G. Lee, X. Li, G. Perry, M.A. Smith, and X. Zhu. 2009a. Impaired balance of mitochondrial fission and fusion in Alzheimer's disease. *J Neurosci*. 29:9090-9103.
Wang, X., B. Su, S.L. Siedlak, P.I. Moreira, H. Fujioka, Y. Wang, G. Casadesus, and X. Zhu. 2008. Amyloid-beta overproduction causes abnormal mitochondrial dynamics via differential modulation of mitochondrial fission/fusion proteins. *Proceedings of the National Academy of Sciences of the United States of America*. 105:19318-19323.
Wang, X., D. Winter, G. Ashrafi, J. Schlehe, Y.L. Wong, D. Selkoe, S. Rice, J. Steen, M.J. LaVoie, and T.L. Schwarz. 2011. PINK1 and Parkin target Miro for phosphorylation and degradation to arrest mitochondrial motility. *Cell*. 147:893-906.
Wang, Z., A. Havasi, J.M. Gall, H. Mao, J.H. Schwartz, and S.C. Borkan. 2009b. Beta-catenin promotes survival of renal epithelial cells by inhibiting Bax. *J Am Soc Nephrol*. 20:1919-1928.
Webber, E., L. Li, and L.S. Chin. 2008. Hypertonia-associated protein Trak1 is a novel regulator of endosome-to-lysosome trafficking. *Journal of molecular biology*. 382:638-651.
Weihofen, A., K.J. Thomas, B.L. Ostaszewski, M.R. Cookson, and D.J. Selkoe. 2009. Pink1 forms a multiprotein complex with Miro and Milton, linking Pink1 function to mitochondrial trafficking. *Biochemistry*. 48:2045-2052.
Wennerberg, K., and C.J. Der. 2004. Rho-family GTPases: it's not only Rac and Rho (and I like it). *Journal of cell science*. 117:1301-1312.
Whistler, J.L., J. Enquist, A. Marley, J. Fong, F. Gladher, P. Tsuruda, S.R. Murray, and M. Von Zastrow. 2002. Modulation of postendocytic sorting of G protein-coupled receptors. *Science (New York, N.Y.*. 297:615-620.
Wilcock, A.C., J.R. Swedlow, and K.G. Storey. 2007. Mitotic spindle orientation distinguishes stem cell and terminal modes of neuron production in the early spinal cord. *Development*. 134:1943-1954.
Wilson, N.H., and E.T. Stoeckli. 2012. Sonic Hedgehog regulates Wnt activity during neural circuit formation. *Vitamins and hormones*. 88:173-209.
Winter, E.E., and C.P. Ponting. 2005. Mammalian BEX, WEX and GASP genes: coding and non-coding chimaerism sustained by gene conversion events. *BMC evolutionary biology*. 5:54.
Wodarz, A., and R. Nusse. 1998. Mechanisms of Wnt signaling in development. *Annual review of cell and developmental biology*. 14:59-88.
Xie, Z., Y. Chen, Z. Li, G. Bai, Y. Zhu, R. Yan, F. Tan, Y.G. Chen, F. Guillemot, L. Li, and N. Jing. 2011. Smad6 promotes neuronal differentiation in the intermediate zone of the dorsal neural tube by inhibition of the Wnt/beta-catenin pathway. *Proceedings of the National Academy of Sciences of the United States of America*. 108:12119-12124.
Yang, Y., Y. Ouyang, L. Yang, M.F. Beal, A. McQuibban, H. Vogel, and B. Lu. 2008. Pink1 regulates mitochondrial dynamics through interaction with the fission/fusion machinery. *Proceedings of the National Academy of Sciences of the United States of America*. 105:7070-7075.
Yoon, J.C., A. Ng, B.H. Kim, A. Bianco, R.J. Xavier, and S.J. Elledge. 2010. Wnt signaling regulates mitochondrial physiology and insulin sensitivity. *Genes & development*. 24:1507-1518.
Yoon, Y., and M.A. McNiven. 2001. Mitochondrial division: New partners in membrane pinching. *Curr Biol*. 11:R67-70.
Yost, C., M. Torres, J.R. Miller, E. Huang, D. Kimelman, and R.T. Moon. 1996. The axis-inducing activity, stability, and subcellular distribution of beta-catenin is regulated in

Xenopus embryos by glycogen synthase kinase 3. *Genes & development*. 10:1443-1454.
Youle, R.J., and D.P. Narendra. 2011. Mechanisms of mitophagy. *Nature reviews. Molecular cell biology*. 12:9-14.
Yu, W., K. McDonnell, M.M. Taketo, and C.B. Bai. 2008. Wnt signaling determines ventral spinal cord cell fates in a time-dependent manner. *Development*. 135:3687-3696.
Yu, W., Y. Sun, S. Guo, and B. Lu. 2011. The PINK1/Parkin pathway regulates mitochondrial dynamics and function in mammalian hippocampal and dopaminergic neurons. *Human molecular genetics*. 20:3227-3240.
Zannis-Hadjopoulos, M., W. Yahyaoui, and M. Callejo. 2008. 14-3-3 cruciform-binding proteins as regulators of eukaryotic DNA replication. *Trends in biochemical sciences*. 33:44-50.
Zechner, D., Y. Fujita, J. Hulsken, T. Muller, I. Walther, M.M. Taketo, E.B. Crenshaw, 3rd, W. Birchmeier, and C. Birchmeier. 2003. beta-Catenin signals regulate cell growth and the balance between progenitor cell expansion and differentiation in the nervous system. *Developmental biology*. 258:406-418.
Zechner, D., T. Muller, H. Wende, I. Walther, M.M. Taketo, E.B. Crenshaw, 3rd, M. Treier, W. Birchmeier, and C. Birchmeier. 2007. Bmp and Wnt/beta-catenin signals control expression of the transcription factor Olig3 and the specification of spinal cord neurons. *Developmental biology*. 303:181-190.
Zhang, Z., N. Wakabayashi, J. Wakabayashi, Y. Tamura, W.J. Song, S. Sereda, P. Clerc, B.M. Polster, S.M. Aja, M.V. Pletnikov, T.W. Kensler, O.S. Shirihai, M. Iijima, M.A. Hussain, and H. Sesaki. The dynamin-related GTPase Opa1 is required for glucose-stimulated ATP production in pancreatic beta cells. *Molecular biology of the cell*. 22:2235-2245.
Zhang, Z., N. Wakabayashi, J. Wakabayashi, Y. Tamura, W.J. Song, S. Sereda, P. Clerc, B.M. Polster, S.M. Aja, M.V. Pletnikov, T.W. Kensler, O.S. Shirihai, M. Iijima, M.A. Hussain, and H. Sesaki. 2011. The dynamin-related GTPase Opa1 is required for glucose-stimulated ATP production in pancreatic beta cells. *Molecular biology of the cell*. 22:2235-2245.
Zhou, X., G. Yang, R. Huang, X. Chen, and G. Hu. 2007. SVH-B interacts directly with p53 and suppresses the transcriptional activity of p53. *FEBS letters*. 581:4943-4948.
Ziegler, S., S. Rohrs, L. Tickenbrock, T. Moroy, L. Klein-Hitpass, I.R. Vetter, and O. Muller. 2005. Novel target genes of the Wnt pathway and statistical insights into Wnt target promoter regulation. *The FEBS journal*. 272:1600-1615.
Zirn, B., S. Wittmann, N. Graf, and M. Gessler. 2005. Chibby, a novel antagonist of the Wnt pathway, is not involved in Wilms tumor development. *Cancer letters*. 220:115-120.